Fatigue and creep in wood based panel products

Thompson, Richard James Hollister

Award date:
1996

Awarding institution:
University of Bath

FATIGUE AND CREEP IN WOOD BASED PANEL PRODUCTS

submitted by Richard James Hollister Thompson
for the degree of PhD
of the University of Bath
1996

COPYRIGHT

Richard Thompson.

Richard J. H. Thompson.

ProQuest LLC
789 East Eisenhower Parkway
P.O. Box 1346
Ann Arbor, MI 48106-1346

SUMMARY

The fatigue performance in bending of representative wood based panel products has been investigated. The research primarily evaluated the effect of the frequency of loading on the fatigue life of structural grade chipboard used for flooring in buildings. Design parameters for flooring are based on deflection and duration of load. However, panel products used in factories or other flooring applications can be subjected to fatigue loading such as vibrating machinery, fork lift truck motion and pedestrian motion. Two other panel products were investigated: oriented strand board (OSB) which is also used for flooring and medium density fibreboard (MDF) which may be used for sports hall flooring in the future.

Parallel tests were carried out in creep and fatigue (at the same peak stress) to enable the results of cyclic and static loading to be compared. Stress versus strain hysteresis loop capture has been used as a non-interruptive method to evaluate fatigue damage in the materials. The parameters derived from the hysteresis loops have been used to evaluate the effects of reducing the level of stress applied and the effect of loading frequency on the fatigue and the relative fatigue performances of OSB, chipboard and MDF.

The fatigue life of chipboard is shown to reduce when the frequency of fatigue loading is reduced. The bending strength of chipboard was also reduced when the rate of loading was reduced for static testing. Observations of the change in the hysteresis loop area between the first and the last loop capture suggest that OSB, chipboard and MDF all have fatigue limits at slightly below the 20% stress level. The fatigue limit for MDF lies slightly below those for OSB and chipboard.

There was no correlation between the constituent particle size and the relative fatigue performances of the three panel products. The fatigue performance of the three panel products normalised by the static strength reduced as follows: chipboard>OSB>MDF. When compared with respect to the applied stress, however, the fatigue performances reduced as follows MDF>OSB>chipboard, which reflects the relative bending strengths.

ACKNOWLEDGEMENTS

It is my pleasure to dedicate this thesis to my parents, Ray and Ros, for their continued support and dedication.

This research and the associated CASE award were funded by Department of the Environment through the Timber Division at the Building Research Establishment (BRE). The studentship part of the CASE award was provided by the Engineering and Physical Sciences Research Council (EPSRC) formerly the Science and Engineering Research Council (SERC). For this support I am very grateful.

Throughout this research I have been very fortunate to have been supported and inspired by my supervisor, **Dr. Martin P. Ansell** and by my industrial liaison officer, **Dr. Peter W. Bonfield**. I would like to thank Martin and Peter for their supervision, guidance and encouragement, and for their contributions in making these three years so rewarding. I was also privileged to be guided by, and to learn from **Prof. John M. Dinwoodie** prior to his retirement in March 1995.

I should like to thank the following people from the University of Bath for their contributions to this work: Simon Bowman for his help with the hysteresis loop capture software and with computing, Dr. Ian Bond and Dr. Clare Hacker for their continued support within the Wood Research group, also Chris Arnold and all of the technical staff for helping to maintain the hydraulic test machinery.

I should also like to thank the staff of the Timber Division at the BRE, in particular Jo-Anne Mundy and Brian Paxton for making me feel very welcome during the time I have spent at BRE and always being keen to help.

Last but not least, I should like to thank Charlotte for her support and encouragement whilst I was writing-up.

ABBREVIATIONS

BS	Bending Strength
BRE	Building Research Establishment
CB	Chipboard
EPSRC	Engineering and Physical Sciences Research Council
FDAS	Fatigue Data Acquisition System
FIDOR	Fibre Building Board Organisation
FIRA	Fibre Building Board Development Organisation
IS	Isocyanate
OSB	Oriented Strand Board
OWB	Oriented Wafer Board
LVDT	Linear Variable Differential Transformer
MC	Moisture Content
MDF	Medium Density Fibreboard
MDFMR	Medium Density Fibreboard Moisture Resistant
MOE	Modulus of Elasticity
MOR	Modulus of Rupture
PB	Particleboard
PC	Personal Computer
PF	Phenol Formaldehyde
R	R ratio
r^2	Correlation Coefficient
RH	Relative Humidity
S_a	Stress Amplitude
S_m	Mean Stress
S_o	Stress Range
SERC	Science and Engineering Research Council
S-N	Stress versus $Log_{(10)}$ Number of Loading Cycles to Failure
UF	Urea Formaldehyde
UMF	Urea Melamine Formaldehyde
UTS	Ultimate Tensile Strength
WPPF	Wood Panel Products Federation

CONTENTS Page Number

1.0 INTRODUCTION

Wood is a natural renewable material used by man in the construction of buildings and ships for over 5000 years. Wood has been extensively used because it is a low density material with excellent specific mechanical properties. However, it has two main drawbacks for use in construction: it has inherently variable mechanical properties, and these properties are anisotropic (different in orthogonal directions). These drawbacks have been overcome in recent times by breaking the wood down into particles or fibres that are pressed together with a resin binder, under the application of heat and pressure, to form particleboards, often referred to as wood based panel products. Wood based panels were first produced about 3500 years ago by the Egyptians (Clarke 1991). They applied hand sawn decorative veneers to lumber cores for pictures, furniture and coffins. There are several types of particleboards. The following three types were tested in the experimental work: wood chipboard, oriented strand board (OSB) and medium density fibreboard (MDF).

Wood based panel products exploit the excellent specific properties of wood, while reducing its inherent variability and anisotropy. The dimensions of wood, or timber, as it is generally referred to in its cut form, are limited by the tree from which it was sawn. Unlike timber, wood based panel products are produced in a wide range of sizes with predetermined mechanical properties and they are widely used for many applications including flooring, roof decking, packaging and furniture. Particleboards used as flooring can be exposed to a combination of creep and fatigue loading throughout their lifetime. Creep loads are produced by static masses, such as heavy machinery standing on a floor, and fatigue loads arise from intermittent loads, such as fork lift trucks or people in motion.

1.1 Research Strategy

The use of these panel products is limited by their creep properties, because they are viscoelastic and they continue to deflect with time when subjected to a constant load. To overcome this, the Building Research Establishment (BRE) has conducted an extensive research programme since 1974 on quantifying and predicting the creep behaviour of particleboards. This research has concentrated on wood chipboard because this maintains the largest UK market, although two other commercially important panel products, MDF and OSB, have also been examined. When particleboard is used as flooring in buildings it is exposed to fatigue as well as creep loading and this is widely ignored.

This thesis extends the work at BRE by examining the response of three selected particleboards to fatigue and creep loading, in order to simulate the loading of factory floors. Creep and fatigue tests were performed on chipboard, OSB and MDF. The fatigue testing of chipboard was carried out at three frequencies determined by the rate of application of stress. The frequency was changed by a factor of ten at each change of loading rate. The three frequencies are termed: low, medium and high. For every fatigue sample tested a side-matched sample was simultaneously tested in creep. This research programme developed and complimented two previous projects at Bath University (Hacker 1991 and Thompson 1992), which were both run in conjunction with BRE, investigating the behaviour of another structural grade chipboard exposed to creep and fatigue loading. This collaborative research has helped to bridge the gap between the existing knowledge of creep in particleboard and the extremely limited knowledge of the fatigue performance of particleboards.

The use of OSB and MDF is increasing annually and these relatively new panel products have replaced chipboard and plywood in many applications. Fatigue test results have been used to examine the fatigue life of different panel products including an evaluation of the effect of wood particle size. OSB is composed of large wood chips/strips, chipboard has smaller chips and MDF is made up of fibre bundles.

During all the tests, stress versus strain hysteresis loops were captured to assess damage to samples without interrupting the tests. The loops were analysed to give the energy dissipated per cycle, the changes in the dynamic modulus of elasticity and underlying creep deflection.

1.2 Thesis Structure

The first five chapters of this thesis provide an introduction to wood and wood based materials in the form of a literature review. Wood is the basic building block for chipboard, oriented strandboard and medium density fibreboard which are the three materials tested in the experimental work. To help understand these materials a brief introduction to the structure of wood is provided, Chapter 2. This is followed by an explanation of each material including their classification, consumption, manufacture, typical properties and uses, Chapter 3. The phenomena of fatigue and creep are covered in the chapters 4 and 5 where the literature for wood based panel products is presented in summary.

Chapter 6 provides details of all the experimental work presented in chapters 7-10. Due to the quantity of data evaluated each section of work is discussed separately to

avoid over complicating the text and interim conclusions are provided at the end of each chapter. These four chapters present results for the static, fatigue and creep testing of the materials. Chapters 7 and 8 examine chipboard exclusively. In Chapter 7 the effect of the rate of loading upon the apparent strength of chipboard is evaluated since this influences the load levels for the fatigue and creep tests. Chapter 8 examines the effect of loading frequency on the fatigue life of chipboard. This work focuses on the use of stress versus strain hysteresis loop capture as a non- interruptive technique to evaluate damage accumulation in the material and to predict a fatigue limit.

Chapters 9 and 10 compare the performances of chipboard, OSB and MDF including evaluation of the effect of wood particle size. In Chapter 9 the relative strengths of the three materials and the magnitude of their inherent variability are investigated. Chapter 10 compares the fatigue performances of the three materials and hysteresis loop capture is again used to evaluate damage accumulation. The emphasis in this work is on parallel fatigue and creep testing, allowing the effects of cyclic loading to be compared to the creep situation which has been more extensively researched.

The interim conclusions are combined in Chapter 11 to consolidate the main findings and references are provided in Chapter 12. Appendices 1-5 contain the equations and computer programmes used in the experimental work and explanations of statistical terms used. Also included are extensive tables containing the dimensions, properties and test conditions for all the samples tested. These have been kept separate from the core text to avoid distracting the reader.

2.0 THE STRUCTURE OF WOOD

This section is a brief description of the structure of wood, since this thesis examines wood chipboard, OSB and MDF, not wood. All three materials are, however, made from wood particles of various sizes, but each material possesses it own characteristic properties. There are some excellent text books available covering the structure and properties of wood/timber, including those by Desch and Dinwoodie (1981), Dinwoodie (1981 and 1989), Bodig and Jayne (1982) and Madsen (1992). This subject is also comprehensively reviewed in PhD theses by Tsai (1987) and Bond (1994).

2.1 Introduction

Wood is a low density, natural, cellular polymer. It is the world's oldest, most widely used structural material and can be classified as a fibre-reinforced composite. The word "material" was derived from the Latin materies, materia: the trunk of a tree. The documented use of wood in ships and buildings dates back over the last 5000 years. The world production of wood is approximately the same as that of iron and steel, and is in the order of 10^9 tonnes per annum (Ashby and Jones 1986, and Dinwoodie 1989).

Woody plants are divide into two main groups:
a) **softwoods** (gymnosperms) also known as conifers or evergreens; and
b) **hardwoods** (dicotyledons, a group of the angiosperms) also called broad-leaved or deciduous.
The distinction is a deceptive one, since many of the softwoods are harder than many of the hardwoods. There are, however, several structural differences between the two types of wood.

In order to understand the structure of wood it must be considered at three separate levels: macroscopic, microscopic and molecular. A more detailed approach is provided by Dinwoodie (1989), and by Bodig and Jayne (1982).

2.2 The Macroscopic Structure of Wood

Most of the growth of a tree takes place in the cambium, a thin layer just inside the protective bark. The tree trunk grows at different rates during the year, in a temperate climate most of the growth occurs in the spring and summer producing one ring per year. Tropical hardwoods, however, may produce more than one ring per year in response to alternating wet and dry growing seasons. Growth rings radiate out from the centre of the trunk and typically consist of two distinct parts. The wood formed early in the growing season is light in weight with large cell cavities and is called early

or spring wood. The primary function of this early wood is to conduct fluids up the tree to the crown. The wood formed in the later part of the growing season is called the late or summer wood, this is darker in colour and has smaller cell cavities. Late wood has a dominant roll in the mechanical properties of the wood due to an increased amount of cell wall material.

If the trunk of a felled tree is examined the growth rings are clearly visible and depending upon the species of tree, the centre of the trunk may be darker in colour than the outer region of the trunk. This change in colour indicates a considerable change in the physiological activity of the wood. The light coloured outer section of the wood is called the sapwood, this conducts mineral solutions up the tree and stores the manufactured food. The darker coloured inner section is the heartwood and extractives are deposited in this region. The heartwood is physiologically inactive, providing only mechanical strength. This region is frequently less permeable and more resistant to decay than the sapwood. The macroscopic features, of a segment of a tree trunk, are shown in figure 2.1.

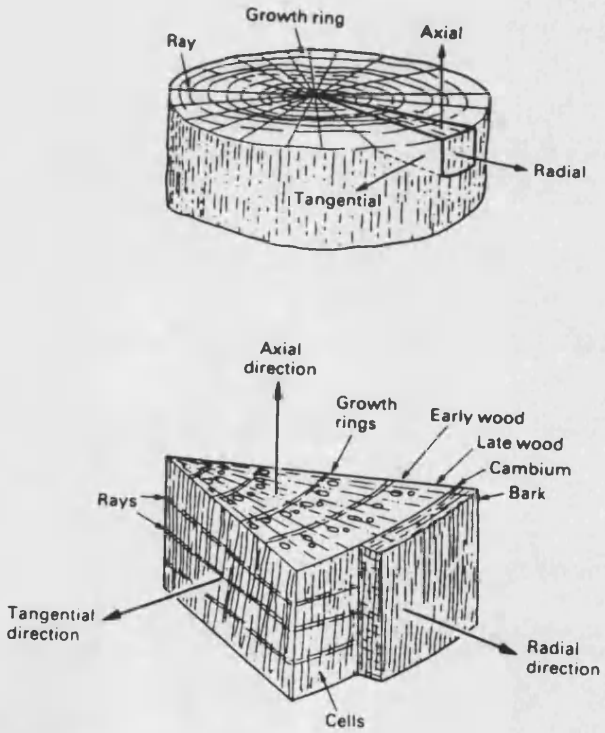

Fig 2.1 The macroscopic structure of wood (Ashby and Jones 1986).

The other main macroscopic features of wood are knots, normally seen in sawn timber. When existing branches enlarge they have to be accommodated by the growing trunk of the tree and this is achieved by the formation of a knot. If the branch was still growing at the point where it fuses to the trunk there is a continuity in growth even

though there is a change in the cell orientation. This forms a live or green knot. If, however, the branch was dead then there is a discontinuity and a dead or black knot is formed. These frequently fall out on sawing.

2.3 The Microscopic Structure of Wood

At a microscopic level, wood is composed of four basic cell types. All four types are present in hardwoods but only two are present in softwoods. In a **softwood** the cells positioned vertically comprise about 90-95% of the volume of the wood and conduct mineral solutions up the tree to the crown and provide support. These cells are the tracheids and are 2-4 mm in length with an aspect ratio of 100:1. The horizontally aligned cells are the parenchyma and form a unit called a ray. These cells store food produced in the leaves and transport fluids to the cambium. They are much smaller than the tracheids and are about 200 X 30 μm. In a **hardwood** the parenchyma cells again store food but these cells can run vertically as well as horizontally. Support is provided by long, narrow cells with tapered ends. These cells are the fibres and are 1-2 mm long, again with an aspect ratio of 100:1. Conduction of fluids is carried out by cells called the vessels, these are cells where the ends have been dissolved away. They are short (0.2-1.2 mm) and relatively wide (<0.5 mm). They run up the axis of the tree providing a transport system to convey fluids, from the roots, to the branches. The generalised microstructure of wood is shown in figure 2.2.

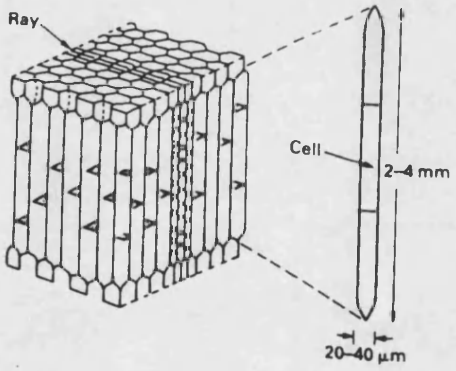

Fig 2.2 The microstructure of wood (Ashby and Jones 1986).

Woods have relative densities in the range 0.07 to >1.0 and fibre-reinforced cell walls. Their properties are very anisotropic, partly because of the cell shape and partly because the cell-wall fibres (microfibrils) are aligned approximately 11° off the axial direction.

2.4 The Molecular Structure of Wood

At a molecular level, wood is considered to be a fibre-reinforced composite material. The cell walls are a matrix of hemicellulose (a partly crystalline polymer of glucose) and lignin (an amorphous polymer composed of carbohydrate compounds), reinforced with fibres of cellulose (in the form of microfibrils). Figure 2.3 shows the ultra structure of a cell wall. The lay-up of the cellulose fibres is complicated but makes an important contribution to the anisotropy of wood (Ashby and Jones 1986). In greatly simplified terms, the fibres are helically wound with the fibre direction nearer the cell axis than across it, producing a modulus for the cell wall three times greater along its length than across.

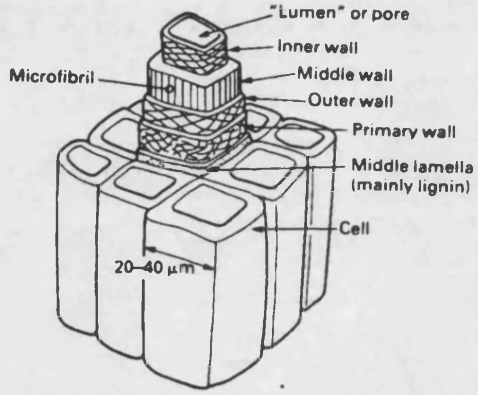

Fig 2.3 The ultra structure of a cell wall (Ashby and Jones 1986).

Cellulose, is a highly crystalline linear polymer, where the molecules are usually located in discrete bundles, called elementary fibrils. Their dimensions are still uncertain but are considered to be in the order of 3.5 X 3.5 nm in cross-section (Bodig and Jayne 1982). Each of these fibrils contains a parallel array of 50-80 cellulose molecules, predominantly aligned with the fibril axis. The fibrils often aggregate into larger units called microfibrils by hydrogen bonding and are thought to be of the order of or 10-30 nm in cross-section (Dinwoodie 1989).

2.5 The Inherent Variability of Wood

Wood is an inherently variable material. This is one of its few deficiencies as a structural material. The same species of tree, grown in different climates and different parts of the same tree, can have different structures and hence different properties. Within an individual tree trunk there can be variations in cell length, grain angle and cell wall thickness. Variability also results from the growth of abnormal reaction wood, produced when a growing tree is leaning, or is exposed to the wind.

3.0 WOOD BASED PANEL PRODUCTS

There are a number of drawbacks that affect the use of wood as a structural material (Dinwoodie 1981):

1) Its performance has a high degree of variability.
2) Its mechanical properties are very anisotropic.
3) Its dimensions are unstable in varying humidity.
4) It is only available in limited widths.

These drawbacks are all improved on by breaking the wood down into smaller units, then reassembling or reconstituting them with resins, to form wood based panel boards/products. Here wood is the raw material for further processing and panels can be tailor made to meet specific design requirements. Wood based panel boards can have similar structural properties in different directions and can be produced in large panels. They have improved dimensional stability in the plane of the board. However this is at the expense of increased thickness swelling, but fortunately this is the smallest and the least critical dimension for swelling. Within any one board type the properties are less variable than for solid wood, this is due to the randomisation of defects, and variation of structure (Gibson 1992). Presently there are a wide variety of wood based panel products available and these divide into three main groups:

3.1 Types of Panel Boards

A) Plywoods are manufactured from wood veneers that are produced by peeling or slicing logs. The international definition for plywood is "panels consisting of an assembly of plies bonded together with the direction of the grain in alternate plies usually at right angles. The outer and inner plies are generally placed symmetrically on both sides of a central ply or core" (Desch and Dinwoodie 1981). At present the market share for plywood is decreasing, this is due to the limited availability of the large diameter logs often required to produce the wood veneers and environmental pressure against the logging of these large trees. (Plywood will not be discussed further since it is not specifically relevant to the research.)

B) Particleboards are panel products manufactured under heat and pressure from particles of wood or other ligno-cellulosic materials and a resin binder (BS5669, the British Standard for Particleboard, 1989). The term particleboard is a general term that encompasses a variety of board types including chipboard, oriented strand board (OSB), waferboard and many others. It is wood particleboard, referred to in the UK as **Chipboard**, and **OSB**, that are important in the context of this review.

Particleboards are generally produced from wood but this is not always the case. For example, commercial particleboards are produced from flax shives in Belgium, and from various husks in India.

C) **Fibreboards** have fibres and fibre bundles as their major constituents. There are many different fibreboards available. The distinction between particleboards and fibreboards is purely arbitrary, based on the size of the constituent particles. **Medium density fibreboard (MDF)** is the fibre board of importance to this review.

3.2 Chipboard

Chipboard is a particleboard composed of a large number of wood chips adhered together using a synthetic resin binder such as urea formaldehyde (UF), urea melamine formaldehyde (UMF), or phenol formaldehyde (PF). The wood chips are generally from coniferous softwoods such as spruce, fir or pine, although hardwoods, for example birch are also used. Additives such as paraffin wax are often included in the wood-resin mix to improve the dimensional stability or other desirable properties of the board. The properties of chipboard show similarities to those of plywood, however, in most strength properties chipboard will be weaker than plywood of the same thickness. Chipboards are available from 3 to 50 mm in thickness (BS 5669, 1989) with uniform or graded density. The properties of the boards are enhanced by using a three or five layer structure with denser outer layers (skins) that support much of the load in structural applications (TRADA 1985a). In the layered boards, the smaller wood chips are used for the outside layers, with an increased resin content and the larger chips are in the core, with a lower resin content. When board thickness is increased it is generally the core that is increased. This means that thinner boards contain a greater proportion of high density material and are generally stronger and stiffer than thicker boards (TRADA 1992).

3.2.1 Classification and Use

Currently, there are six grades of chipboard available, these are specified by the strength and moisture resistance of the boards, in BS5669: Part 2, 1989. Each grade has a specific range of properties designed to suit individual applications. The six grades are as follows:

C1: Wood chipboard for general uses. Applications include: wall and ceiling linings, and fittings and fitments for use in dry conditions (WPPF Ref PD/11, 1992).

C1A: Wood chipboard with slightly higher mean quality levels for a number of properties. This is primarily used for: furniture and fitments, and as a substrate for veneers, laminates and foils for use in dry conditions (WPPF Ref PD/12, 1992).

C2: Wood chipboard with enhanced mechanical properties. This is used for light duty non-domestic flooring in dry conditions, and for situations where a higher density board than Type C1 is required (WPPF Ref PD/13, 1992).

C3: Wood chipboard with major improvements in moisture resistance compared to Type C1 (WPPF Ref PD/14, 1992). This is used as decking for flat roofs, wall and ceiling linings, as a substrate for veneers in kitchen and other work tops. It is suitable for use where relative humidity (RH) is fairly high but where its moisture content (MC) should not normally exceed 17%.

C4: Wood chipboard with the same degree of moisture resistance as Type C3 but with a specified impact resistance. This is mainly used for domestic or other light duty flooring and for decking to flat roofs. Other uses include wall and ceiling linings, and fittings and fitments in situations of relatively high humidity (WPPF Ref PD/15, 1992).

C5: Wood chipboard with enhanced moisture resistance and mechanical properties. It is intended for use where full structural design or prototype testing is required. This is used for structural mezzanines, I and box beams, heavy duty: suspended flooring, shelving and racking, and for construction in accordance with BS 5268: Part 2 (WPPF Ref PD/16, 1992a). It was introduced into BS5669 in 1989 but manufactures are still encountering difficulties in achieving this grade of chipboard due to the limits imposed on the formaldehyde content of boards.

The principal difference between the different types of chipboard is that on drying following a period of wetting, MUF and PF bonded boards are capable of considerable recovery, while UF bonded boards show very little recovery. Moreover, the permanent strength loss of UF boards in the presence of moisture increases markedly in raised temperatures (BRE 1992a).

3.2.2 Consumption of Chipboard

The consumption of chipboard in the UK peaked in 1988 at 3.28 million cubic metres. With the construction industry in recession in 1990 consumption was still 2.75 million cubic metres (BRE 1992a). Provisional figures show European consumption at 43.51

million cubic metres in 1990 (Mundy 1993). Of the UK consumption 55% is home produced, with about 40% of the overall consumption used as floor decking and a large proportion of the remainder used in furniture manufacture (BRE 1992a).

3.2.3 Manufacture of Chipboard

Chipboard was first produced in Brenen, Germany in 1941 following the advent of synthetic thermosetting resins (Clarke 1991) and has been manufactured in the UK since the 1940s. At first this was a method of using up the waste wood chips from saw mills. The production of chipboard now uses vastly more wood than can be provided in this way and small trees known as round woods currently provide a large proportion of the wood chips. The chips are cut by rotating knives, dried and then sprayed with adhesive. Usually the chips are then blown on to flat cauls or platens forming a mat in a manner that leaves the finer chips (from the round wood) on the surfaces and the coarser chips in the centre. This is the process used to produce the modern three and five layer boards. In early boards there was a random distribution of particle sizes and no density profile and this contributed to the inferior properties of early chipboard.

On average about 8% of the dry weight of a three layer board is synthetic resin, this is a mean value with 9-11% in the surface layers and 5-7% in the core. The mats are compressed in a heated press at around 200°C. The rate of closing the press has an important influence on the properties of the board produced (Desch and Dinwoodie 1981). This is the batch platen method of production and accounts for the majority of the market. Recently significant production has used a continuous pressing process instead.

Chipboard may also be produced by the Mendé method, although this is only appropriate for thin chipboard of 6 mm or less. This is analogous to paper manufacture in that the board is sufficiently flexible as to pass between and over large heated rollers.

Chipboard may also be extruded. This method of manufacturing chipboard is cheaper than the batch platen method but produces boards with inferior mechanical properties. There is a distinct zone of weakness across the length of the panel as extruded. These boards are still quite suitable for use as the core of doors.

3.3 Oriented Strand Board (OSB)

OSB is a wood based panel board made from flakes, wafers or strands of wood that are bonded together with about 2.5% by weight of powdered synthetic resin, producing a board with similar strength properties to plywood. It is sometimes referred to as flakeboard but in the UK this is a general term for particleboards with large particles, which includes OSB and waferboard. In the USA, however, flakeboard is a specific product (BRE 1986). The resin is the most expensive component of a board and OSB has a lower resin content than chipboard. The application of liquid resins is cheaper than applying powders but the resin content has to be increased.

The panels are made up of three layers: in the bottom layer comprising 25% of the panels thickness, the strands are oriented parallel to the panel's length. In the middle layer comprising 50% of the panel, the strands are oriented perpendicular to the panel's length. In the top layer, comprising 25% of the panel, the strands are again oriented parallel to the panel's length. This creates a three ply effect, although the core is not always oriented. The use of large flakes enhances the strength and stiffness properties of the panels compared to chipboard.

OSB is a relatively new material and was developed from waferboard, which itself was first produced in Idaho in 1955 according to Anderson (1995) or in 1962 according to TRADA (1985a). Waferboard is no longer available in the UK and production has almost ceased in North America, originally the main producer (BRE 1992b). It was not until the early 1980s that oriented wafer board (OWB) and OSB were produced. Like chipboard OSB originated as a use for waste forestry material. It is now replacing plywood and chipboard in many applications. In order to produce plywood large diameter logs are required to peel the veneers. OSB, however, is produced from much smaller logs, 50 - 450 mm in diameter. At present the world supply of large diameter logs is reducing due to deforestation, reforestation with fast growing plantation timber and environmental pressures, but this should not affect the supply of raw material for OSB production.

3.3.1 Classification and Use

OSB is an alternative to plywood for many uses and to chipboard for flooring. Present applications of OSB include flooring, timber frame sheathing, flat roofing, sarking on pitched roofs, site hoarding and boarding up, cases, pallet tops, packaging, cladding for agricultural buildings, roofs, floors and walls for mobile/relocatable buildings, and furniture frames. Novel uses include cabinet making in Germany and the web component of "I" beams in North America.

In 1986 the production of OSB began in Scotland, using Scots pine logs, (in the USA and Canada aspen and pine are used) and OSB was introduced to the UK market. There was no existing British Standard for OSB and accreditation by the British Board of Agrement was sought before OSB could be sold. The first certificate was achieved for use in wall sheathing and Sterling Board (OSB) has since replaced plywood in almost 70% of the UK timber frame industry (Anderson 1995). Certificates for roofing and flooring have since been achieved. OSB was included in BS5669, the particleboard standard, as part 3, in November 1992 where it is divided into two grades:

F1: Boards use adhesives that are inherently moisture resistant. They recover an acceptable degree of strength after exposure to water and/or high humidity for limited periods, although such exposure may cause non-reversible dimensional changes. They do not necessarily resist prolonged exposure to weather, attack by micro organisms, or persistent damp conditions (BS5669, 1989, part 3 and WPPF Ref PD/17, 1992).

F2: Boards that have enhanced properties in relation to strength, moisture resistance and resistance to fungal attack (BS5669, 1989 and WPPF Ref PD/18, 1992).

3.3.2 Consumption of OSB

In Europe there are two OSB mills at present with a third mill soon to be opened in Ireland. Norbord predict OSB demand in Europe to triple over the next three years, bringing consumption up to 1.4 million cubic metres by the year 2000 (Anderson 1995). Consumption is also growing in North America and Japan.

3.3.3 Manufacture of OSB

Firstly the bark is stripped from the logs, dried and used to provide heat for drying the wafers, heating the press and the offices, and for drying more bark. This uses up 50% of the bark and the remaining 50% is used for making garden mulch and playground bark.

The debarked logs are cut to length and fed into a waferiser that reduces them to strands about 75 mm by 35 mm (the width is about half the length). These are subsequently dried and stored for further processing. A synthetic resin PF or MUF is mixed with the wood strands and a proportion of wax emulsifier. The mix is then subjected to pressure and heat in a multi-opening press to form three layer mats with the required density and thickness. Once cool the boards are trimmed and sanded to suit their end use. Little if any timber is wasted during the entire process.

3.4 Medium Density Fibreboard (MDF)

MDF is one of the fourteen types of fibre building board described in BS 1142, 1989. These can be divided into three broad groups based upon their densities: hardboards (density exceeding 800 kg/m^3), mediumboards (density 350 kg/m^3-800 kg/m^3) and softboards (density less than 350 kg/m^3). MDF was first made in the USA in 1966, although wood fibre building boards were first produced by Sundeala in Middlesex, UK in 1898.

3.4.1 Classification and Use

Two types of MDF are specified in BS 1142, 1989:

MDF: FIDOR and FIRA define MDF as "a sheet material manufactured from fibres of ligno-cellulosic material felted together with the primary bond normally derived from a bonding agent. Other agents may be added during or after the manufacture to modify the particular properties of the material. "Panels are usually smooth on both sides and the surface finish is usually superior to that of chipboard or OSB. (WPPF Ref PD/6, 1994).

MDFMR: Medium Density Fibreboard Moisture Resistant has all the properties of standard MDF with an improved resistance to moisture (WPPF Ref PD/7, 1994).

MDF is used in the furniture industry for cabinet carcasses, drawers, doors, and unit tops, in particular where profiled edges are required. MDFMR is used as a substitute for solid timber, for consistent straight lengths of mouldings such as: skirting boards, window boards, architraves, cornice mouldings, joinery components, stair treads, landings, shop fittings and partition systems. Modified forms of MDFMR with further improved moisture resistance, not covered in the British Standard are used for business signs, shop-fronts and facias, exterior display stands and marine craft interiors. Most manufactures produce a range of MDF types suited for different applications.

3.4.2 Consumption of MDF

New Zealand has by far the greatest consumption of MDF compared to its population at 63 m^3 per 1000 people. MDF is manufactured from radiata pine in New Zealand and from sitka spruce and pine in Ireland and the USA. It is generally accepted that MDF manufactured from softwood gives better quality MDF than if it was manufactured from hardwood. In 1993 the European consumption of MDF was 2.7 million m^3 and 85% of new houses in the UK had their window boards made out of MDF.

3.4.3 Manufacture of MDF

The manufacture is a dry process in which the primary bond is achieved by the added 6-8 dry weight per cent of synthetic resin. Generally this is UF in standard MDF and MUF in the moisture resistant material. The early stages of manufacture are the same as those used in the wet process for manufacturing fibre building boards.

The raw material is produced by chipping forest thinnings, sawmill waste and plywood peeler log cores. These are reduced to fibres by the defibrillator method. Low pressure steam is used to soften the lignin, and to preheat the chips that are fed into an Archimedean screw between segmented grinding disks, one of which rotates. Resin and wax emulsion are added to the fibres, and the mix is dried in a drying tube. The dry fibre is then stored in silos prior to further processing.

Mats are dry-formed on caul plates and gradually compressed by steel belts, then consolidated by batch or continuous pressing. Panels are reduced from about 600 mm down to about 20 mm in thickness. Finally it is cured under heat and pressure, trimmed and sanded. Panels produced range in thickness from 1.6 to 60 mm.

The performances of the boards depend upon the type and amount of adhesive added, the make-up of the mat and the degree of pressing (BRE 1991).

3.5 Strength Properties of Different Panels

The strength of chipboard increases with the increasing average length of chip for a given resin content. Waferboard and OSB are the extreme cases where the chips are approximately 30 mm or more long and waferboard chips are often as wide. Both these board types compete with plywood. The differences in the bonding mechanisms in particleboards, fibreboards and plywoods are of great importance to the strength of the panels. Lignin provides a large portion of the bonding between the fibres in some fibreboards, although this is not the case for MDF where the primary bonding is produced by the added resin. In plywoods there is a continuous layer of the adhesive between the veneers. Particleboards, and in particular chipboard, have a significantly larger surface area of wood than plywood. Since the adhesive is the most expensive component of particleboard the quantity consumed is minimised by spot gluing and the chips are bonded at random contact points instead of by a continuous layer of adhesive. This means that the mechanical properties of chipboard are influenced by the particle properties, the quantity of adhesive used and the particle size.

The degree of orientation of OSB particles varies depending on the producer (BRE 1986). In the plane of the board OSB is weaker than plywood but across the board it is about the same. The difference is reduced when using large sheets because plywood contains knots and defects. OSB has similar strength and slightly higher stiffness than a structural grade chipboard (BRE 1986) but thickness swell is three times greater. Table 3.1 provides a **rough guide** to the relative properties of chipboard, OSB and MDF although it must be remembered that there will be overlaps between good brands of one board type and poorer brands of another board type. This table is a summary of the data presented in the Wood Panel Products Federation folder "The Facts on Board" (1994).

Table 3.1 The relative strengths of chipboard, OSB and MDF.

		Chipboard Grade C4	OSB Grade F2	MDF Grade MR
Thickness of boards (mm)		Up to 25	18-20	13-19
Bending Strength (N/mm^2)		19	28	30
MOE major axis, bending (N/mm^2)		3000	4000	2500
Tensile Strength * (N/mm^2)		0.5	0.5	N/A
Density Range (kg/m^3)		640-720	640-720	600-900
Length Change for a 1% change in MC (mm/m)		0.3	0.3	0.4
% increase in	Length	0.25	0.15	0.4
(RH change from 65 to 85%)	Width	0.25	0.2	0.4
	Thickness	7	10	6

*90° to the plane of the board

3.6 Environment and Moisture

Wood is hygroscopic and can be expected to change dimensions by several percent over a single season (Kyanka 1980). Clad and Schmidt (1981a) showed that the surrounding climate influences the deflection and the moisture content of particleboards. However, Suzuki and Saito (1987) indicated no significant differences in static bending behaviour with temperature between three board types bonded with PF, UMF and UF adhesives. In general the bending strength decreased with increasing temperature as shown in fig. 3.1. The modulus of elasticity (MOE) did not decrease at all with increasing temperature above 40°C for all boards and there were no significant differences between the MOE versus temperature relationships for the different board types. Kajita *et al* (1991) exposed four commercially produced particleboards to various accelerated ageing tests with phenol and phenol (face)/isocyanate (core) bonded boards proving more durable than urea and melamine urea bonded boards.

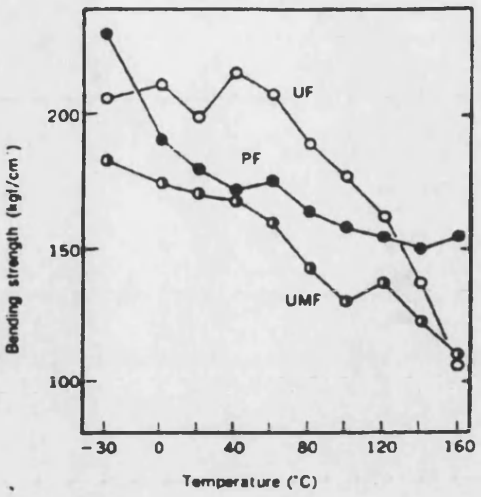

Fig 3.1 Relationships between bending strength and temperature for PF, UMF and UF bonded boards (Suzuki and Saito 1987).

3.7 The Use of Wood Based Panel Products for Flooring

Many materials, mainly wood based, are used for flooring including solid timber, plywoods, chipboards, OSB, MDF and several combinations using panels coated with wood veneers. BS 8201 (1987) is the Code of Practice for flooring of timber, timber products and wood based panel products. Also, the use of wood based panels for flooring is explained in the TRADA information sheet ref: TRADA (1985b) and in the Wood Panel Products Federation folder "The Facts on Board" (1994). The panels are usually supported on joists and figure 3.2 shows the use of tongued and grooved chipboard as an example.

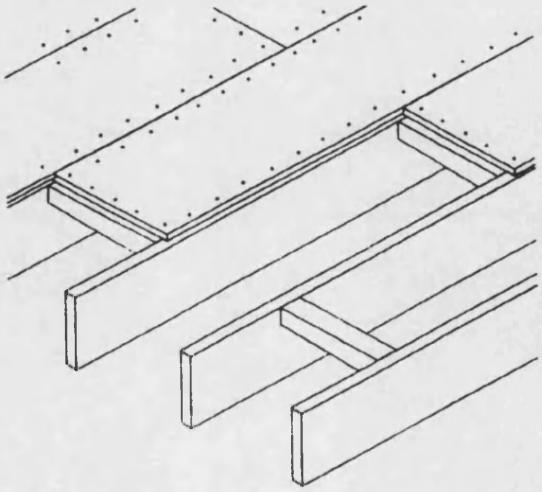

Fig 3.2 Tongued and grooved edge structural decking - this should be laid across the joists with the short edges supported (WPPF Ref AD/15, 1994).

4.0 FATIGUE LITERATURE

In the context of this thesis, fatigue is repeated stress cycling of a component to failure below its short-term static strength (samples are not notched prior to loading). There are several methods of fatigue loading, these include bending (flexure), axial tension/compression, rotating bending and torsion as shown in figure 4.1.

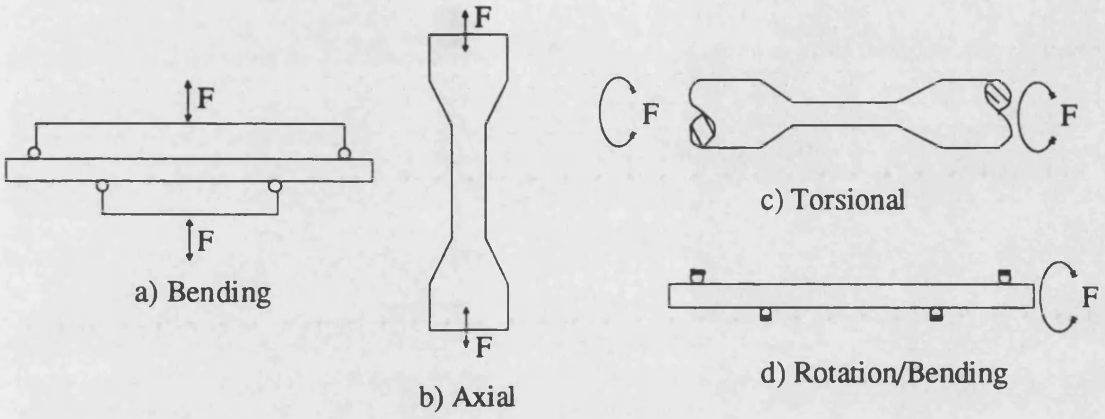

Fig 4.1. Fatigue test configurations (Ansell 1983).

Fatigue results are generally presented in the form of a stress versus life relationship referred to as an S-N diagram. In such a diagram the stress is plotted as a function of the $\log_{(10)}$ cycles to failure using the Wöhler convention as in figure 4.2.

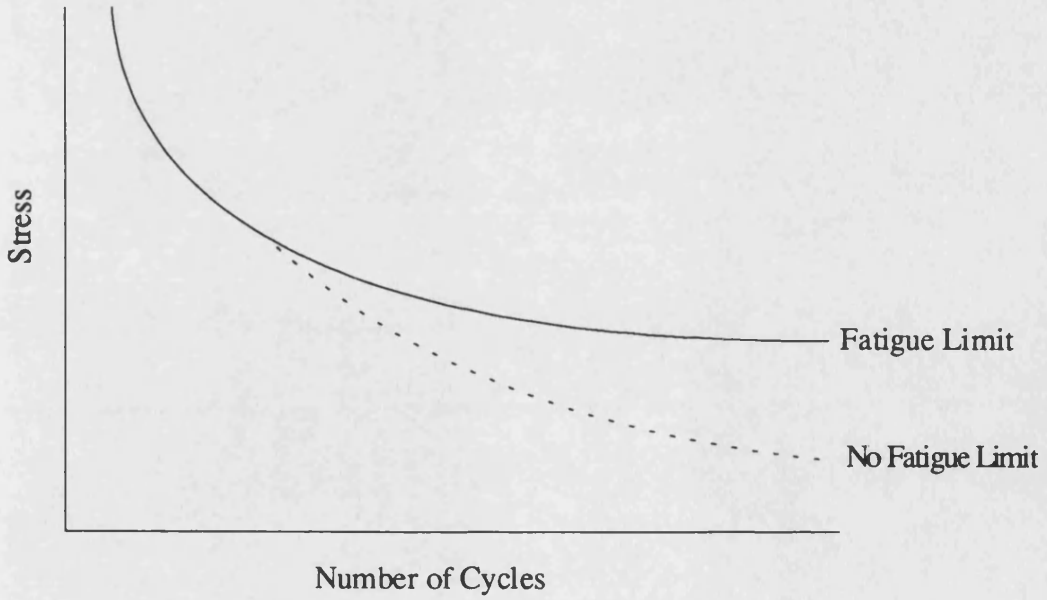

Fig 4.2. Typical stress-life (S-N) curves (Cranne and Charles 1985).

Cyclic loading generally produces failure even at low stresses. There are, however, some materials where the curve of the S-N diagram levels off at a certain known stress level and these are referred to as having a fatigue limit. This is demonstrated in figure 4.2. Below the fatigue limit infinite life can be expected. This was not found for chipboard in the previous work (Hacker 1991 and Thompson 1992) but stress levels below 50% were not tested so this is inconclusive.

Cyclic loading is widely performed with the stress varying sinusoidally as a function of time (constant amplitude testing). However, modern servo-hydraulic testing machines allow complete control of the applied load, making it possible to load with complex wave forms. The following definitions are fundamental to constant amplitude fatigue testing.

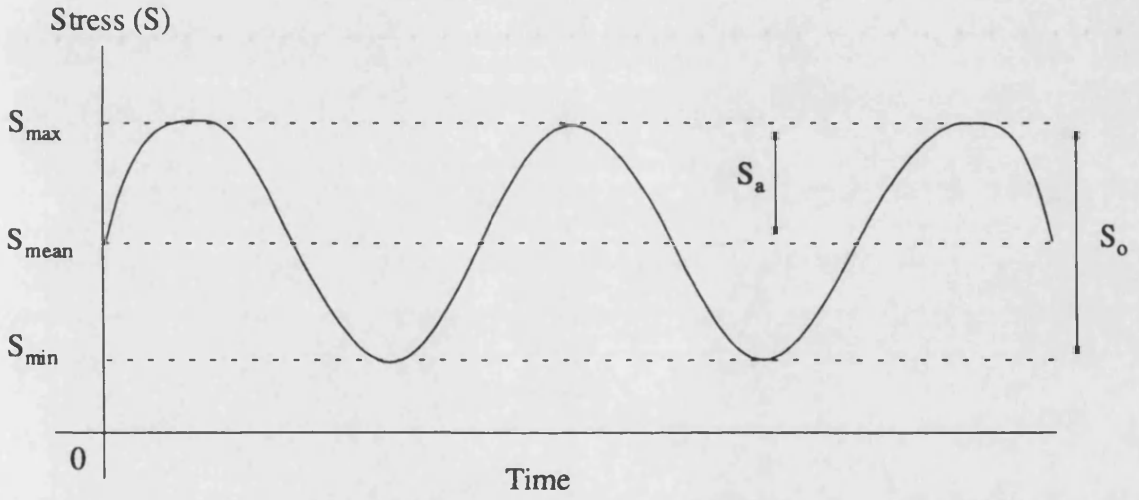

Fig 4.3 Terms relating to constant amplitude fatigue testing (Ansell 1983).

Stress range (S_o) is the difference between the maximum and minimum stress.

$$S_o = S_{max} - S_{min} \qquad (1)$$

Stress amplitude (S_a) is half of the stress range.

$$S_a = 1/2(S_{max} - S_{min}) \qquad (2)$$

Mean stress (S_m) is the stress mid way between the maximum and minimum stress. This is the stress about which the sine wave oscillates.

$$S_m = 1/2(S_{max} + S_{min}) \qquad (3)$$

R ratio (R) is the minimum stress divided by the maximum stress.

$$R = S_{min}/S_{max} \qquad (4)$$

This thesis considers mainly R ratios between zero and one, referred to as partial, non-reversed loading. (The test sample is cyclically stressed in bending with the minimum stress always positive.) The maximum stress level may be set to be a predetermined percentage of the short term bending strength. At R=0.1 the loading has a relatively low mean stress with a large alternating stress. At an R ratio closer to R=1.0 say R=0.75, there is a high mean stress with a small alternating stress. Figure 4.4 shows how altering the R ratio changes the stress wave.

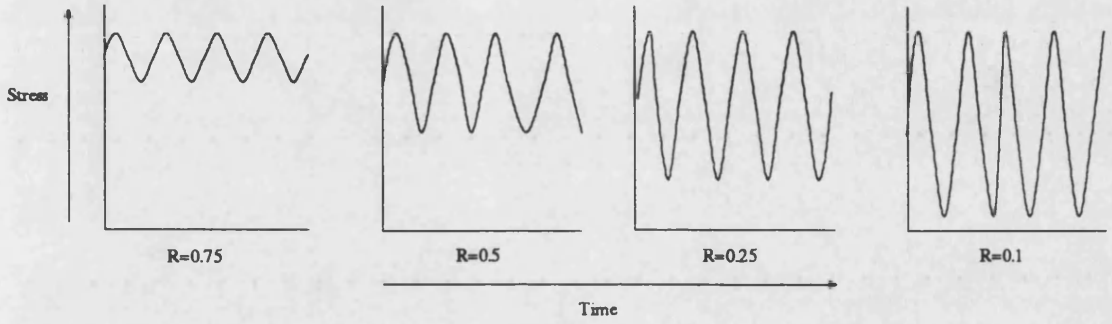

Fig 4.4 Changes in the stress wave for different R ratios in non-reversed loading.

Fatigue results from testing at different R ratios with different stress levels tested at each R ratio can be used to produce a series of S-N lines as in figure 4.5.

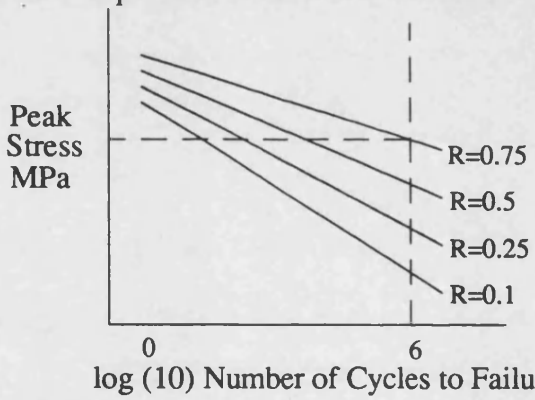

Fig. 4.5. A series of S-N lines.

By plotting a vertical line at a given life the peak stress to give that life can be determined for each R ratio. This information makes it possible to produce a constant life diagram which is a plot of mean stress versus alternating stress. Knowing the peak stress and the R ratio, the minimum stresses can be calculated from equation (4). Both the alternating and the mean stresses can be obtained from equations (2) and (3) respectively. A diagram of this type allows safe combinations of alternating and mean stresses to be predicted as in figure 4.6. Here S_e is the alternating stress at R=-1, and S_u is the ultimate strength, (R=1).

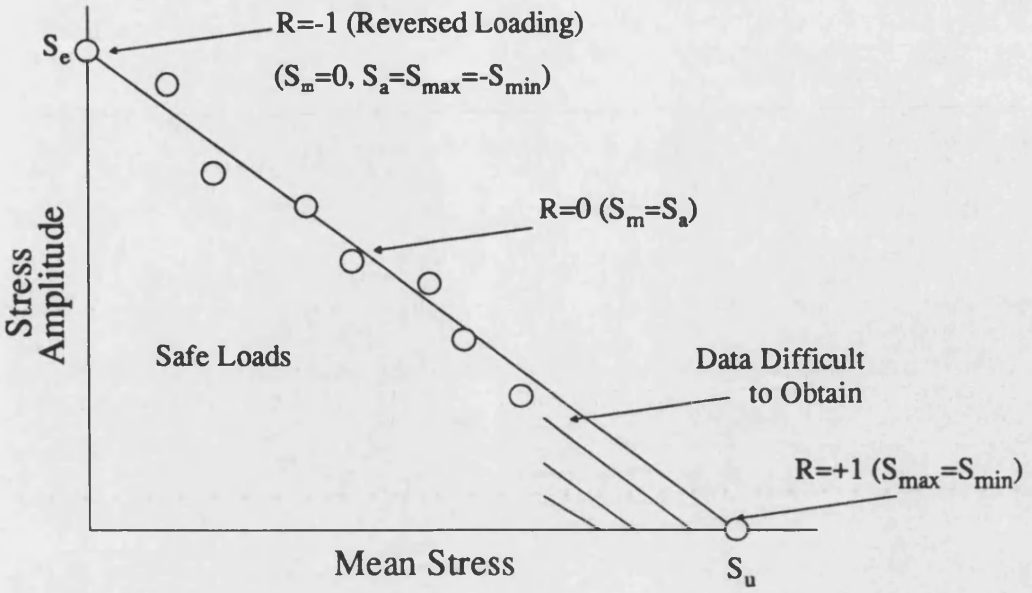

Fig 4.6 Constant life or Goodman line for (N_f) cycles to failure (Ansell 1983).

Two alternative expressions to the Goodman line can be plotted. The Gerber line is slightly less conservative than the Goodman line, producing a curve rather than a straight line. The Soderberg line, primarily plotted for metals with ultimate stress replaced by the yield stress, gives a more conservative prediction than the Goodman line, as in figure 4.7.

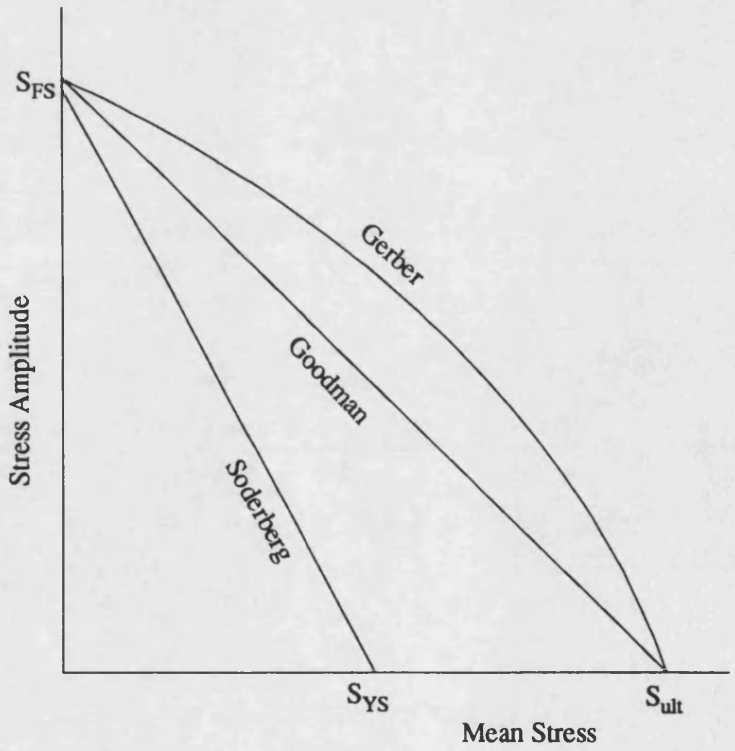

Fig 4.7 Constant life diagram showing predictions of Goodman, Gerber and Soderberg lines (Crane and Charles 1985).

The equations of these lines are as follows:-

The Goodman line: $\Delta S_m = \Delta S_0(1-S_m/S_{ult})$

The Gerber line: $\Delta S_m = \Delta S_0(1-S_m/S_{ult})^2$

The Soderberg line: $\Delta S_m = \Delta S_0(1-S_m/S_{yield})$

where: ΔS_m = mean stress for failure in N_f cycles

ΔS_0 = cyclic stress range for failure in N_f cycles

S_{ult} = ultimate strength (for this thesis the bending strength)

S_{yield} = yield stress (often used for metals)

4.1 Fatigue in Wood and Wood Laminates

The experimental work presented in this thesis examines the fatigue performance of three wood based composite panels and not solid wood so a comprehensive literature review on the fatigue performance of wood will not be attempted. Instead because the materials are all wood based the subject will be introduced and several representative publications will be discussed. The literature in this area has been reviewed comprehensively by Tsai and Ansell (1990), Tsai (1987), Bonfield (1991), Bond (1994) and Hacker (1995).

Wood has been used by man for thousands of years and in the construction of ships for over four hundred years. Despite this extensive history the fatigue of wood was not considered until the 1940s when wood was used in the manufacture of aircraft and research in this area was concentrated during World War II. The lack of research prior to this time is explained by one comment from Dr. Fokker, a noted German aircraft designer. He is quoted as saying "fatigue in properly seasoned wood is unknown" (Lewis 1960). This was prior to failures of Fokker aircraft from 1920 to 1930. These failures are likely to have been fatigue failures but were attributed to other causes. This is understandable because static and fatigue failures in wood have been shown to have the same appearance unlike metals where they can be distinguished (Kyanka 1980).

After Word War II ended research on the fatigue of wood was reduced because metals replaced wood in the manufacture of aircraft. Since then wood research has focused on strength, creep and duration of load because wood is generally used in civil engineering applications where loading is mainly static.

The results from the early research such as that by Kommers (1943) and Freas and Werren (1959) are of only limited use now because the equipment available at the time meant that testing was deflection controlled. Wood is viscoelastic and its deflection will increase with time under constant amplitude loading. Applying a constant deflection means that the applied load will decrease with time as the fatigue cycling continues. This means that the samples tested were unlikely to fail at low loads and the prediction of a fatigue endurance limit at an optimistically high stress was inevitable.

In recent years only limited fatigue research on wood and wood laminates has been reported. A large section of this work resulted from the use of wood laminates for constructing wind turbine blades. Initial testing was performed in four point bending on Khaya ivorensis, Sitka spruce and compressed beech laminates by Tsai and Ansell (1990) and Tsai (1987). They found that increased moisture content reduced both the

static strength and the fatigue life of the laminates. They also demonstrated that fatigue damage in wood laminates is progressive and commences on the face loaded in compression. This work has continued at the University of Bath to the present day. The focus of this work changed after the initial work and axial loading replaced four point bending. The extensive results of the axial testing are reported in PhD theses by Bonfield (1991), Bond (1994) and Hacker (1995). These results will not be reported in this section but some are referred to when the results of hysteresis loop captures are discussed in chapters 8 to 10.

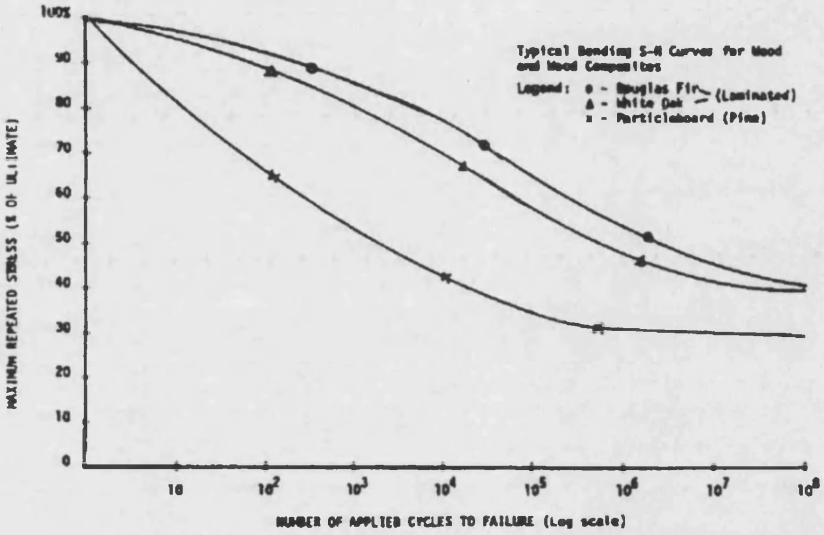

Fig 4.8 The number of applied cycles to failure ($\log_{(10)}$ scale) for wood laminates and particleboard (Kyanka 1980).

Kyanka (1980) compared the fatigue performance of two laminated woods and a particleboard (figure 4.8). It is not clear from this figure how many replicates were tested at each stress level and no justification is given for the fatigue limits that are predicted beyond the last data point for all three materials. For this reason the fatigue limits must be ignored and the main observation is that particleboard has a considerably inferior fatigue performance compared to the laminated woods. This consolidates the need for the fatigue performance of particleboards to be evaluated. Kyanka states that: "Wood and wood based materials do have a definite endurance limit" but no value is predicted for this endurance limit and again no justification is provided.

The fatigue performance of wood and wood composites relative to their static strengths is reported to be superior to that of crystalline materials (Kyanka 1980 and Dinwoodie 1989). This has contributed to fatigue in wood being generally ignored. It was once considered that due to the large stresses and strains endured by a tree during its lifetime that wood was "fatigue conditioned".

Lewis (1962) performed fatigue loading in bending on quarter scale wooden material for railway stringers, used in bridges. The design parameter required for use in service was the fatigue strength for no failures at 2 million cycles. The results indicated this to be 50% of the static strength for straight-grained material and 60% of the static strength, for material with 1:12 slope of grain. He observed that until the actual fatigue failure starts the strength is not impaired and that increasing the stress level reduced the fatigue life. These tests were deflection controlled but the load was checked at intervals to ensure that it was within 5% of the desired level at any time. The loading configuration used was three point loading which has since been generally replaced by four point loading.

Very few workers have reported work performed in load control. Tsai and Ansell (1990) suggest that the fatigue limit for wood loaded in compression under load control was less than 25% of its static strength. This agreed with Kommers (1943), although the testing performed by Kommers was in deflection control. If this fatigue limit is correct then the fatigue limit for particleboards would be at a lower percentage stress than 25% since Kyanka showed that the fatigue performance of particleboard was inferior to that of laminated woods relative to their static strengths. Tsai and Ansell (1990) found that the fatigue performance of wood and laminated wood were not significantly different as did Kommers (1943). In contradiction to this, Maku and Sasaki (1963) found that when loaded in rotation bending the fatigue performance of glue laminated wood was superior to that of wood. When, however, the results were normalised with respect to the relative static strengths both were very similar. Tsai and Ansell (1990) showed that the compressive strength of wood was only about one third of the tensile strength, indicating that failure in bending is likely to be controlled by the zone loaded in compression. When normalised with respect to the static strength the fatigue life was found to be largely independent of the species of wood.

Imayama and Matsumoto (1970) subjected wood to reversed loading in bending at 40 Hz and found that the temperature increased throughout testing with maximum increases of up to 20°C. This implies that adiabatic heating had occurred which would have dried the wood and that the frequencies were far too high for the fatigue testing of wood. When testing at these high frequencies there is not only the internal heating of the wood to consider but also that wood is viscoelastic and will not have sufficient time to respond to the applied loads. Sterr (1963) measured the temperature of laminated wood and solid wood beams in repeated loading at 5.6 Hz. He found that the fatigue resistance of laminated wood was 23% better than that of solid wood. The deflection of the beams he tested increased most towards the end of testing. The mode

of failure for fatigue was different to that for static loading although both types of failure were initiated on the compressive side as found by Tsai and Ansell (1990). This contradicts the findings of Kyanka (1980) where the failure modes were found to be indistinguishable. The mean strengths for laminated wood and solid wood were very similar but the distribution of strengths was narrower for laminated wood which is safer for design and should be acknowledged in national standards. Sterr observed that the temperature increased due to progressive destruction of the test piece and was greater in the zone loaded in compression than in the zone loaded in tension. This confirms that damage initiates in the compressive zone as found by Tsai and Ansell (1990). The temperature increase was lowest in the neutral zone. The greatest temperature rise was in the zone of subsequent failure with localised temperature increases of up to 70°C. Bond (1994) also looked at localised temperature increases close to joints in tension to evaluate the initiation of failure by using thermal imaging.

Fuller and Oberg (1943) subjected several types of compressed wood to repeated loading in rotation bending. These tests were performed at very high frequencies of 60 and 180 Hz. These tests were appropriate because the material was to be used for aircraft propellers. These results are only useful if the wood is to be used for other high velocity applications. They found no difference in the fatigue limit at these two frequencies but it is likely that the tests were above a threshold value for the response of the wood. Also the material tested was compressed wood, so the cellular structure of the wood had been destroyed.

Freas and Werren (1959) found that repeated bending loads of up to 50% of the ultimate strength, for up to 9 million loading cycles could be applied to laminated oak without producing an appreciable change in the bending strength, or the stiffness. Also in all the failures they observed it was the wood that failed and not the glue bond. They made no attempt to continue the fatigue tests to determine the fatigue lives. Ibuki *et al* (1962) showed that glue-laminated wood bonded with UMF resin was superior in fatigue to that bonded with PF. Sekhar *et al* (1963) found that loading wood in repeated torsion was more damaging than repeated bending.

Nakai and Grossman (1983) found that the deflections for clear wood loaded in bending were lower when intermittently loaded than when constantly loaded in creep. The Boltzman principle of superposition was confirmed except at high stresses. No evidence was found to suggest that beams loaded intermittently (seven days loaded, seven days unloaded and two days loaded, twelve days unloaded) had shorter lives compared to constant loading. In more recent work Grossman and Nakai (1987)

examined shorter loading cycles and showed the principle of superposition still to apply below the 50% stress level. It was concluded that when the intervals between loading periods are longer than the duration of the loading periods, then the cumulative effects are negligible.

Salmén *et al* (1985) and Salmén (1987) have used hysteresis loop capture to evaluate the fatigue of wood. The later work examined the effect of frequency of loading on the fatigue performance of wood, but this work was performed at temperatures above 80°C. Salmén concluded that higher temperatures and lower frequencies favour the structural breakdown of wood. This research was aimed at the pulping of wood rather than its structural use and so it is not directly relevant.

The most important feature highlighted by the literature is that particleboards have a worse fatigue performance than wood and laminated wood. This means that it is not acceptable to assume that fatigue damage does not occur in wood based materials as was wrongly assumed for wood for so many years. The available literature on the fatigue of particleboard is reviewed in section 4.2.

4.2 Fatigue in Wood Based Composites Loaded in Bending

Fatigue tests on wood based composites have been performed in bending, axial tension/compression and interlaminar shear. There is, however, only a limited amount of published literature which examines these loading modes because the main use of wood based composites is as panels for building and the loading is mainly static. Hence research has always concentrated on the time dependent properties of panels under static loading (creep). This section concentrates on bending fatigue since this is directly applicable to the use of wood composites in flooring. Most of the literature concerns chipboard because this is the most widely used wood composite and has been produced for longer than panels such as OSB and MDF. Section 4.4 discusses the axial and interlaminar shear fatigue properties of wood composites separately. The main sources of information about the bending fatigue performance of wood based composites are the collaborative work of BRE with Bath University, Japanese research published in "Mokuzai Gakkaishi" and German research published in "Holz als Roh- und Werkstoff". Unfortunately the German research and most of the Japanese research have never been published in English and so only the abstracts and figures are available.

By far the most relevant literature available are publications from the two previous programmes of testing performed at Bath University in collaboration with BRE. Both of these programmes used stress versus strain hysteresis loop capture to evaluate fatigue damage for a structural chipboard. The chipboard tested was grade C5 as explained in section 3.2.1, manufactured in accordance with BS 5669 (1989) and was exposed to a range of fatigue loading regimes. The first programme tested a structural chipboard at R=0.01, at four stress levels, all at 65% RH and results are reported by Ansell and Bonfield (1990), Hacker (1991) and Bonfield *et al* (1993 and 1994a). The second programme tested the same chipboard at R=0.25, R=0.5 and R=0.75, at four stress levels, also all at 65% RH and is reported by Thompson (1992) and Thompson *et al* (1994). The creep of chipboard has been comprehensively researched at BRE and is reviewed in Chapter 5. Recently BRE has investigated the slow cyclic fatigue of chipboard. In the work to date matched samples of chipboard were loaded in four point bending under the following conditions: a 7 hours loaded/17 hours unloaded cycle, a 17 hours loaded /7 hours unloaded cycle and under constant loading. These were carried out at three humidity levels (30, 45 and 90% RH) and three stress levels (30, 45 and 60% of their short term strength), this work is reported by Dinwoodie *et al* (1995a) and Bonfield *et al* (1995).

4.2.1 Fatigue Life in Bending

The most important parameter when evaluating the fatigue performance of a material is the fatigue life, that is the number of loading cycles it will survive. Bonfield *et al* (1994a) generated an S-N curve for structural chipboard tested at R=0.01 using the Wöhler convention (Wöhler 1867). This was later incorporated into a series of S-N curves for chipboard, figure 4.9, by Thompson *et al* (1994).

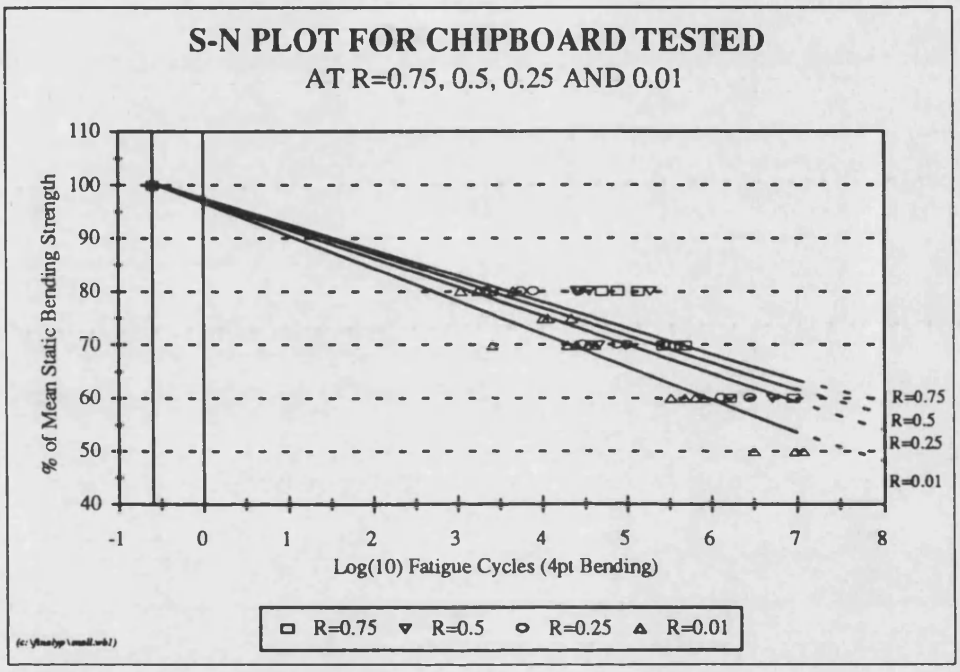

Fig 4.9 S-N plot for chipboard loaded in 4 point bending (Thompson *et al* 1994).

These S-N curves were then used to produce a constant life diagram for chipboard, figure 4.10, showing the combination of alternating and mean stress for a 50% probability of failure at a given fatigue life. Since static strength values were included in the S-N curves, these are also incorporated in the constant life lines. It was found that the fatigue life increased with decreasing stress level for all four R ratios and with increasing R ratio from R=0.75 to R=0.01. Hence the life was reduced by the increase in the stress range rather than by increasing the mean stress. Hacker (1991) found no endurance limit for lives of less than 10^7 cycles and neither did Thompson *et al* (1994) for lives less than $5*10^6$ cycles. This does not prove that chipboard lacks a fatigue limit but if there is a fatigue limit, it occurs lower than the 50% stress level which was the lowest stress level tested. This agrees with the observations of Kyanka (1980), and Tsai and Ansell (1990) which indicated that the fatigue limit for a particleboard would be at a stress level of less than 25%. Also Kollmann and Krech (1961) and Gillwald *et al* (1966) both showed wood based composites to have worse fatigue performances than solid wood.

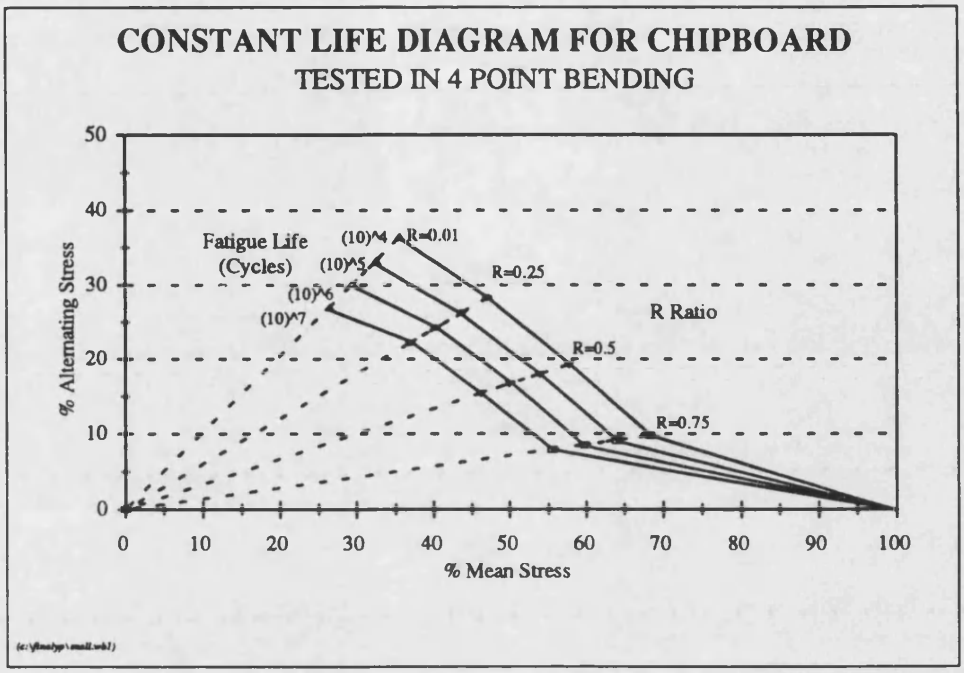

Fig 4.10 Constant life diagram for chipboard loaded in 4 point bending (Thompson *et al* 1994).

Kyanka (1980) reports that some morphological studies of fracture surfaces have shown that the fracture process may combine individual glue and wood failure and that it may also depend upon processing variables such as pressing time, temperature and chip geometry.

4.2.2 Residual Strength

Bonfield *et al* (1994a) and Thompson *et al* (1994) both reported results for the residual strength of only two runout samples each, while it is possible that there was a slight decrease in strength as a result of fatigue loading the results were far from conclusive. Rotem (1988) developed and tested a model to predict the residual strength of a multi-directional laminated composite material subjected to tensile fatigue and predicted with a good correlation that the residual strength only begins to degrade within the final 10% of the fatigue life. Fatigue failure in chipboard will be the combined result of many complex fracture paths, as is the case for the composite material tested by Rotem. In metals the propagation of a lone crack is the usual cause of a fatigue failure. Sekino and Okuma (1985) found the fatigue strength of samples after 10^7 cycles to be 38-44% of the static strength. It does, however, appear from the S-N diagrams presented by Sekino that the chipboards tested were lower grade materials than those tested by Thompson and Hacker.

4.2.3 Damage Mechanism and the Principle of Superposition

Bonfield *et al* (1994a) observed that the fracture path travelled in the vicinity of the wood chip-resin interface in preference to through the wood chips and that the fatigue samples always failed before their side-matched creep partners. Superposition of the strain data for samples loaded in fatigue and creep was attempted but was unsuccessful indicating that the mechanisms of deformation are different. Thompson *et al* (1994) observed the same general fracture paths, but at the higher R ratios the creep samples sometimes failed first. Dinwoodie *et al* (1995) also found that the principle of superposition did not apply for chipboard samples loaded intermittently and loaded in creep. This implies that recovery occurs whilst the samples are unloaded and that the two deformation mechanisms are different and contradicts the findings of Nakai and Grossman (1983) for clear wood in bending.

4.2.4 Effect of Environmental Conditions

Dinwoodie *et al* (1995) and Bonfield *et al* (1995) both showed that increasing the RH from 30 to 65% has only a small effect on the relative creep rate for chipboard subjected to slow cyclic fatigue. When, however, the RH was increased from 65 to 90% there was a marked increase in the relative creep rate. The effect of environmental conditions on the creep of wood based composites has been more extensively researched than the effect on the fatigue properties and is discussed in Chapter 5.

4.2.5 Effect of Resin Content and Type

The resin content contributes to the mechanical properties of a particleboard due to the influence this has upon the number of bonding points per unit volume. Similarly the resin type will be a factor in determining the strength of the inter-chip bonds. Tanaka and Suzuki (1984) examined the effect of resin content (between 4% and 11.5%) on the bending fatigue of four different flakeboards (two random, one oriented and one shavingsboard) at 1 Hz. They observed that at stress levels between 65 and 95% of static bending strength the number of cycles to failure increased markedly as the resin content of the particleboard was increased. There was also an increase in the fatigue strength with increasing strength of the adhesive bond. This agreed with the earlier findings of Clad and Schmidt (1981b) who found that particleboards with a high resin content displayed comparatively superior behaviour in both fatigue and strength properties. Sekino and Okuma (1985) performed similar experiments on four types of commercial particleboard with different resin types: isocyanate (IS), phenol formaldehyde (PF), urea formaldehyde (UF) and melamine-urea formaldehyde (MUF). These fatigue tests were performed at frequencies of 1.0-2.0 Hz, at various stress

levels between 60% and 90% of the static bending strength. Unlike the other researchers they observed no significant difference between the results for the different resin types. Sekino also showed the maximum deflection to increase gradually until a critical deflection was reached followed by rapid failure and the critical deflection for the same type of board was constant for different cyclic stress levels. Only small reductions in MOR and MOE of a few percent were observed prior to failure.

4.2.6 Cyclic Creep

Cyclic creep can be defined as the maximum deflection during cyclic loading and is the development of deformation in the material under cyclic loading. Tanaka and Suzuki (1984) found the cyclic creep rate to increase gradually at first and then increase rapidly before failure. Failure eventually occurred when the maximum deflection equalled the critical deflection for the particleboard. At high cyclic stress levels burst type acoustic emissions were not present in the initial stages of tests but appeared frequently during fatigue cycling in the latter stages of testing. These were attributed to the microfracture of local points of weakness in the particleboard. Park and Mataki (1990a) observed that the cyclic relaxation (i.e. the relaxation within each loading cycle) of three layer particleboard was linear before the critical deflection was reached. This is thought to be due to the gradual growth of cracking elements between wood chips. They also found that the fatigue life was reduced as the rate of cyclic relaxation was reduced. Dinwoodie *et al* (1995) found that on an elapsed time basis the samples loaded for the shortest time showed less creep deformation for the range of stress levels and humidities tested. The cyclic creep rate for samples increased linearly with increasing stress level.

4.3 Stress Versus Strain Hysteresis Loop Capture

The quantification of damage is difficult to achieve by either non-destructive or non-interuptive processes. The capture of stress versus strain hysteresis loops during fatigue testing, however, is a method that enables quantitative measurements of damage accumulation to be continuously made without the need to stop the test. Analysis of the hysteresis loops allows changes in the dynamic moduli, energy dissipated per cycle and the underlying creep effects following fatigue loading, to be determined (Bonfield *et al* 1993).

The use of stress versus strain hysteresis loop capture and the parameters derived from the loops are explained in depth as part of the experimental detail in section 6.3. The concept of loop capture will, however, be introduced briefly here to make it possible to understand this section of the fatigue literature.

4.3.1 The Concept of Hysteresis Loop Capture

When a load is applied to any material that does not respond in a perfectly elastic manner there is a lag between the applied load/stress and the strain produced in the material. This is shown in figure 4.11.

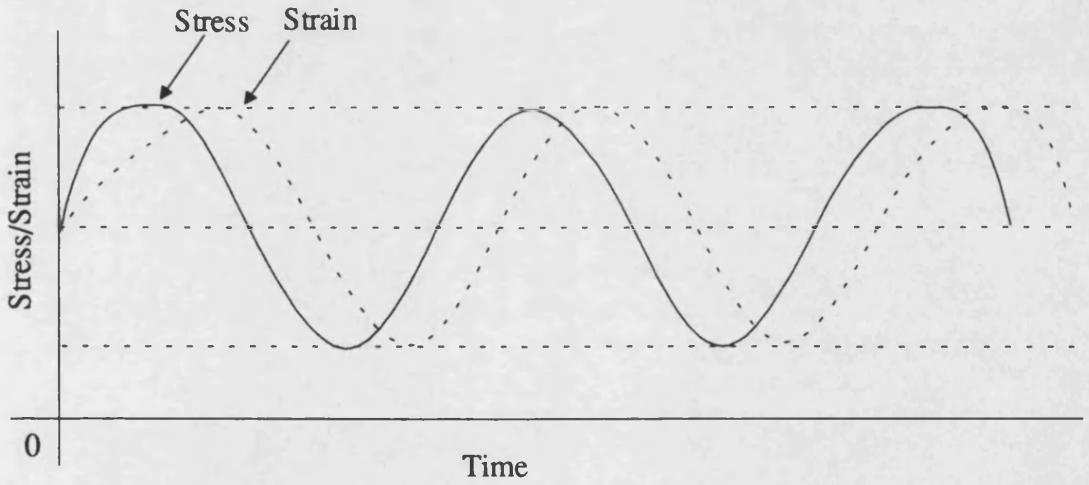

Fig 4.11 The lag between the applied stress and the resulting strain that produces hysteresis.

Wood and wood based composites are viscoelastic, so there is a lag between the applied stress and the resulting strain producing hysteresis. The lag is caused by internal friction and the breaking of bonds, representing a dissipation of energy in the sample.

4.3.2 Loop Capture for Wood and Wood Composites

Hysteresis loop capture has been used to evaluate fatigue damage occurring in chipboard when loaded in bending and is reported by Hacker (1991), Bonfield *et al* (1994a) and Thompson *et al* (1994). It has also been used for the axial fatigue loading of wood laminates to predict fatigue damage when they are used in wind turbine blades. This work will be referred to in chapters 8 to 10.

Another area of research where hysteresis loop capture has been used is modelling the effect of earthquake loading on timber joints and buildings. This work is of limited relevance because it evaluates the damping of vibrations and damage to metal connectors, not damage accumulation in the wooden material. A recent and comprehensive review of this field is provided by Foliente (1994).

4.3.3 Creep and Fatigue Strain Curves for Chipboard

Hacker (1991) and Bonfield *et al* (1993) found that for samples loaded in creep there was an initial rapid build up of strain, followed by continuous deflection at an ever decreasing rate until close to failure when the deflection increased rapidly leading to failure. The fatigue samples also experienced three stages of deformation to failure. The first stage was rapid as in creep, followed by a second stage, frequently close to linear and a third rapid stage leading to failure. The third stage was not always captured because hysteresis loops were captured at predetermined time intervals and this third stage was rapid, normally occurring in between loop captures. Creep strain was nearly always greater than the maximum fatigue strain. However, the fatigue samples always failed before the side-matched creep samples and the creep and fatigue strain curves were similar at all stress levels. Thompson *et al* (1992 and 1994) found the deflection to increase as the R ratio was increased from 0.01 to 0.75. This was due to the increased mean stress and the reduction in recovery time resulting from increasing the R ratio. In all cases the higher the percentage stress level the greater the microstrain produced. Figure 4.12 shows an example of creep and fatigue microstrain curves for a side-matched pair of chipboard samples (Thompson *et al* 1994).

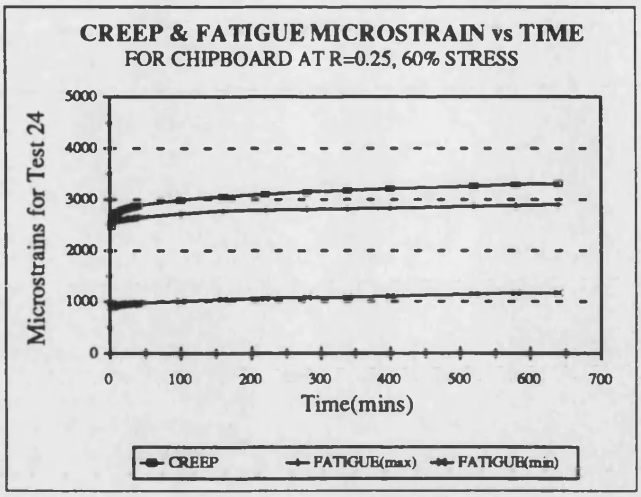

Fig 4.12 Creep and fatigue microstrains for chipboard loaded at R=0.25, at 60% stress (Thompson *et al* 1994).

4.3.4 Dynamic Moduli For Chipboard

Initial values of dynamic moduli found by Bonfield *et al* (1994a) were between 4.7 GPa and 5.6 GPa and appeared to be independent of stress level. Initially at the 50 and 60% stress levels the dynamic moduli increased slightly before levelling out, then eventually decreased gradually. At 70 and 80% stress levels there was a gradual decrease in dynamic modulus throughout testing. Thompson *et al* (1994) also found stress level to have little effect upon the dynamic modulus for each of the three R ratios tested, although values were marginally higher at lower stress levels. Figure 4.13 is an example showing the change in dynamic moduli with time for two chipboard samples tested at R=0.25 at 60% stress.

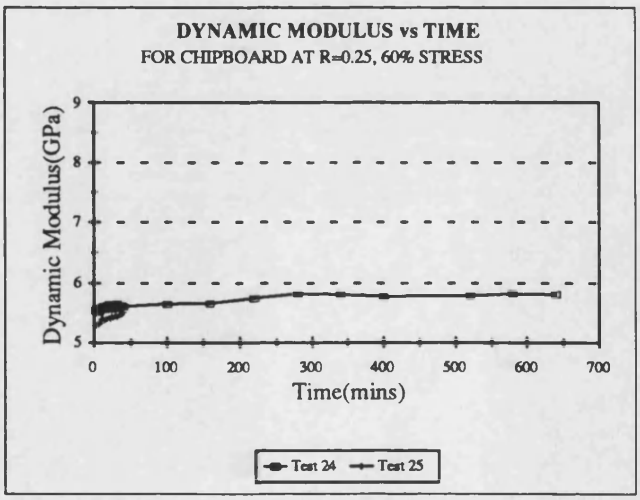

Fig 4.13 Dynamic moduli for chipboard (Thompson *et al* 1994).

In these tests the dynamic moduli increased slightly during the tests and in some cases fell away towards the end. The dynamic moduli increased with increasing R ratio (increasing the R ratio increases the mean stress and decreases the stress amplitude). This is different to the results of Bonfield *et al* (1993) for laminated wood fatigued axially at R=-1, where the dynamic modulus decreased in a three stage process. The structures of wood laminates and particleboards are however very different.

4.3.5 Hysteresis Loop Areas

Hacker (1991) found that the initial hysteresis loop areas for chipboard were greater at higher stress levels and changed from around 1.5 kJ/m^3 at 50% stress, to around 5.0 kJ/m^3 at the 80% stress level. The rate of increase of loop area throughout tests was higher at higher stress levels. Final hysteresis loop areas also increased with increasing stress level. The increase in loop area was almost linear between 60 and 80% of life, after which the loop area increased more rapidly (Bonfield *et al* 1993). In general testing at R=0.01 revealed a tendency for an increase in loop area and a decrease in dynamic modulus with an increase in loading cycles, implying that damage accumulates during fatigue tests resulting in a less stiff, more flawed structure (Bonfield *et al* 1994a). The hysteresis loops captured for chipboard were more open than those captured for laminated wood, indicating that more energy was dissipated per cycle, i.e. more damage was occurring. The loop area for laminated wood increased rapidly close to failure, (Bonfield *et al* 1993). Thompson *et al* (1994) found that the last hysteresis loop captured was at a greater microstrain than the first loop captured, i.e. further along the X axis due to an increase in the underlying creep strain, for every test, at all three R-ratios. Figure 4.14 illustrates how the hysteresis loop area increased with time for two samples tested at R=0.25 at the 60% stress level.

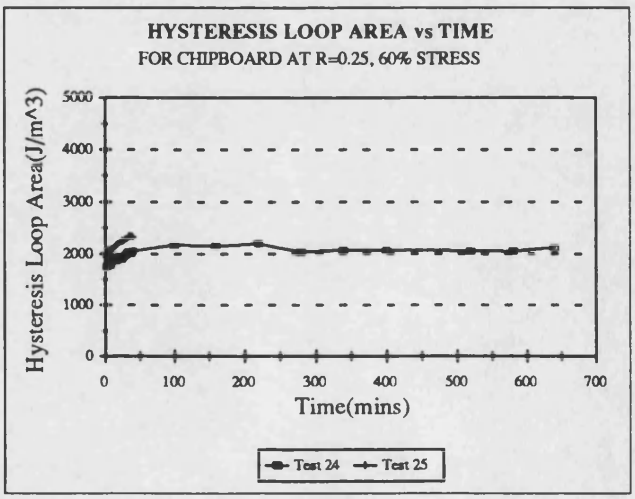

Fig 4.14 Hysteresis loop areas for chipboard (Thompson *et al* 1994).

The loop areas captured for different samples at the same stress levels for each of the R ratios were similar. The loop area increased with increasing stress level for all R ratios showing that the greater the stress level the greater the damage produced within the sample per loading cycle. The R ratio had a profound effect on the loop area with the loop areas at R=0.01 more than ten times greater than those at R=0.75. This demonstrates that it was the magnitude of the alternating stress component that caused most of the damage in the samples but it was the level of the mean stress that influenced the deflections.

4.4 Axial Fatigue in Wood Based Composites

The axial fatigue of particleboard is reviewed here for two reasons:

1) To gain an insight into whether damage in panel products subjected to bending fatigue loading would be expected to be predominantly on the tensile or the compressive side of the specimen, or distributed evenly on both sides.

2) To compare the fatigue results from axial fatigue with those from bending fatigue.

The majority of the literature on the axial fatigue of wood composites is from Japan and again not all of the papers are available in English. Consequently references to these papers are based on abstracts and figures only. As mentioned previously literature on the axial fatigue testing of wood laminates will not be reviewed here. No literature could be found about the relative fatigue performances of wood based composites loaded in tension and compression. However, it is reported that grade C5 structural chipboard is 40% weaker in tension than in compression (WPPF Ref PD/16, 1992). This is an important finding because wood laminates are stronger in tension. When chipboard is fatigue loaded in bending it is probable that the fatigue failure will initiate on the side loaded in tension. For this reason the tests reported in section 8.8 were performed for clarification.

4.4.1 Fatigue Life, Residual Strength and Environmental Effects

Suzuki and Saito (1984) performed tensile fatigue tests on three particleboards loaded perpendicular to the surface of the board at 10 Hz. This testing was used to evaluate the durability of the boards rather than their in-service fatigue performance. The fatigue strengths after being subjected to 10^7 loading cycles were at 45 to 52% of the UTS depending upon the resin type. It was concluded that there was no reduction in the internal bond strength or residual strength until immediately prior to fatigue failure. No attempt was made to define a fatigue limit.

McNatt and Werren (1975) evaluated the fatigue life of three particleboards loaded in tension parallel to the surface of the board for 10^6 cycles at R=0.1, at 15 Hz. None of the samples survived 10^6 cycles at stress levels as low as 45% of the static tensile strength. This implies that the particleboards were of a lower grade than those tested by Hacker (1991) and Thompson *et al* (1994) but this is deceptive. When particleboards are loaded in bending, the highest stresses are produced in the surfaces of the boards where the wood chips are smaller and the resin content is higher. When testing in tension parallel to the board's surface, the low grade core material is also

stressed. The worst scenario is tensile loading perpendicular to the surface of the board because the core material will take all of the applied stress.

Suzuki and Saito (1988) loaded two particleboards and one MDF in axial tension parallel to the surface of the board. This was similar to McNatt's tests but at 15 Hz. The effect of ageing the boards and applying repeated stresses was combined. Again the fatigue strength at 10^7 cycles was found to be 45% of the original strength. These results are almost identical to the bending fatigue results reported by Sekino and Okuma (1985). Suzuki and Saito (1988) also found a linear relationship between repetitive stress parallel to the surface of the board and $\log_{10}$ of the number of cycles to failure for different levels of exposure to increased temperature and/or humidity. Kato *et al* (1990) found that the number of cycles to failure was sensitively affected by the maximum stress and the stress amplitude in agreement with the results of Thompson (1994) for changing R ratio. Kato *et al* (1990) also found that the fatigue life could be predicted from the slope of the second stage in a cyclic creep curve.

Particleboards subjected to ageing treatments characteristically absorb moisture and as a result their mechanical properties are degraded. Ageing treatments in this context may be any of the following: 1) submersion in water, 2) conditioning at increased humidity and/or temperature, or 3) drying in an oven. Suzuki and Saito (1988) looked at the effects of ageing treatments on the tensile properties of particleboards. They found that the thickness of particleboard specimens increased with increasing cycles of ageing. Specimens continually subjected to the same treatment conditions will generally swell rapidly at first but swelling will level off with further ageing cycles. UF bonded particleboards generally swell to a greater extent than other particleboards.

Suzuki and Saito (1986) found that the internal bond strength of UF and PF bonded particleboards to decrease with increased moisture content. The decrease was more pronounced for UF than PF bonded boards. The fatigue life was reduced by increasing the moisture content. A linear relationship was observed between the periodically applied maximum stress and $\log_{10}$ of the number of cycles to failure. This relationship can be used to estimate the static internal bond strength at a specific moisture content. The static internal bond strength can then be used in turn to predict the fatigue strength of particleboard at the moisture content specified. The main reason for the decrease in internal bond strength as the moisture content increased was considered to be due to the swelling stresses induced by the uptake of moisture, causing a deterioration in the mechanical strength of the resin binder. It was shown by Suzuki and Saito (1984) that a large thickness swelling resulted in a low estimated fatigue strength. Suzuki and

Saito (1986) suggested that a high initial swelling indicated a poor fatigue performance but this was not a firm conclusion. The initial strength loss was considered to be one of the most important factors affecting the fatigue strength when the MC was increased.

4.4.2 Effects of Resin Type

Suzuki and Saito (1984) found that after being subjected to an ageing treatment the estimated fatigue strength of PF bonded board was higher than that of UF and UMF bonded boards. It was demonstrated that the resistance of PF bonded boards to repeated stress was slightly better than that of UF or UMF bonded boards, despite PF bonded boards having the lowest average internal bond strength. The regression lines fitted to the fatigue data for each of the particleboards intersected the Y axis at less than 100% stress.

4.4.3 Cyclic Creep

Suzuki and Saito (1988) concluded that cyclic creep behaviour in tension can be divided into two main stages. Kato *et al* (1990), however, reported later that there were four stages of cyclic creep for particleboard, as shown in figure 4.15 where the maximum stress level was 61% with a stress amplitude 24%. The maximum strains at the transient points from the first to the second and from the second to the third stage, decreased with increasing stress amplitudes within the same stress level. Also, the time required for the first stage in the creep curve was almost equal to that from the third to the fourth stages and was 1/15 - 1/10 of that of the second stage under any loading conditions. The creep test was considered to be a special case of partial non-reversed loading in fatigue where the stress amplitude was zero (R=1).

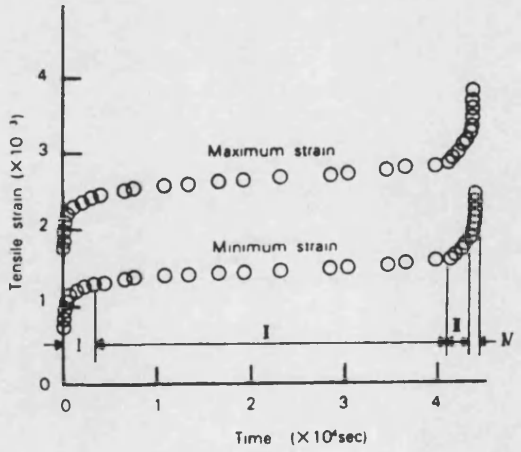

Fig 4.15 Example of cyclic creep behaviour in a partial non-reversed fatigue test (Kato *et al* 1990).

5.0 CREEP IN WOOD BASED PANELS

Solid timber and wood based panels are viscoelastic materials, so when they are subjected to constant load the deflection will increase with time. This phenomenon is referred to as creep. In this chapter, attention is focused on work at the UK's Building Research Establishment (BRE) by Dinwoodie, Bonfield, Mundy (previously Higgins), Paxton, Robson and Pierce. At BRE an extensive programme of work on quantifying and predicting the creep behaviour of wood based panels has been undertaken for over twenty years. The research is especially relevant to this thesis because the test methodology and loading configuration used are the same as for the work reported here.

A literature review on creep in solid wood will not be attempted here. Dinwoodie and Bonfield (1995), stress the need for further European research into the creep in wood based panels due to their increasing use in structural applications. In this chapter the creep performances of different panel boards and timber are compared. A good introduction to this subject is provided by Andriamitantsoa (1995) while a comprehensive literature review of European research in this area by Dinwoodie and Bonfield (1995) provides a list of references.

Creep testing is generally performed in bending rather than axial tension or compression for wood and wood based panels. The primary reason for this is that in everyday applications these materials are almost always exposed to loads in bending. Very little effort has been made to evaluate the effect of the mode of loading on creep properties. In one study Kliger (1991) found relative creep in four point bending to be greater than or about the same as for shear loading.

5.1 Introduction to Creep Testing at BRE

Approximately 95% of all creep tests at BRE have been performed in four point bending, in preference to three point bending, to minimise the shear forces within the samples. In previous studies the same load was applied to all samples while comparing the creep behaviour of markedly different board materials. This resulted in widely different materials being stressed at different percentages of their short-term ultimate strength. At BRE the loads applied to samples have been applied as percentages of the short-term ultimate strength, estimated by testing to failure an adjacent sample, or samples from the same board. In addition to this, creep deflections have been expressed as relative creep values where:

$$\text{Relative Creep} = \frac{\text{Total Deflection - Initial Elastic Deflection}}{\text{Initial Elastic Deflection}}$$

This allows more meaningful comparisons to be made between boards with markedly different strengths. Caution must be used in comparing relative creep values because other workers have used different definitions.

5.2 Steady-State Environmental Conditions

Dinwoodie *et al* (1990b, 1991a, 1991b and 1995), and Dinwoodie and Bonfield (1995) found that for a range of different board types, loaded under steady-state environmental conditions the creep deflections were dependent upon three primary variables:

A) temperature
B) relative humidity and
C) stress level.

In general, an increase in any of these three variables results in an increased creep deflection. The other main factors affecting the creep of wood based panels are the resin type, the resin content and the type of board, loosely described by the wood particle size.

5.2.1 Temperature

It is generally agreed that an increase in temperature produces a small increase in creep rate. Over a narrow range of temperatures (10 to 30°C) this was shown for a range of boards by Dinwoodie *et al* (1990b, 1991b and 1995), and by Dinwoodie and Bonfield (1995). Andriamitantsoa (1995) considered the effect of temperature to be negligible on creep in timber below 50°C. However, Kingston and Budgen (1972) showed that the creep of wood (hoop pine) loaded in compression increased by a factor of about 2.5 when the temperature was increased from 20°C to 50°C. Also Dinwoodie *et al* (1991b), and Dinwoodie and Bonfield (1995) demonstrated that deflection increases to a greater extent at higher temperatures, with solid wood affected to a greater extent than board materials.

5.2.2 Relative Humidity

Increased relative humidity has a far greater effect on the creep deflections of wood based boards and timber than increased temperature. There is agreement in the literature that increasing the steady-state relative humidity and moisture content result in increasing creep deflections and reduced time to failure (Dinwoodie *et al* 1981, 1984, 1991b, 1992a and Kliger 1991). It is also reported by Dinwoodie *et al*

that the increase in deflection is greatest above 70% RH and there is a very marked increase in creep deflection between 60% and 95% RH, which is clearly demonstrated in figure 5.1. This is supported by Kliger (1991) who demonstrated that the relative creep of particleboards after six months at 94% RH was double that at 65% RH.

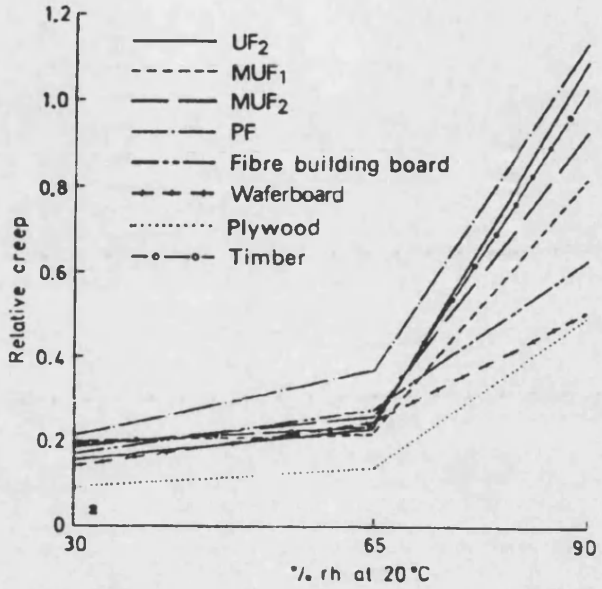

Fig 5.1 Relative creep variation for a loading time of 990 minutes, at different relative humidities, at 20°C (Dinwoodie *et al* 1990b).

5.2.3 Stress Level

A linear increase in relative creep with increasing stress level between 30 and 75% of the ultimate stress was found for chipboard, OSB and plywood by Dinwoodie *et al* (1991a, b and c), and Dinwoodie and Bonfield (1995). Wood on the other hand displayed non-linearity at stress levels above 45 to 50%.

5.2.4 Effect of Resin Type, Resin Content and Board Type

The effects of resin type and content are still an area of controversy. In general, however, the propensity to creep for different resin types increases in the following order: melamine-urea formaldehyde; urea formaldehyde; phenol formaldehyde; isocyanate and high alkaline cured phenol formaldehyde, due to its high equilibrium moisture content (Dinwoodie and Bonfield 1995). Pierce *et al* (1986) demonstrated that there is disagreement as to whether resin type has an effect on the creep behaviour of particleboard. However, Kliger (1991) showed consistently higher relative creep for UF bonded chipboard than for MUF bonded at two different environmental conditions i.e. 20°C/65% RH and 20°C/94%.

There is no proof that increasing the resin content in boards reduces the propensity to creep but it does increase the elastic modulus which may in turn reduce creep.

Examining creep in different board types Andriamitantsoa (1995) found that creep was highest in particleboard, then plywood and then solid wood. Dinwoodie *et al* (1991a), and Dinwoodie and Bonfield (1995) compared several board types over a range of stress levels and found that plywood and waferboard had consistently low values of relative creep. In the same tests high alkaline cured PF bonded chipboard and non-British Standard chipboard showed consistently high values of relative creep. Hall and Haygreen (1978) loaded boards in creep over two years and found the total creep to increase with board type as follows: 1) oriented particleboard, 2) waferboard, 3) plywood and 4) shavings particleboard. Schober (1987) found the absolute creep deformation to increase with decreasing particle size for MDF, particleboard and solid timber, although particle board showed greater creep deflection than MDF at above 70% humidity. McNatt and Hunt (1982) found that hardwood flakeboards deflected to a greater extent than the equivalent plywood. All these results agree with the general rule for wood based panel products presented by Bonfield *et al* (1994b), and Dinwoodie and Bonfield (1995) that as the particle size increases the resistance to creep is improved. This is a generalisation as there are overlaps between board types (Dinwoodie and Bonfield 1995). Creep in wood was only greater than that in particleboard at high temperatures (Dinwoodie *et al* 1984).

5.2.5 Creep Modulus

The creep modulus is defined as "the ratio of applied stress to the creep strain, at any time after the initial loading". Under all conditions the creep modulus of MUF bonded chipboard decreased with increasing $\log_{(10)}$ time and this decreased with increasing stress level (Dinwoodie *et al* 1991b).

5.3 Unsteady-State Environmental Conditions

At BRE a range of particleboards were tested under protected external conditions. Relative creep under these conditions was slightly less than at 20°C and 90% RH as demonstrated in figure 5.2 (Dinwoodie *et al* 1990b). A comprehensive review of work in this area is provided by Dinwoodie *et al* (1992a). It is generally considered that a protected external condition is the worst possible "internal" condition to which boards can be exposed, with the exception of swimming pools (Dinwoodie 1992a).

McNatt and Hunt (1982) performed 90 day duration creep tests on hardwood flakeboards and plywood to simulate snow loading on roof decking. They determined

the creep deflections under 65% constant humidity to be 44 to 69% of the initial deflection. Under cyclic humidity this increased to 145 to 276% of the initial deflection. Armstrong and Grossman (1972) concluded that deflections in particleboard during moisture cycling were mainly due to desorption. Similar behaviour was observed for particleboard, hardboard and wood although the effects were greatest for particleboard and hardboard.

Under protected external conditions Dinwoodie *et al* (1992a) found relative creep to be low for waferboard, high for PF bonded particleboard and high for fibre building board. Solid timber displayed a pronounced mechanosorptive behaviour (cyclic behaviour in relative creep due to changing humidity). Waferboard was the only board material to display this mechanosorptive behaviour but to a lesser extent than for timber.

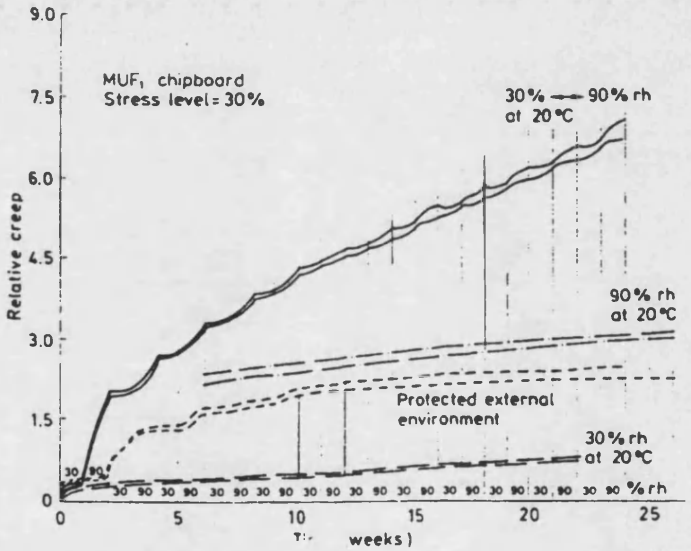

Fig 5.2 Variation in relative creep for samples of one MUF particleboard, subjected to constant, variable and cyclic relative humidity (Dinwoodie *et al* 1990b).

The same pattern was repeated for cyclic changes in temperature, enhancing the evidence of strong interactions between board types and environmental conditions. There remains controversy as to whether or not board materials are mechanosorptive but it was apparent that cyclic annual changes in temperature had little or no effect on the magnitude of creep deflections (Dinwoodie 1992b).

5.4 Predicting Creep

There is a definite need to be able to predict the creep behaviour of particleboards. There are two methods by which this can be approached:

1) Mathematical modelling - this has been very successful in describing actual deflections and predicting future deflections (Gressel 1984). Power law equations are particularly appropriate but there is no theoretical justification for this approach.

2) Rheological models - this was the method chosen by BRE and the models are derived from first principles. Rheological models have also been applied to describe creep in wood by Urakami and Fukuyama (1982). Rheological models provide the best description of the viscoelastic behaviour of wood and wood based materials (Dinwoodie *et al* 1990b). The argument is that the elastic springs of the model are analogous to the crystalline cellulosic core of the microfibril and the time-dependent dashpots symbolize the viscoelastic and viscous behaviour of the matrix materials: lignin, hemicellulose and non-crystalline cellulose. Hence this method is expanded upon in the following text.

Four, spring and dashpot rheological models are proposed from the work at BRE (Pierce *et al* 1985, Robson 1988 and Dinwoodie *et al* 1990a, b, 1991b). In the models Y is the deflection at time t, β_1 is the elastic deformation, $\beta_2[1-\exp(-\beta_3 t)]$ is viscoelastic deformation and $\beta_4 t$ is the viscous deformation.

5.4.1 The 3-Element Model

$$Y=\beta_1+\beta_2[1-\exp(-\beta_3 t)]$$

The 3-element model (Pierce *et al* 1985) is capable of accurately describing creep deflection for short periods of time but is of little use in the prediction of long term creep from short term data, since it incorrectly assumes that no further creep occurs beyond the last data point. The further forward the prediction, the greater the underestimate. The model assumes that there is no viscous behaviour, which is certainly not the case in reality.

5.4.2 The 4-Element Model

$$Y=\beta_1+\beta_2[1-\exp(-\beta_3 t)]+\beta_4 t$$

This model (Pierce *et al* 1985) always predicts deflection values that are too high since it assumes that the viscous behaviour is linear with time after the last data point, rather than the decreasing rate that occurs in practice.

5.4.3 The 5-Parameter 4-Element Model

$$Y=\beta_1+\beta_2[1-\exp(-\beta_3 t)]+\beta_4 t^{\beta_5}$$

This model (Pierce *et al* 1985) contains a non-linear viscous component where $0<\beta_5<1$ and the viscous component has a gradually reducing flow rate, rather than a constant flow rate β_4 as in the 4-element model. Thus the 5-parameter model is superior to the 4-element model for long-term prediction of creep deflections, especially at low stress levels as in figure 5.3. However the 4-element model is better at representing the separate components of deflection.

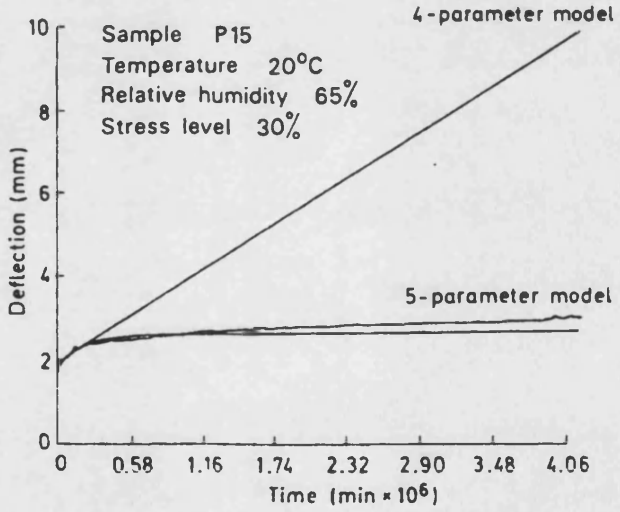

Fig 5.3 Comparison of 4-element and 5-parameter model curves from 24 weeks data: Errors in prediction were 230% for the 4-element model and 11% for the 5-parameter model (Dinwoodie *et al* 1990b).

5.4.4 The 11-Parameter Model

$$Y=\beta_1+\beta_2[1-\exp(-\beta_3 t)]+\beta_4[1-\exp(-\beta_5 t)]+\beta_6[1-\exp(-\beta_7 t)]+\beta_8[1-\exp(-\beta_9 t)]+\beta_{10}[1-\exp(-\beta_{11} t)]$$

This model (Robson 1988 and Bennet 1993) has no viscous component and five viscoelastic components, two of which are predicted from the three fitted viscoelastic components. Initial fittings of this model to existing data show this model to predict creep more accurately than the 5-parameter model. The 11-parameter model followed the shape of the creep curve more closely and is justified in terms of current theory of creep deformation.

In conclusion the application of the 4-element and 5-parameter models to creep data accumulated over seven to nearly ten years showed that the 5-parameter model is superior to the 4-element model as a predictive tool (Dinwoodie *et al* 1990a). This consolidated the earlier view of Pierce et al (1985) that the 4-element model should not be used to predict beyond about 12 months forward projection from 6 months accumulated data. The 11-parameter model proposed by Robson (1988) seems to be an improvement on the 5-parameter model but requires further verification.

The rheological approach to modelling used at BRE was confirmed by Kliger (1991) who tested the 4-element model against seven other models including power law models.

5.5 Creep Mechanism

It is only recently that investigation into the mechanism of creep has commenced. The hydrogen bond is considered to be of significant importance in determining the extent of creep deflection for solid wood. This view is supported by initial tests on acetylated thin wood strips at BRE. This work should lead to the creation of a model for creep based upon chemical kinetics. Initial findings have indicated that the activation energy level is equivalent to the dissociation of 4 to 6 hydrogen bonds (Dinwoodie *et al* 1991b).

The reason why the creep shown by particleboard is greater than that for solid wood is not yet certain, although it is considered to be due to either higher creep of the resin binder or the propagation of microcracks in the wood flakes.

6.0 EXPERIMENTAL DETAIL

6.1 Materials Tested

Three types of wood based panels were tested:

A) a structural grade **chipboard;**

B) a moisture-resistant **oriented strandboard (OSB)** and

C) a moisture-resistant **medium density fibreboard (MDF).**

These were selected by the Building Research Establishment and were intended to be for similar applications, within the limitations of the boards and their relevant standards. The brand names and the manufacturers of the boards will not be given in this thesis to maintain product confidentiality.

A) Chipboard was the material tested most intensively and this occupied about 70% of the testing time. The chipboard selected was a structural board, grade C4, manufactured in accordance with BS 5669 part 2 1989, this was the manufacturer's replacement for the chipboard tested in the previous programmes by Thompson *et al* (1994) and by Hacker (1991). The resin formulation had been changed to comply with legislation to reduce formaldehyde emissions. This board was marketed as being almost identical to the previous board, but it was different in appearance and performance. The chipboard consisted of softwood particles of spruce or fir bonded with an MUF resin and was a three layered board as described in section 3.2. The MUF resin is a copolymer of melamine formaldehyde and urea formaldehyde mixed in the ratio 2:3 respectively.

B) The OSB selected was a moisture resistant board, grade F2, manufactured in accordance with BS 5669: Part 3: 1992, composed of soft wood particles, in this case Scots Pine bonded with about 2.5 weight percent of PF resin. This was also a three layered board, as described in section 3.3. The testing of OSB occupied about 15% of testing time as did the testing of MDF.

C) The MDF selected was a moisture-resistant board manufactured in accordance with BS 1142 (1989). Again this was a softwood board composed from fibres and fibre bundles of sitka spruce and pine bonded with 6-8 weight percent of MUF resin. The material can easily be identified since the core is dyed green. MDF panels produced from softwoods are generally superior to the equivalent panels manufacture from hardwoods. The MDF has a density profile and the density changes from 1000-1100 kg/m^3 at the surface down to about 600 kg/m^3 in the core and the particle/fibre size is homogeneous. The data sheet supplied by the manufacturer states that this

for use in non-stressed applications. MDF is, however used for stair treads which receive fatigue loading and is being considered for many applications including flooring for sports halls. It is also stated in the data sheet that this material is not suitable for external use, despite being classed as moisture resistant. There are, however, exterior grades of MDF manufactured but these are not recognised in any British or European standard.

BRE provided conditioned matched sets of four samples of: chipboard, OSB and MDF, all 50 mm wide by 330 mm long. The chipboard and MDF samples provided were 18 mm thick and the OSB samples were 19 mm thick. The chipboard samples were cut from panels 8'x4', providing seventy samples (seven strips of ten) from each panel, and a total of eight chipboard panels were tested. The OSB and MDF samples were cut from panels 8'x8', providing one hundred and fifty four samples (seven strips of twenty two) from each panel, and two panels were tested for each material.

Side-matched sets of four samples were employed to minimise the effect that the inherent variability of chipboard would have upon the scatter of the fatigue data collected. The properties of chipboard vary considerably from panel to panel within the same batch, and vary between different samples cut from the same panel. The use of adjacent samples minimises this variability. Side-matched sets of four were also used for the testing of OSB and MDF. The strength of OSB samples is more variable than that of chipboard samples and the strength of MDF samples is less variable. Figure 6.1 is an example of a side-matched set of four samples.

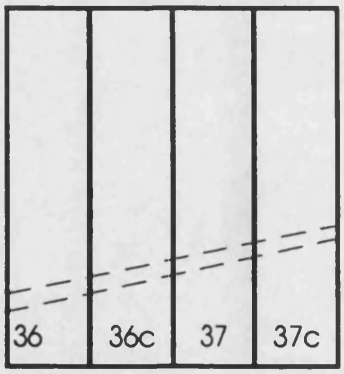

Fig 6.1 A side-matched set of four samples of chipboard, OSB or MDF.

The two outer samples from each side-matched set of four were loaded to failure to determine the mean short term bending strength in four point bending. The left of the centre two samples in each set became the fatigue sample and the right hand one became the creep sample.

All samples of each of the three board types were conditioned and stored at 20°C ± 2°C and ~65% relative humidity. This was to maintain the moisture content of the samples close to 9%. Since wood and wood based materials are hygroscopic changes in moisture content of samples can significantly affect the mechanical properties.

6.2 Test Equipment

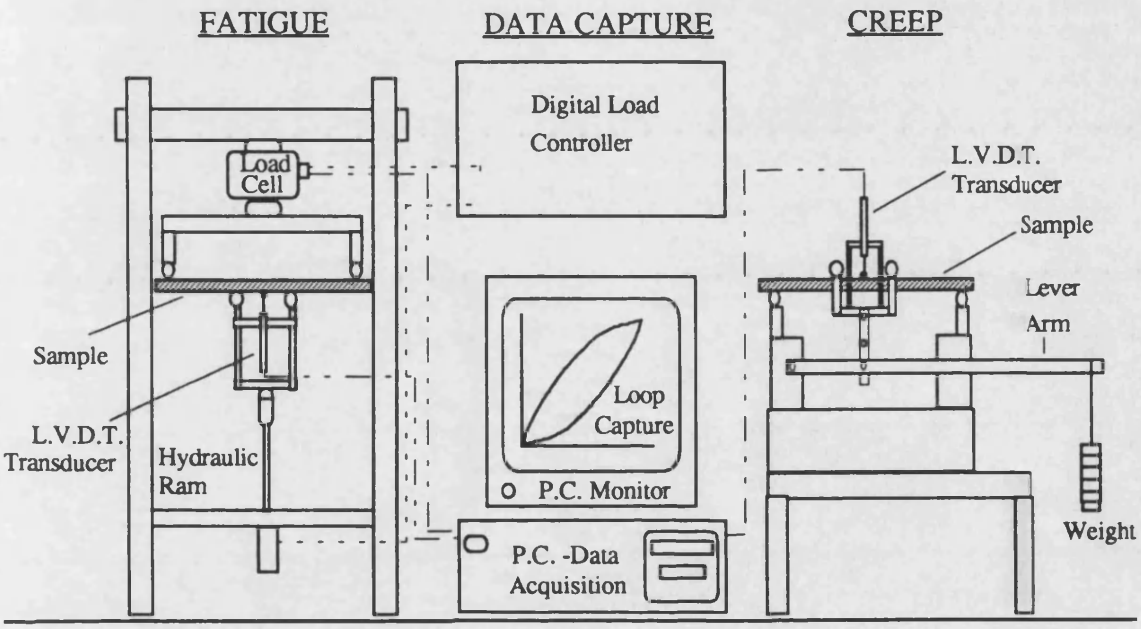

Fig 6.2 Diagram of the, parallel fatigue and creep, testing equipment.

All the tests in fatigue, creep and static loading were performed using the equipment shown in figure 6.2. Loads were applied in four point bending in accordance with BS 5669 Pt. 1 1989 using an identical loading configuration to that used by Thompson *et al* (1994), Hacker (1991), and in the creep testing at BRE. This loading configuration uses a span to depth ratio of approximately 16:1 in quarter point loading with the distance between the outer supports fixed at 300 mm. In the fatigue rig, the supports were rollers of 25 mm diameter instead of the 8 mm rollers used in the creep rig. A larger diameter was required to minimise the possibility of compression damage to the surface of the board that may be inflicted by cyclic loading. In 4-point bending the stress is distributed uniformly throughout the region between the inner supports unlike 3-point bending where the stress is concentrated at the centre and shear stresses are induced. This means that a larger proportion of the sample surface is stressed and this stress is uniformly distributed between the inner supports, not concentrated at a central support as in 3-point bending, providing more representative results (Hammant 1971).

The short term static tests, and the fatigue tests, were performed on a Dartec 5 kN servo-hydraulic fatigue machine operating under load control using a Dartec M9500 digital controller. The digital controller replaced the pervious analogue controller used by Thompson *et al* (1994), and by Hacker (1991) which allowed the load to drift slightly as the sample deflection increased during fatigue testing. The new digital controller operates on a feed back loop which allows accurate control of the applied load during fatigue and static testing.

The creep testing was performed in parallel with the fatigue testing using a creep rig provided by BRE. The loads were applied to the creep samples via a lever arm and pivot arrangement with the same roller configuration as for the fatigue tests. The supports on this rig were rollers with the smaller diameter of 8 mm as used in the creep tests at BRE. Compression damage is less likely in creep because there is no movement at the rollers.

The true centre point deflection of the matched creep and fatigue samples were measured throughout all tests using linear variable differential transformer (LVDT) displacement transducers. In both cases the transducer was mounted between the central rollers in contact with the sample surface and the deflection is measured with respect to the central pair of rollers. Deflections measured with respect to the outer pair of rollers do not enable the surface strains to be calculated. These deflections and the load measurements were captured and manipulated by a custom made computerised fatigue data acquisition system (FDAS). The equations used for the data manipulation are enclosed as Appendix 1.

Humidity was maintained at ~65% RH by enclosing both the fatigue and the creep rig within polyethylene membranes within which were located beakers containing a saturated solution of sodium nitrite ($NaNO_2$).

Fig 6.3 Dartec fatigue rig, controller and fatigue data acquisition system.

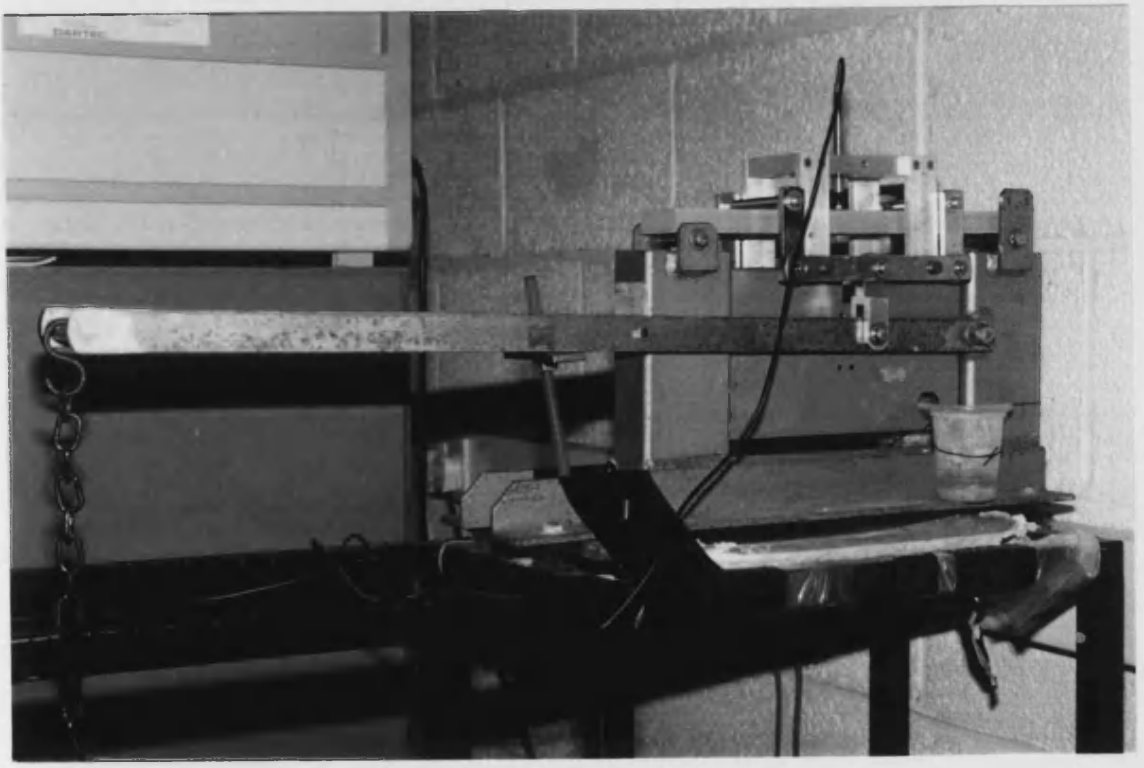

Fig 6.4 Creep rig provided by BRE.

6.3 Experimental Methods

Initially the outside two samples of each side-matched set of four were statically tested to failure in bending to determine the mean bending strength (BS) for the set. The left inner sample was loaded sinusoidally in fatigue at R=0.1, referred to as non-reversed loading, i.e. the stress on the sample is always positive. Figure 6.5 demonstrates that R=0.1 produces a relatively low mean stress, with a large cyclic stress, referred to as the stress range, and the maximum/peak applied stress is ten times greater than the minimum applied stress. The right inner sample was loaded in creep at the same peak stress level.

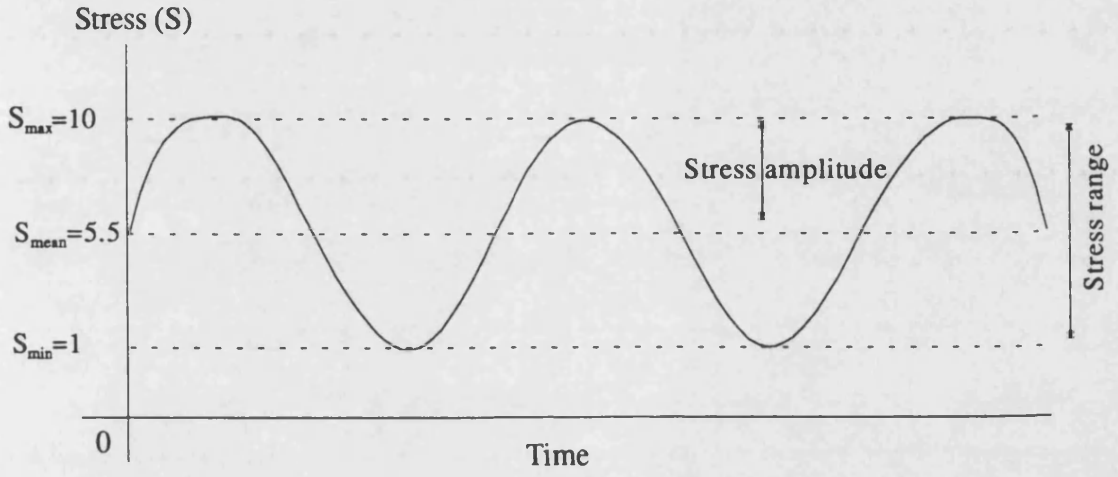

Fig 6.5 The stress wave form applied to the fatigue sample at R=0.1.

The fatigue tests on chipboard were performed at three frequency ranges determined by the loading rates of 1.2 MPa/s, 12 MPa/s and 150 MPa/s. The implementation of these loading rates in fatigue testing produced test frequencies increasing by an order of magnitude each time, resulting in low frequencies (0.015-0.15 Hz), medium frequencies (0.15-3.0 Hz) and high frequencies (3.0-15.0 Hz). The aim was to bridge the gap between existing fatigue and creep data, and to establish differences between fatigue and creep damage mechanisms.

OSB and MDF were both tested at the medium frequency only. The aim of this testing was to compare the fatigue performances of these two materials with that of chipboard and to relate the findings to the difference in particle size between the materials. Again an identical loading rate was used for both the static and fatigue testing of these two materials. Using the same loading rate does however result in lower test frequencies for stronger samples as shown in Appendix 2. This applies when samples of the same material have different strengths, and when samples of one material are stronger than

another material. For example OSB is significantly stronger than chipboard so the OSB samples would be tested at slightly lower frequencies than chipboard samples for the same percentage stress level. The load is applied as a sine wave providing an average loading rate equivalent to applying a triangular wave form.

The mean BS of the outside two samples was taken as the 100% stress level and was used to calculate the percentage stress levels to set up the fatigue and creep tests. Chipboard samples were tested at all three test frequencies at stress levels of 80, 70, 60, 50, 40, 30 and 20% (i.e. percentage of the mean BS of the outside two samples). Medium frequency testing of OSB and MDF was also performed at 80, 70, 60, 50, 40, 30 and 20% stress levels.

The parallel fatigue and creep tests of side-matched samples were started almost simultaneously. In each test the fatigue sample was sinusoidally cycled up to the percentage of the mean BS (peak stress level) while the creep sample was constantly loaded at that peak stress level.

The applied load and the centre point deflection from both samples were monitored by the FDAS and they were entered into standard beam equations to calculate the surface stresses and strains. Stress versus strain hysteresis loops were captured at pre-determined time intervals. Wood based materials are viscoelastic, so when the load is applied to a sample the strain lags behind the applied stress and energy is dissipated due to internal friction and damage taking place. When a full loading and unloading cycle has taken place then a loop is produced and can be plotted as stress versus strain. These hysteresis loops were captured and printed at two minute intervals at first, then less frequently as time progressed. The FDAS calculated the creep microstrain, maximum and minimum fatigue microstrain, hysteresis loop area, dynamic modulus and fatigue loading frequency. (The hysteresis loop parameters are explained in section 6.6.) All this information was stored by the computer for analysis. The cycle counter on the load controller was stopped when a fatigue sample failed, recording the number of cycles to failure.

If the fatigue sample had not failed after 10^5 loading cycles for low frequency loading, 10^6 cycles for medium frequency and 10^7 cycles for high frequency loading it was considered to be a runout, and testing was stopped. Runout samples were statically tested to failure at a later date to determine their residual bending strengths.

Computer programmes were written to calculate the parameters required for setting up the creep and fatigue tests using the mean BS, the dimensions of both samples, and the R ratio. These programmes are included as Appendix 3.

All of the samples were labelled as in figure 6.6, this shows chipboard Panel 3 as an example. The dimensions were measured at three points along central section of each sample using a digital vernier gauge to obtain values of the mean width and thickness. The weight and length were also measured before storing the samples in a moisture conditioned cupboard at ~65% RH until required for testing.

In figure 6.6 S, F and C represent static, fatigue and creep samples respectively. Each cross-section of the panels of chipboard contained ten samples that were divided into three matched sets of four. For example samples 76 and 77C are the outside samples to fatigue sample 76C and creep sample 77. However, sample 77C is also the left side static sample in the matched set of four samples including 78, 78C and 79. In the panels of OSB and MDF each cross-section contained twenty two samples that were divided into seven side-matched sets of four. The outside two samples in each set were statically tested in four point bending using the Dartec 5 kN servo hydraulic test machine, as used for the fatigue tests, to obtain the mean bending strength for the set. All of the static tests were performed at the same loading rate, as used in the respective fatigue tests. These rates were 0.0864 kN/s for the low rate/frequency, 0.864 kN/s for the medium rate/frequency and 10.8 kN/s for the high rate/frequency. The reasons for this are discussed later in section 7.

The dimensions for all samples tested, the parameters for setting up the creep and fatigue tests, the stresses applied and the number of loading cycles for all the samples tested are included in appendices 4A-F.

S	F	C	S	F	C	S	F	C	S
101	101C	102	102C	103	103C	104	104C	105	105C
S	F	C	S	F	C	S	F	C	S
96	96C	97	97C	98	98C	99	99C	100	100C
S	F	C	S	F	C	S	F	C	S
91	91C	92	92C	93	93C	94	94C	95	95C
S	F	C	S	F	C	S	F	C	S
86	86C	87	87C	88	88C	89	89C	90	90C
S	F	C	S	F	C	S	F	C	S
81	81C	82	82C	83	83C	84	84C	85	85C
S	F	C	S	F	C	S	F	C	S
76	76C	77	77C	78	78C	79	79C	80	80C
S	F	C	S	F	C	S	F	C	S
71	71C	72	72C	73	73C	74	74C	75	75C

Fig 6.6 Example of panel numbering, chipboard Panel 3.

6.4 Experimental Difficulties

Initially the new chipboard (referred to as A) was tested at R=0.25 to evaluate the new controller and the test set up prior to starting testing on the effect of frequency. Also chipboard A was compared to the chipboard tested previously by Thompson *et al* (1994) and Hacker (1991) (referred to as chipboard B), that had been tested at R=0.25. Only the S-N plot from this testing is included in the results section since this allows comparisons to be made between the results reported in this thesis and those from previous work.

A major cause for concern when running the fatigue experiments at R=0.25 was perturbations in the captured hysteresis loops as shown in figure 6.7 below.

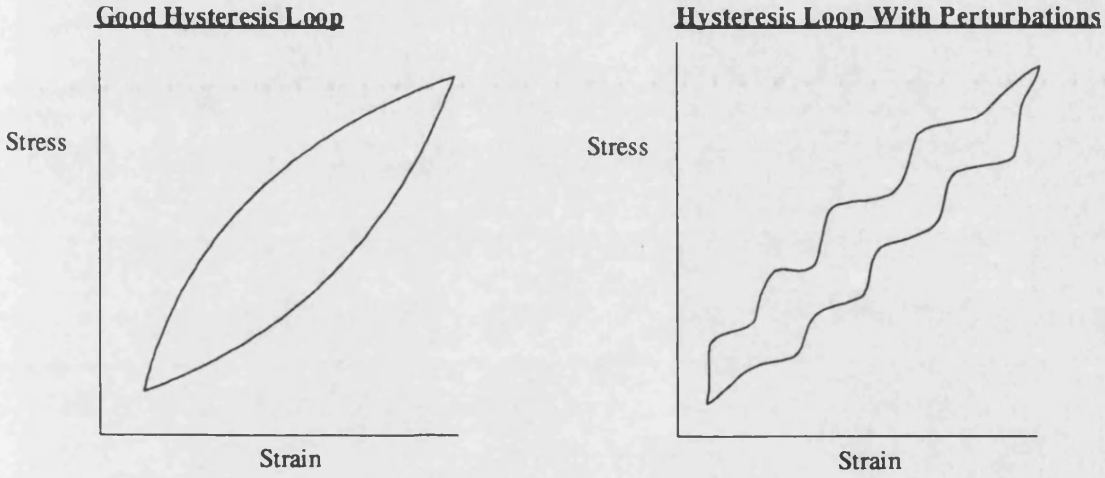

Fig 6.7 Hysteresis loop perturbations.

It was considered essential to resolve the cause of the perturbations prior to starting the core testing. First an accelerometer was used to eliminate natural frequency effects and interference on the electricity supply as possible causes. Following this the perturbations were shown to be caused by the load signal, not the displacement signal. The displacement signal from the transducer was monitored and was shown to be a smooth sine wave when measured from above or below the centre point of the sample, demonstrating that despite the perturbations observed the samples were being loaded sinusoidally.

Monitoring the signal from the load cell revealed that the perturbations were initiated when the ram changed direction, these were then damped out, before initiating again every time the ram changed direction. At lower frequencies, i.e. less than 5 Hz. the magnitude of the perturbations was almost unnoticeable but as the frequency was increased the magnitude of the perturbations increased progressively.

The perturbations were also related to sample stiffness because stiffer samples produced smaller displacements of the ram and reduced the effect of the ram changing direction. It was considered possible that friction between the rollers and sample might be contributing to the perturbations but tests using different materials, P.T.F.E. tape and lubricating spray showed this not to be the case.

Improvements were made by the implementation of several measures. Lashback was checked for at all joints, with the joint between the load cell and inner rollers re-machined to tighter tolerance. The outer rollers were also replaced, as slight flats had worn into them, and the Moog valve was serviced, but all measures resulted in only limited success. Despite these problems the first two panels of chipboard samples were tested at R=0.25, evaluating the new chipboard and the load controller.

This problem was however resolved prior to any testing at R=0.1. Previously the load cell was mounted on the ram and seems to have behaved as an accelerometer unable to respond to the rapid changes in direction occurring at the higher frequencies used. New fittings were machined and the load cell was fixed above the top set of rollers. The sample loading configuration remained unchanged and the perturbations in the captured hysteresis loops were eliminated for frequencies in excess of the highest required for testing.

6.5 Experimental Regime

Once the hysteresis loop capture problems were resolved the following testing commenced.

Testing of chipboard

To determine the effect of frequency upon the fatigue performance:

1) Initial static testing of side-matched samples to evaluate whether changing the loading rate affects the apparent strength of chipboard.
2) High frequency fatigue testing of chipboard.
3) Medium frequency fatigue testing of chipboard.
4) Low frequency fatigue testing of chipboard.
5) Extensive static testing of side-matched samples at the three different loading rates, to determine the extent to which changing the loading rate for the static bending tests, affects the strength of the chipboard.
6) Axial testing of chipboard to evaluate whether the fatigue failure of chipboard in bending is dependent upon the face of the sample that is loaded

in tension or the face loaded in compression. Also to compare the energy dissipated per loading cycle for tensile and compressive loading.

Testing of OSB and MDF

To evaluate the relative fatigue performances of the three materials and to relate the results to the size of the constituent particles of each board type.

1) Medium frequency fatigue testing of OSB.
2) Extensive static testing of OSB at the medium rate to determine the distribution of sample strengths.
3) Medium frequency fatigue testing of MDF.
4) Extensive static testing of MDF at the medium rate to determine the distribution of sample strengths.

6.6 Hysteresis Loop Parameters

Hysteresis loops were captured at predetermined time intervals for all the tests on all three materials. The fatigue data acquisition system (FDAS) was custom made at Bath University and subsequently modified to capture hysteresis loop at all three frequencies for chipboard and for all three materials. The load and centre point deflection for both the fatigue sample and the creep sample were fed into a PC where they were entered into the standard beam equations given in Appendix 3. This converts the loads into the applied stresses and the deflections into the resulting microstrains for the fatigue and creep tests. To evaluate the damage occurring in the samples it is useful to monitor the strains for both samples, primarily the maximum and minimum microstrains. Three parameters for the fatigue sample are calculated from the hysteresis loops, these are: the dynamic modulus and the hysteresis loop area that are calculated by the FDAS, and the fatigue modulus that can be calculated from the data provided by the FDAS.

a) Dynamic Modulus

The dynamic modulus is the average stiffness of the sample during the fatigue test. It is the gradient of the individual hysteresis loop at a specific time in the test and is measured from the two extreme points of each loop as shown in figure 6.8. This value makes it possible to examine how the stiffness of the fatigue sample changes as a result of the cyclic loading. If the stiffness of the samples decreases, then they are being damaged.

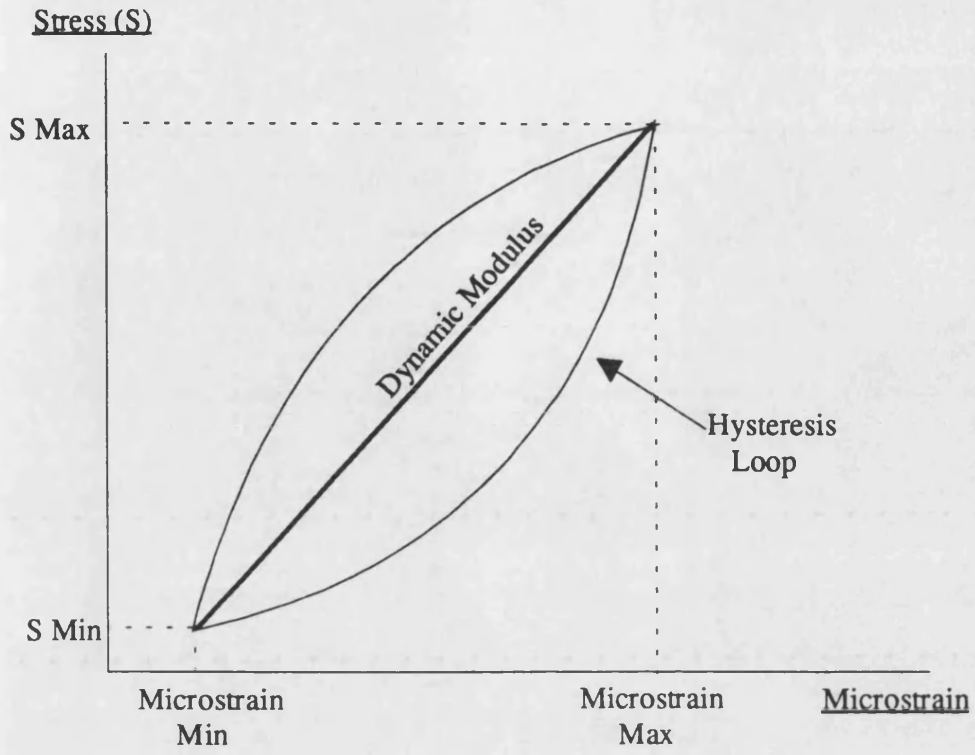

Fig 6.8 Dynamic modulus.

b) Fatigue Modulus

The fatigue modulus is the gradient of the line from the starting point of loading at the beginning of a test (the origin), to the stress versus strain maximum for each hysteresis loop. This measurement of sample stiffness differs from the dynamic modulus in that it takes account of the creep occurring in the sample, as well as any fatigue damage causing a decrease in the average stiffness. The definition is shown pictorially in figure 6.8. This parameter has been used by Yang *et al* (1992) to predict fatigue life for polymer composites and by Hacker (1993 and 1995) to predict fatigue life for wood laminates used in wind turbine blades.

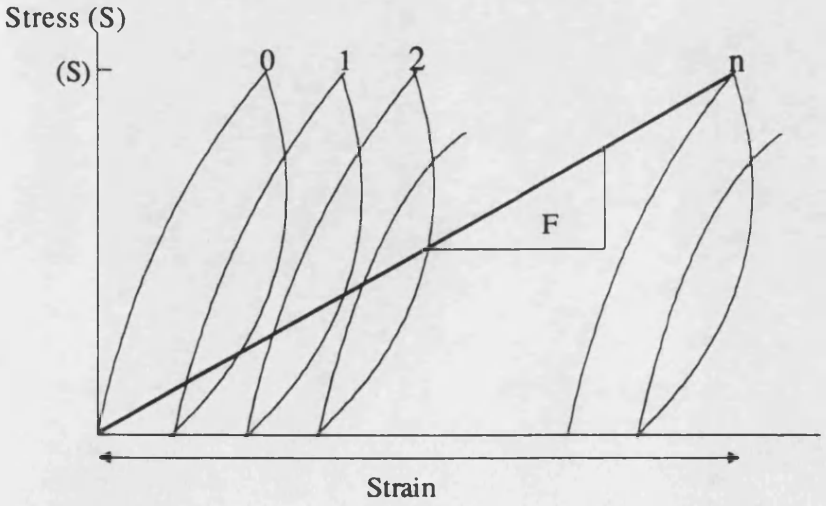

Fig 6.9 Definition of the fatigue modulus F.

The fatigue modulus is therefore based on the calculation of the stress range divided by the strain range, where the strain is increasing throughout a fatigue test due to both fatigue damage, and creep, which occur simultaneously.

c) Hysteresis Loop Area

The area of a stress versus strain hysteresis loop is the total energy dissipated in the sample during an individual loading and unloading cycle. This is a measure of the energy dissipated by the sample and an indication of the damage produced in that sample. It may also include losses due to the hydraulic system depending upon the oil flow rate, frictional effects and the loading configuration. This makes the loop area a good measure for comparing the energy lost per cycle throughout individual tests and between different tests but it is unlikely to be an absolute quantity.

6.7 Axial Testing of Chipboard

It is generally accepted that wood is stronger in tension than it is in compression. This means that when wood is tested in bending it can be assumed that it is the side of the wood that is loaded in compression that initiates failure, even though the fracture may only be easily visible on the tensile side. This is true for the fatigue of wood as well as for static testing and has been shown for wood laminates by Hacker (1995) and by Bond (1994). This is not necessarily the case for chipboard and the literature (WPPF Ref PD/16, 1992) indicates that the reverse of this is true and that chipboard is stronger in compression than it is in tension, this could have a significant impact on the design of chipboard panels used for flooring. Definite information was not available for the chipboard tested here, so it was decided to perform a limited number of axial static tests to determine the approximate tensile and compressive strengths of the chipboard. These values were then used to set up two fatigue tests, one in compression and the other in tension and to capture stress versus strain hysteresis loops for both tests. The objective of this was to determine whether more damage was produced per loading cycle by compressive or tensile fatigue loading at the same percentage stress level. The magnitude of the hysteresis loops captured in each case were also of interest to evaluate comparative damage rates.

7.0 STATIC TESTING OF CHIPBOARD

7.1 Qualitative Evaluation of Loading Rate Effect on Strength

In the work reported by Thompson *et al* (1994) and by Hacker (1991) which pre-dates this thesis but which is complimentary to it, the loading rate for the static bending strength tests was not stated. This was because the rate at which the analogue load controller applied the load was determined by the rate at which the operator turned the load dial. When the digital controller was installed at the beginning of this work it became possible to precisely control the rate at which the load was applied. This meant that the rate of loading for the static testing of the outside samples from the side-matched sets of four had to be determined before the fatigue testing at R=0.25, at high frequency could commence. Chipboard is inherently variable, so it was decided that the best method of examining the effect of the loading rate upon the strength of the chipboard was to test side-matched samples at considerably different loading rates.

Four cross-sections (strips) of Panel 1 consisting of forty side-matched samples were statically tested to determine their bending strengths at different loading rates. The strengths of all these samples are shown in figures 7.1a and 7.1b. In both these plots each column shows the ultimate failure stress of a side-matched sample. The positions of the samples relative to each other are the same as they were within the panel. For example, in figure 7.1a the first two columns show the strength for sample 1 tested at 10.8 kN/s next to the strength of its side matched partner, sample 1C, tested at 0.1 kN/sec. Sample 1C is also side-matched to sample 2 and so on for the ten samples in that cross section of the chipboard panel.

Figure 7.1a shows the strengths for samples 1-5C loaded at 10.8 kN/s and 0.1 kN/s, and for an entire cross-section of the panel, samples 21-25C, all loaded at 10.8 kN/s. This entire cross-section was tested because 10.8 kN/s is equivalent to 150 MPa/s, the rate of application of stress to be used for the fatigue tests at R=0.25. This was also the rate used for all the fatigue tests performed by Hacker (1991), and by Thompson *et al* (1994) at R=0.25. Figure 7.1b shows the strengths for samples 6-10C loaded at 0.2 and 0.01 kN/s together with samples 11-15C loaded at 0.5 kN/s and 0.005 kN/s.

Fig. 7.1a

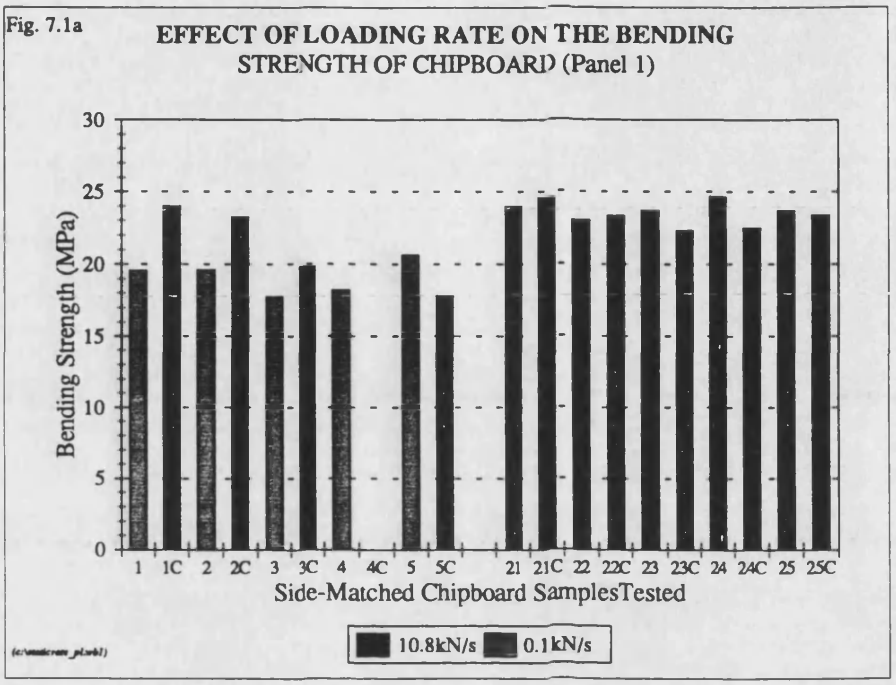

Fig. 7.1b

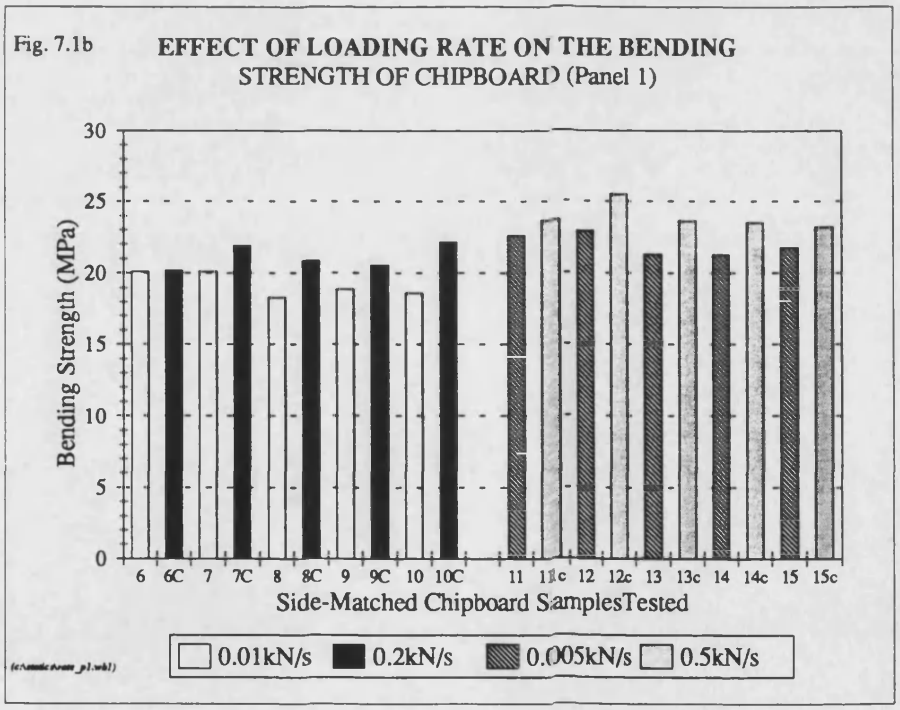

Discussion

Twenty nine strengths for side-matched samples tested at different loading rates were measured (the value for sample 4C was not captured) and in all but two cases the sample loaded at the higher loading rate had a higher bending strength than its side-matched samples. There was one occurrence where two side-matched samples loaded at different rates had the same bending strength and one where the sample loaded at the lower rate had the higher strength. Also table 7.1 demonstrates that the side-matched samples tested at the higher loading rates had higher mean bending strengths than those loaded at lower rates.

Table 7.1 Bending strengths of side-matched chipboard samples loaded at different rates.

Loading Rate kN/sec	Number of Samples	Mean Bending Strength MPa	Standard Deviation ($\sigma n-1$) MPa	Standard Deviation as a % of BS	Sample Numbers
0.1	5	19.15	1.19	6.2	1-5
10.8	4	21.21	2.90	13.7	1C-5C
0.01	5	19.21	0.86	2.9	6-10
0.2	5	21.13	0.85	4.0	6C-10C
0.005	5	21.97	0.76	3.5	11-15
0.5	5	23.88	0.91	3.8	11C-15C
10.8	10	23.51	0.79	3.4	21-25C

Gerhards and Link (1986) observed a similar rate effect for Douglas fir lumber loaded in bending. They found the strengths to increase linearly with the logarithm of loading rate and also reviewed the effect of loading rate on the strength of wood. Gerhards *et al* (1984) also found the tensile strength of Douglas fir lumber to increase slightly with increased loading rate. However, they found that the weakest lumber was weaker still when loaded at an increased rate. Bender *et al* (1988) also observed an increase in the tensile strength of southern pine lumber when the loading rate was increased by seventeen times.

The standard deviation for the strengths of chipboard samples 1C-5C is higher than for the other tests as only four valid results were collected. Only one of the standard deviations is of statistical significance (samples 21-25C) since eight data points are required for a statistically significant standard deviation, but they are still a useful guide

to the spread of the data. A comprehensive evaluation was carried out at a later stage and is reported in section 7.3.

It was decided from this information that increasing the loading rate did produce a small increase in the apparent strength for the material. The loading rate of 10.8 kN/s was chosen to test the outside samples from the matched sets of samples. Although this is a fast rate of loading, approaching that for an impact test, it is representative of what is endured by the samples during the high frequency fatigue tests and is in agreement with the findings of McNatt (1977). The choice of a lower value of loading rate would have been unrelated to the fatigue testing and not as appropriate.

The loading rates used for the static tests by Thompson *et al* (1994) and Hacker (1991) are not known but it is certain that they were considerably lower than 10.8 kN/s. The stress levels quoted in this thesis for high frequency tests will be slightly higher than those reported previously due to the increase in the static strength values obtained at the higher loading rate. The magnitude of this increase is evaluated in section 7.3.

7.2 Bending Strengths

Altogether ten panels of chipboard were tested. Panels 1 and 2 were used to investigate the effect of the loading rate on the strength of the chipboard and then for fatigue testing at R=0.25. This was to allow the results of this thesis to be compared to previous work where a different chipboard product had been investigated. Panels 3 and 4 were tested at high frequency at R=0.1. Panels 5 and 6 were tested at medium frequency at R=0.1, and panels 7 and 8 were tested at low frequency at R=0.1. Panels 9 and 10 were used to quantitatively examine the effect of loading rate upon the strength of the samples and this work is presented in section 7.3.

As was explained in Chapter 6, for each matched set of four samples containing a central pair of fatigue and creep samples, the outside pair of samples were statically loaded to failure to obtain the mean bending strength for the set. It was decided that an entire cross-section of each panel should be statically tested, to indicate the variability in the bending strengths of the samples, across each panel. The results of this testing are presented in this section.

All the static tests performed on samples from panels 3 and 4 were carried out at the loading rate of 10.8 kN/s. This loading rate is equivalent to the rate of application of stress used during the high frequency fatigue tests performed on these panels. With hindsight this loading rate would have been set at 8.64 kN/s instead of 10.8 kN/s because it was found that the rate of application of stress for the fatigue testing required reducing from 150 MPa/s used previously for testing at R=0.25, to 120 MPa/s for testing at R=0.1. The aim was to keep the upper limit for the high frequency fatigue tests at about 8 Hz to minimise adiabatic heating in the fatigue samples. This rate change has a minimal effect upon the results because the rate of loading used for the low rate was a factor of ten lower than for the medium loading rate and a factor of one hundred and twenty five lower than that for the high loading rate. The reason that 10.8 kN/s was used originally was to allow the strengths of the samples from panels 3 and 4 to be compared with those from panels 1 and 2. Thirty two samples from Panel 3 and thirty four from Panel 4 were tested to failure in four point bending. In each case, these were composed of the outside two samples of each matched set of four, together with an entire cross section of ten samples.

All the samples tested from panels 5 and 6 were loaded at 0.864 kN/s, which is equivalent to 12 MPa/s, the rate of application of stress for the medium frequency fatigue tests performed on these panels. Twenty eight samples from Panel 5 and twenty two from Panel 6 were tested to failure. In each case these comprised the outside two

samples of each matched set of four together with an entire cross section of ten samples from Panel 6. It was not possible to test an entire cross section of Panel 5 because at the time the samples were needed for fatigue testing. Three of the seven cross-sections of Panel 6 were not tested and have been stored in the conditioning cupboard in case they are required for comparative testing by BRE at a later date.

For panels 7 and 8 all the samples were loaded at 0.0864 kN/s, which is equivalent to 1.2 MPa/s, the rate of application of stress used for the low frequency fatigue tests performed on these panels. Thirty four samples from Panel 7 and thirty four from Panel 8 were tested to failure in four point bending. For both panels these comprised the outside two samples of each matched set of four together with an entire cross section of ten samples from each panel.

Figures 7.2a-f show the bending strengths for the samples in the entire cross-sections of panels 3-8 respectively. The samples are shown in their relative positions in the panels. This gives a good indication of the scatter of strengths across each panel and within side-matched sets of four samples. Table 7.2 displays the bending strength data and statistics for all the samples statically tested to failure from panels 3-8. This allows the variation in strength of the samples to be examined for the different panels, tested at the three different loading rates (low, medium and high) and indicates the strength variations within individual panels and within side-matched sets of four. Figure 7.3 shows strength intervals plotted against the numbers of samples loaded at each loading rate within that strength interval. This allows the range and distribution of sample strengths to be compared for each loading rate.

Fig. 7.2a

BENDING STRENGTH OF CHIPBOARD
Panel 3, Cross-Section, High Rate

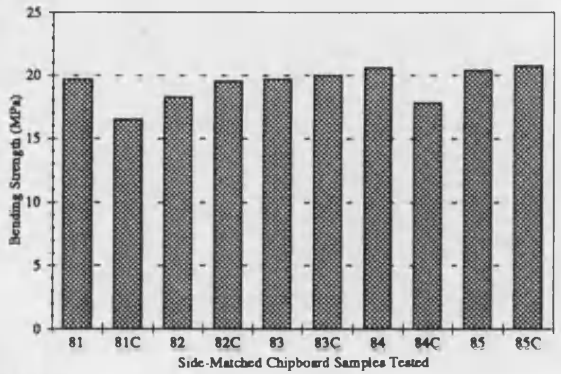

Fig. 7.2b

BENDING STRENGTH OF CHIPBOARD
Panel 4, Cross-Section, High Rate

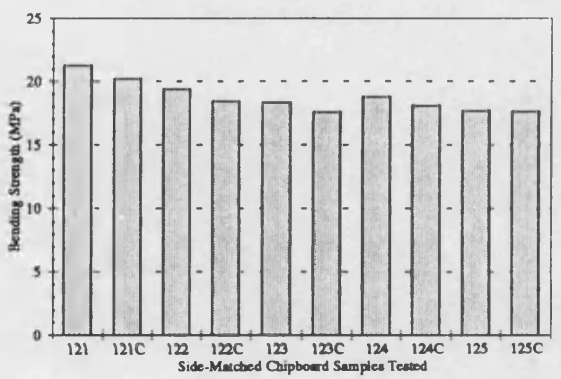

Fig. 7.2c

No cross-section of Panel 5 was tested because the samples were required for fatigue testing.

Fig. 7.2d

BENDING STRENGTH OF CHIPBOARD
Panel 6, Cross-Section, Medium Rate

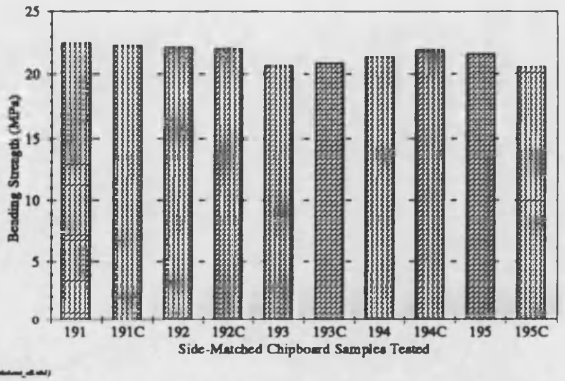

Fig. 7.2e

BENDING STRENGTH OF CHIPBOARD
Panel 7, Cross-Section, Low Rate

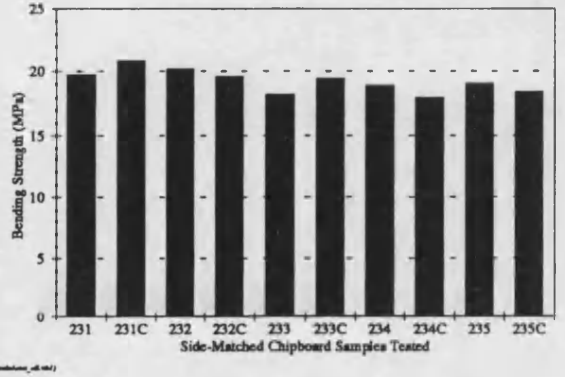

Fig. 7.2f

BENDING STRENGTH OF CHIPBOARD
Panel 8, Cross-Section, Low Rate

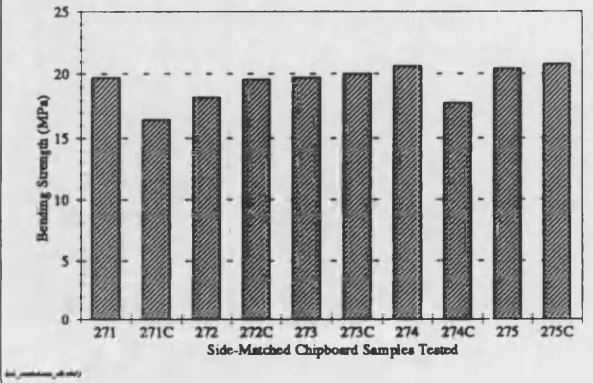

Table 7.2 Bending strength data for chipboard tested at three loading rates.

1	Loading rate (kN/s)	10.8 kN/s (High)					0.864 kN/s (Medium)					0.0864 kN/s (Low)				
2	Panel Number	3		4		3 & 4	5		6		5 & 6	7		8		7 & 8
3	Samples Tested	**Total**	**X**	**Total**	**X**	**Total**	**Total**	**X**	**Total**	**X**	**Total**	**Total**	**X**	**Total**	**X**	**Total**
4	Number of samples	32	10	34	10	66	28	--	22	10	50	34	10	34	10	68
5	Mean Bending Strength (MPa)	19.6	19.3	19.3	18.6	19.5	21.1	--	20.9	21.6	21.0	18.5	19.2	18.7	17.3	18.6
6	SD from Mean (MPa)	1.4	2.0	2.1	1.2	2.0	2.2	--	1.5	0.7	1.9	1.2	0.9	2.0	1.3	1.6
7	SD as % of Mean Bend. Strength	10.2	7.1	11.0	6.6	10.6	10.4	--	7.1	3.2	9.0	6.6	4.6	10.5	7.7	8.7
8	Mean Diff. Matched Sets (%)	4.9	2.3	6.0	6.2	5.5	3.8	--	3.2	3.0	3.6	6.1	2.2	3.3	3.6	4.7
9	SD from the Mean Diff. (%)	4.6	N/A	9.5	N/A	7.5	1.9	--	1.4	N/A	1.71	5.4	N/A	2.3	N/A	4.3
10	(8) excluding out of bound sets	3.8	N/A	3.0	2.2	3.3	N/A	--	N/A	N/A	N/A	4.3	N/A	N/A	N/A	3.8
11	SD of (10) %	3.1	N/A	2.1	N/A	2.6	N/A	--	N/A	N/A	N/A	3.2	N/A	N/A	N/A	2.7
12	Strength Range (MPa) Min	15.6	16.5	12.9	17.6	12.9	18.0	--	17.8	20.6	17.8	16.4	18.0	14.2	16.5	14.2
	Max	24.5	20.8	23.1	21.3	24.3	26.4	--	23.3	22.5	26.4	20.8	20.8	21.4	20.8	21.4
13	Strength Range (MPa)	8.9	4.3	10.2	3.7	11.4	8.4	--	5.5	1.9	8.6	4.4	2.8	7.2	4.3	7.2

Notes:-

X = Cross section of each panel consisting of 10 samples.

S.D. = Standard Deviation.

Mean Diff. Matched Sets of Four = the mean difference in strength between the outside two samples of each set of four when tested to failure.

Out of bound sets were those where the difference between the static strengths of the outside two samples was greater than 10.5% of the mean strength obtained from those two samples.

A cross section of Panel 5 was not statically tested to failure as the samples were required for dynamic tests.

3/7 of Panel 6 has not been tested and is stored in the conditioning cupboard in case the samples are needed at a later date.

Fig. 7.3

BENDING STRENGTH OF CHIPBOARD
AT THREE LOADING RATES IN 4pt. LOADING

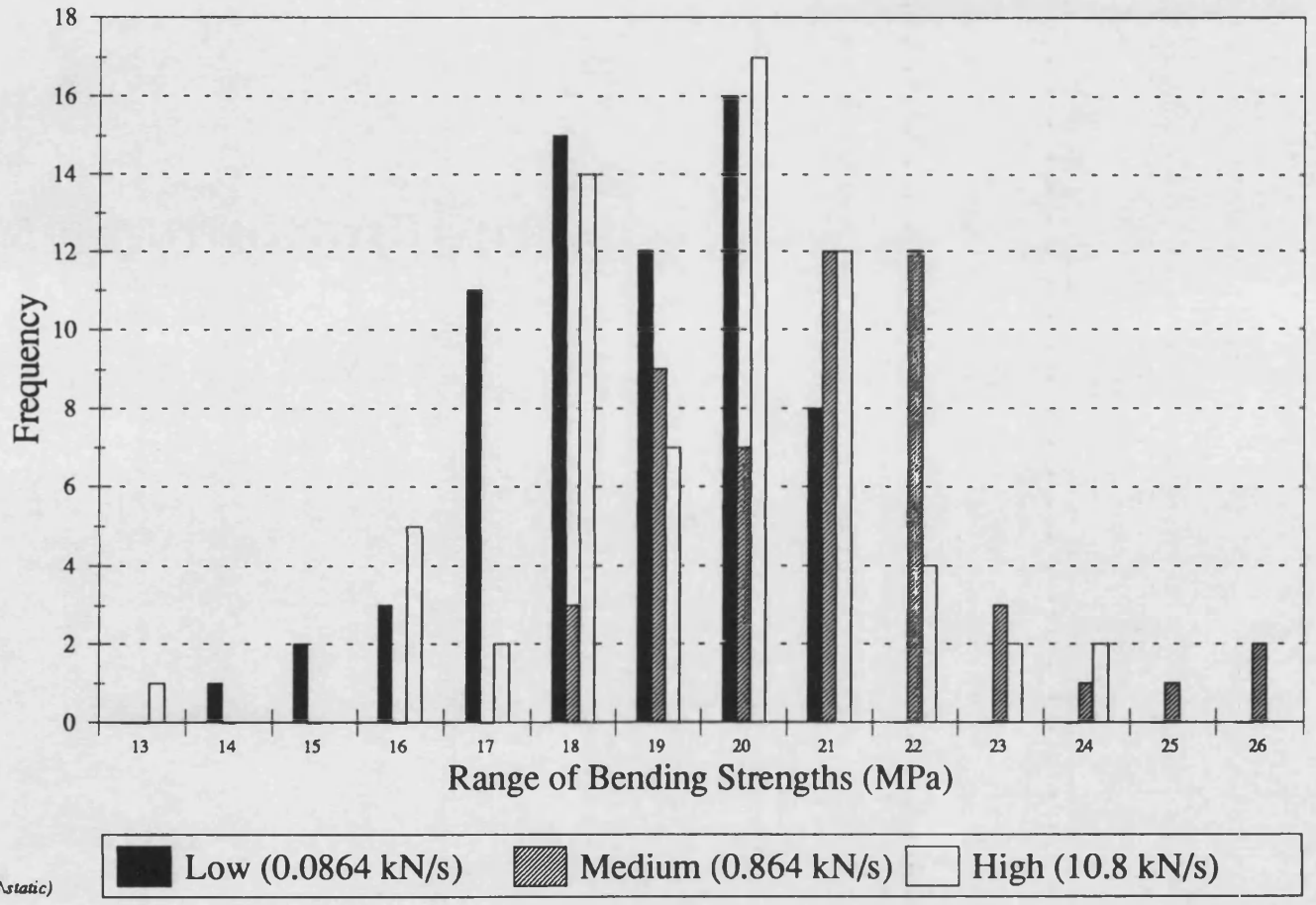

Discussion

The bending strengths of the samples tested to failure at the low loading rate (panels 7 and 8) shown in table 7.2 ranged from 14.2 to 21.4 MPa. This was 17.8 to 26.4 MPa for the medium rate (panels 5 and 6) and 12.9 to 24.3 MPa for the high rate (panels 3 and 4). The distribution of these strengths is shown in figure 7.3. Table 7.2 also shows that the range of strengths for the low rate was 7.2 MPa. This increased to 8.6 MPa for the medium loading rate and then to 11.4 MPa for the high loading rate. The variability of the static strengths is increased by increasing the rate of application of the load. So the variability of the fatigue results should be lower at lower test frequencies, because the static data is used to set the percentage stress levels for dynamic testing.

It can be seen from table 7.1 that the mean bending strength for Panel 7 is 18.5 MPa and for Panel 8 is 18.7 with both panels tested at 0.0864 kN/s (low). The mean bending strengths for panels 5 and 6, tested at 0.864 kN/s (medium), were 21.1 and 20.9 MPa respectively. For panels 3 and 4, tested at 10.8 kN/s (high) mean strengths were 19.6 and 19.3 MPa respectively. Finally the mean bending strengths for panels 1 and 2 tested at 10.8 kN/s (high) were 22.5 and 20.7 MPa respectively. These are shown in Appendix 4D. It can be seen from these strengths and from figure 7.3 that the mean bending strength of all samples tested at the low loading rate (panels 7 and 8) were lower than those from both the higher loading rates tested. The results of the rate of loading experiments presented in section 7.1 strongly suggest that the strengths for the samples tested at the medium rate should fall between those for the low and the high loading rate. This expected trend did not, however, occur. The mean strength for the medium loading rate was slightly higher than for the high loading rate. When the loading rate was reduced from 10.8 kN/s to 0.864 kN/s the variation in strengths between the panels must have been greater than the reduction in strength as a result of the reduction in loading rate. These results were inconclusive and reinforced the need to quantitatively assess the effect of loading rate on the strength of samples, and the results of further comprehensive tests are reported in section 7.3.

The effect of strength variability between boards and within the same board is minimised by using side-matched sets of four samples. This is proved by the figures in rows seven and eleven of table 7.2. These show that, the standard deviation as a percentage of the mean bending strength for the entire panels, is considerably greater than for the side-matched sets of four samples, for all the panels where data is available. The use of sample matching and of normalised percentage values means that only localised differences are encountered.

A good indication of the localised differences within panels 3-8 can be seen from figures 7.2a-f. These show the strengths of the samples from the entire cross section of their respective panels and clearly the differences between side matched samples are usually small. It is, however, always going to be possible for one sample to be significantly stronger than its adjacent partners. For example in figure 7.2f, the bending strength for sample 274C was 2.6 MPa less than both of its adjacent partners. If this group of samples had been a matched set of four, then sample 274C would have been the fatigue sample and the stress level imposed would have been 15% higher than stated for that sample and a shorter fatigue life would have resulted. Even though this circumstance cannot be prevented sample 274C is exceptional and the matched sets of four samples are normally very similar.

Matched sets with a difference in strength between the outside two samples of greater than 10.5% of their mean bending strength were not used. This resulted in three sets of four samples being excluded from Panel 7, none from Panel 8, none from panels 5 and 6, two sets from Panel 3 and three sets from Panel 4.

7.3 Quantification of Loading Rate Effect on Bending Strength

The results presented in section 7.1 indicated that, increasing the loading rate for static tests by orders of magnitude, in order to relate them to the fatigue tests, would produce a small increase in the bending strengths of the samples. Since the low loading rate is one hundred and twenty five times slower than the high loading rate it was considered important to evaluate this rate effect. Due to the inherent variability of chipboard and the possibility that the resulting increase in strength would only be small it was decided that a large population of side-matched samples would have to be tested to produce a conclusion with a reasonable degree of validity.

To satisfy this requirement within the time available it was decided that a population of one hundred and twenty samples would be tested. The samples from panels 9 and 10 were all side-matched to provide three sets of forty samples to be loaded at low, medium and high rates. These were divided as shown in figure 7.3a. This figure shows all the samples loaded to failure from Panel 9. L, M and H represent low (0.0864 kN/s), medium (0.864 kN/s) and high (10.8 kN/s) rates respectively. It has already been seen in section 7.2 that the use of side-matched sets means that only localised differences in strength are encountered which minimises the variability of the bending strengths. All the static tests were performed using the same methods and equipment described in sections 6.2 and 6.3 for side-matched sets of four samples. The only difference between the samples was the rate at which they were loaded.

Table 7.3 presents the results for bending strengths for all three loading rates. This table allows the mean and median, the standard deviations, and the range of the bending strengths to be compared for the three loading rates. The length, breadth, thickness and weight of all the samples were measured and recorded prior to testing. This allowed the specific bending strength of all the samples to be calculated by dividing the bending strength of each sample by its relative density (also referred to as the specific gravity). Table 7.4 presents the same data as table 7.3 but for the specific bending strengths instead of the bending strengths to allow the two to be compared.

The distribution of the bending strengths for the forty samples tested at each loading rate are presented in the histograms, figures 7.4a-c. These show the frequency of samples strengths in each range for the low, the medium and the high rates respectively. Figure 7.5 shows the mean bending strength and the standard deviation for all the samples tested at all three loading rates and figure 7.6 shows the specific values.

L	M	H	L	M	H	L	M	H	L
311	311C	312	312C	313	313C	314	314C	315	315C
M	H	L	M	H	L	M	H	L	M
306	306C	307	307C	308	308C	309	309C	310	310C
H	L	M	H	L	M	H	L	M	H
301	301C	302	302C	303	303C	304	304C	305	305C
L	M	H	L	M	H	L	M	H	L
296	296C	297	297C	298	298C	299	299C	300	300C
M	H	L	M	H	L	M	H	L	M
291	291C	292	292C	293	293C	294	294C	295	295C
H	L	M	H	L	M	H	L	M	H
286	286C	287	287C	288	288C	289	289C	290	290C
L	M	H	L	M	H	L	M	H	L
281	281C	282	282C	283	283C	284	284C	285	285C

Fig 7.3a Example of the panel numbering for the matched bending strength samples (Panel 9).

Table 7.3 Bending strength data for evaluating the effect of loading rate.

Loading Rate for the side-matched chipboard samples		**Low (0.0864 kN/s)**	**Medium (0.864 kN/s)**	**High (10.8 kN/s)**
Mean Bending Strength (MPa)		19.5	20.2	20.6
Median Bending Strength (MPa)		19.7	20.4	20.6
Standard Deviation (σn-1) (MPa)		1.5	1.8	1.7
Number of Side-Matched Samples Tested		40	40	40
Range of Strengths (MPa)	Max	16.4	16.6	17.3
	Min	22.2	24.0	25.0
Range of Strengths (MPa) (Max - Min)		5.8	7.4	7.7

Table 7.4 Specific bending strength data for evaluating the effect of loading rate.

Loading Rate for the side-matched chipboard samples		**Low (0.0864 kN/s)**	**Medium (0.864 kN/s)**	**High (10.8 kN/s)**
Mean Specific Bending Strength (MPa)		27.1	28.0	28.6
Median Specific Bending Strength (MPa)		27.3	27.9	28.7
Standard Deviation (σn-1) (MPa)		1.8	2.2	2.2
Number of Side-Matched Samples Tested		40	40	40
Range of Specific Strengths (MPa)	Max	22.8	23.2	24.2
	Min	29.5	31.6	32.9
Range of Sp. Strengths (MPa) (Max-Min)		6.7	8.4	8.7

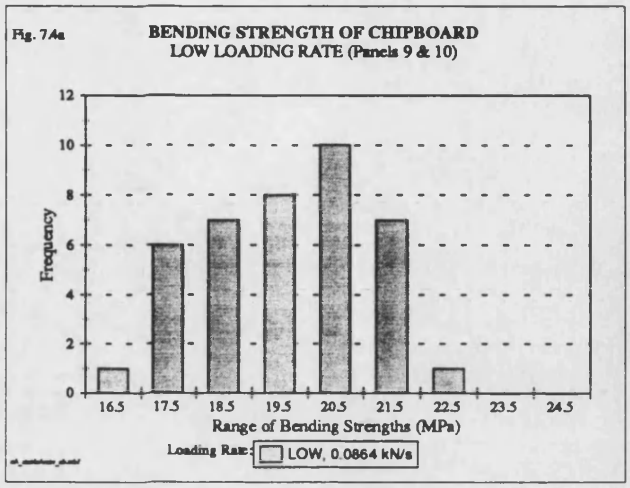
Fig. 7.4a
BENDING STRENGTH OF CHIPBOARD
LOW LOADING RATE (Panels 9 & 10)
Frequency
0
2
4
6
8
10
12
16.5
17.5
18.5
19.5
20.5
21.5
22.5
23.5
24.5
Range of Bending Strengths (MPa)
Loading Rate:
LOW, 0.0864 kN/s

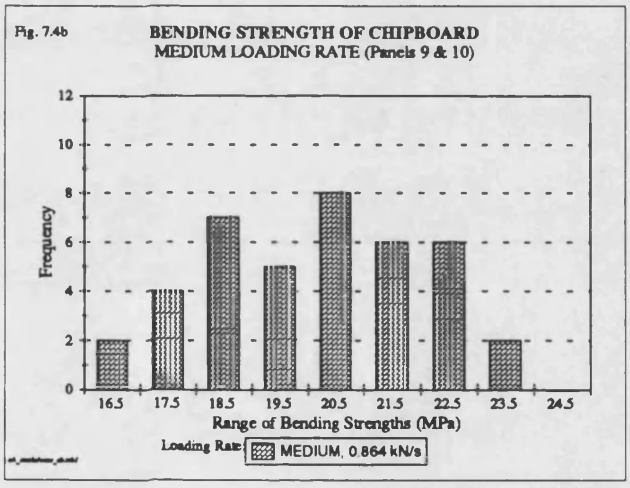
Fig. 7.4b
BENDING STRENGTH OF CHIPBOARD
MEDIUM LOADING RATE (Panels 9 & 10)
Frequency
0
2
4
6
8
10
12
16.5
17.5
18.5
19.5
20.5
21.5
22.5
23.5
24.5
Range of Bending Strengths (MPa)
Loading Rate:
MEDIUM, 0.864 kN/s

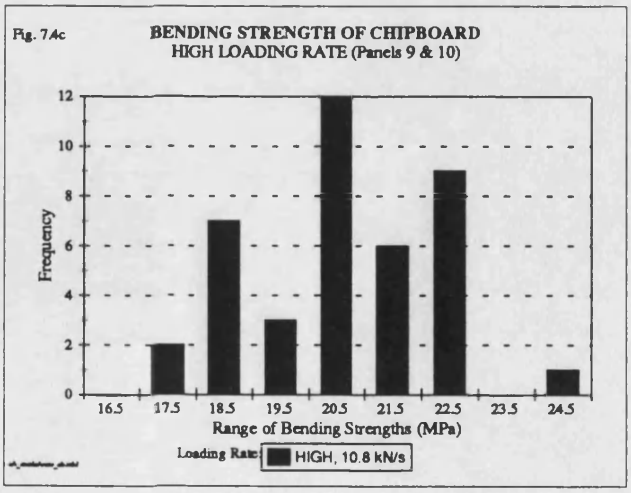
Fig. 7.4c
BENDING STRENGTH OF CHIPBOARD
HIGH LOADING RATE (Panels 9 & 10)
Frequency
0
2
4
6
8
10
12
16.5
17.5
18.5
19.5
20.5
21.5
22.5
23.5
24.5
Range of Bending Strengths (MPa)
Loading Rate:
HIGH, 10.8 kN/s

Fig. 7.5

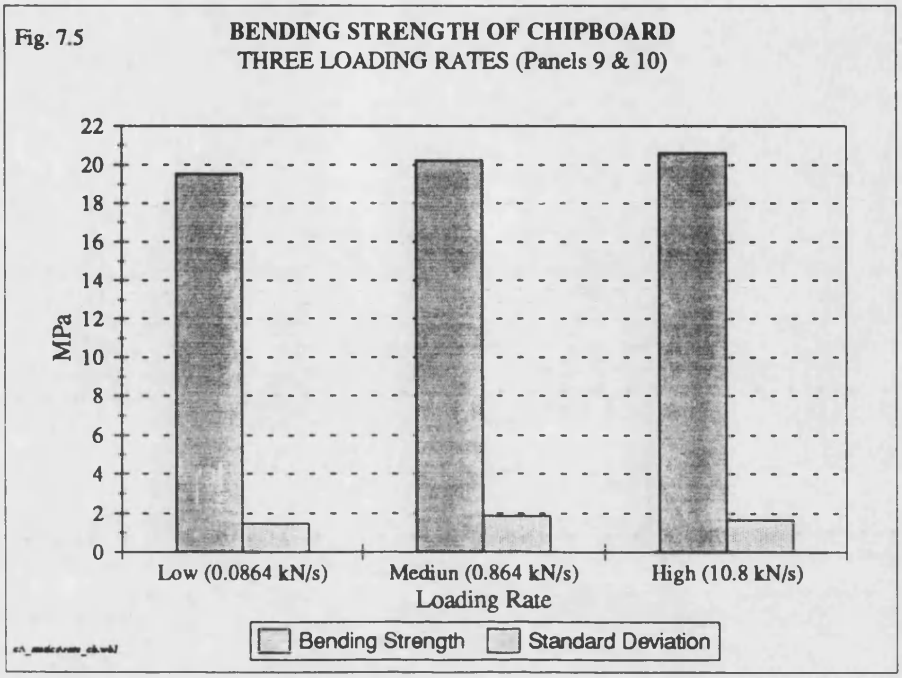
BENDING STRENGTH OF CHIPBOARD
THREE LOADING RATES (Panels 9 & 10)
MPa
22
20
18
16
14
12
10
8
6
4
2
0
Low (0.0864 kN/s)
Mediun (0.864 kN/s)
High (10.8 kN/s)
Loading Rate
Bending Strength
Standard Deviation

Fig. 7.6

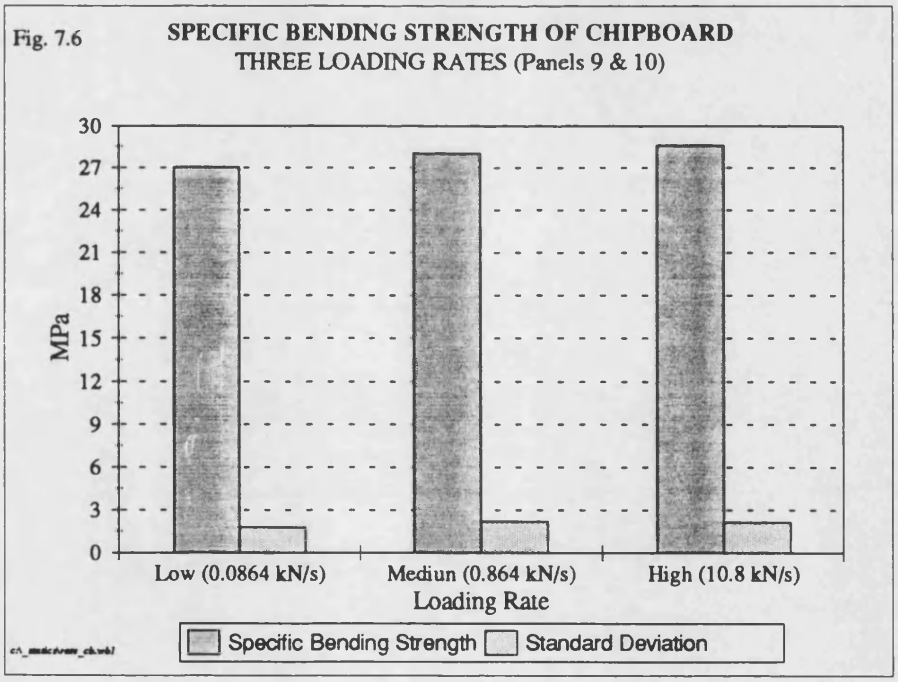
SPECIFIC BENDING STRENGTH OF CHIPBOARD
THREE LOADING RATES (Panels 9 & 10)
MPa
30
27
24
21
18
15
12
9
6
3
0
Low (0.0864 kN/s)
Mediun (0.864 kN/s)
High (10.8 kN/s)
Loading Rate
Specific Bending Strength
Standard Deviation

Discussion

The mean bending strengths can be seen to increase as the loading rate is increased from low to medium and from medium to high. These increases were only small compared to the mean strengths as predicted and represent an increase of 3.5% from low to medium and of 1.9% from medium to high. These values were 3.8% and 2.1% for the specific bending strengths. Before it is possible to confirm this trend as a real one, a statistical test must be performed to confirm that the means of the bending strengths are not from the same population and that there is a statistically significant difference between them. However, the trend does agree with the literature. Lyon and Barnes (1978) showed the MOR of particleboard decking to decrease by 6% for a ten fold increase in time to failure. They also found that particleboard was less sensitive to rate of loading than solid wood and that the MOE for particleboard in the tests performed was independent of the loading rate.

The median values are all very close to the mean values, so this indicates that the strengths may be symmetrically distributed. The histograms, figures 7.4a-c appear to be normally distributed but since it is important to confirm that data are normally distributed before applying statistical tests a distribution analysis has been carried out and this is presented in section 7.4.

The range of strengths for all the samples tested increased as the loading rate was increased which concurs with the use of side-matched sets of four samples. This means that higher loading rates result in greater scatter of data collected and this also holds for specific bending strengths (table 7.4).

The scatter of the specific bending strengths does not fall compared to the bending strengths so there is no reason to evaluate the specific properties further. The strength of wood and wood based materials are often closely related to density, so it is possible that some of the variation in the strength of the samples could have been explained by variations in their density. This however, was not the case.

7.4 Distribution Analysis

The aim of this section is to reinforce the hypothesis that a normal distribution provides the most appropriate fit to the static strength data for chipboard. Although the probability plots (figures 7.4a-c) suggest that the data are normally distributed, it has been shown that the static strength of some materials is described better by alternative distributions. For example the strength of composite materials has been described by a Weibull distribution (Talreja 1981) as has the strength of Aluminium (Weibull 1952).

For these reasons it was decided to test the static strength data for chipboard with respect to three possible distributions. The normal distribution, log normal distribution and a two parameter (2P) Weibull distribution were applied to the data for chipboard tested at the low loading rate, and are included as figures 7.7a-c respectively. Least squares linear regression was the applied to this data and the quality of the fits compared.

Discussion

Initial data analysis for the three loading rates provided skewness values (defined in Appendix 5A) of -0.23 for the low rate, -0.05 for the medium rate and 0.11 for the high rate. The closer to zero the skewness value is the less skewed the data is which indicates that the strengths for the low loading rate are skewed to a greater extent than for the higher loading rates. This makes the strengths for the low rate the least likely set of data to be normally distributed. If the strengths for the low loading rate are normally distributed, it follows that the strengths for the higher rates are also normally distributed.

The cumulative distribution function (defined in Appendix 5B) for the low loading rate strengths was plotted on respective probability paper for the three distributions (D'Agostino 1986). The correlation coefficients (r^2 values) for the linear regression fits to these plots were as follows:

Normal:	$r^2 = 0.98$
$Log_{(10)}$ Normal	$r^2 = 0.97$
2P Weibull	$r^2 = 0.96$

Since the correlation for the normal distribution is the highest this implies that the data is best described by a normal distribution.

Fig 7.7a

NORMAL DISTRIBUTION - EVALUATION
CHIPBOARD, AT R=0.1, AT LOW FREQUENCY

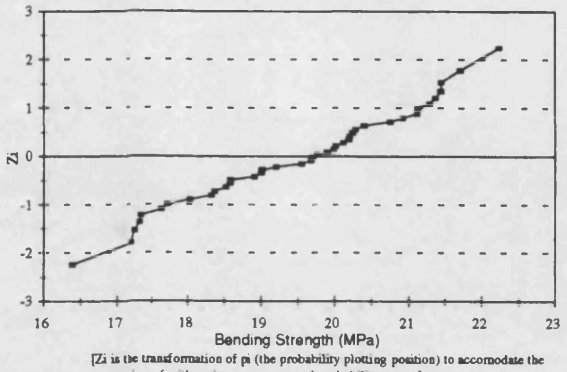

[Zi is the transformation of pi (the probability plotting position) to accomodate the conversion of arithmetic paper to normal probability paper.]

Fig 7.7b

LOG NORMAL DISTRIBUTION - EVALUATION
CHIPBOARD, AT R=0.1, AT LOW FREQUENCY

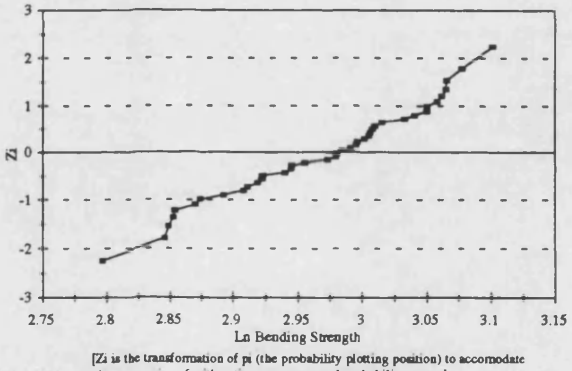

[Zi is the transformation of pi (the probability plotting position) to accomodate the conversion of arithmetic paper to normal probability paper.]

Fig 7.7c

2P WEIBULL DISTRIBUTION - EVALUATION
CHIPBOARD, AT R=0.1, AT LOW FREQUENCY

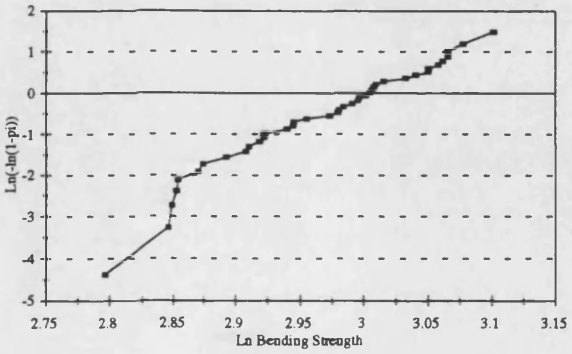

[pi is the probability plotting position]

7.5 Statistical Evaluation

With confidence in the hypothesis that the data belong to a normal distribution, it is appropriate to apply a statistical test based on this distribution, to provide a level of confidence that the mean strengths are different. The means only differ by a small amount, consequently it was decided to test whether the mean strengths for the low and high rates are significantly different. A t-test, paired two-sample for means, was applied to the data, for the low and high loading rates. This was the most appropriate test because it compares the difference between the strengths for the matched pairs of samples and the differences in the strengths are not lost as a result of the differences within the panels.

Discussion

The t-test concluded that the mean strengths for the low and high loading rates are different at the 95% level. The mean strength for the samples loaded at the medium rate falls between the means for the low and the high rates, so it is reasonable to assume that this also represents a real, but small difference. In conclusion the strength of the samples increased with the rate at which the load was applied from the low to the medium and from the medium to the high rate. The magnitude of this change in the measured strength is an increase of approximately 5% when the loading rate is increased from low to high, representing a rate increase of 125 times.

7.6 Interim Conclusions 1

1) The range/scatter of bending strengths increased as the rate of loading was increased from 0.0864 kN/s to 0.864 kN/s and from 0.864 kN/s to 10.8 kN/s.

2) The effect of the strength variability between boards and within the same board is minimised for chipboard by using side-matched sets of four samples.

3) The bending strength of the chipboard tested increased as the rate of application of stress was increased. The strength increase was 3.5% from the low to the medium rate and 1.9% from the medium to the high rate. These increases are masked by the inherent variability in chipboard unless side-matched samples are tested.

4) Strength variations between samples were not reduced when allowing for density variations by using the specific strengths.

5) Distribution analysis indicated that the bending strength data for chipboard is best represented by a normal distribution.

6) The increase in the strength of chipboard produced by increasing the loading rate from low to high was statistically significant at the 95% level.

8.0 FATIGUE IN CHIPBOARD

In this section the fatigue life performance for chipboard is reported in the form of S-N plots (stress versus $\log_{10}$ loading cycles to failure). This type of plot was introduced in Chapter 4. In figure 8.1a fatigue results for testing chipboard (referred to as chipboard A) at R=0.25, at high frequency, are compared to those for the chipboard (referred to as chipboard B) tested previously at R=0.25 by Thompson (1992) and Hacker (1991). The figures allow the fatigue performance of chipboard A to be compared with that of chipboard B tested previously. The fatigue life performance of chipboard A tested at R=0.25 and tested at R=0.1 can be compared in figure 8.1b.

The core work reported here evaluates the effect of frequency on the fatigue life performance of chipboard A. An S-N plot compares the performance at each of the three frequencies tested at R=0.1. In each plot the lines fitted to the fatigue data are least squares linear regression fits where approximately half of the data falls on each side of the line giving a 50% probability of failure below the line.

It is merely convention to plot fatigue data in the S-N format (Wöhler 1867) and for regression analysis the axes should be set out as an N-S plot. The independent variable should be plotted on the X-axis, and the dependent variable plotted on the Y-axis, as stated by McNatt (1977). This procedure is followed in this chapter to produce the regression lines despite them being plotted in the S-N format using the Wöhler convention. The regression equations are produced with stress treated as the independent variable, then inverted in the S-N plots.

Unless stated otherwise, chipboard refers to chipboard A, tested to evaluate the effect of frequency on the fatigue performance of chipboard.

8.1 Fatigue Performances of Chipboards A and B

Figure 8.1a is a normalised S-N plot comparing the fatigue life for chipboard A, to that for chipboard B tested previously by Thompson (1992) and Hacker (1991). The plot has been normalised with the strength of the side-matched static samples. Static bending strengths have been included in the regression analysis but runout values have been ignored. Both sets of data are for fatigue testing at R=0.25.

The equations for the regression lines in figure 8.1a and their respective correlation coefficients (r^2 values) were as follows:

Chipboard B (previous/old) tested at R=0.25 at high frequency, static data included, runouts excluded.

1) $\text{Log}(N) = -0.183(S) + 17.96 \qquad r^2 = 0.98$

Chipboard A (replacement/new) tested at R=0.25 at high frequency, static data included, runouts excluded.

2) $\text{Log}(N) = -0.151(S) + 14.61 \qquad r^2 = 0.99$

Fig. 8.1a

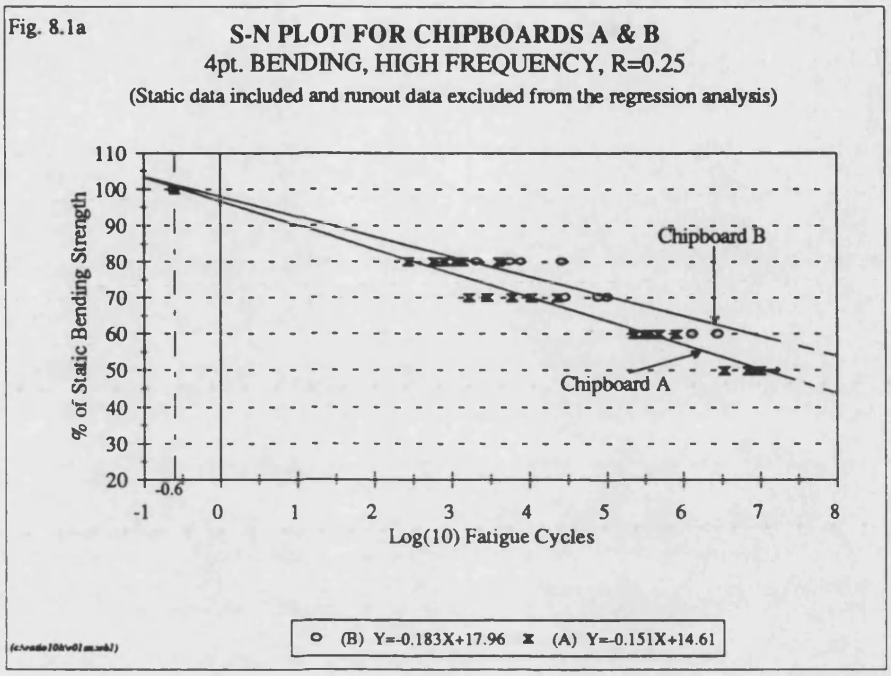

Fig. 8.1b

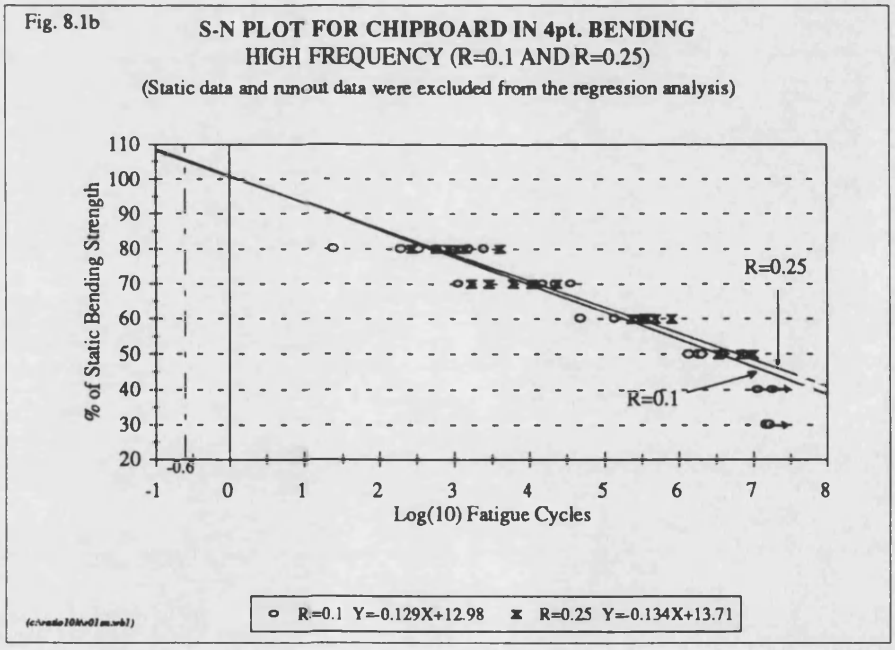

Discussion

The static bending strength data was included in the regression analysis for figure 8.1a and later in figure 8.3b but not in any of the other S-N plots. There are two opposing views regarding the inclusion of static strength data in the regression analysis of fatigue results. One view is that the ramp loading of samples to failure is not consistent with fatigue data because fatigue is repeated loading below the strength of the material. The problem with this view is that setting a given number of loading repetitions for a test to qualify as fatigue would be arbitrary. The second view point is that when a sample is ramp loaded to failure it has endured 1/4 of a fatigue loading cycle and should be included at this point on the S-N curve (-0.6 on the $\log_{(10)}$ cycles scale).

However, including static data in regression analysis forces the fitted line to intersect the one quarter fatigue cycle line close to the static strength (or 100% stress level). This means that the regression lines might be conservative at the high stresses but they may be dangerously optimistic for the lower stresses and for attempted extrapolations. For this reason static data is not generally included in the regressions. Static data was included in figure 8.1a because there were limited data points to fit regression lines for chipboard B and is later included in figure 8.3b as a comparison to figure 8.3a.

Including runout values in the regression analysis falsely assumes that unbroken samples have failed. This leads to an unjustified prediction of pessimistic fatigue lives and so runout points have been excluded from all regression analyses in this thesis.

At first it appears from figure 8.1a that chipboard B had a greater fatigue life than chipboard A. At high stress levels the two regression lines converge but as the stress level is lowered chipboard B has a steadily greater fatigue life than chipboard A. This view is distorted because of the following three factors:

1) The static tests for chipboard A were performed at significantly higher loading rates than those for chipboard B. This means that equivalent percentage stress levels are not identical. It was demonstrated in Chapter 7 that static tests performed at higher loading rates increase the apparent strength of the sample. Since the static strengths determine the percentage stress levels for the fatigue tests this means that the percentage stress values for chipboard A were of the order of 5% higher than those for chipboard B. Without this bias the two regression lines would move closer together.

2) In the testing of chipboard A the number of cycles chosen for a run out sample was 10^7. The limiting number of cycles for chipboard B tested previously was $5*10^6$

because of the limited testing time available. (Both sets of data contain runout points.) This causes the data for chipboard B to be distorted to a lower number of cycles to failure than chipboard A. This causes the regression lines to converge.

3) The lowest stress level tested for chipboard B was 60% of the static strength. This value was 50% for chipboard A. If 50% stress level tests had been performed for chipboard B the results may have caused the regression lines to converge.

Despite the appearance of figure 8.1a the inference from factors (1)-(3) is that the fatigue performances of chipboards A and B were indistinguishable when normalised by the static strengths. The two chipboards were marketed as the same product, from the same manufacturer but they were different in appearance. Chipboard A had a reduced formaldehyde content compared to chipboard B that was no longer in production.

8.2 Fatigue at R=0.25 and R=0.1 for Chipboard A

Figure 8.1b is a normalised S-N plot comparing the fatigue performance for chipboard A loaded at high frequency, at R=0.25 and at R=0.1. Static bending strengths and runout values were not included in the regression analysis.

The equations for the regression lines in figure 8.1b and their respective correlation coefficients were as follows:

Chipboard A tested at R=0.1 at high frequency, static data and runout data excluded.

3) $\text{Log}(N) = -0.129(S) + 12.98 \qquad r^2 = 0.90$

Chipboard A tested at R=0.25 at high frequency, static data and runout data excluded.

4) $\text{Log}(N) = -0.134(S) + 13.71 \qquad r^2 = 0.92$

Discussion

The fatigue performance of chipboard tested at R=0.1 was slightly inferior to that tested at R=0.25 as shown in figure 8.1b. This agrees with the S-N lines and constant life diagram produced by Thompson *et al* (1994), included as figures 4.9 and 4.10 respectively, in section 4.2.1. In these figures, it can be seen that the fatigue life reduces sequentially as the R ratio is reduced, from 0.75 to 0.5, to 0.25, to 0.01. In figure 4.9 the S-N line for R=0.1 would be expected to fall just below that for R=0.25 as it does in figure 8.1b. This result indicates that the constant life diagram for the replacement chipboard may be similar to that presented by Thompson et al (1994).

8.3 Effect of Frequency Upon Fatigue Life

Figure 8.2 is an S-N plot comparing the normalised fatigue life data for chipboard tested at R=0.1, at low, medium and high frequencies. The sets of fatigue data correspond to stress application rates of 1.2, 12 and 150 MPa/s respectively. The static samples used to obtain the 100% stress values were tested at a loading rate of 0.0864 kN/s for the low frequency tests, 0.864 kN/s for the medium frequency tests and 10.8 kN/s for the high frequency tests. These rates label the test frequencies as low, medium and high as explained in section 6.3. Static bending strengths and runouts values are again not included in the regression analysis.

The fatigue lives (cycles to failure) for the low, medium and high frequency tests are provided in tables 8.1 and 8.2. Table 8.1 provides a comparison between the mean sample lives at each stress level for the different frequency ranges. Where runout results have been included they are at values of 10^5 loading cycles for low frequency testing, 10^6 for medium frequency testing and 10^7 for the high frequency testing.

Table 8.2 is similar to table 8.1 but compares the median lives for each stress level at each of the three frequencies instead of the mean lives. Using the median prevents unusually high or low values from adversely influencing the data analysis. The median and mean values are very similar implying that the spread of the sample lives is close to a normal distribution as would be expected from the distribution analysis for bending strengths that was reported in section 7.4. The populations of samples tested at each stress level, for each loading condition, are not large enough to justify distribution analysis of the fatigue results.

The equations for the regression lines in the normalised plot for evaluating the effect of frequency on the fatigue performance of chipboard and their respective correlation coefficients were as follows:

Chipboard tested at R=0.1 at low frequency, static and runout data excluded.

5) $\text{Log}(N) = -0.099(S) + 9.79 \qquad r^2 = 0.89$

Chipboard tested at R=0.1 at medium frequency, static and runout data excluded.

6) $\text{Log}(N) = -0.119(S) + 11.76 \qquad r^2 = 0.96$

Chipboard tested at R=0.1 at high frequency, static and runout data excluded.

7) $Log(N) = -0.129(S) + 12.98$ $r^2 = 0.90$

The r^2 values show that the correlation was greatest at the medium frequencies.

8.3.1 Fatigue Life as a Function of Bending Strength

The regression lines for the low, medium and high frequency testing of chipboard have been re-evaluated using the stress values in MPa instead of the normalised values. Figure 8.3a shows the three regression lines calculated with the static strengths and runout results excluded. This has then been re-plotted in figure 8.3b with the static data included to draw the lines closer together close to the one quarter loading cycle point to highlight the trends.

The equations for the regression lines in figure 8.3a showing the stress data for chipboard tested at all three frequencies and their respective correlation coefficients were as follows:

Chipboard tested at R=0.1 at low frequency, static and the runout data excluded.

8) $Log(N) = -0.410(S) + 8.30$ $r^2 = 0.73$

Chipboard tested at R=0.1 at medium frequency, static and the runout data excluded.

9) $Log(N) = -0.360(S) + 8.89$ $r^2 = 0.60$

Chipboard tested at R=0.1 at high frequency, static and the runout data excluded.

10) $Log(N) = -0.554(S) + 11.62$ $r^2 = 0.82$

The equations for the regression lines in figure 8.3b and their respective correlation coefficients were as follows:

Chipboard tested at R=0.1 at low frequency, static data included but runouts excluded.

9) $Log(N) = -0.456(S) + 8.10$ $r^2 = 0.72$

Chipboard tested at R=0.1 at medium frequency, static data included but runouts excluded.

10) $\text{Log}(N) = -0.489(S) + 9.99 \qquad r^2 = 0.78$

Chipboard tested at R=0.1 at high frequency, static data included but runouts excluded.

11) $\text{Log}(N) = -0.579(S) + 11.04 \qquad r^2 = 0.75$

In order to confirm that fitting least squares linear regression lines to the fatigue data are appropriate, the residuals have been plotted in figures 8.4a-c. The residuals are the differences between the values predicted by the regression equations and the experimental observations corresponding to the regression lines fitted to the normalised fatigue life data for the low, medium and high frequency testing plotted in figure 8.2.

A 50% chance of failure, as predicted by the least squares regression plots, is not safe enough for use by designers so the lower bounds of the 95% confidence intervals have been plotted, figure 8.5, for the regression lines in the normalised plots. The 95% confidence interval means that there is a 2.5% chance that the true population mean is below the lower interval.

Fig. 8.2

S-N PLOT FOR CHIPBOARD IN 4pt. BENDING
R=0.1, LOW, MEDIUM & HIGH FREQUENCIES
(Static data and runout data were excluded from the regression analysis)

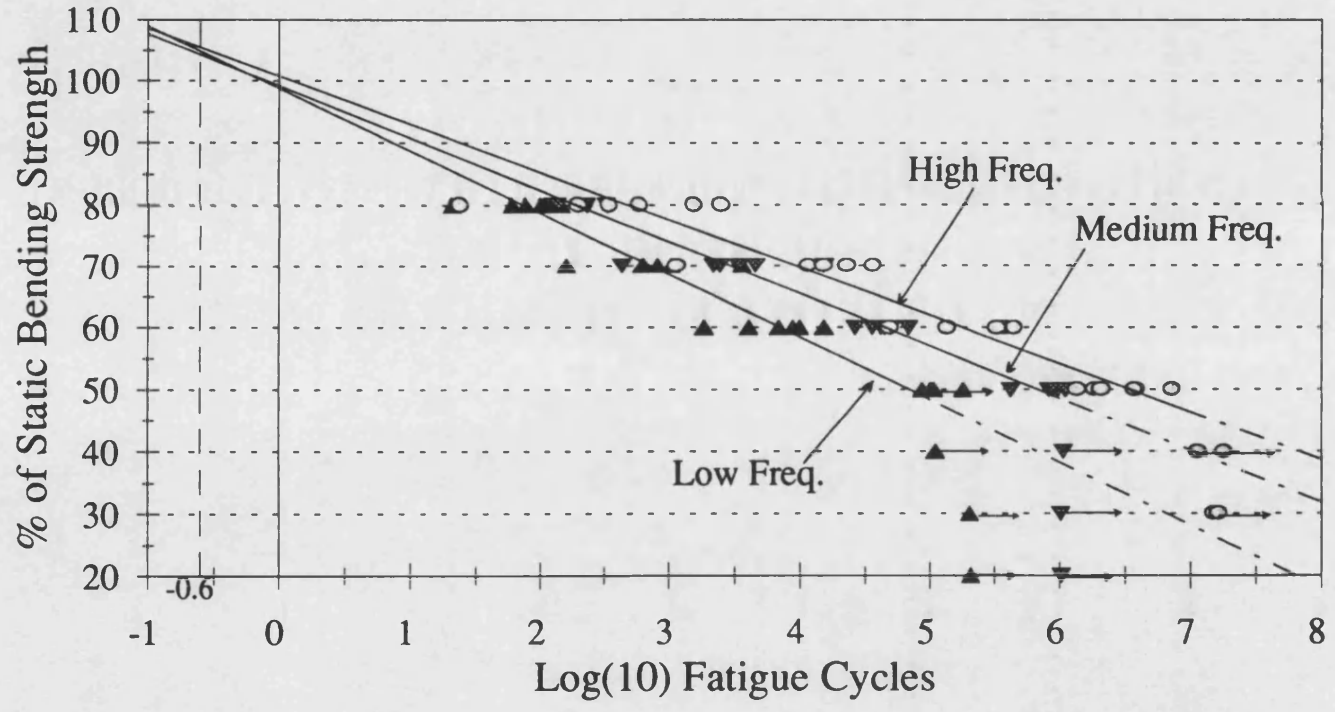

▲ Low Freq. Log(N)=-0.099(S)+9.79
▼ Medium Freq. Log(N)=-0.119(S)+11.76
○ High Freq. Log(N)=-0.129(S)+12.98

(c:\cost508\sn_low.wb1)

Table 8.1 Effect of loading frequency on the mean fatigue life of chipboard.

	LOW FREQUENCY (0.0864 kN/s)		MEDIUM FREQUENCY (0.864 kN/s)			HIGH FREQUENCY (10.8 kN/s)		
Relative Rate	**1**		**10**			**125**		
Stress Level	Mean Fatigue life ± Standard Deviation (No of Cycles)	Fraction of Samples Failed	Mean Fatigue Life ± Standard Deviation (No of Cycles)	Fraction of Samples Failed	Increased Life Compared to Low Freq. (Multiplied by)	Mean Fatigue Life ± Standard Deviation (No of Cycles)	Fraction of Samples Failed	Increased Life Compared to Low Freq. (Multiplied by)
80%	86 ± 43	6/6	212 ± 75	6/6	**2.5**	873 ± 972	6/6	**10.2**
70%	1146 ± 1250	6/6	4 731 ± 5 375	6/6	**4.1**	17 134 ± 11 834	6/6	**15.0**
60%	7768 ± 4777	6/6	44 737 ± 14 632	6/6	**5.8**	286 678 ± 157 954	6/6	**36.9**
50%	N/A	1/6	784 587 ± 242 185	4/6	NA	3 358 866 ± 2 135 773	6/6	NA
40%	100 000(Runout)	0/1	1 000 000(Runout)	0/1	NA	10 000 000(Runout)	0/2	NA
30%	100 000(Runout)	0/1	1 000 000(Runout)	0/1	NA	10 000 000(Runout)	0/2	NA
20%	100 000(Runout)	0/1	1 000 000(Runout)	0/1	NA	Freq. too high to test	0/0	NA

NA = applies to those conditions where few or no samples failed for the duration of the tests.
Means calculated from failed samples only.

Table 8.2 Effect of loading frequency on the median fatigue life of chipboard.

	LOW FREQUENCY		MEDIUM FREQUENCY			HIGH FREQUENCY		
Relative Rate	**(0.0864 kN/s) 1**		**(0.864 kN/s) 10**			**(10.8 kN/s) 125**		
Stress Level	Sample Lives (Cycles) and **Median Life (M)**	Fraction of Samples Failed	Sample Lives and **Median Life (M)**	Fraction of Samples Failed	Increased Life Compared to Low Freq. (Multiplied by)	Sample Lives and **Median Life (M)**	Fraction of Samples Failed	Increased Life Compared to Low Freq. (Multiplied by)
80%	21, 60,78,100 108,147 **M = 89**	6/6	130,139,202,228, 236,334 **M = 215**	6/6	**2.4**	24,200,349,583, 1564,2519 **M = 466**	6/6	**5.2**
70%	164,614,638,806 1024,3632 **M = 722**	6/6	436,2183,2457,3359, 4616,15336 **M = 2 908**	6/6	**4.0**	1146,11468,15335, 15459,22964,36434 **M = 15 397**	6/6	**21.3**
60%	1852,4079,6871, 8963,9260,15580 **M = 7 917**	6/6	26352,35629,41938, 44558,50554,69393 **M = 43 248**	6/6	**5.5**	49477,139037, 337511,346277, 385810,461955 **M = 341 894**	6/6	**43.2**
50%	88285,101075+, 103121+,105911+ 183598+	1/6	431184,837667, 895045,974452, 1088931+,1123401+ **M = 934 749**	4/6	NA	1534263,1862866, 2086482,3698783, 3823711,7269408 **M = 2 892 633**	6/6	NA
40%	(1 Sample)	0/1	1075351+	0/1	NA	18240189+, 11380003+	2	NA
30%	(1 Sample)	0/1	1019403+	0/1	NA	16567032+, 15299002+	2	NA
20%	(1 Sample)	0/1	1043001+	0/1	NA	Freq. too high to test	0	NA

NA = applies to those conditions where few or no samples failed for the duration of the tests.
+ denotes a runout samples.

Fig. 8.3a

S-N PLOT FOR CHIPBOARD IN 4pt BENDING
R=0.1, LOW, MEDIUM & HIGH FREQUENCIES
(Static data and runout data excluded from the regression analysis)

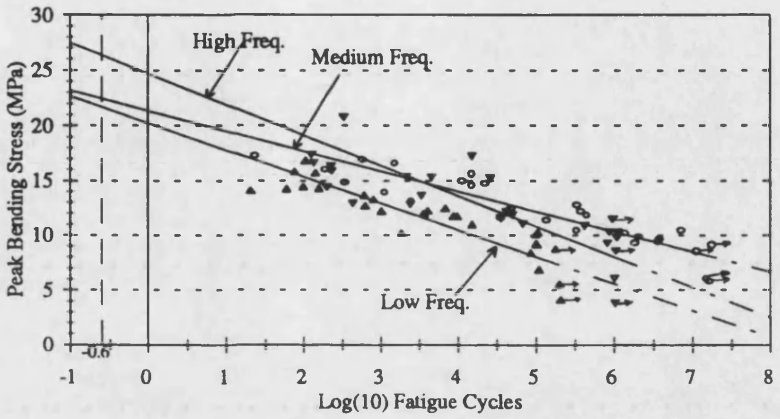

▲ Low Freq. Log(N)=-0.410(S)+8.30 ▼ Medium Freq. Log(N)=-0.360(S)+8.89
○ High Freq. Log(N)=-0.544(S)+11.62

Fig. 8.3b

S-N PLOT FOR CHIPBOARD IN 4pt BENDING
R=0.1, LOW, MEDIUM & HIGH FREQUENCIES
(Static data included and runout data excluded from the regression analysis)

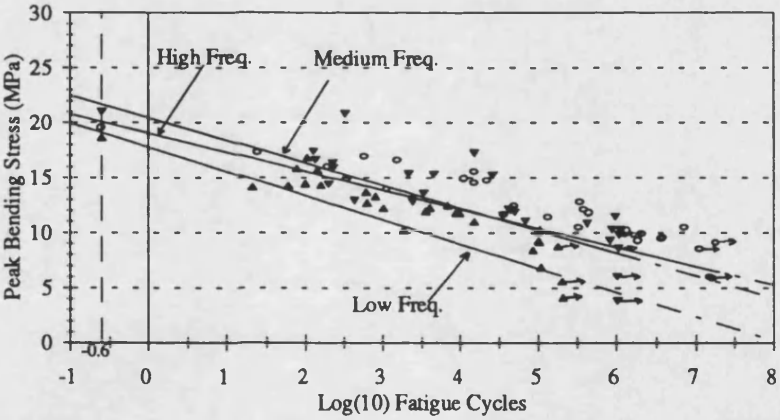

▲ Low Freq. Log(N)=-0.456(S)+8.10 ▼ Medium Freq. Log(N)=-0.489(S)+9.99
○ High Freq. Log(N)=-0.579(S)+11.04

Fig. 8.4a

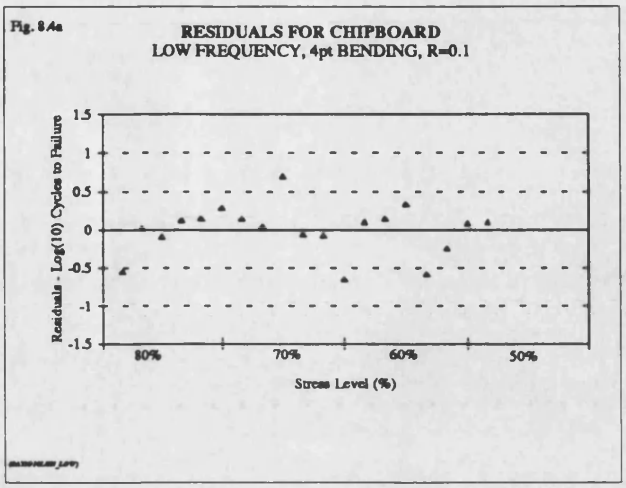

Fig. 8.4b

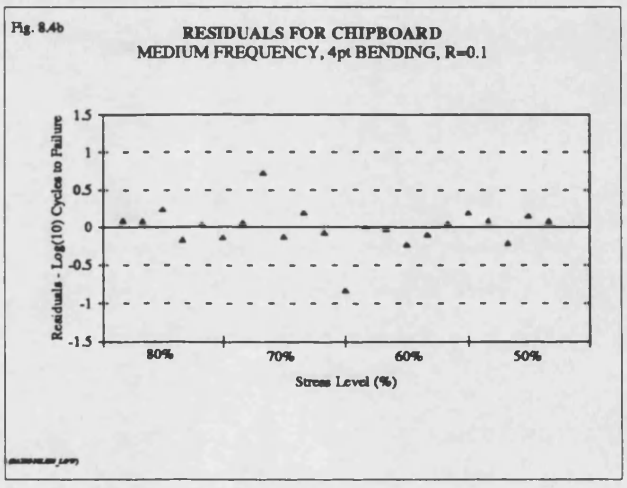

Fig. 8.4c

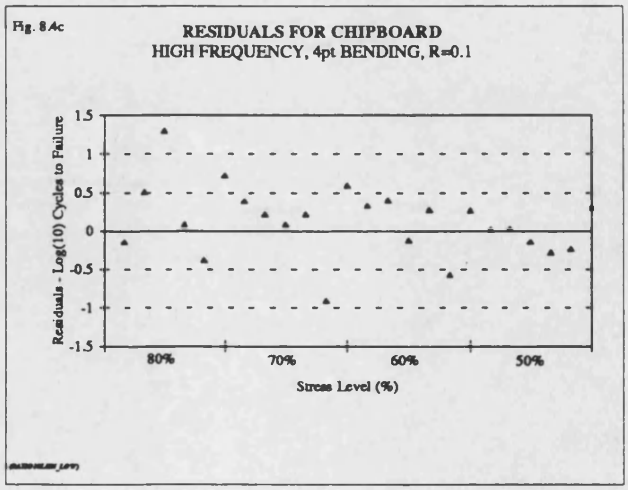

Fig. 8.5

95% CONFIDENCE INTERVALS FOR CHIPBOARD
R=0.1, LOW, MEDIUM & HIGH FREQUENCIES
(Static data and runout data were excluded from the regression analysis)

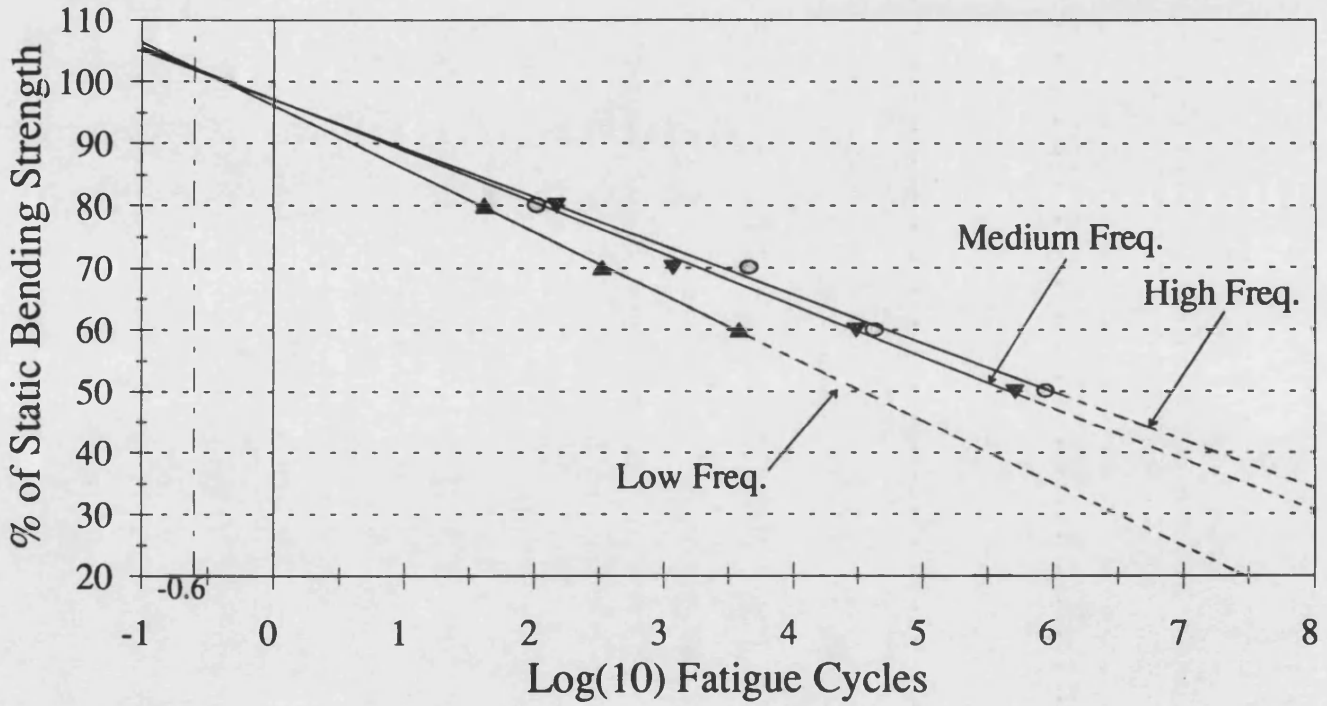

▲ Low Freq. Log(N)=-0.098(S)+9.43
▼ Medium Freq. Log(N)=-0.120(S)+11.68
○ High Freq. Log(N)=-0.127(S)+12.34

(c:\cost508\sn_low.wb1)

Discussion

The three sets of data and regression lines plotted in figure 8.2 for the low, medium and high frequency loading allow the three loading regimes to be compared. All testing was performed using identical loading configurations. The fatigue and static tests for each frequency were performed at equivalent rates. These were 1.2 MPa/s for low frequency, 12 MPa/s for medium frequency and 150 MPa/s for high frequency. The only difference is the number of data points included in the regression analysis at the 50% stress level. One point is included for low frequency, four points for medium frequency and six points for high frequency. The regression line for the low frequency loading intersects the 1/4 cycle point ($Log_{(10)}$ N = -0.6) at 105.0% of the ultimate stress. This value was 104.3% for the medium frequency and 105.6% of the ultimate stress for the high frequency loading. All three values are close to the 100% stress value showing that the static tests are closely related to the fatigue tests.

The regression lines demonstrate that, for the same stress level, testing at frequencies reduced by approximately one and then two orders of magnitude causes failure at fewer fatigue cycles than testing at the higher frequencies. This is displayed numerically in table 8.1. For the tests at the 80, 70 and 60% stress levels the mean fatigue life is reduced by 2.5, 4.1 and 5.8 times respectively by reducing the frequency of loading by a factor of ten (medium to low). Reducing the frequency by a factor of 125, (high to low) reduces the mean fatigue life at the same three stress levels by 10.2, 15 and 36.9 times respectively. A very similar trend can be seen for the change in median life as a result of the change in loading frequency. At the 50% stress level there was only one sample failure for the low frequency testing so this has not been used for comparison with the higher frequencies. However, there was a significant number of failures at this stress level for the medium and high frequencies. The fatigue life was reduced by a factor of 3.92 by reducing frequency by 12.5 times (high to medium).

This has serious implications for design when applying fatigue data for chipboard to practical situations. The frequency of loading that will be encountered during service must be evaluated carefully because if data from high frequency testing was used to predict the fatigue life for a load history at a lower frequency, a potentially dangerous overestimate of the material's life might occur. It will be essential to include a safety/scaling factor to account for the frequency of loading in fatigue design.

Loading at lower frequencies allows the chipboard time to respond viscoelastically. At higher frequencies the material does not have enough time to respond to the changing load and behaves almost elastically leading to the increased fatigue life. It must be

remembered that the stress levels for the high frequency loading are essentially about 5% higher than those for the low frequency. The static tests were performed at the same rate as the fatigue tests so the higher frequency tests were performed at slightly higher stress levels because the static samples were about 5% stronger due to the rate of loading at which they were tested. The lower stress levels have not been included in this discussion as it is uncertain what life the runout samples would have survived to.

McNatt (1977) stated that the S-N curves for wood and wood based materials should be double concave: concave downwards at high stress levels to pass through the 100% stress level at one cycle of stress and concave upward at the lower stress levels as shown by Kyanka (1980), see figure 4.8. This often results in the portion of the curve that passes through the captured data being a straight line. This is confirmed by the regression lines in figure 8.2 which all pass through the one stress cycle point slightly greater than the 100% stress level at about 105% stress and by plotting the residuals. Kyanka (1980) indicated a fatigue limit for wood based materials, this would account for the concave upward portion of the curve and agrees with section 8.7 of this thesis.

Comparing figure 8.2 with figure 8.3a demonstrates that the fatigue results for chipboard are less variable when normalised than when plotted as stress values in MPa. The correlation coefficients are considerably higher when the data has been normalised. The reason for this is that the normalised data reflects the variation within matched sets of four samples not the variations for the whole panels as in figure 8.3a. It has already been shown in Chapter 7 that the use of matched sets of four samples reduces the inherent variability of chipboard.

The inclusion of the static strength data in the regression lines with the Y axis plotted as stress values (MPa), as in figure 8.3b, improves the correlation coefficients compared with figure 8.3a but not to the same degree as using the normalised values.

Plotting the residuals for the low, medium and high frequency normalised fatigue lives shown in figures 8.4a-c justifies the use of straight line regression fits. In each of the three plots the residuals ($\log_{(10)}$ cycles to failure) lie in approximately even proportions on each side of the zero line for residuals indicating that a straight line fit is appropriate. If the regression lines in figure 8.2 were extrapolated they would probably still be double concave but there is no way of knowing when the runout samples would have failed. This means that if extrapolation of the S-N curve is attempted care should be taken to be conservative and the straight line should be adopted.

8.3.2 95% Confidence Intervals

The lower bounds of the 95% confidence intervals, figure 8.5, were calculated for each stress level using the mean lives and the associated standard errors (Rowntree 1981). Least squares linear regression was applied to the resulting confidence intervals to produce the straight lines plotted. Figure 8.5 shows that the fatigue life for low frequency loading, which is by far the worst case, exceeds 10^7 loading cycles at the 20% stress level. However, this would be reduced by numerous safety factors in a real life situation that would considerably reduce the design life. The regression lines also demonstrate that increasing the loading frequency still increases the fatigue lives with the variability in the sample lives accounted for since the regression lines are in the same order as in figure 8.2.

The life prediction for the low stress levels at all three frequencies remains very conservative because the lives are predicted from the high stress level tests where the samples failed. This highlights the need for other methods of predicting the fatigue life beyond the measured failures such as the use of hysteresis loop capture.

8.4 Runouts

Runouts are samples that did not fail when subjected to a pre-determined number of fatigue loading cycles after which the testing was stopped. The designated number of cycles for a runout reduced as the frequency was reduced due to time limitations. This resulted in the fatigue tests being stopped after 10^7 cycles for high frequency loading, 10^6 cycles for medium frequency and 10^5 cycles for low frequency loading. The surviving samples (runouts) and their side-matched creep partners were then statically tested to failure to determine their residual bending strengths. This allowed the change in strength resulting from fatigue and creep loading to be compared.

For the high frequency loading at R=0.25 there was only one runout sample from the twenty three fatigue samples tested. This was sample C-53 which was tested at the 50% stress level. Twenty eight samples were tested at R=0.1 at high frequency, producing four runout samples, but all four were for stress levels of less than 50%. The residual strengths of these runout samples and their side-matched creep partners are shown in table 8.3. None of the creep partners failed within the duration of the runout fatigue tests.

Table 8.3 Residual bending strengths of runout samples and their side-matched creep partners (high frequency loading) at R=0.25 and R=0.1.

Fatigue Sample	R ratio	Stress Level %	Width mm	Thickness mm	Failure Load KN	Residual Strength MPa	Strength Change %
C-53	0.25	50	50.0	17.9	1.3762	19.30	-8.0
C-78	0.1	40	50.1	17.9	1.6981	23.80	+4.8
C-111C	0.1	40	50.1	17.9	1.5457	21.66	+1.6
C-89C	0.1	30	50.0	17.9	1.5978	22.44	+15.4
C-134C	0.1	30	49.6	17.9	1.3107	18.56	-7.2

Creep Sample		Stress Level %	Width mm	Thickness mm	Failure Load KN	Residual Strength MPa	Strength Change %
C-53C	NA	50	49.9	17.9	1.3113	18.38	-12.0
C-78C	NA	40	50.0	17.9	1.7151	24.09	+6.1
C-112	NA	40	50.1	18.0	1.5143	20.99	-1.5
C-90	NA	30	50.1	17.9	1.5219	21.33	+9.7
C-135	NA	30	50.1	18.0	1.3968	19.36	-3.2

Twenty seven fatigue samples were tested at R=0.1 at medium frequency and five samples survived more than 10^6 loading cycles required for a runout, two of these were tested at the 50% stress level. This set of samples was stored in the conditioning cupboard until this section of testing was complete before the residual bending strengths of the runouts were measured. The residual strengths of the runout samples are shown in table 8.4 together with those for the side-matched creep partners. Again none of the creep partners had failed within the duration of the fatigue runout tests.

Table 8.4 Residual bending strengths of runout samples and their side-matched creep partners (medium frequency loading) at R=0.1.

Fatigue Sample	R ratio	Stress Level %	Width mm	Thickness mm	Failure Load kN	Residual Strength MPa	Strength Change %
C-174C	0.1	50	17.87	50.08	1.1089	15.6	-20.53
C-183	0.1	50	17.91	49.97	1.1465	16.09	-21.82
C-161C	0.1	40	18.01	50.16	1.6281	22.52	+4.74
C-184C	0.1	30	17.90	50.04	1.3928	19.51	+3.65
C-166C	0.1	20	17.94	50.14	1.3889	19.37	-1.41
Creep Sample		Stress Level %	Width mm	Thickness mm	Failure Load kN	Residual Strength MPa	Strength Change %
C-175	NA	50	17.83	50.03	1.1770	16.65	-15.18
C-183C	NA	50	17.94	50.01	1.2066	16.87	-18.03
C-162	NA	40	18.01	50.02	1.5749	21.84	+1.56
C-185	NA	30	17.94	50.01	1.3826	19.33	+4.5
C-167	NA	20	17.92	49.99	1.3481	18.89	+1.10

Eight out of the twenty seven fatigue samples tested at R=0.1 at low frequency were runouts, surviving more than the 10^5 cycles, with five of the runouts tested at the 50% stress level. Like the runouts for the medium frequency testing this set of runout samples was also stored in the conditioning cupboard until this section of testing was completed before the residual bending strengths were measured. The residual strengths of these runout samples are shown in table 8.5 together with the residual strengths of the side-matched creep partners. Three of the creep partners failed within the duration of the fatigue tests at this frequency.

Table 8.5 Residual bending strengths of runout samples and their side-matched creep partners (low frequency loading) at R=0.1.

Fatigue Sample	R ratio	Stress Level %	Width mm	Thickness mm	Failure Load kN	Residual Strength MPa	Strength Change %
C-213	0.1	50	50.0	17.9	1.1311	15.97	-8.6
C-220	0.1	50	49.9	17.9	1.2512	17.56	-5.2
C-226C	0.1	50	50.0	18.0	1.2987	18.01	-2.0
C-253C	0.1	50	49.9	17.9	1.2896	18.14	-10.0
C-268	0.1	50	49.2	18.0	1.1379	16.11	-21.8
C-236C	0.1	40	50.0	17.9	1.1250	17.51	+3.2
C-249C	0.1	30	50.0	17.9	1.2865	18.15	-2.6
C-264C	0.1	20	50.0	18.0	1.3662	19.03	-7.5

Creep Sample		Stress Level %	Width mm	Thickness mm	Failure Load kN	Residual Strength MPa	Strength Change %
C-213C	NA	50	NA	NA	NA	NA	Failed
C-219C	NA	50	NA	NA	NA	NA	Failed
C-227	NA	50	49.9	18.0	1.3409	18.68	+1.7
C-253C	NA	50	49.9	17.9	1.2791	18.02	-10.6
C-268C	NA	50	NA	NA	NA	NA	Failed
C-237	NA	40	49.9	17.9	1.2848	16.13	-4.9
C-250	NA	30	49.7	17.9	1.2848	18.20	-2.3
C-265	NA	20	49.8	18.0	1.4589	20.41	-0.8

Discussion

There was no consistent trend in residual strength versus static strength for both the fatigue and creep samples from the high frequency testing at R=0.25 and R=0.1. The change in strength for the fatigue samples range from a strength reduction of 8.0%, to an increase of 15.4% with respect to the mean strength of the outside two samples from their respective matched sets of four samples. Both results could be due to an unusually weak or strong sample respectively not predicted from the mean static strength of the outside samples in the respective side-matched sets. Increases in strength may be due to drying of the chipboard during fatigue cycling and the strength reductions may be due to fatigue damage. However, no conclusions can be drawn from such varied results. The same results were observed for the creep samples where values for the change in strength varied from a 12.0% decrease in strength to a 9.7% increase. Again no conclusions can be drawn from this. The strength increases observed for the fatigue samples may be due to drying of the chipboard as a result of adiabatic heating at the higher frequencies. This is, however, unlikely because similar increases were observed for creep samples where adiabatic heating is definitely not an influencing factor.

These results are similar to those observed by Thompson (1992) for high frequency testing of chipboard. The two runout samples (tested at R=0.5 and R=0.75) tested in this work showed strength reductions of approximately 5% but were not conclusive.

The residual strength results for the medium frequency testing are more useful. Both of the runout samples tested at the 50% stress level show strength decreases of more than 20% compared to the mean bending strength of their respective outside matched partners. When the scatter of strengths within side-matched sets of four samples is considered this shows that the samples have definitely been damage as a result of the fatigue loading. This appears reasonable because four out of the six of the fatigue samples tested at this stress level failed so it is likely that the two surviving samples were close to failure when the fatigue tests were stopped. For the high frequency loading it is possible that any decrease in strength resulting from fatigue loading was not observed due to the static test rate being too high for the damage incurred during fatigue to contribute to the fracture of the samples. The side-matched creep partners to these two medium frequency runouts also showed similar strength decreases implying that they were also approaching failure when the load was removed. As the frequency was reduced from high to medium, and from medium to low, the time duration of the fatigue and creep tests increased. This is why the creep partners to the high frequency runouts do not show a strength decrease but some of those at the lower frequencies

do. Four out of six of the fatigue samples failed at the 50% stress level, at medium frequency but none of the creep samples failed. This implies that more damage is produced by the fatigue loading than creep loading at this stress level, and frequency.

The lower stress level samples tested at medium frequency (<50%) showed no consistent result. One sample reduced very slightly in strength whilst the other two increased. However, none of these changes was close to the magnitude of decrease seen for the 50% stress samples. The reason for this is thought to be that the runout samples from the tests at stress level below 50% were not close to failure when the testing was stopped unlike those samples at the 50% stress level.

The runout results from the low frequency testing were similar to those for the medium frequency testing. There were five runouts at the 50% stress level all of which displayed reductions in strength. However, two of these increases were inconclusive because they were not large enough and two others were borderline at about 10%. The fifth sample showed a strength reduction of over 20%. These results imply that fatigue loading at 50% stress and above does reduce the strength of the chipboard but for the 50% stress level not until close to the failure life of the material. This agrees with the literature. Rotem (1988) showed that the strength of fibrous composite materials did not degrade until the final 10% of the fatigue life. Suzuki and Saito (1984) showed that there was no decrease in the internal bond strength of chipboard fatigued in tension until immediately prior to failure.

For the low frequency testing three of the creep samples failed prior to their side-matched fatigue partners. This means that creep loading may be more damaging than fatigue loading once the fatigue loading is below a threshold frequency. Again the changes in strength for the samples loaded at stress levels below 50% showed no conclusive trends. This enhances the view that these samples were not approaching failure when the tests were stopped.

8.5 Stress versus Strain Hysteresis Loops (First and Last)

The following section examines captured hysteresis loops and the parameters derived from them. The results for the high frequency testing of chipboard at R=0.25 will not be discussed because the tests were used to set-up and adapt the FDAS to capture hysteresis loops using the digital load controller.

Figures 8.6a-c show the first and last hysteresis loops captured by the FDAS for a sample tested at medium frequency at each of the stress levels 70, 50 and 30%. These plots provide a pictorial view of the changes in the hysteresis loop parameters as a result of fatigue loading. The first loops captured are not the loops for the first cycle of loading and each fatigue test may have continued long after the last loop was captured. At this stage of the tests hysteresis loops were captured at hourly intervals for the 70% stress level and at daily intervals for the 50 and 30% stress level. Hysteresis loops were captured throughout all the fatigue tests, for all stress levels, at each of the three frequencies. They contain the loop parameters described in section 6.6. Figure 8.7 shows an example of the hard copy of a hysteresis loop produced at the printer for a sample loaded at R=0.1 at 70% stress at medium frequency. All of the printouts displayed the starting date and time of the test, the elapsed time, the loop number, the fatigue test frequency, the maximum and minimum fatigue stresses, the maximum and minimum fatigue strains, the hysteresis loop area, the loop slope (dynamic modulus) and the stress and strain for the creep samples.

The hysteresis loops had the same appearance for all three frequencies but changed with the stress level applied and so first and last hysteresis loops are not presented for the low and high frequency tests. They are also very similar to the loops shown by Thompson *et al* (1994). However the parameters from the captured hysteresis loops for all the stress levels at all three frequencies are discussed in the following sections of this chapter.

Discussion

The hysteresis loops reduce in size with decreasing stress level as smaller stresses produce smaller strains. In each test the last loop increases in area and moves to a greater microstrain compared to the first loop. This shows that damage has been produced in the sample and therefore the energy dissipated per cycle of loading has increased and creep has occurred. The parameters derived from the loops are discussed in the sections that follow.

Fig. 8.6a FIRST & LAST CAPTURED HYSTERESIS LOOPS
CHIPBOARD TESTED AT R=0.1, 70% STRESS

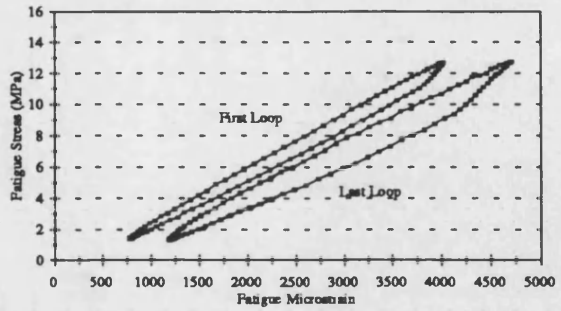

Fig. 8.6b FIRST & LAST CAPTURED HYSTERESIS LOOPS
CHIPBOARD TESTED AT R=0.1, 50% STRESS

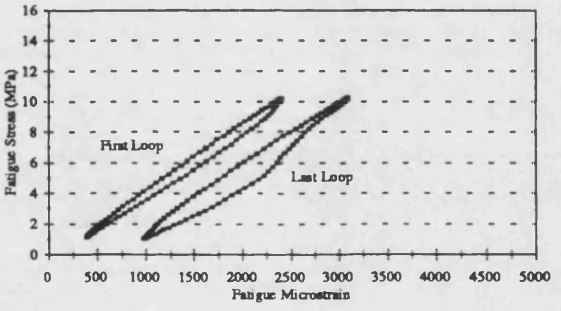

Fig. 8.6c FIRST & LAST CAPTURED HYSTERESIS LOOPS
CHIPBOARD TESTED AT R=0.1, 30% STRESS

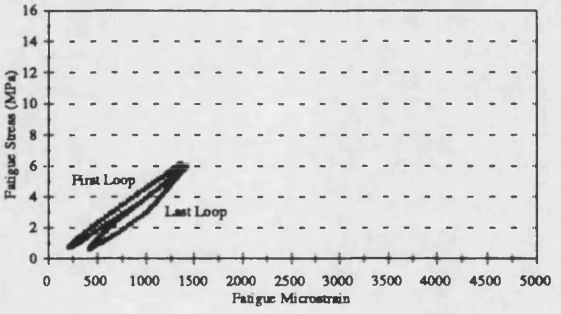

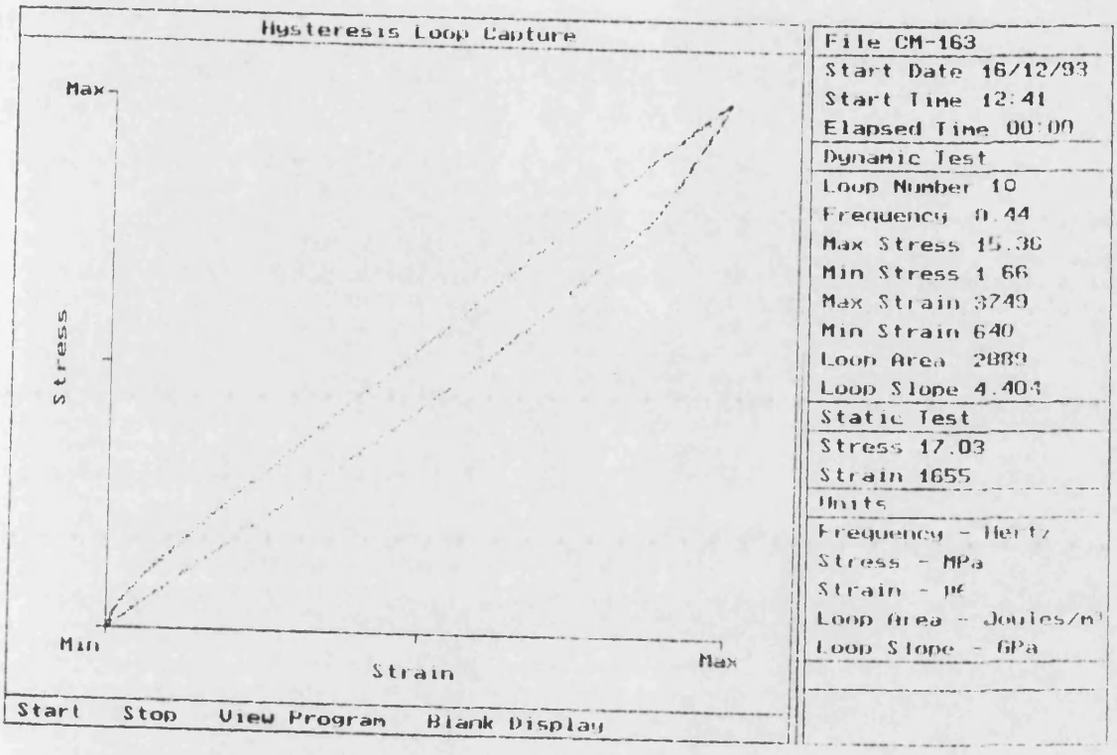

Fig 8.7 Hysteresis loop captured for medium frequency loading of chipboard at the 60% stress level, at R=0.1.

8.6 Creep and Fatigue Deflections

Throughout all testing the centre point deflections of the creep and the fatigue samples were measured using LVDT displacement transducers, as was explained in Chapter 6. The centre point deflection measurements and the applied loads were fed into the beam equations shown in Appendix 1. Parameters including the creep, maximum fatigue and minimum fatigue microstrains were calculated. The maximum fatigue microstrain is the microstrain produced at the surface of the sample when the hydraulic ram is at the top of its stroke and the minimum fatigue microstrain is the microstrain produced at the surface of the sample when the ram is at the bottom of its stroke.

Before examining the values and graphs it is essential to remember that the first hysteresis loop and hence the first microstrain measurement is for the first loop captured by the FDAS, rather than the loop from the first loading cycle. The first loop captured, will be the loop from the first or the second loading cycle for samples tested at low frequency. For the medium frequency testing this will be after approximately thirty to sixty cycles and for the high frequency testing this may have been captured anything up to a few hundred cycles after the start of the test. Also, for all three frequencies the last hysteresis loop captured and hence the last fatigue microstrain measurement may be for the last loading cycle, or they may have been captured up to twenty four hours before this for the longer, lower stress level tests. The same is true for the ultimate strain produced during the creep tests. Once the tertiary stage of creep is reached in which the strain rate increases dramatically, the sample fails rapidly and it is unlikely that the last creep strain value will be captured by the FDAS. However, the last loop capture and hence fatigue microstrain will be the smallest number of cycles away from the end of the test at the lowest frequencies and the highest stress levels. This is because in the shortest tests the loop captures are still in close succession and have not reached the stage when the capture interval is considerably increased.

For each of the three frequencies, six samples were tested at the 80, 70, 60 and 50% stress levels. At the low and medium frequencies one sample was tested at the 40, 30 and 20% stress levels because these tests were always runouts and required a large proportion of the machine time available. At the high frequency two samples were tested at the 40 and 30% stress levels. However, a sample was not tested at the 20% stress level because the frequency would have been too high. For this reason the data for the stress levels where six replicates were tested can be considered with greater confidence than those where only one or two replicates were tested.

Figures 8.8a-c, 8.9a-c and 8.10a-c show the median initial, median final and median changes in microstrain for chipboard with changing stress level from 80% to 20%. Figures 8.8a-c show the median microstrain trends for the side-matched creep samples tested. Figures 8.9a-c show the median maximum microstrains for the fatigue samples, with the ram at the top of its stroke, with the peak stress applied to the sample and figures 8.10a-c show the median minimum microstrains for the fatigue samples, with the ram at the bottom of it's stoke, with 10% of the peak stress applied to the sample.

Table 8.6 shows the median values for the initial, final and change in microstrain for the creep samples and the maximum and minimum initial, final and change in microstrain for the fatigue samples. This is for all the stress levels tested at all three frequencies. The ranges of values for the initial and final microstrains for the fatigue and creep samples are shown in table 8.7 to give an indication of the spread of the data for different samples tested at the same stress levels and frequencies.

The colour plot, figure 8.11, shows the maximum fatigue microstrains for all twenty seven fatigue samples tested at low frequency plotted with respect to the factored time. This considers the test time as a proportion of the total time required for the fatigue sample to fail or for the fatigue test to be stopped.

One representative plot showing the maximum and minimum fatigue microstrains and the creep microstrain have been included for almost every stress level tested at each of the three frequencies. Figures 8.12a-f show representative plots for the low frequency tests performed at the 80, 70, 60, 50, 30 and 20% stress levels respectively. Figures 8.13a-f show representative plots for the medium frequency tests performed at the 80, 70, 60, 50, 40 and 20% stress levels respectively. Then figures 8.14a-f show representative plots for the high frequency tests performed at the 80, 70, 60, 50, 40 and 30% stress levels respectively. All of these figures have been plotted with identical Y axes showing microstrain from 0 to 6000 to allow the creep, maximum fatigue and minimum fatigue microstrains to be compared between different samples at different stress levels for the three frequencies tested, as well as for the individual samples. There is a vast difference between the time axes since they are a measure of the life of the sample. Sample life has already been considered in the S-N results in sections 8.1-8.3.

Figure 8.15, shows the microstrains for sample 174C tested at medium frequency at R=0.1. This plot also shows the maximum and minimum loads applied to the fatigue sample. The loads were measured at the load cell which was NAMAS calibrated to be

accurate to within a fraction of one percent of the load. This demonstrates the accuracy of the digital controller at forcing the hydraulic ram to follow the intended loading regime. The final plot, figure 8.15b, shows the microstrains for sample 183 also tested at medium frequency at R=0.1. This plot also shows the temperature and relative humidity with in the polythene cover. The temperature and humidity were measured accurately using a Protimeter loaned from the BRE.

Fig. 8.8a MEDIAN INITIAL MICROSTRAINS, CHIPBOARD
SIDE-MATCHED PARTNERS LOADED IN CREEP

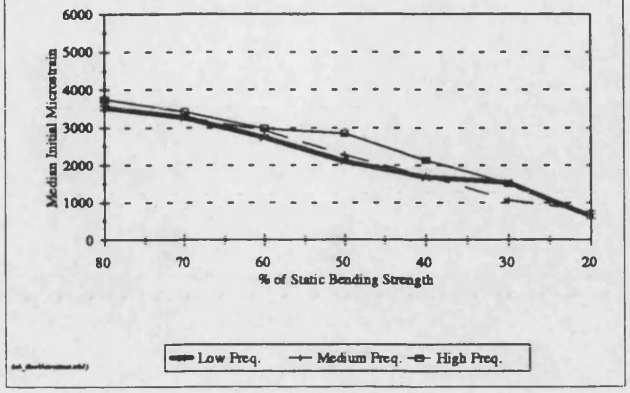

Fig. 8.8b MEDIAN FINAL MICROSTRAINS, CHIPBOARD
SIDE-MATCHED PARTNERS LOADED IN CREEP

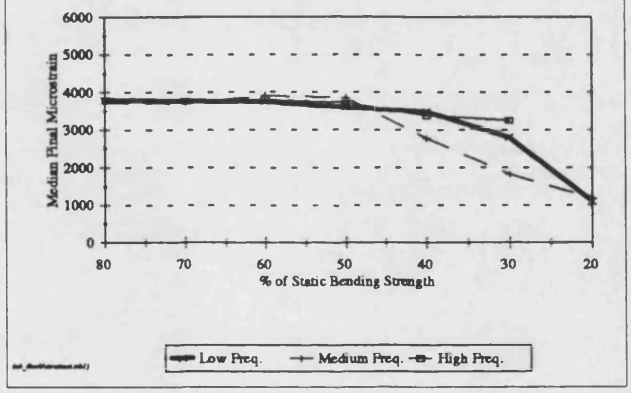

Fig. 8.8c MEDIAN MICROSTRAIN CHANGES, CHIPBOARD
SIDE-MATCHED PARTNERS LOADED IN CREEP

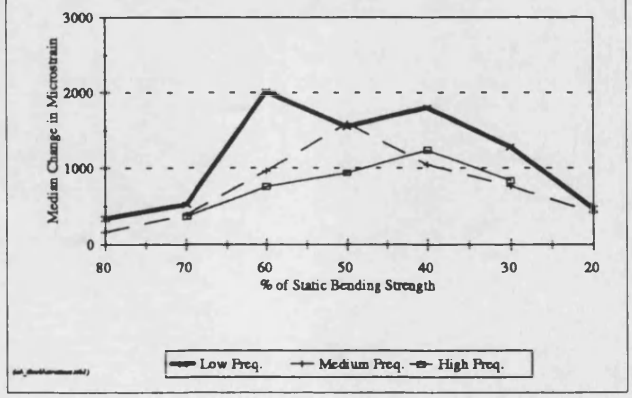

Fig. 8.9a MEDIAN INITIAL MAX FATIGUE MICROSTRAIN FOR CHIPBOARD LOADED AT R=0.1

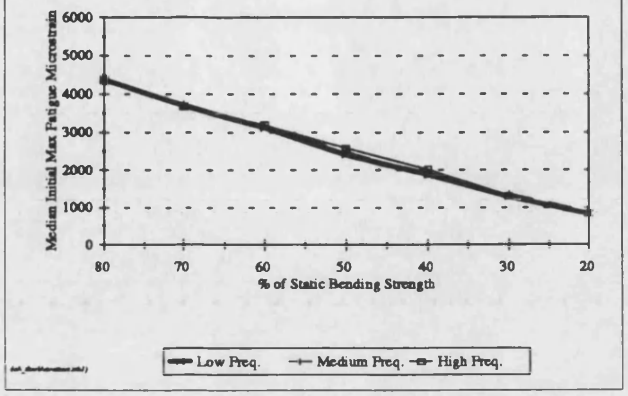

Fig. 8.9b MEDIAN FINAL MAX FATIGUE MICROSTRAIN FOR CHIPBOARD LOADED AT R=0.1

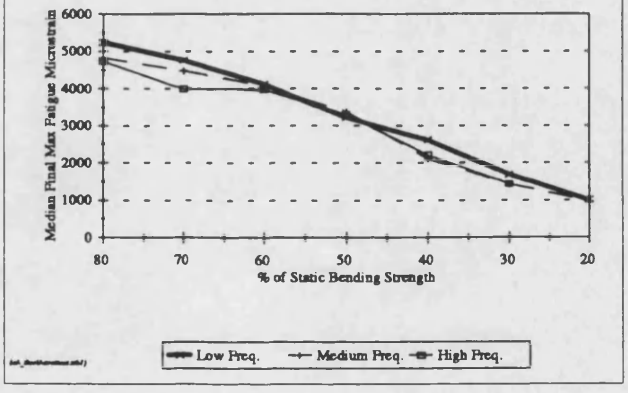

Fig. 8.9c MEDIAN CHANGE IN THE MAXIMUM FATIGUE MICROSTRAIN, CHIPBOARD LOADED AT R=0.1

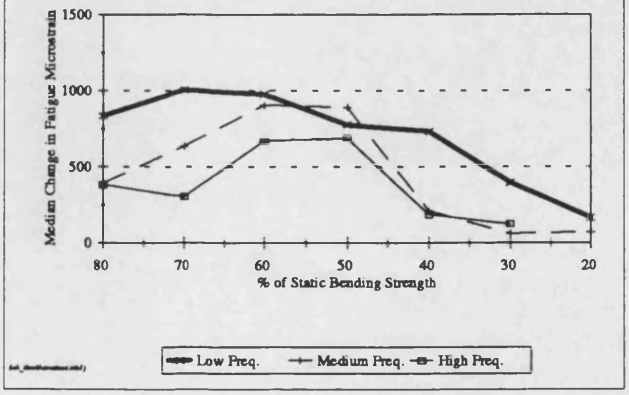

Fig. 8.10a MEDIAN INITIAL MIN FATIGUE MICROSTRAIN FOR CHIPBOARD LOADED AT R=0.1

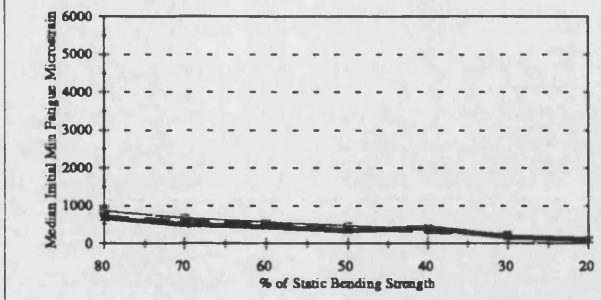

Fig. 8.10b MEDIAN FINAL MIN FATIGUE MICROSTRAIN FOR CHIPBOARD LOADED AT R=0.1

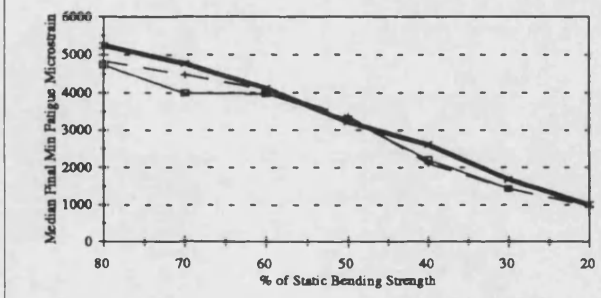

Fig. 8.10c MED CHANGE IN MIN FATIGUE MICROSTRAIN FOR CHIPBOARD LOADED AT R=0.1

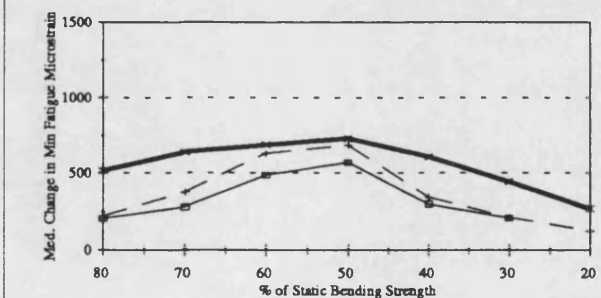

Table 8.6 Median creep and fatigue microstrains for chipboard tested at R=0.1, at low, medium and high frequencies.

Stress Level	Initial Median Creep Microstrain	Final Median Creep Microstain	Median Change in Creep Microstrain	Initial Median Max Fatigue Microstrain	Final Median Max Fatigue Microstrain	Median Change in Max Fatigue Microstrain	Initial Median Min Fatigue Microstrain	Final Median Min Fatigue Microstrain	Median Change in Min Fatigue Microstrain
Chipboard, Low Frequency, R=0.1									
80%	3540	3804	340	4386	5250	834	674	1188	514
70%	3262	3776	523	3703	4764	1005	490	1180	635
60%	2740	3746	2012	3131	4121	978	432	1125	684
50%	2113	3593	1547	2412	3222	776	323	1102	727
40%	1681	3483	1802	1887	2618	731	411	1017	606
30%	1527	2805	1278	1289	1685	396	178	621	443
20%	628	1093	465	835	999	164	101	369	268
Chipboard, Medium Frequency, R=0.1									
80%	3573	3729	168	4405	4840	393	736	972	221
70%	3284	3706	392	3746	4471	635	605	1018	374
60%	2926	3913	960	3177	4078	904	518	1158	626
50%	2285	3867	1593	2490	3379	890	384	1064	684
40%	1725	2775	1050	1898	2109	211	273	617	344
30%	1061	1821	760	1367	1429	62	201	411	210
20%	775	1188	413	901	971	70	139	264	125
Chipboard, High Frequency, R=0.1									
80%	3751	N/A	N/A	4351	4734	383	867	1046	203
70%	3424	3774	4351	3674	4000	305	681	956	278
60%	2990	3807	3674	3209	3977	670	568	1136	485
50%	2853	3721	3209	2594	3304	688	461	1044	569
40%	2142	3383	2594	2033	2217	184	366	662	297
30%	1519	2352	2033	1312	1437	125	242	291	208

Table 8.7 The range of creep microstrains, and fatigue microstrains at high, medium and low frequencies, at R=0.1 for chipboard.

Stress Level	Initial Creep Microstrain	Final Creep Microstrain	Initial Maximum Fatigue Microstrain	Final Maximum Fatigue Microstrain	Initial Minimum Fatigue Microstrain	Final Minimum Fatigue Microstrain
LOW FREQUENCY, R=0.1						
80%	3332-3667	3725-3935	4077-4824	4847-5617	565-753	1041-1336
70%	3138-3453	3740-3928	3371-3914	4203-5046	396-613	820-1265
60%	2381-3040	3031-3203	2914-3203	3914-4405	390-512	932-1305
50%	1581-2666	3464-3972	2214-2523	2742-4094	279-357	839-1647
40%	1681	3483	1887	2618	411	1017
30%	1527	2805	1287	1685	178	621
20%	628	1093	835	999	101	289
MEDIUM FREQUENCY, R=0.1						
80%	3392-3580	3535-3786	4032-4816	4311-5321	660-815	792-1103
70%	2796-3640	3676-3904	3402-4032	3830-4708	539-784	800-1188
60%	2585-3215	3644-3919	3014-3281	3698-4443	455-613	955-1320
50%	2023-2796	3768-3928	2416-2531	3099-3635	310-450	929-1328
40%	1725	2775	1898	2109	273	617
30%	1061	1821	1367	1429	201	411
20%	775	1188	901	971	139	264
HIGH FREQUENCY, R=0.1						
80%	3745-3751(1 pt only)		4179-4351	4415-4874	817-921	867-1257
70%	3286-3467	3638-3887	3440-4086	3652-4632	549-796	777-1195
60%	2846-3455	3676-3952	2914-3492	3484-4195	507-730	937-1258
50%	2633-3068	3607-3920	2411-2687	2960-3562	445-531	898-1164
40%	1819-2464	3276-3490	1981-2085	2113-2320	357-374	590-730
30%	1388-1649	2057-2646	1312	1359-1562	218-265	304-515

Fig 8.11

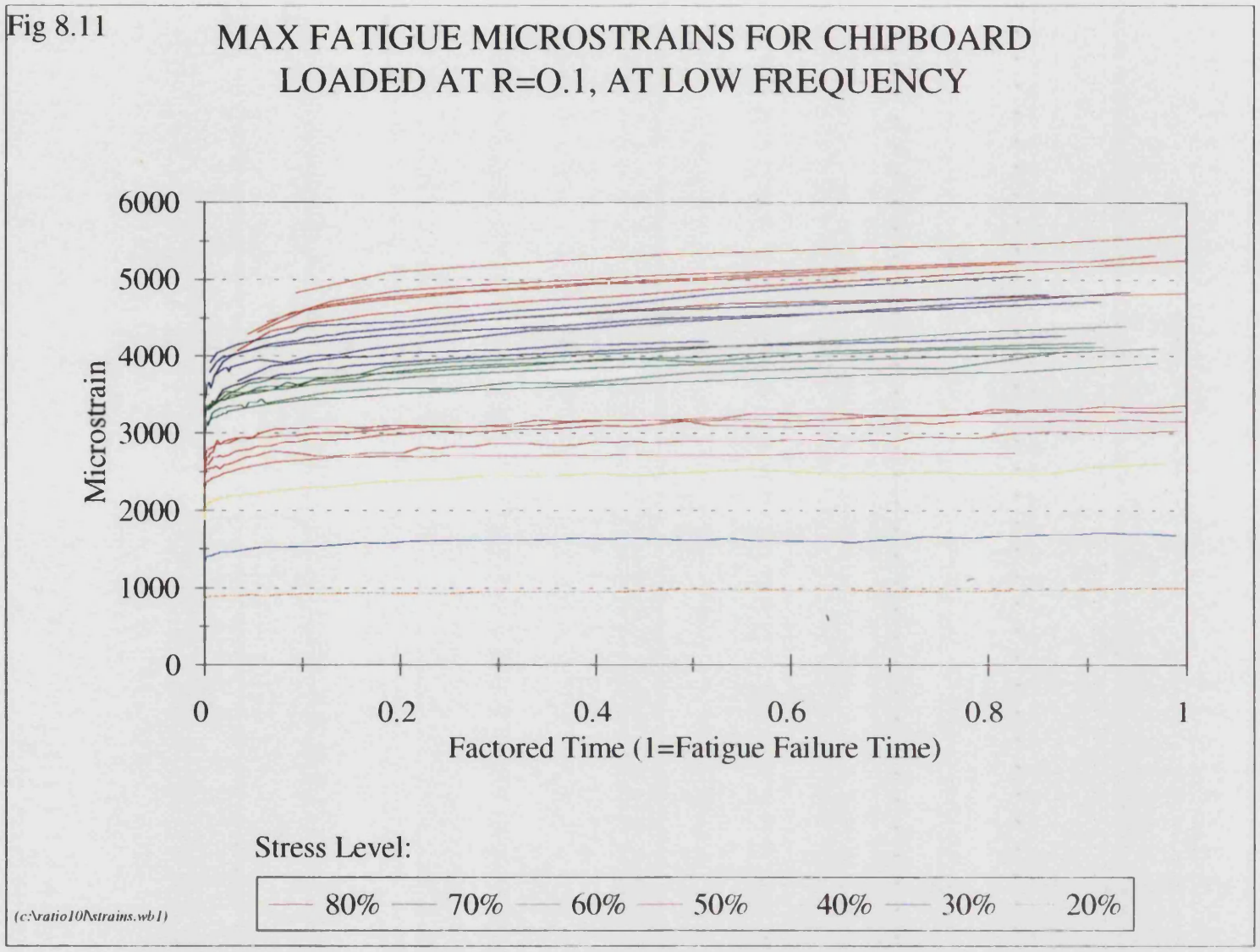
MAX FATIGUE MICROSTRAINS FOR CHIPBOARD
LOADED AT R=O.1, AT LOW FREQUENCY
Microstrain
6000
5000
4000
3000
2000
1000
0
0
0.2
0.4
0.6
0.8
1
Factored Time (1=Fatigue Failure Time)
Stress Level:
80%
70%
60%
50%
40%
30%
20%
(c:\ratio10\strains.wb1)

Fig 8.12a

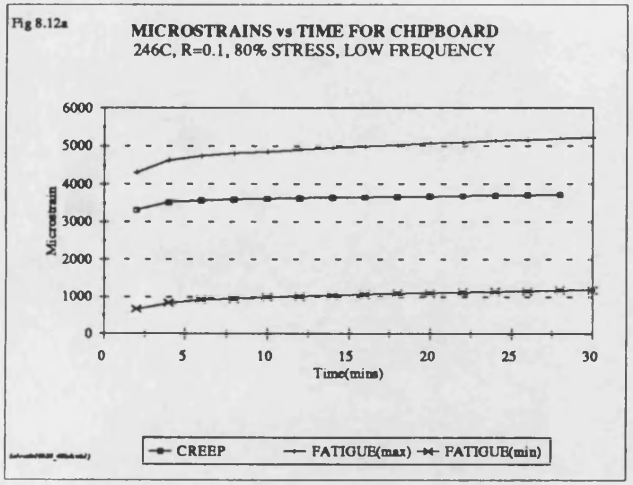

Fig 8.12b

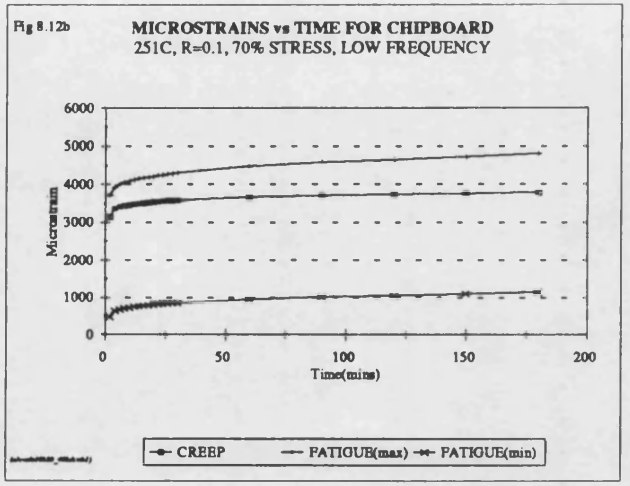

Fig 8.12c

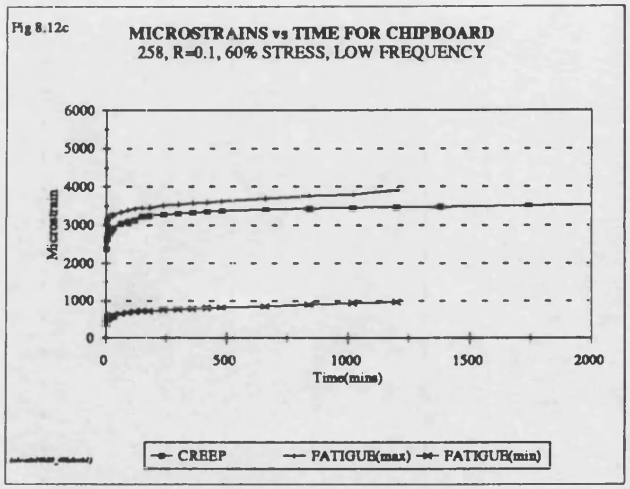

Fig 8.12d

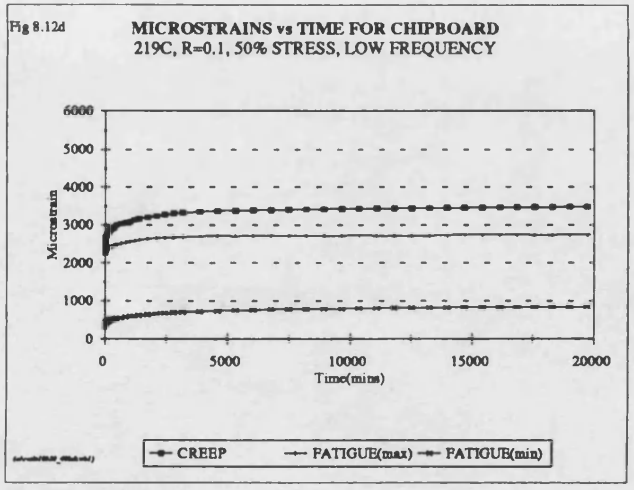

Fig 8.12e

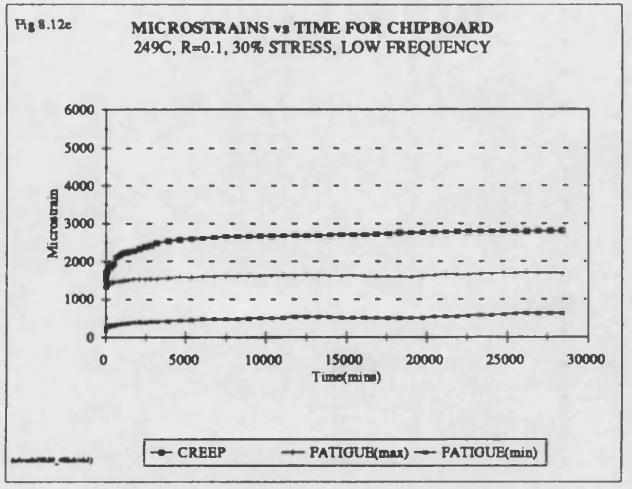

Fig 8.12f

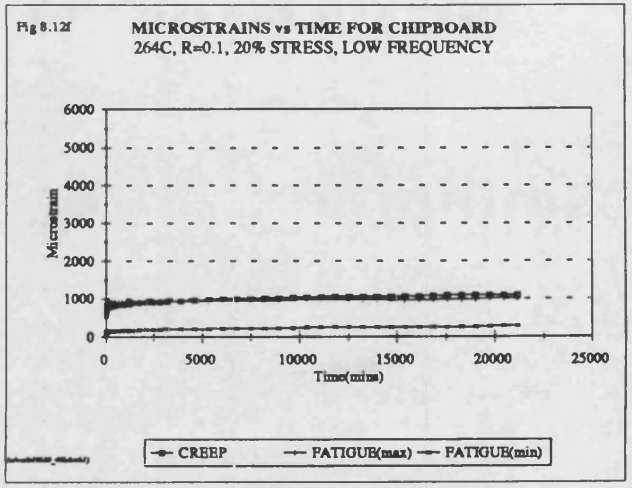

Fig 8.13a MICROSTRAINS vs TIME FOR CHIPBOARD
154C, R=0.1, 80% STRESS, MEDIUM FREQ.

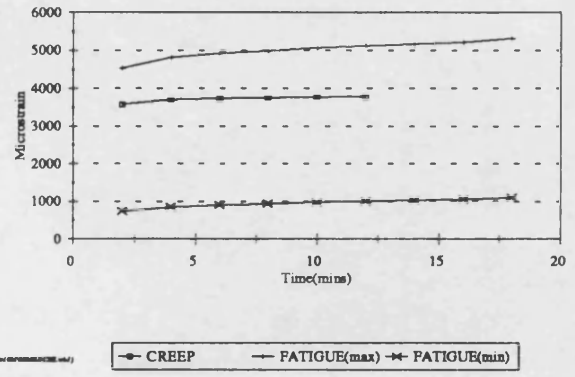

Fig 8.13b MICROSTRAINS vs TIME FOR CHIPBOARD
143, R=0.1, 70% STRESS, MEDIUM FREQ.

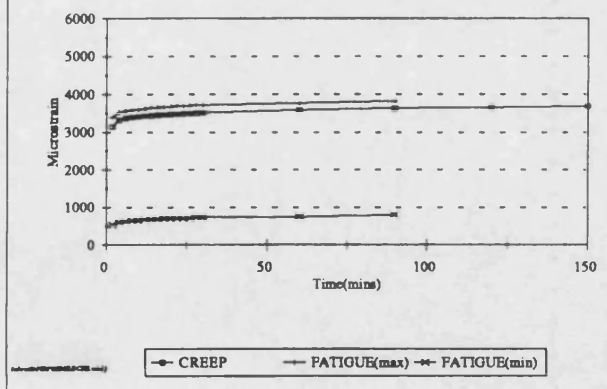

Fig 8.13c MICROSTRAINS vs TIME FOR CHIPBOARD
171C, R=0.1, 60% STRESS, MEDIUM FREQ.

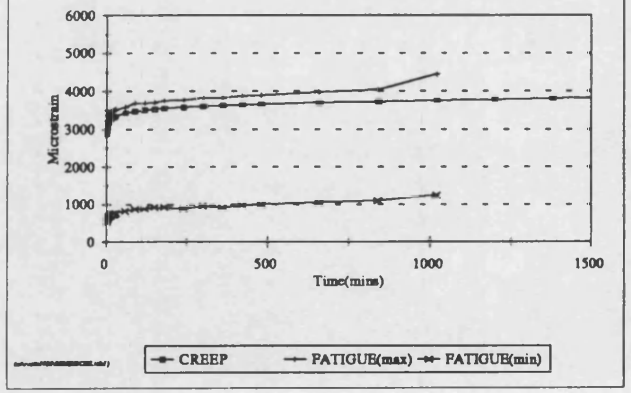

Fig 8.13d MICROSTRAINS vs TIME FOR CHIPBOARD
148, R=0.1, 50% STRESS, MEDIUM FREQ.

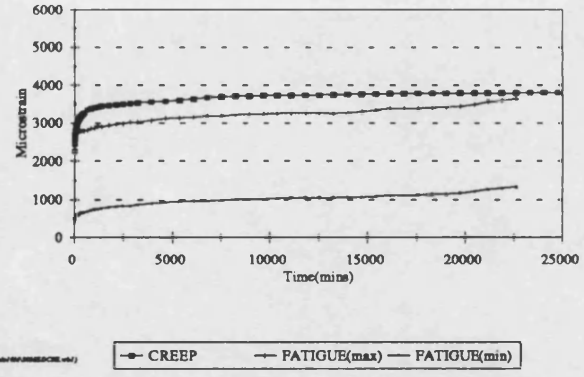

Fig 8.13e MICROSTRAINS vs TIME FOR CHIPBOARD
161C, R=0.1, 40% STRESS, MEDIUM FREQ.

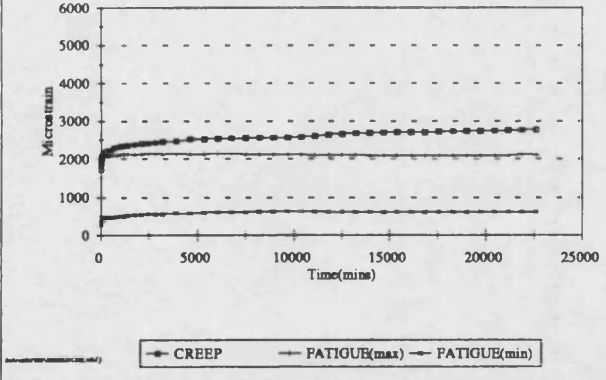

Fig 8.13f MICROSTRAINS vs TIME FOR CHIPBOARD
166C R=0.1 20% STRESS MEDIUM FREQ.

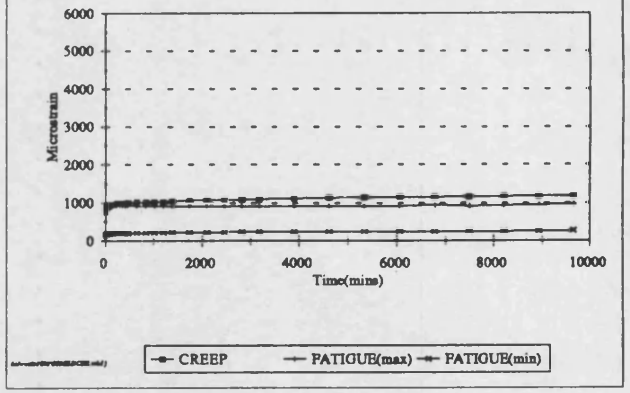

Fig 8.14a

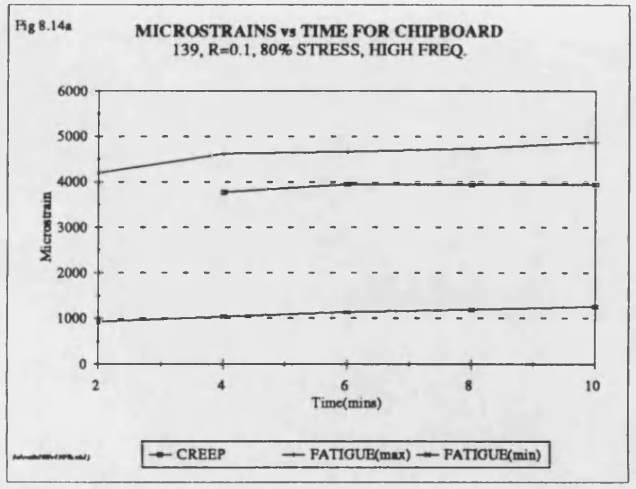

Fig 8.14b

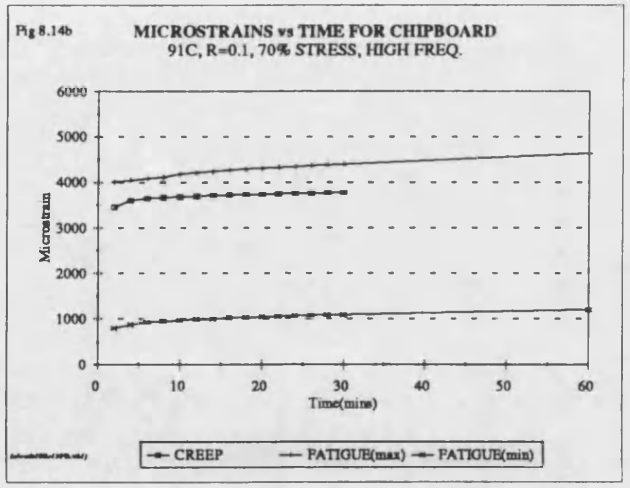

Fig 8.14c

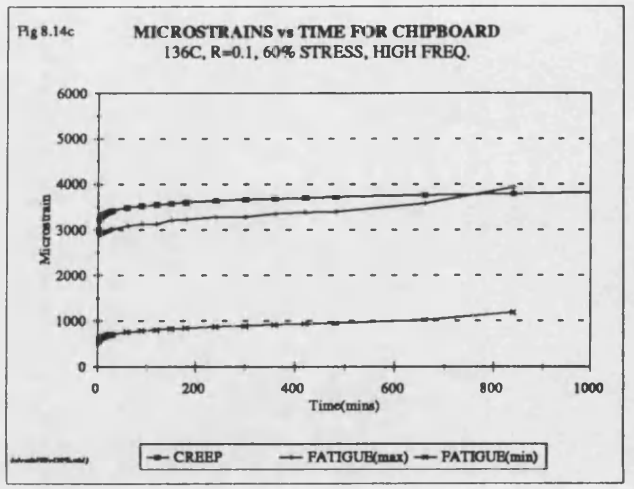

Fig 8.14d

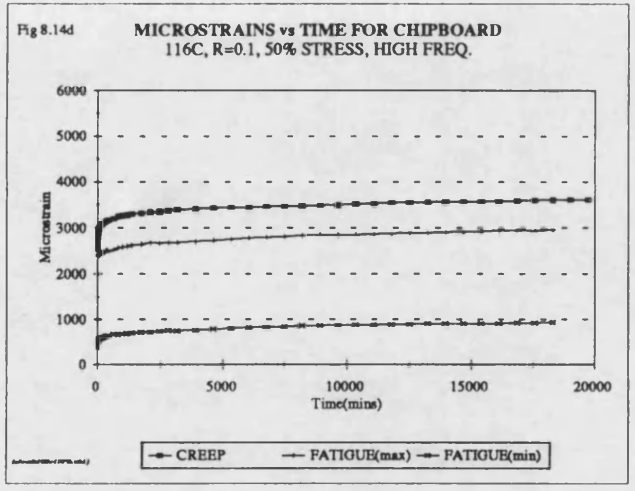

Fig 8.14e

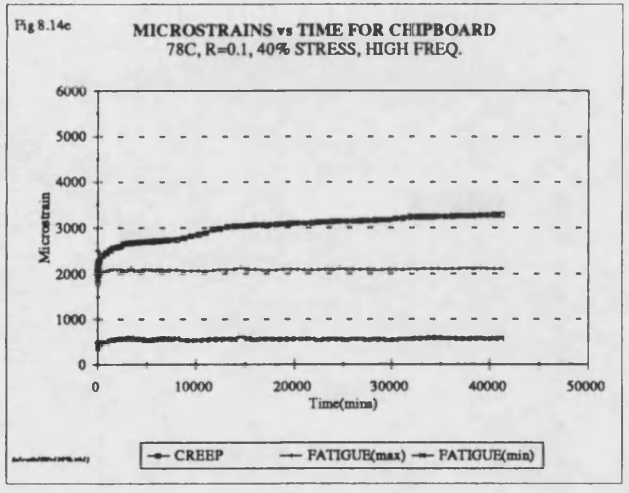

Fig 8.14f

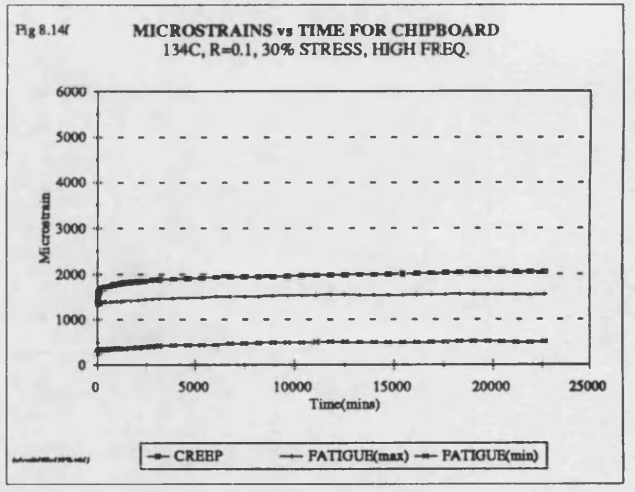

Fig 8.15

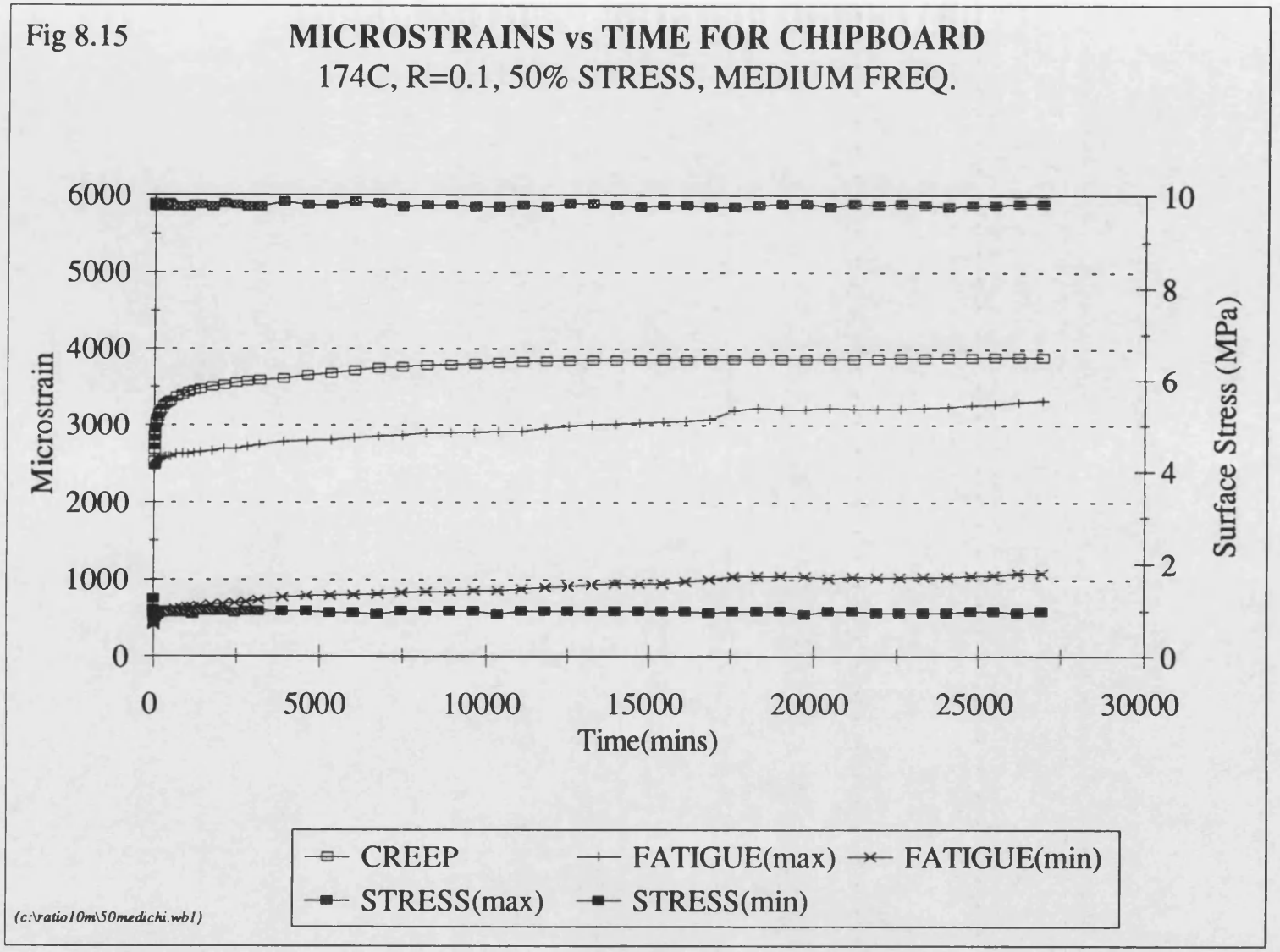
MICROSTRAINS vs TIME FOR CHIPBOARD
174C, R=0.1, 50% STRESS, MEDIUM FREQ.
Microstrain
Surface Stress (MPa)
Time(mins)
0
1000
2000
3000
4000
5000
6000
0
2
4
6
8
10
0
5000
10000
15000
20000
25000
30000
CREEP
FATIGUE(max)
FATIGUE(min)
STRESS(max)
STRESS(min)
(c:\ratio10m\50medichi.wb1)

Fig 8.15b

FATIGUE ENVIRONMENT & STRAINS v TIME

R=0.1, 50% STRESS, MEDIUM FREQUENCY

FOR CHIPBOARD SAMPLE CM-183

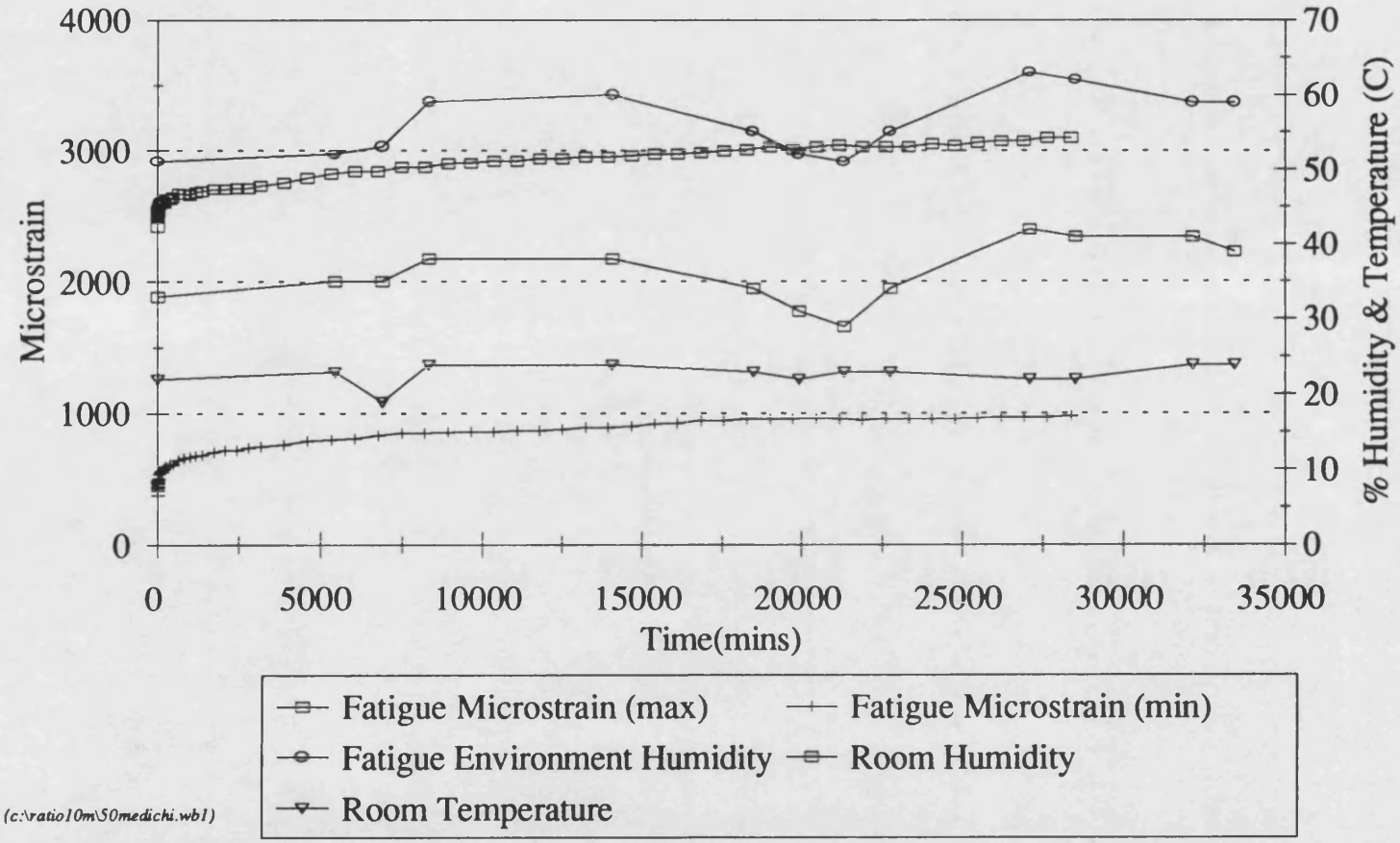

Discussion

The main observation from figures 8.8a-c, 8.9a-c and 8.10a-c is that the magnitudes of the microstrains for all three frequencies are almost identical. This appears unlikely at first because the fatigue lives reduced significantly as the frequency was reduced. However, there is no reason why the strain should change for the same applied stress because the loading frequency has been changed.

The first set of plots, figures 8.8a-c did not show any differences for the three frequencies because they are for the side-matched creep samples and frequency was not applicable to these tests. All three sets of tests on the creep samples were essentially identical and can be considered as constants against which the fatigue samples can be examined. However, as has already been demonstrated in Chapter 7 there will be some variation due to the inherent variability of the chipboard despite the use of side-matched sets of samples and the normalisation of the stresses. The initial microstrains for the creep samples were highest at the highest stress levels and reduced as the stress level was reduced. This is because a greater load produces a greater instantaneous deflection. The final microstrains for the creep samples were almost constant for the 80, 70, 60 and 50% stress levels at approximately 3800 microstrain implying that this is a critical strain for the samples. It may be possible to use this critical strain to predict sample failure. Because these are the last values captured not the last values experienced by the sample it is probable that this is the maximum creep microstrain before the final stage of creep is reached leading to the rapid failure of the samples. The final microstrain values for the 40, 30 and 20% stress levels must be treated with caution because none of the samples failed this was also the case for some of the samples tested at the 50% stress level. This is the cause of the decrease in the final creep microstrain and the change in the creep microstrain seen at below the 40% stress level in figures 8.8b and 8.8c. The change in the creep microstrain increases from the 80% to the 50% stress level because the initial values are lower for the lower stress levels. For the prediction of creep deflections the work of Dinwoodie *et al* should be referred to as reported in Chapter 5. Dinwoodie *et al* (1991a and 1991b), and Dinwoodie and Bonfield (1995) reported a linear increase in relative creep as a result of increasing the stress level between 30 and 75%. Relative creep was not plotted for the creep data reported in this thesis because the tests performed were relatively short in duration.

The short term static tests were performed at high rates of load application compared to the creep loading, especially for the medium and high rates, the strengths measured are higher than those that would have been measured if the load was applied slowly.

This means that the 80% stress levels for the creep tests are very high (approximately 85%) when applied as dead weights and cause the creep samples to fail almost immediately.

The initial and final median maximum fatigue microstrains were almost identical for all three frequencies. The initial values were expected to be very similar because the same loads were applied to all the samples at the equivalent stress levels regardless of the loading frequency and very little time has elapsed. As for the creep samples, the initial maximum fatigue microstrains decreased with decreasing stress level. Again greater stresses produce greater instantaneous deflections. However, the final maximum fatigue microstrains also decrease with decreasing stress level. This is because the samples have not failed at stress levels below 40%. For stress levels between 80% and 50% the median values are calculated from failed samples, except for the 50% stress level for the low frequency loading. However, the final stage of deflection is not captured so it is not possible to determine the magnitude of the ultimate microstrains to failure. The changes in the maximum fatigue microstrains increase as the stress level is reduced from 80% to 70% or 60% and then decrease with reducing stress level down to the 20% stress level. These changes are shown on a magnified scale in figure 8.9c and so the differences between the different frequencies are smaller than they appear. The change at the 80% stress level is greater for the low frequency than for the medium and high frequencies because the final loops were captured at fewer loading cycles before the end of the tests and so the strain values are higher.

The plots of the minimum fatigue microstrains, figures 8.10a-c, show the same features as those for the maximum fatigue microstrains, figures 8.9a-c. The only difference is that the magnitudes of the strains are lower because only 10% of the peak stress was being applied to the samples.

It is clear in the colour plot, figure 8.11, that the maximum fatigue microstrains decrease as the stress level is reduced for the low frequency loading. This is the same for the medium and high frequency testing and the trend is seen for the maximum fatigue microstrains in figures 8.13a-f and 8.14a-f. Tables 8.6 and 8.7 also show that all three microstrains reduce in magnitude as the stress level is reduced for all three frequencies. Also the values of the initial maximum, final maximum, initial minimum and final minimum fatigue microstrain are not significantly changed by changing the loading frequency (low, medium or high). Figure 8.11 demonstrates that when plotted with respect to factored time the strains for the different samples tested at the same

stress level are very similar and that there is very little overlap between the strains produced for different stress levels.

The creep and fatigue microstrains were both found to increase in three stages, demonstrated by figures 8.11, 8.12a-f, 8.13a-f and 8.14a-f, as was previously found by Hacker (1991) and Thompson *et al* (1994). In both creep and fatigue there is an initial rapid increase in deflection followed by a more gradual almost linear stage, then a rapid increase leading to failure. The final rapid stage of the deflection is rarely captured due to the pre-set loop capture interval.

In figures 8.12a-f, 8.13a-f and 8.14a-f, the graphs for the 80% stress level tests, figures 8.12a, 8.13a and 8.14a are the least comprehensive, due to the short length of time taken for the samples to fail. Failure times were 7 to 58 minutes for the low frequency tests, which was significantly longer than the 6 to 16 minutes for the medium frequency testes and the 1 to 8 minutes for the high frequency test. Hysteresis loops can only be captured at a minimum of two minute time intervals and so the number of loops captured was greater as the frequency was reduced at the 80% stress level. In all eighteen tests for the three frequencies at 80% stress the fatigue sample failed after the creep sample, however, the maximum fatigue microstrain was always significantly greater than the creep microstrain as demonstrated in figures 8.12a, 8.13a and 8.14a.

At the 70% stress level for the low and medium frequency testing, demonstrated by figures 8.12b and 8.13b the fatigue microstrain was above the creep microstrain for the duration of all twelve tests performed at this stress level. At high frequency, demonstrated by figure 8.14b, the fatigue microstrain was above the creep microstrain for three out of six of the tests, almost identical for two tests and below for one test, for sample C-138. The graphs show that the difference between the maximum fatigue microstrain and the creep microstrains was less than at the 80% stress level. At the 70% stress level the fatigue samples failed before the creep samples in three out of the six tests at low frequency, compared to five out of five for the medium frequency testing and one out of six for the high frequency testing.

With the stress level reduced to 60%, demonstrated by figures 8.12c, 8.13c and 8.14c for the low, medium and high frequencies respectively, the creep microstrain was generally very close to the maximum fatigue microstrain. The maximum fatigue microstrain then increased at a greater rate than the creep microstrain until the fatigue sample failed. This was the case for all six samples tested at this stress level, at low frequency, with four of the samples showing a third rapid stage to the deformation

leading to failure. In four out of six of the tests at the medium frequency, the maximum fatigue microstrain was just greater than the creep microstrain and in the other two tests the fatigue microstrain started below the creep microstrain but increased more rapidly and overtook the creep microstrain prior to the failure of the fatigue samples. With the stress level reduced to 60% for the high frequency testing the creep microstrain exceeded the maximum fatigue microstrain. This was the case for five out of six of the tests although the fatigue microstrain exceeded the creep microstrain prior to failure for three of the tests. The one test where the fatigue microstrain was greatest was a very early fatigue failure. At this stress level the fatigue sample failed first in all tests at low and medium frequencies and five out of six tests at the high frequency.

At the 50% stress level for the low, medium and high frequencies, demonstrated by figures 8.12d, 8.13d and 8.14d the creep microstrain was generally greater than the maximum fatigue microstrain. This was the case in four out of six tests at the low frequency and all twelve tests for the medium and high frequencies. The other two samples tested at low frequency were ignored because the sample had moved out of position on the rollers. The microstrains were greater for the creep samples than for the fatigue samples at all three frequencies, as observed at the 60% stress level for the high frequency tests. The reason that this change occurred at a higher stress level for the high frequency loading is thought to result from the relative loading rates for the static tests. As was explained in Chapter 7 the static strengths for the high rate were approximately 5% higher than those for the low rate. Only one out of six fatigue samples and one out of six creep samples failed during low frequency testing at this stress level. For the medium frequency testing the fatigue sample failed before the creep sample in all of the tests and in five out of six cases for the high frequency testing. This tells us that although it is the static component of the load that produces the strain, it is the cyclic component that causes more of the damage producing sample failure, except for the 80% stress level tests. This contradicts the findings of Nakai and Grossman (1983) for wood, that there was no evidence to suggest that wooden beams loaded intermittently had shorter lives than when loaded in creep. However, wood and particleboard are fundamentally different materials and intermittent loading is different to fatigue cycling. The creep microstrains and maximum fatigue microstrains were very close at 50% stress which was also the case at 60% stress for the higher frequencies.

At the lowest stress levels of 40, 30 and 20%, figures 8.12e-f, 8.13e-f and 8.14e-f the trend continues with the creep microstrain above the maximum fatigue microstrain in all cases, considerably so in some cases. Now the maximum fatigue microstrain curves are almost flat meaning that after the initial elastic deflection, creep deformation was

almost non existent over the time scale of the tests, possibly even approaching a fatigue limit for the material. The plots for the 20% stress levels for the low and medium frequencies, figures 8.12f and 8.13f respectively suggests that if there is a fatigue limit, it would occur at marginally below 20% stress. This is because the maximum fatigue microstrain increases very slightly throughout the duration of the test. This is very similar to the observations for the high frequency loading at the 30% stress level shown in figure 8.14f.

The maximum fatigue microstrain curves flatten out with reducing stress level because less deformation is taking place. The fatigue samples failed first at all but the highest stress levels despite the creep samples deflecting to a greater extent than the fatigue samples below 50 or 60% of the ultimate stress.

The load applied to the sample was accurately controlled throughout testing. Figure 8.15 demonstrates that as the fatigue microstrains increase the load applied to the fatigue sample is unchanged. The changes in temperature and relative humidity shown in figure 8.15b have no effect on the fatigue microstrains for the sample tested. This is because enclosing the sample in polythene means that there is limited air flow over the sample minimising the effect of these changes. Also the longest tests were two to three weeks in duration and the changes observed were relatively brief.

To generalise the results, all three microstrains reduced in magnitude as the stress level was reduced. At the highest stress level only, the creep samples failed first at all frequencies but the fatigue loading was more damaging than creep loading for 70, 60 and 50% stress. This changed at approximately 40% stress for the testing at all three frequencies where the fatigue cycling produced less deformation than the creep loading as demonstrated by figures 8.12-e-f, 8.13e-f and 8.14e-f. In figure 8.12f for low frequency testing at 20% stress the creep and maximum fatigue microstrain are closer than for the medium and high frequencies but this is probably due to the variation between side-matched samples. Although only one or two replicates were tested for the 40, 30 and 20% stress levels the results can be accepted with a fair degree of confidence because all three sets of data agree. Also the results compliment those observed for the higher stress levels where there were three sets of six replicates.

8.7 Dynamic Moduli

The dynamic modulus is the average stiffness of a sample when subjected to cyclic loading and the data analysis software computes a value for every captured hysteresis loop. It is the gradient of the line joining the two extreme points of each hysteresis loop (see section 6.6). Before examining the results of this section it must again be emphasised that the first and last hysteresis loops captured do not correspond to the first and last cycles of fatigue (see section 8.4).

Figures 8.16a-c show how the median dynamic moduli change as a result of changing the stress level, for all the samples tested, at all stress levels, for all three frequencies. Figure 8.16a compares the initial median dynamic moduli for all three frequencies, figure 8.16b the final median dynamic moduli and figure 8.16c the median changes in the dynamic moduli.

Table 8.8 provides a numerical summary of the dynamic moduli for all the fatigue samples tested, at all stress levels, for all three frequencies. Median values for the initial, the final, and the change in the dynamic moduli from the six samples tested at 80, 70, 60 and 50% stress levels have been used. This is to minimise variations in moduli which relate to the scattered strengths of the chipboard samples, although when tested the mean values were similar to the medians. For 40, 30 and 20% stress levels only one sample was tested. The median change in the dynamic moduli, is the median of the changes in the dynamic moduli for the individual samples, from the start to the finish of the tests. This shows how the average stiffness of the fatigue samples changes as a result of fatigue cycling. Also included in the table are the ranges of the initial, final and changes in the dynamic moduli, to provide a numerical indication of the spread of the dynamic moduli.

Figures 8.17a-e, 8.19a-e and 8.21a-e show the dynamic moduli as a function of time for all the samples tested at the 80, 70, 60, 50, 40, 30 and 20% stress levels for the low, medium and high frequencies respectively. This allows direct comparisons to be made between the different samples at the same stress level and at different stress levels. Time is plotted on the X axis and varies greatly as it represents the duration of the tests. These figures have also been plotted with respect to factored time and are included as figures 8.18a-e, 8.20a-e and 8.22a-d for the low, medium and high frequencies respectively. A graph for the 80% stress level for high frequency loading has not been plotted with respect to factored time due to the short duration of the tests. All the graphs have been plotted with dynamic modulus ranging from 2-6 GPa on the Y axis. The factored time plots help compare tests with greatly different lives.

Fig. 8.16a

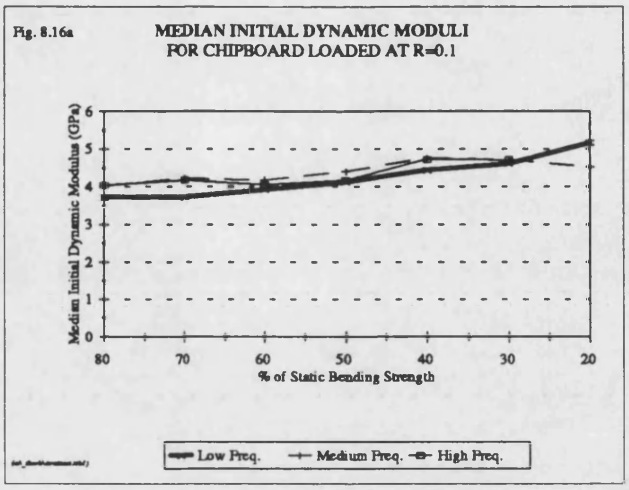

Fig. 8.16b

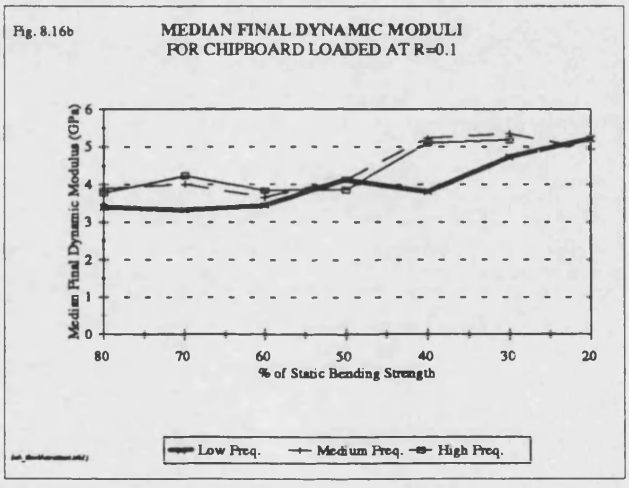

Fig. 8.16c

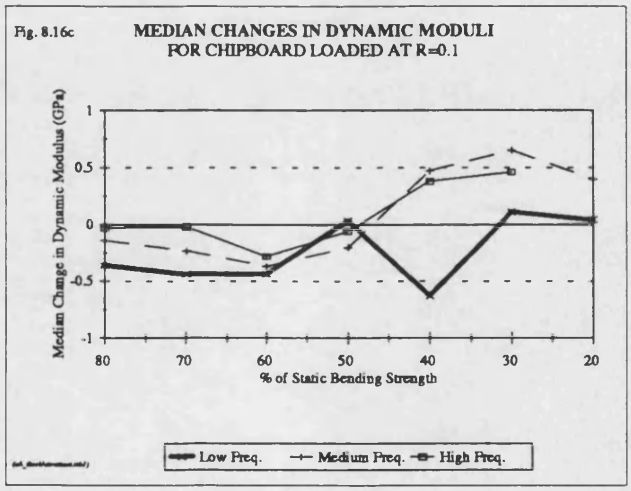

Table 8.8 Median dynamic moduli for chipboard tested at R=0.1, *at low, medium* and high frequencies.

Stress Level	Median Initial Dynamic Modulus GPa	Median Final Dynamic Modulus GPa	Median Change in Dynamic Modulus GPa	Range of Initial Dynamic Moduli GPa	Range of Final Dynamic Moduli GPa	Range of Change in Dynamic Modulus GPa
LOW FREQUENCY, R=0.1						
80%	3.72	3.40	-0.36	3.16-4.10	2.99-3.75	(-0.11)-(-0.58)
70%	3.72	3.31	-0.44	3.39-4.08	2.83-3.82	(-0.26)-(-0.56)
60%	3.93	3.44	-0.44	3.47-4.21	2.93-3.74	(-0.39)-(-0.57)
50%	4.13	4.13	0.03	3.84-4.40	3.85-4.39	(-0.14)-(+0.47)
40%	4.44	3.81	-0.63	1 Sample	1 Sample	1 Sample
30%	4.62	4.73	+0.11	1 Sample	1 Sample	1 Sample
20%	5.17	5.21	+0.04	1 Sample	1 Sample	1 Sample
MEDIUM FREEQUENCY, R=0.1						
80%	4.02	3.89	-0.14	3.59-4.84	3.50-4.43	(-0.09)-(-0.15)
70%	4.23	4.01	-0.23	3.51-4.87	3.29-4.43	(-0.17)-(-0.44)
60%	4.18	3.65	-0.37	3.61-4.86	3.26-4.55	(-0.27)-(-0.65)
50%	4.41	4.13	-0.20	3.90-4.87	3.58-4.64	(-0.13)-(-0.42)
40%	4.76	5.23	+0.47	1 Sample	1 Sample	1 Sample
30%	4.71	5.36	+0.65	1 Sample	1 Sample	1 Sample
20%	4.53	4.93	+0.40	1 Sample	1 Sample	1 Sample
HIGH FREQUENCY, R=0.1						
80%	4.04	3.78	-0.03	3.37-4.31	3.22-4.34	(-0.15)-(+0.03)
70%	4.18	4.23	-0.02	3.74-4.56	3.59-4.62	(-0.19)-(+0.09)
60%	4.06	3.84	-0.28	3.76-4.74	3.41-4.50	(-0.47)-(-0.04)
50%	4.17	3.85	-0.06	3.73-4.63	3.54-4.65	(-0.19)-(0.46)
40%	4.73	5.11	+0.38	2 Samples	2 Samples	2 Samples
30%	4.72	5.18	+0.46	2 Samples	2 Samples	2 Samples

Fig 8.17a DYNAMIC MODULUS vs TIME FOR CHIPBOARD
R=0.1, 80% STRESS, LOW FREQUENCY

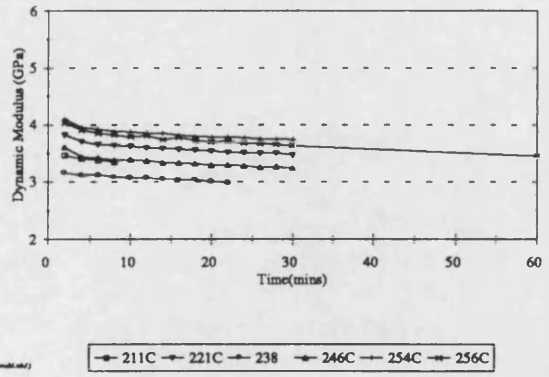

Fig 8.17b DYNAMIC MODULUS vs TIME FOR CHIPBOARD
R=0.1, 70% STRESS, LOW FREQUENCY

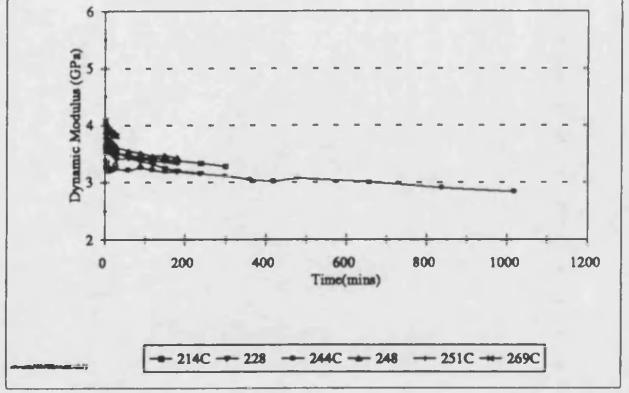

Fig 8.17c DYNAMIC MODULUS vs TIME FOR CHIPBOARD
R=0.1, 60% STRESS, LOW FREQUENCY

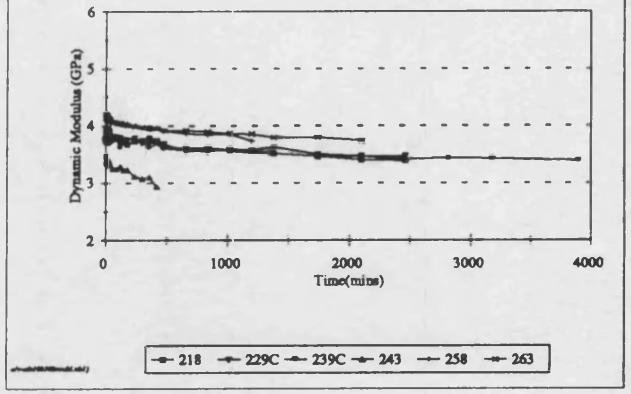

Fig 8.17d DYNAMIC MODULUS vs TIME FOR CHIPBOARD
R=0.1, 50% STRESS, LOW FREQUENCY

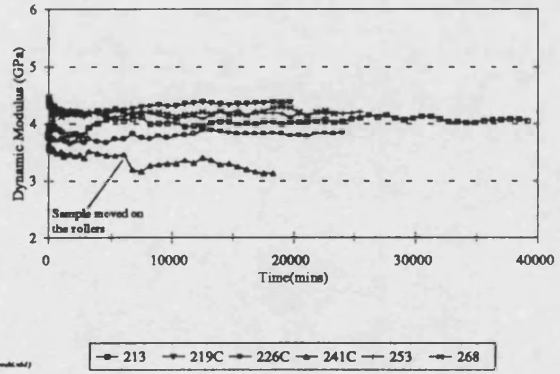

Fig 8.17e DYNAMIC MODULUS vs TIME FOR CHIPBOARD
R=0.1, 40, 30 & 20% STRESS, LOW FREQ.

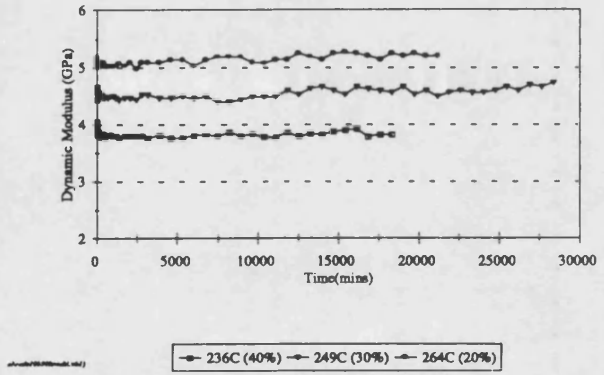

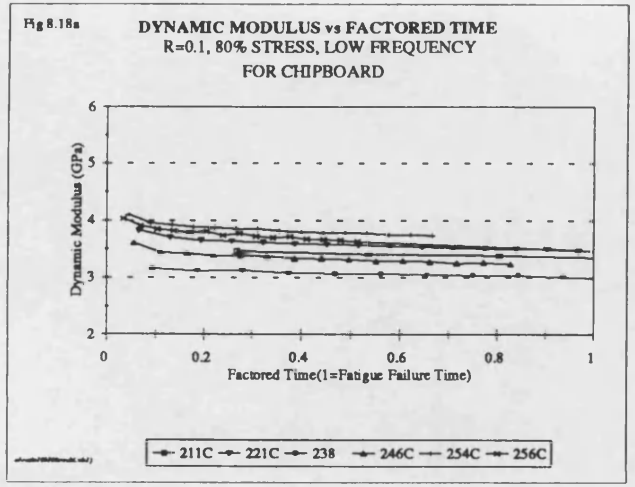
Fig 8.18a
DYNAMIC MODULUS vs FACTORED TIME
R=0.1, 80% STRESS, LOW FREQUENCY
FOR CHIPBOARD
Dynamic Modulus (GPa)
Factored Time(1=Fatigue Failure Time)
211C 221C 238 246C 254C 256C

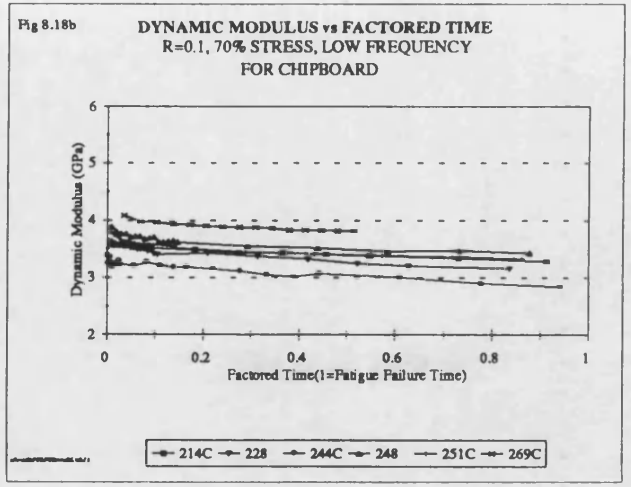
Fig 8.18b
DYNAMIC MODULUS vs FACTORED TIME
R=0.1, 70% STRESS, LOW FREQUENCY
FOR CHIPBOARD
Dynamic Modulus (GPa)
Factored Time(1=Fatigue Failure Time)
214C 228 244C 248 251C 269C

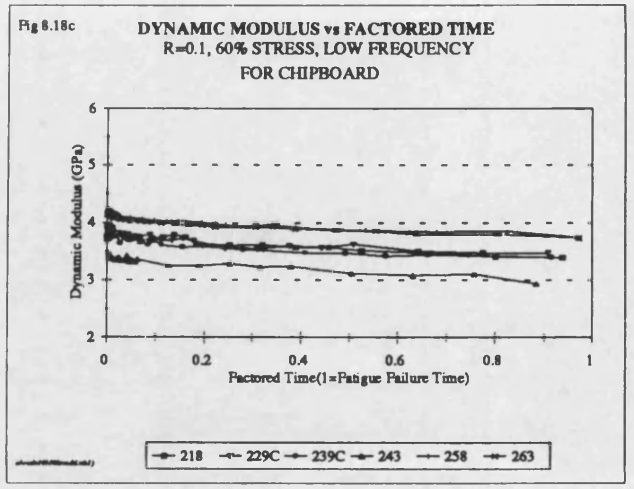
Fig 8.18c
DYNAMIC MODULUS vs FACTORED TIME
R=0.1, 60% STRESS, LOW FREQUENCY
FOR CHIPBOARD
Dynamic Modulus (GPa)
Factored Time(1=Fatigue Failure Time)
218 229C 239C 243 258 263

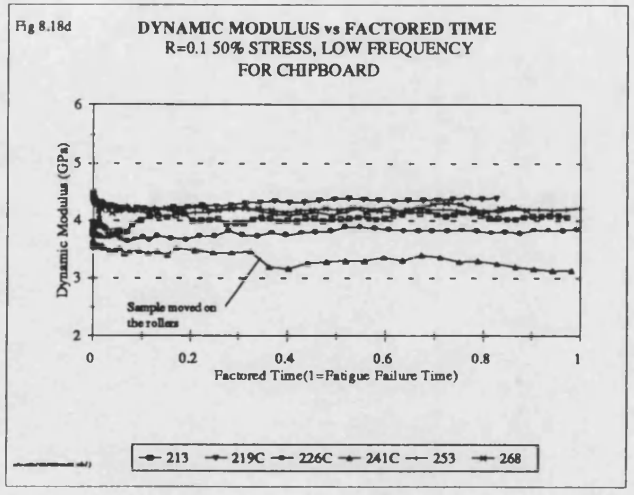
Fig 8.18d
DYNAMIC MODULUS vs FACTORED TIME
R=0.1 50% STRESS, LOW FREQUENCY
FOR CHIPBOARD
Dynamic Modulus (GPa)
Sample moved on the rollers
Factored Time(1=Fatigue Failure Time)
213 219C 226C 241C 253 268

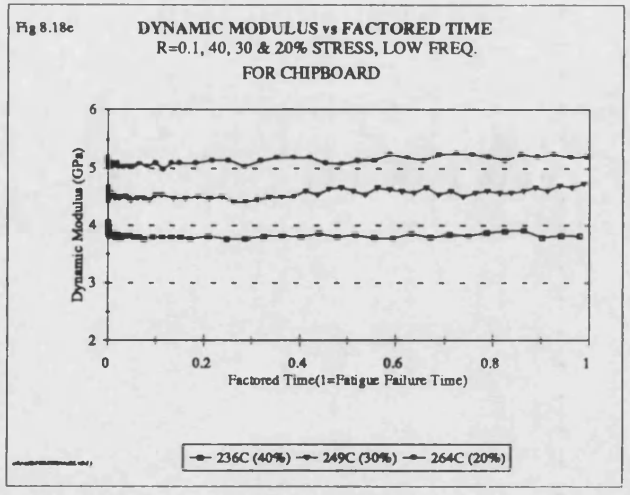
Fig 8.18e
DYNAMIC MODULUS vs FACTORED TIME
R=0.1, 40, 30 & 20% STRESS, LOW FREQ.
FOR CHIPBOARD
Dynamic Modulus (GPa)
Factored Time(1=Fatigue Failure Time)
236C (40%) 249C (30%) 264C (20%)

Fig 8.19a **DYNAMIC MODULUS vs TIME FOR CHIPBOARD**
R=0.1, 80% STRESS, MEDIUM FREQUENCY

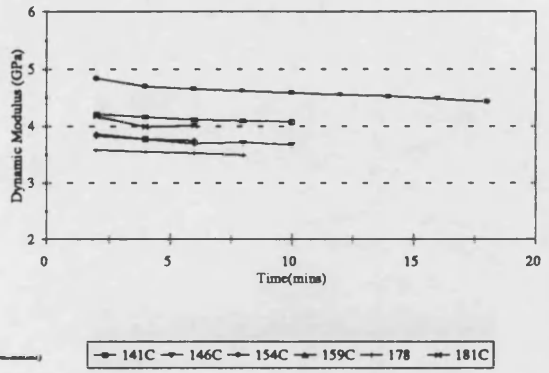

Fig 8.19b **DYNAMIC MODULUS vs TIME FOR CHIPBOARD**
R=0.1, 70% STRESS, MEDIUM FREQUENCY

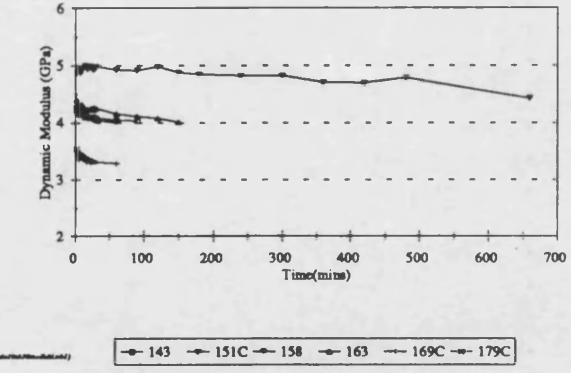

Fig 8.19c **DYNAMIC MODULUS vs TIME FOR CHIPBOARD**
R=0.1, 60% STRESS, MEDIUM FREQUENCY

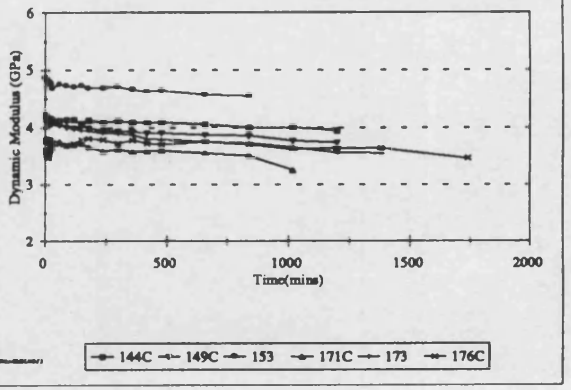

Fig 8.19d **DYNAMIC MODULUS vs TIME FOR CHIPBOARD**
R=0.1, 50% STRESS, MEDIUM FREQUENCY

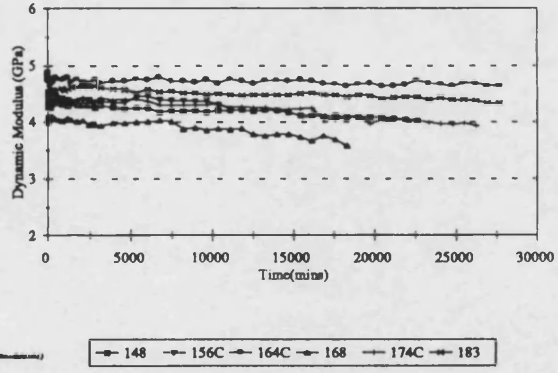

Fig 8.19e **DYNAMIC MODULUS vs TIME FOR CHIPBOARD**
R=0.1, 40, 30 & 20% STRESS MEDIUM FREQ

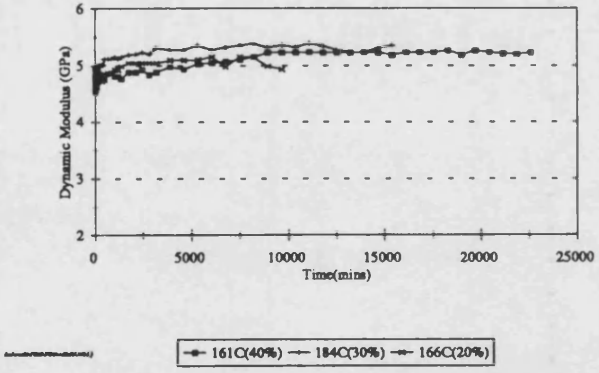

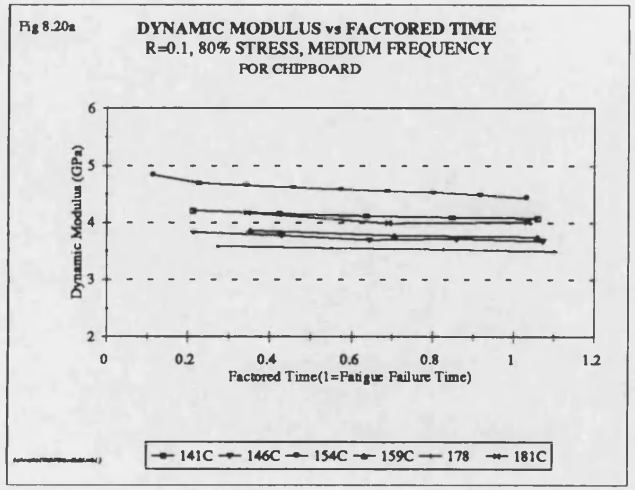
Fig 8.20a
DYNAMIC MODULUS vs FACTORED TIME
R=0.1, 80% STRESS, MEDIUM FREQUENCY
FOR CHIPBOARD
Dynamic Modulus (GPa)
Factored Time(1=Fatigue Failure Time)
141C 146C 154C 159C 178 181C

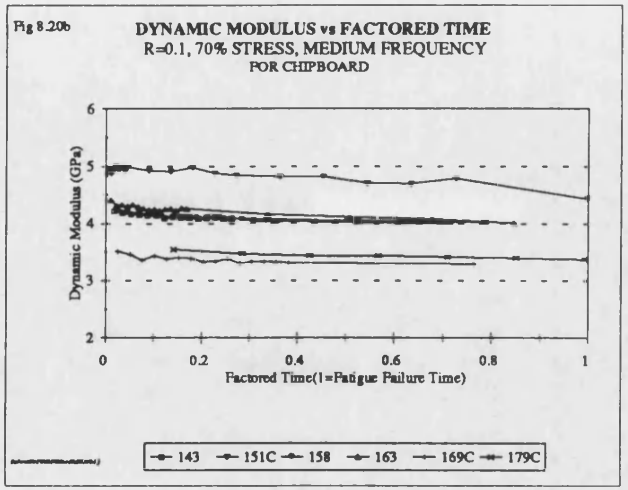
Fig 8.20b
DYNAMIC MODULUS vs FACTORED TIME
R=0.1, 70% STRESS, MEDIUM FREQUENCY
FOR CHIPBOARD
Dynamic Modulus (GPa)
Factored Time(1=Fatigue Failure Time)
143 151C 158 163 169C 179C

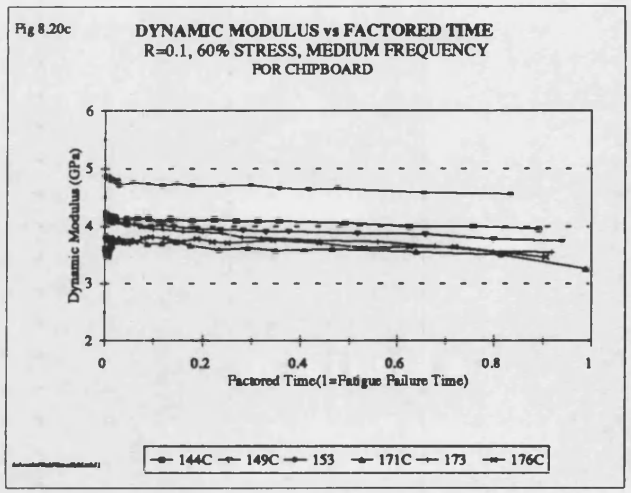
Fig 8.20c
DYNAMIC MODULUS vs FACTORED TIME
R=0.1, 60% STRESS, MEDIUM FREQUENCY
FOR CHIPBOARD
Dynamic Modulus (GPa)
Factored Time(1=Fatigue Failure Time)
144C 149C 153 171C 173 176C

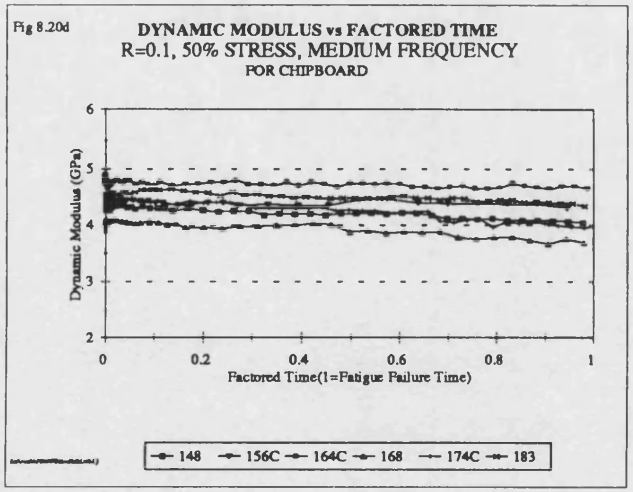
Fig 8.20d
DYNAMIC MODULUS vs FACTORED TIME
R=0.1, 50% STRESS, MEDIUM FREQUENCY
FOR CHIPBOARD
Dynamic Modulus (GPa)
Factored Time(1=Fatigue Failure Time)
148 156C 164C 168 174C 183

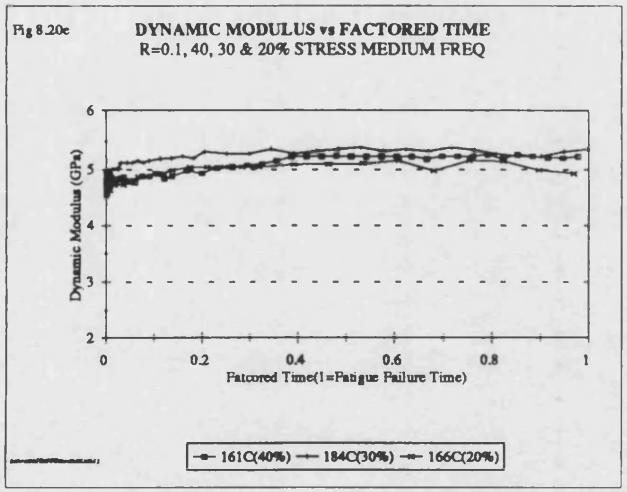
Fig 8.20e
DYNAMIC MODULUS vs FACTORED TIME
R=0.1, 40, 30 & 20% STRESS MEDIUM FREQ
Dynamic Modulus (GPa)
Patcored Time(1=Fatigue Failure Time)
161C(40%) 184C(30%) 166C(20%)

Fig 8.21a DYNAMIC MODULUS vs TIME FOR CHIPBOARD
R=0.1, 80% STRESS, HIGH FREQUENCY

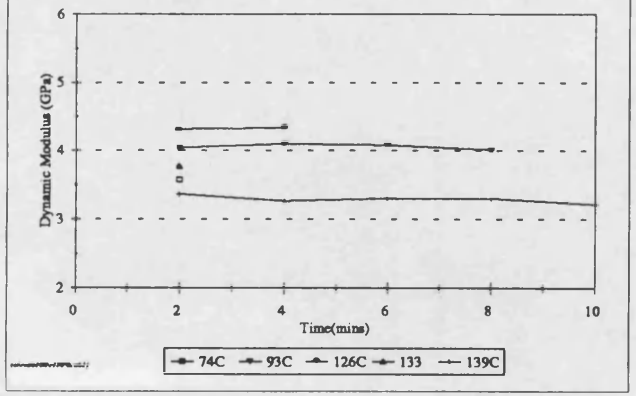

Fig 8.21b DYNAMIC MODULUS vs TIME FOR CHIPBOARD
R=0.1, 70% STRESS, HIGH FREQUENCY

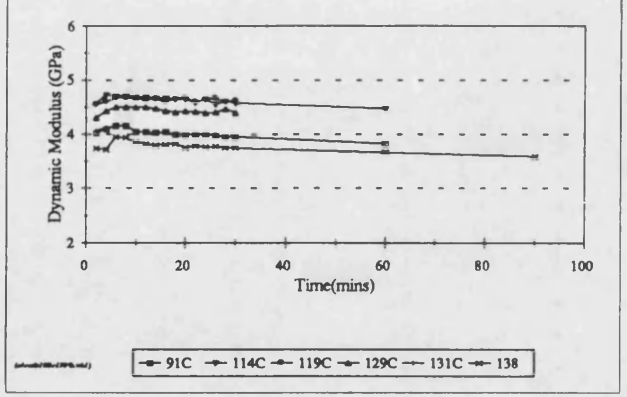

Fig 8.21c DYNAMIC MODULUS vs TIME FOR CHIPBOARD
R=0.1, 60% STRESS, HIGH FREQUENCY

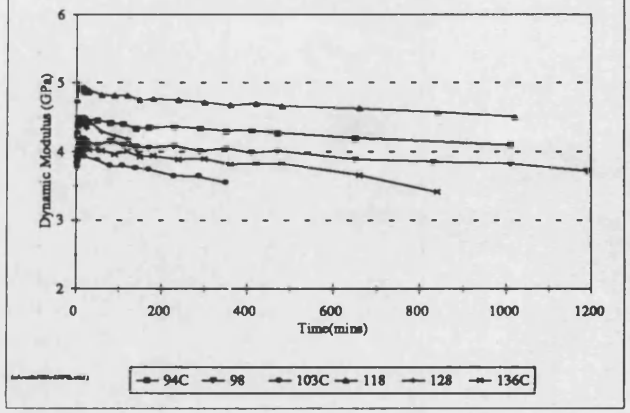

Fig 8.21d DYNAMIC MODULUS vs TIME FOR CHIPBOARD
R=0.1, 50% STRESS, HIGH FREQUENCY

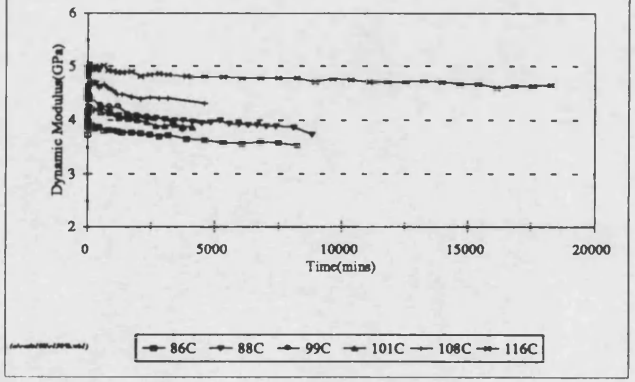

Fig 8.21e DYNAMIC MODULUS vs TIME FOR CHIPBOARD
R=0.1, 40 & 30% STRESS, HIGH FREQUENCY

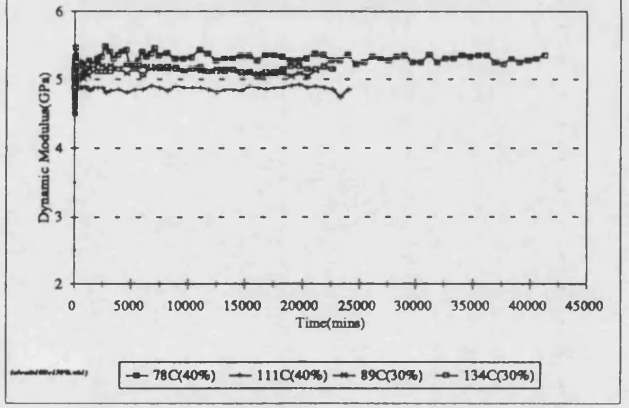

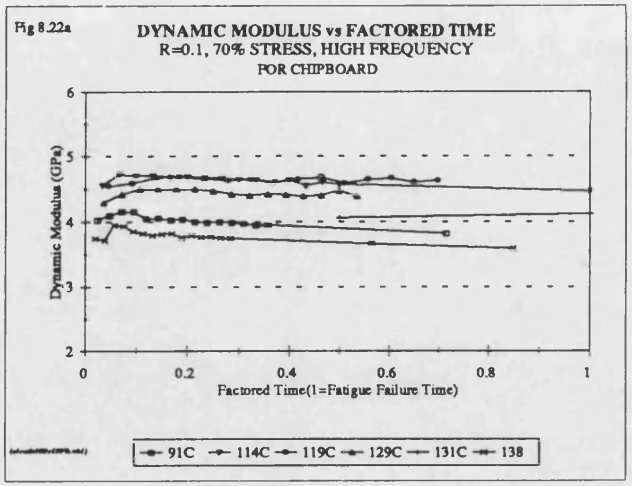
Fig 8.22a
DYNAMIC MODULUS vs FACTORED TIME
R=0.1, 70% STRESS, HIGH FREQUENCY
FOR CHIPBOARD
Dynamic Modulus (GPa)
Factored Time(1=Fatigue Failure Time)
91C 114C 119C 129C 131C 138

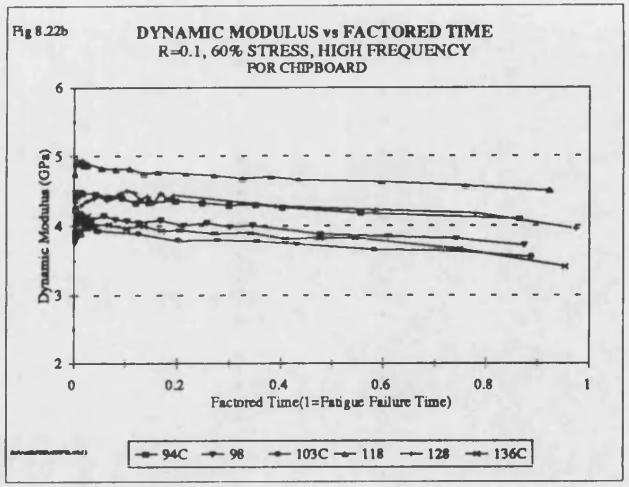
Fig 8.22b
DYNAMIC MODULUS vs FACTORED TIME
R=0.1, 60% STRESS, HIGH FREQUENCY
FOR CHIPBOARD
Dynamic Modulus (GPa)
Factored Time(1=Fatigue Failure Time)
94C 98 103C 118 128 136C

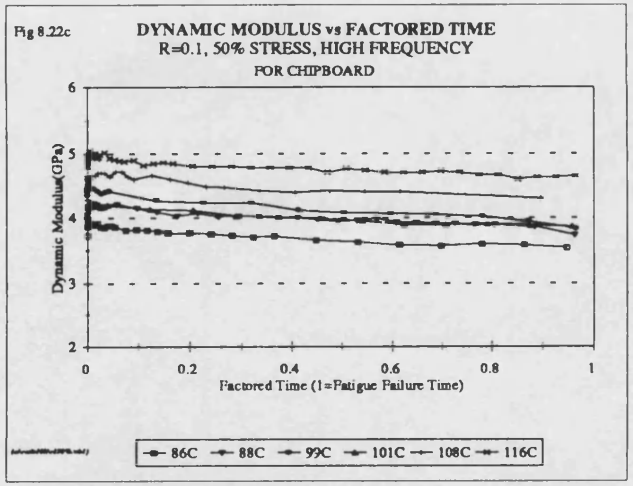
Fig 8.22c
DYNAMIC MODULUS vs FACTORED TIME
R=0.1, 50% STRESS, HIGH FREQUENCY
FOR CHIPBOARD
Dynamic Modulus(GPa)
Factored Time (1=Fatigue Failure Time)
86C 88C 99C 101C 108C 116C

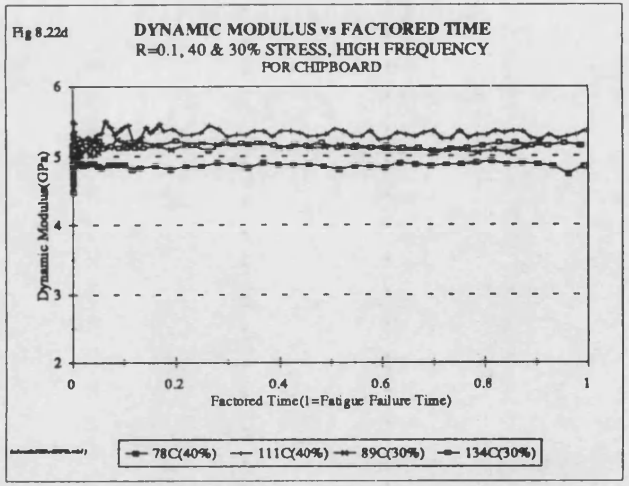
Fig 8.22d
DYNAMIC MODULUS vs FACTORED TIME
R=0.1, 40 & 30% STRESS, HIGH FREQUENCY
FOR CHIPBOARD
Dynamic Modulus(GPa)
Factored Time(1=Fatigue Failure Time)
78C(40%) 111C(40%) 89C(30%) 134C(30%)

Discussion

The values for the median initial, median final and the change in the median dynamic moduli are very similar for all three frequencies, figures 8.16a-c and show the same general trends with changing stress level. The only exception to this similarity is the change in loop area for the low frequency testing at the 40% stress level. However, this result is based on only one test and the initial loops captured for this test suffered from interference, so they should be considered with caution. The values for the dynamic moduli, table 8.8, are very similar to those reported by Hacker (1991) for testing at R=0.01 and by Thompson *et al* (1994) for testing at R=0.25 (see section 4.3.4). Both the initial and final values of dynamic moduli are greater than the static bending moduli reported in the literature for grade C4 structural chipboard (WPPF PD/15, 1992). This indicates that the chipboard tested is of a high standard for grade C4 material.

The median initial and median final dynamic moduli increased with decreasing stress level for all three frequencies. The lower the stress level the less the samples are damaged at the start of the tests, so the samples will be stiffer. At the lowest stress levels (<50%) there was a slight increase in the dynamic moduli. It is possible that this was due to drying of the samples at the higher test frequencies but this is unlikely for the low and medium frequencies tested.

To compare changes in the dynamic moduli during individual tests it is clearer to look at the figures plotted with respect to factored time rather than those plotted with respect to time, where the data is compacted close to the Y axis.

At the 80% stress level, figures 8.17a and 8.18a, for low frequency testing, there is a definite decrease in the dynamic moduli throughout testing for all six samples. The same trend is observed for the medium frequency testing, figures 8.19a and 8.20a, but for the high frequency loading, figure 8.21a, there was very little change in the dynamic moduli. This was probably due to the short duration of the tests and because the samples failed before there was time to see any reduction in moduli. Although the number of cycles to failure for the low frequency testing was less than for the medium frequency testing, which was in turn less than for the high frequency, the time duration of the tests increased with decreasing frequency. This allowed time for a measurable decreases in dynamic moduli to occur at the low and medium frequencies.

With the stress level reduced to 70, 60 and 50%, figures 8.17a-c and 8.18a-c for low frequency, figures 8.19a-c and 9.20a-c for medium frequency, and figures 8.21a-c and

8.22a-c for high frequency, the dynamic moduli continued to decrease throughout testing for all the samples tested. This can also be seen from the median changes in dynamic moduli in table 8.8 and from figure 8.16c. Hacker (1995) also found the dynamic moduli to decrease throughout fatigue testing for khaya-epoxy wood laminates loaded tension at R=0.1. The decreases observed for the wood laminates were of a far greater magnitude than those for chipboard. The magnitude of these changes in dynamic moduli for chipboard were always small, 0.65 MPa or less. The initial increases in dynamic moduli observed for high frequency loading were not observed for any of the samples tested at low frequency and only for a few samples at medium frequency. For many of the samples the dynamic moduli increased slightly at the start of the tests and then gradually decreases for the duration of the test. It is possible that the samples become slightly stiffer at the start of the tests due to compaction of the core material. After this, the wood-resin interfaces (glue lines) must start to break with cracks propagating between wood chips, resulting in a reduction in the stiffness of the samples. This reduction in stiffness eventually results in sample failure.

For the low frequency testing at 40, 30 and 20% stress levels the dynamic moduli increased at first and then remained almost constant for the duration of the tests. This implies that the samples were not significantly damaged by the continuous fatigue loading. This seems reasonable as the samples survived the allotted 10^6 loading cycles resulting in runouts. The tests were stopped and no failures occurred. This agrees with the creep microstrain curves which show no increase in microstrain after initial elastic deformation. The dynamic modulus for the 30% stress level test at medium frequency continued to increase throughout the test. This means that the sample became stiffer throughout the test with the sample surviving to become a runout sample. The dynamic modulus also increased as a result of cyclic loading for the 40 and 30% stress level tests at high frequency, possibly due to drying from adiabatic heating of the samples, although this is considered improbable. The dynamic moduli for the 40, 30 and 20% stress level tests at low frequency also remained almost unchanged for the duration of the tests. These samples did not show the initial increase in modulus observed at the higher frequencies but also survived to become runouts and showed no change in microstrain. Grossman and Nakai (1987) observed slight increases in the dynamic moduli for clear wood specimens loaded in bending at stress levels of 30% and below. These increases were attributed to a slight work hardening but the increases were not statistically significant. Tsai (1987) also observed increases in the dynamic moduli for Khaya and Sitka spruce when fatigue loaded in bending at low load levels.

The plots of dynamic modulus versus factored time show all the same features as the plots with non-factored time. They also show that the trends in dynamic modulus as a function of factored time between different samples at the same stress levels are very similar.

8.8 Fatigue Moduli

The fatigue modulus, defined in section 6.6, differs from the dynamic modulus because it incorporates the changing stiffness and the creep strain of the sample during a fatigue test.

Figures 8.23a-c show the median initial, median final and the median change in fatigue moduli, respectively, for chipboard at all three frequencies, at stress levels from 80% to 20% of the static strength. Median values have been plotted again to minimise variations from unusually weak or strong samples. Fig 8.23a is, as would be expected, the same as fig 8.16a for the initial dynamic moduli.

Table 8.9 provides a numerical summary of the median fatigue moduli for all the fatigue samples tested, at all stress levels, for all three frequencies. This table displays the median initial, median final and the median change in fatigue moduli. Also included are the ranges of the initial, final and the change in the moduli for the different samples tested at each stress level for each frequency. The initial fatigue moduli are the first captured fatigue moduli and the final fatigue moduli are the last captured fatigue moduli. They are not usually the true first and last values, as was explained previously (see section 8.6). At the 80% stress level for the low frequency the second hysteresis loop has been considered as the starting points for the tests because the first loading cycle begins at zero stress, not one tenth of the peak stress, as required for an R ratio of 0.1 and unclosed loops were captured for the first loading cycle. The second loop was also used for the high frequency tests at 30% stress as the maximum and minimum stresses were not obtained by the time the first hysteresis loop was captured. Two of the six samples tested at 50% stress at low frequency were excluded from the calculations because they had moved on the rollers.

Figures 8.24a-e, 8.27a-e and 8.30a-e show the fatigue moduli as a function of time for all the samples tested at the 80, 70, 60, 50, 40, 30 and 20% stress levels for the low, medium and high frequencies respectively. This allows direct comparisons to be made between the different samples at the same, and at different stress levels. Time is plotted on the X axis and varies greatly as it represents the duration of the tests. Because tests are of greatly different time duration these figures have also been plotted with respect to factored time and are included as figures 8.25a-e, 8.28a-e and 8.31a-d for the low, medium and high frequencies respectively. A graph for the 80% stress level for high frequency loading has not been plotted with respect to factored time due to the short duration of the tests. All of the graphs have been plotted with the fatigue modulus ranging from 0-6 GPa on the Y axis. The plots with respect to factored time provide a

better comparison between tests of greatly different time duration. When the hysteresis loops were captured, to measure the fatigue moduli values, there was a concentration of data points at the beginning of the tests. For this reason the fatigue moduli have also been plotted with respect to $\log_{(10)}$ time to remove the confusion produced by the clustering of data points close to the Y axis.

Fig. 8.23a

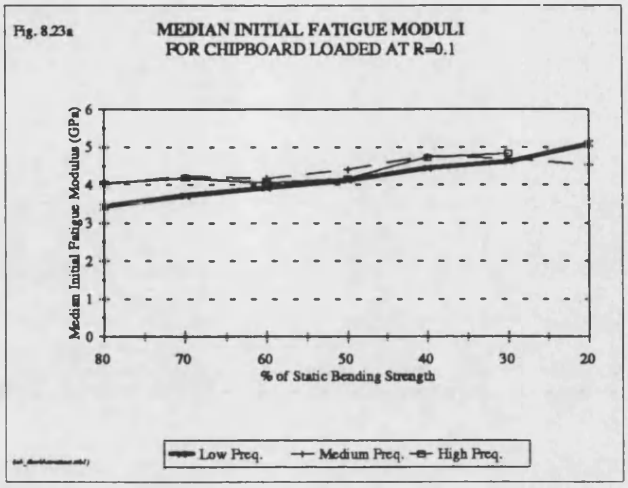

Fig. 8.23b

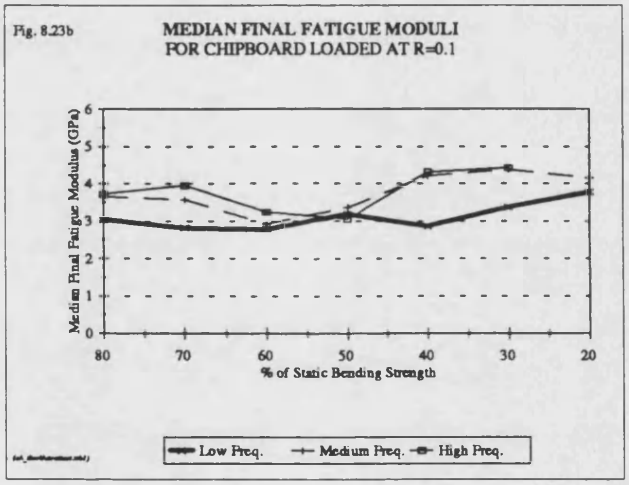

Fig. 8.23c

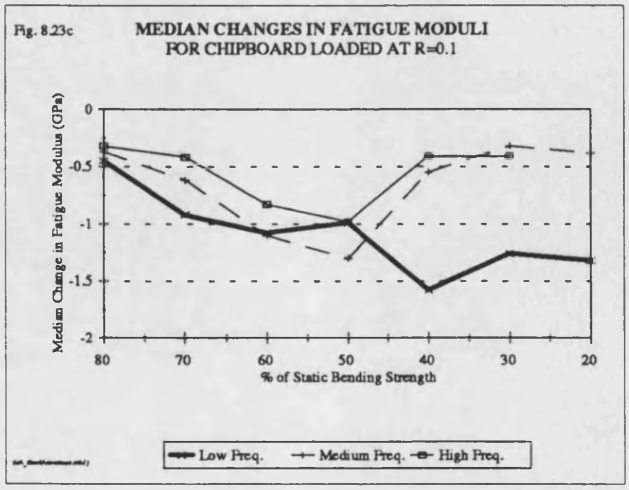

Table 8.9 Median fatigue moduli for chipboard tested at R=0.1, at low, medium and high frequencies.

Stress Level	Median Initial Fatigue Modulus GPa	Median Final Fatigue Modulus GPa	Median Change in Fatigue Modulus GPa	Range of Initial Fatigue Moduli GPa	Range of Final Fatigue Moduli GPa	Range of Change in Fatigue Modulus GPa
LOW FREQUENCY, R=0.1						
80%	3.43	3.04	-0.45	3.16-4.10	2.64-3.36	(-0.14)-(-0.77)
70%	3.72	2.82	-0.92	3.39-4.08	2.28-3.50	(-0.58)-(-1.11)
60%	3.92	2.77	-1.08	3.47-4.21	2.53-3.13	(-0.94)-(-1.29)
50%	4.13	3.18	-0.99	3.84-4.40	2.84-3.18	(-0.93)-(-1.22)
40%	4.44	2.86	1.58	1 Sample	1 Sample	1 Sample
30%	4.62	3.36	1.26	1 Sample	1 Sample	1 Sample
20%	5.09	3.77	1.32	1 Sample	1 Sample	1 Sample
MEDIUM FREEQUENCY, R=0.1						
80%	4.02	3.65	-0.37	3.59-4.84	3.25-4.03	(-0.31)-(-0.81)
70%	4.23	3.57	-0.62	3.51-4.87	2.91-3.73	(-0.48)-(-1.14)
60%	4.18	2.91	-1.10	3.61-4.86	2.63-3.86	(-0.73)-(-1.42)
50%	4.41	3.35	-1.30	3.90-4.87	2.69-3.41	(-1.46)-(-1.09)
40%	4.76	4.21	-0.55	1 Sample	1 Sample	1 Sample
30%	4.70	4.38	-0.32	1 Sample	1 Sample	1 Sample
20%	4.53	4.15	-0.38	1 Sample	1 Sample	1 Sample
HIGH FREQUENCY, R=0.1						
80%	4.04	3.72	-0.32	3.37-4.31	2.87-4.09	(-0.22)-(0.50)
70%	4.18	3.95	-0.42	3.74-4.56	3.09-4.24	(-0.17)-(0.65)
60%	4.06	3.23	-0.83	3.83-4.74	2.74-3.88	(-0.76)-(-1.14)
50%	4.17	3.04	-0.98	3.73-4.63	3.73-4.63	(-0.75)-(-1.27)
40%	4.73	4.32	-0.41	2 Samples	2 Samples	2 Samples
30%	4.84	4.43	-0.41	2 Samples	2 Samples	2 Samples

Fig 8.24a

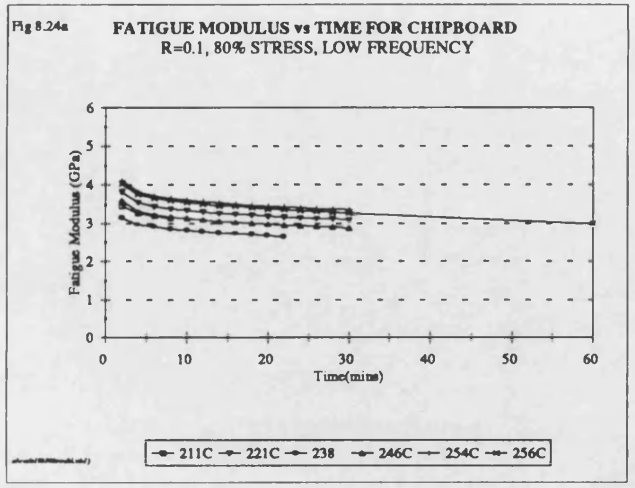

Fig 8.24b

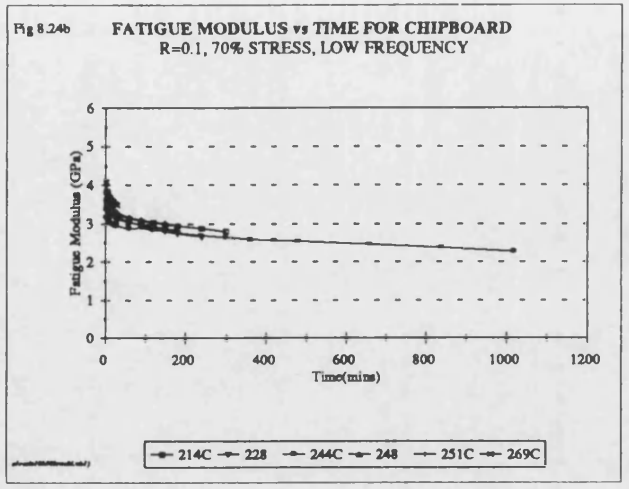

Fig 8.24c

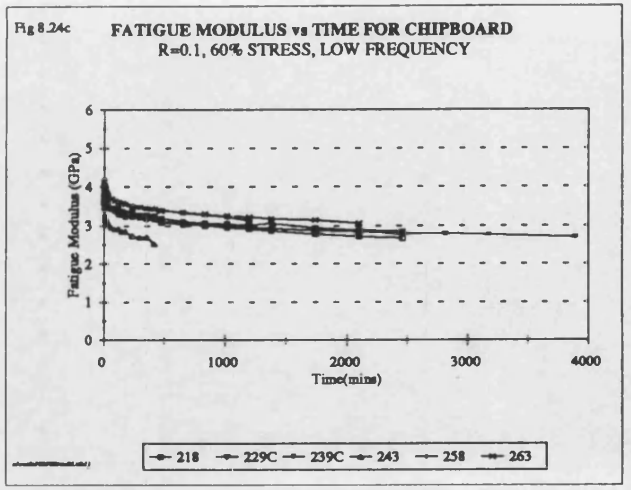

Fig 8.24d

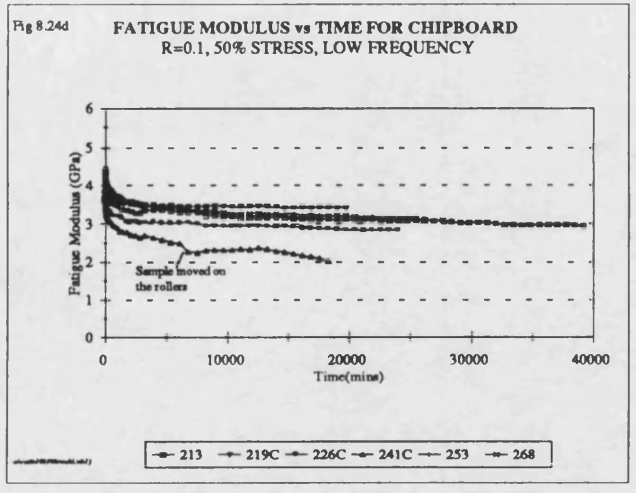

Fig 8.24e

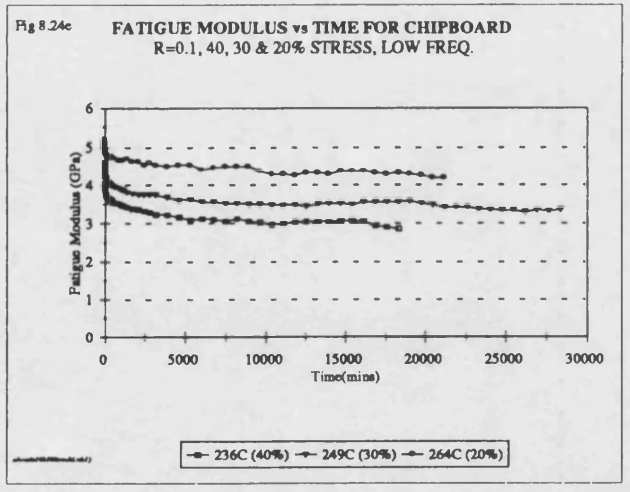

Fig 8.25a

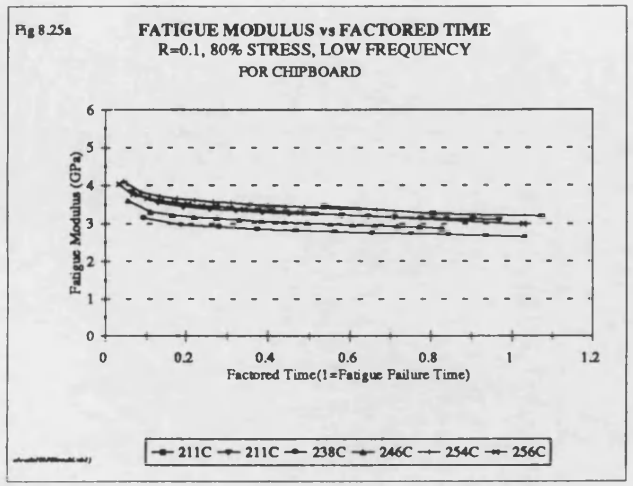

Fig 8.25b

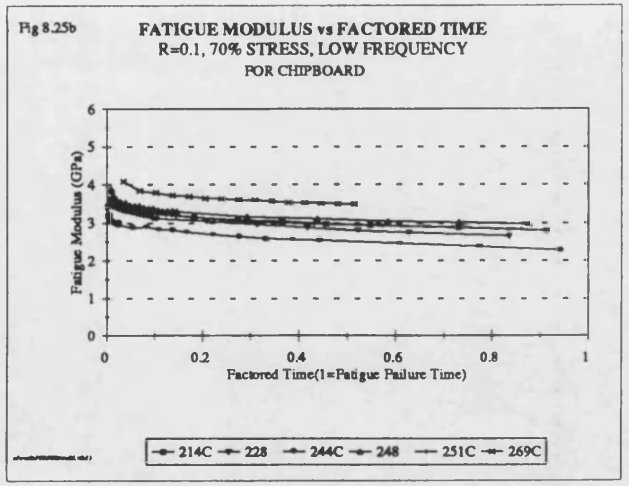

Fig 8.25c

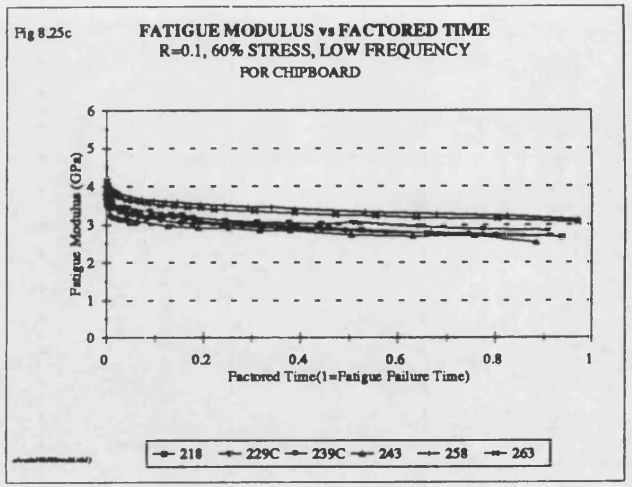

Fig 8.25d

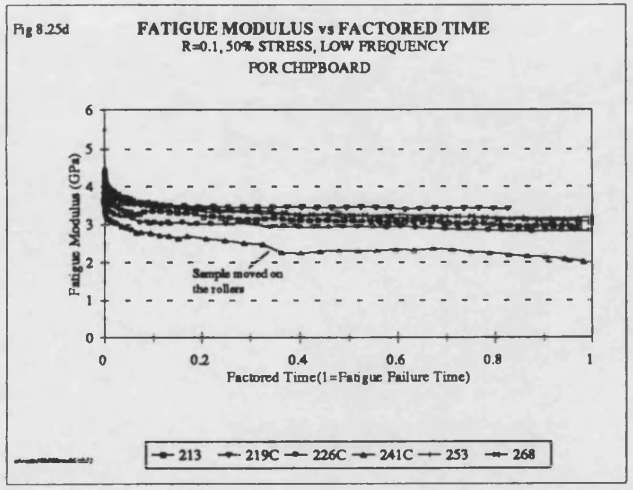

Fig 8.25e

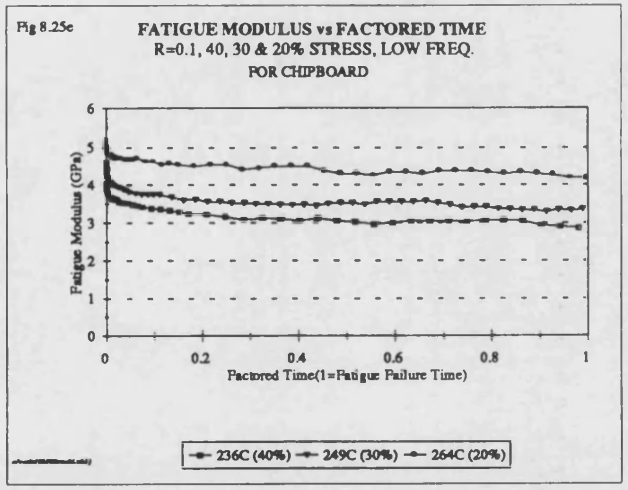

Fig 8.26a **FATIGUE MODULUS vs LOG TIME, CHIPBOARD**
R=0.1, 80% STRESS, LOW FREQUENCY

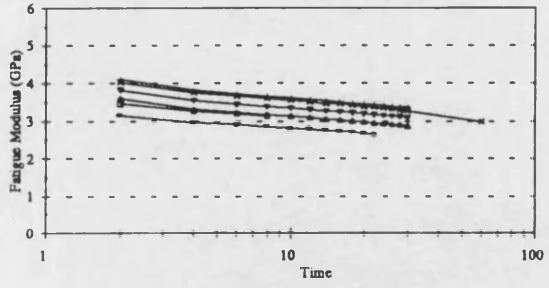

Fig 8.26b **FATIGUE MODULUS vs LOG TIME, CHIPBOARD**
R=0.1, 70% STRESS, LOW FREQUENCY

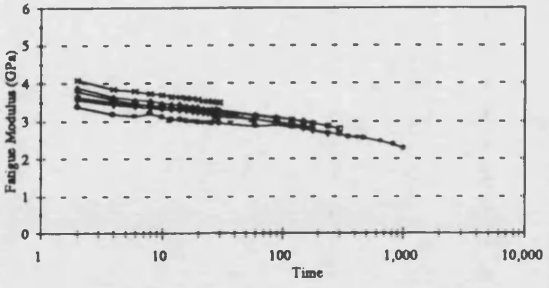

Fig 8.26c **FATIGUE MODULUS vs LOG TIME, CHIPBOARD**
R=0.1, 60% STRESS, LOW FREQUENCY

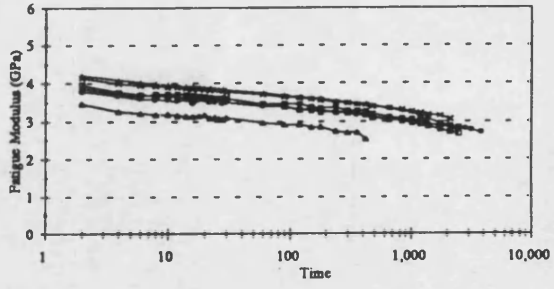

Fig 8.26d **FATIGUE MODULUS vs LOG TIME, CHIPBOARD**
R=0.1, 50% STRESS, LOW FREQUENCY

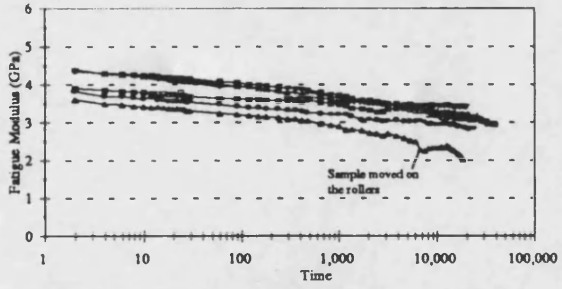

Fig 8.26e **FATIGUE MODULUS vs LOG TIME, CHIPBOARD**
R=0.1, 40, 30 & 20% STRESS, LOW FREQ.

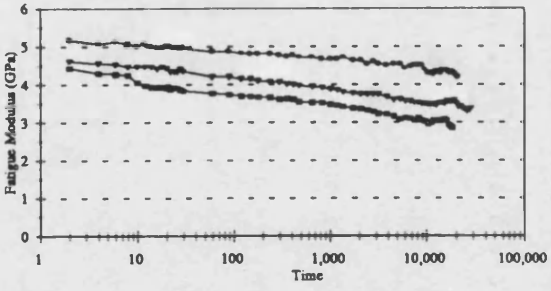

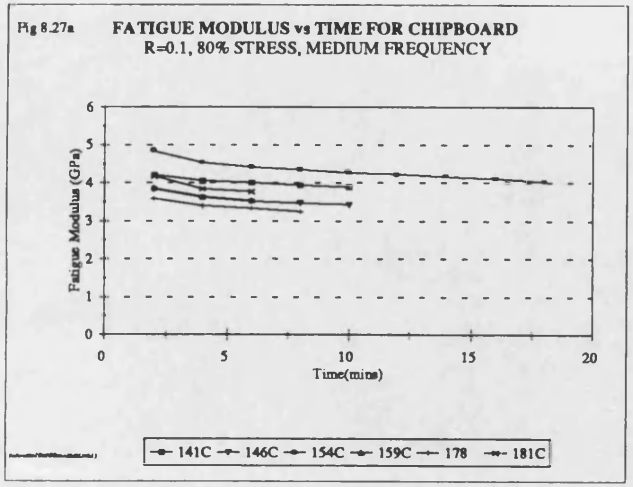
Fig 8.27a
FATIGUE MODULUS vs TIME FOR CHIPBOARD
R=0.1, 80% STRESS, MEDIUM FREQUENCY
Fatigue Modulus (GPa)
Time(mins)
141C 146C 154C 159C 178 181C

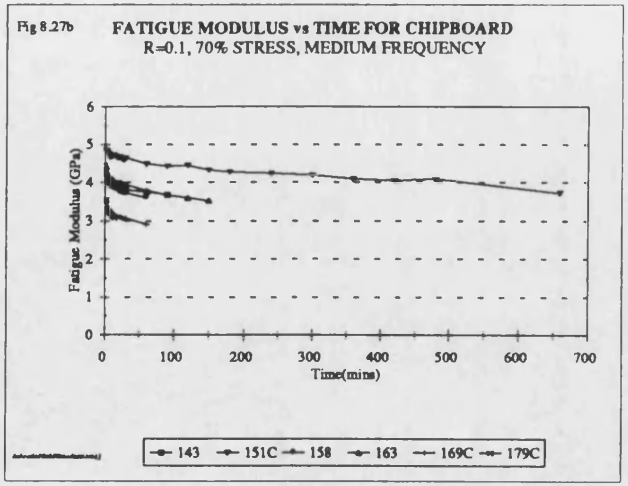
Fig 8.27b
FATIGUE MODULUS vs TIME FOR CHIPBOARD
R=0.1, 70% STRESS, MEDIUM FREQUENCY
Fatigue Modulus (GPa)
Time(mins)
143 151C 158 163 169C 179C

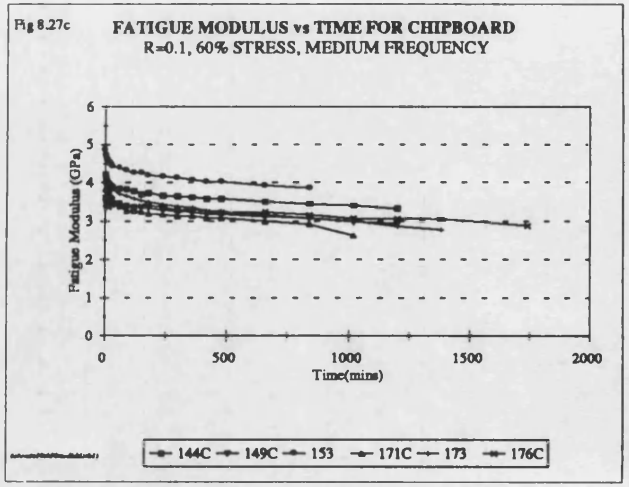
Fig 8.27c
FATIGUE MODULUS vs TIME FOR CHIPBOARD
R=0.1, 60% STRESS, MEDIUM FREQUENCY
Fatigue Modulus (GPa)
Time(mins)
144C 149C 153 171C 173 176C

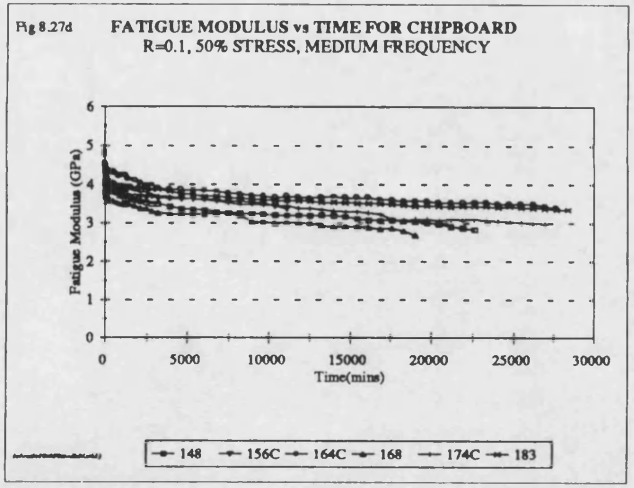
Fig 8.27d
FATIGUE MODULUS vs TIME FOR CHIPBOARD
R=0.1, 50% STRESS, MEDIUM FREQUENCY
Fatigue Modulus (GPa)
Time(mins)
148 156C 164C 168 174C 183

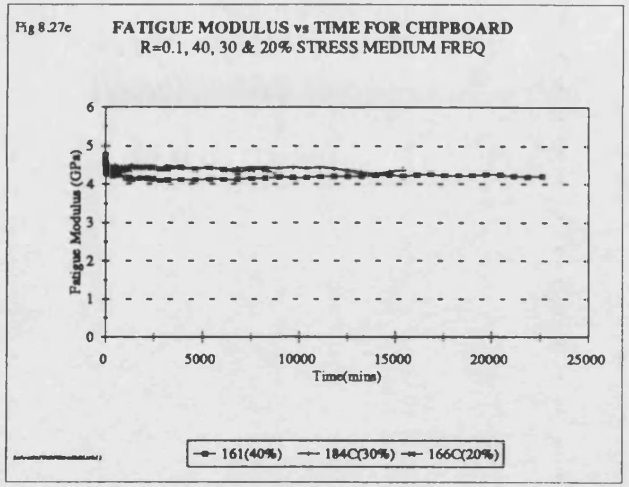
Fig 8.27e
FATIGUE MODULUS vs TIME FOR CHIPBOARD
R=0.1, 40, 30 & 20% STRESS MEDIUM FREQ
Fatigue Modulus (GPa)
Time(mins)
161(40%) 184C(30%) 166C(20%)

Fig 8.28a

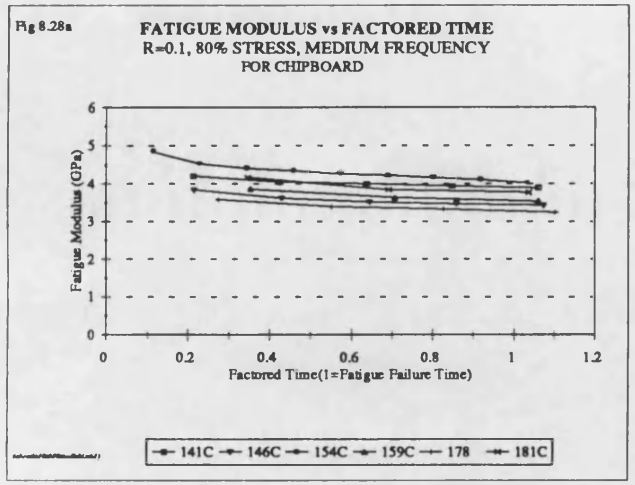

Fig 8.28b

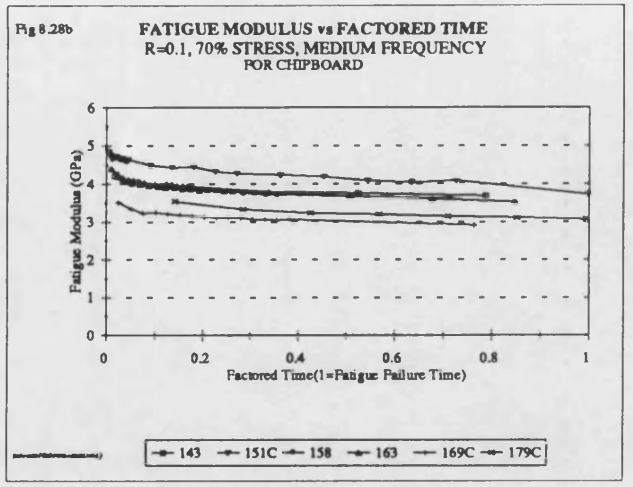

Fig 8.28c

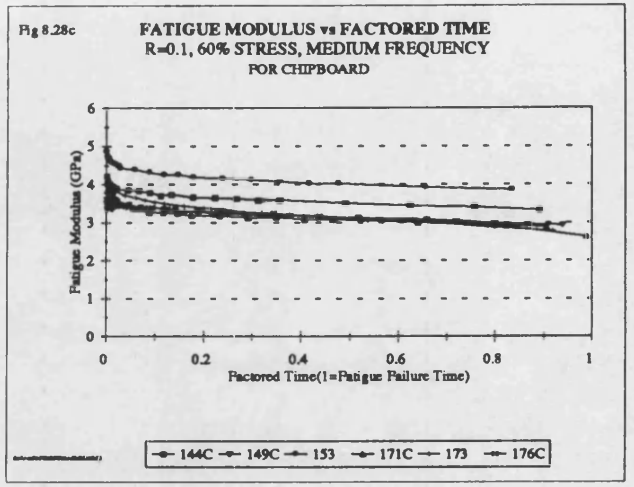

Fig 8.28d

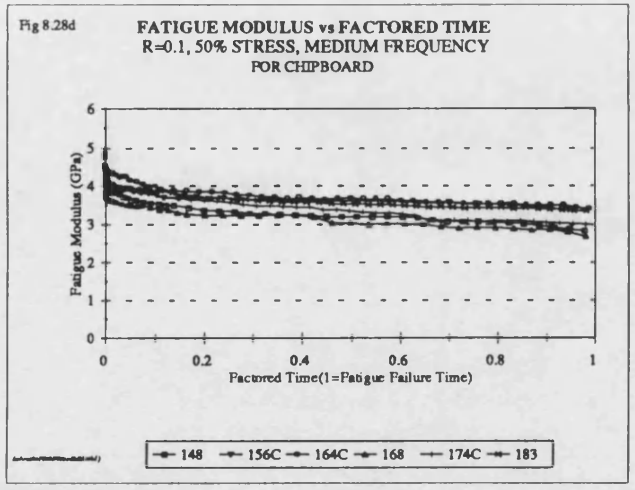

Fig 8.28e

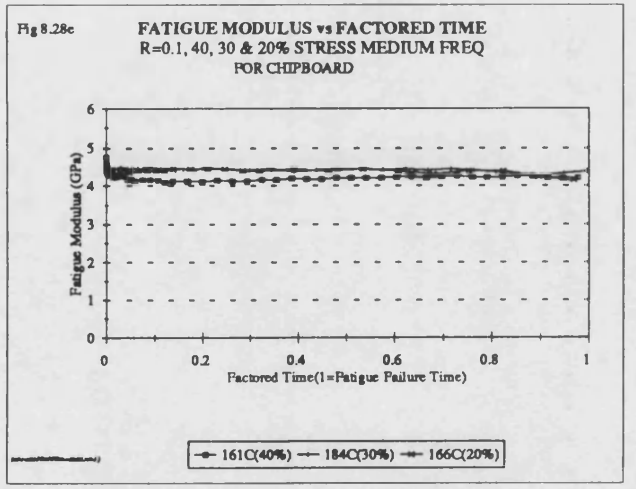

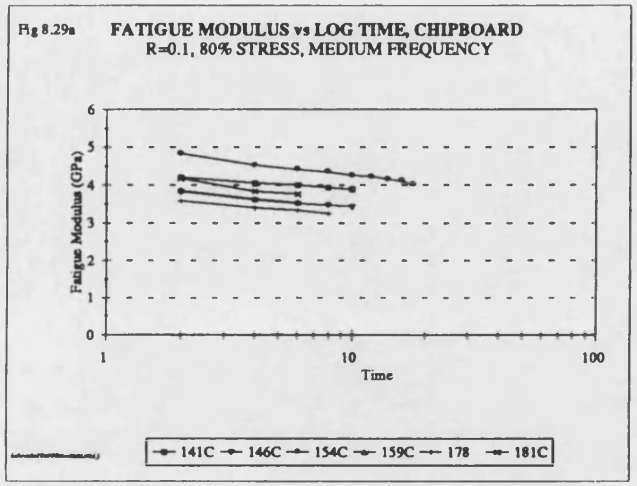
Fig 8.29a
FATIGUE MODULUS vs LOG TIME, CHIPBOARD
R=0.1, 80% STRESS, MEDIUM FREQUENCY
Fatigue Modulus (GPa)
Time
141C 146C 154C 159C 178 181C

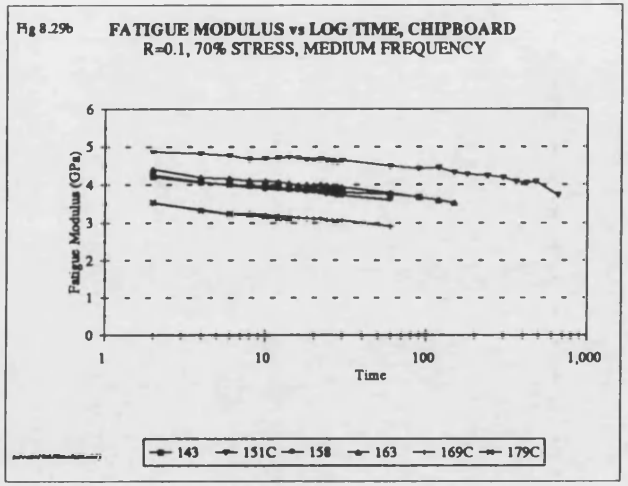
Fig 8.29b
FATIGUE MODULUS vs LOG TIME, CHIPBOARD
R=0.1, 70% STRESS, MEDIUM FREQUENCY
Fatigue Modulus (GPa)
Time
143 151C 158 163 169C 179C

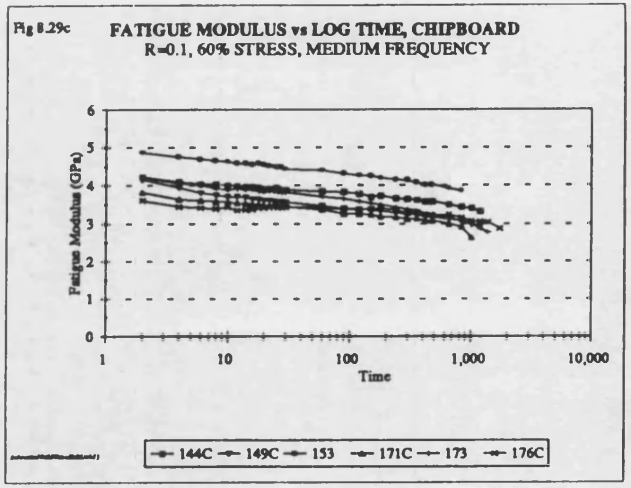
Fig 8.29c
FATIGUE MODULUS vs LOG TIME, CHIPBOARD
R=0.1, 60% STRESS, MEDIUM FREQUENCY
Fatigue Modulus (GPa)
Time
144C 149C 153 171C 173 176C

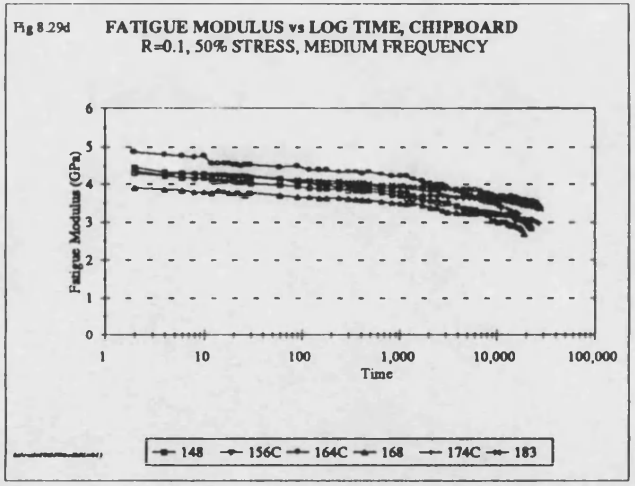
Fig 8.29d
FATIGUE MODULUS vs LOG TIME, CHIPBOARD
R=0.1, 50% STRESS, MEDIUM FREQUENCY
Fatigue Modulus (GPa)
Time
148 156C 164C 168 174C 183

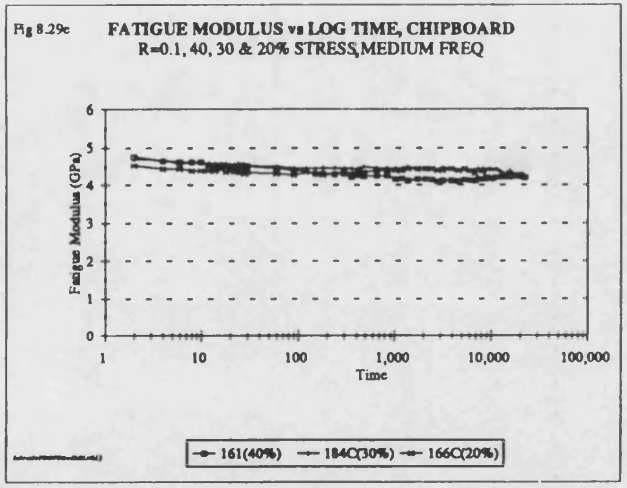
Fig 8.29e
FATIGUE MODULUS vs LOG TIME, CHIPBOARD
R=0.1, 40, 30 & 20% STRESS, MEDIUM FREQ
Fatigue Modulus (GPa)
Time
161(40%) 184C(30%) 166C(20%)

Fig 8.30a FATIGUE MODULUS vs TIME FOR CHIPBOARD
R=0.1, 80% STRESS, HIGH FREQUENCY

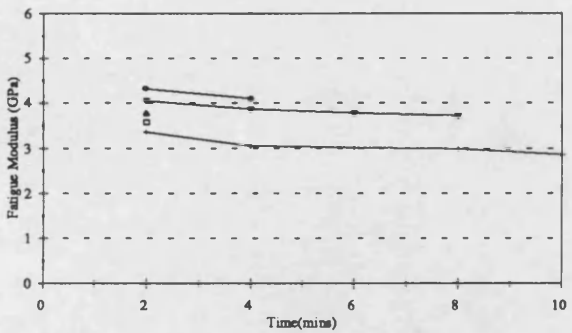

Fig 8.30b FATIGUE MODULUS vs TIME FOR CHIPBOARD
R=0.1, 70% STRESS, HIGH FREQUENCY

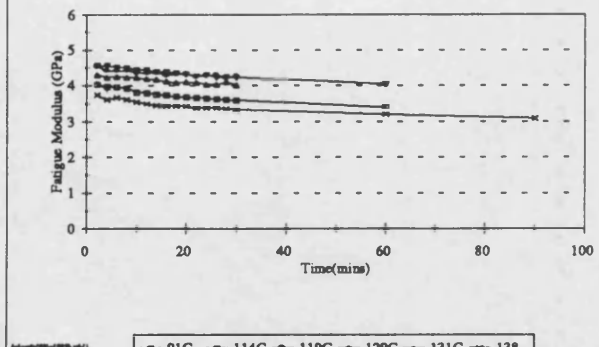

Fig 8.30c FATIGUE MODULUS vs TIME FOR CHIPBOARD
R=0.1, 60% STRESS, HIGH FREQUENCY

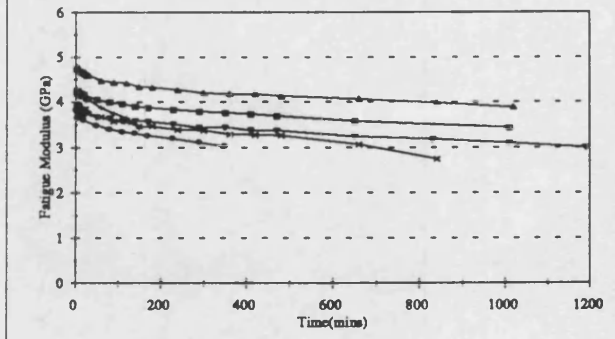

Fig 8.30d FATIGUE MODULUS vs TIME FOR CHIPBOARD
R=0.1, 50% STRESS, HIGH FREQUENCY

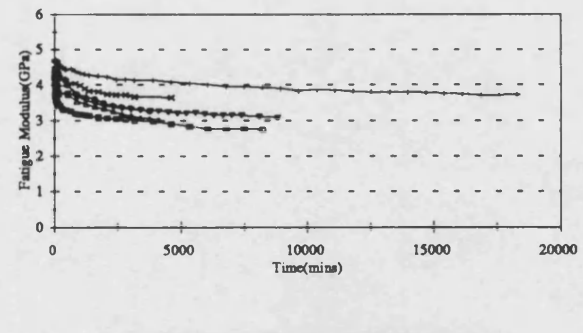

Fig 8.30e FATIGUE MODULUS vs TIME FOR CHIPBOARD
R=0.1, 40 & 30% STRESS, HIGH FREQUENCY

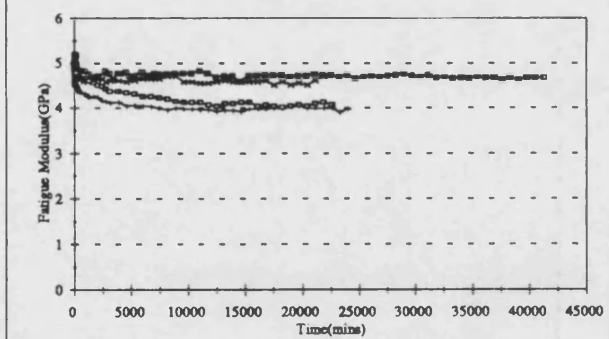

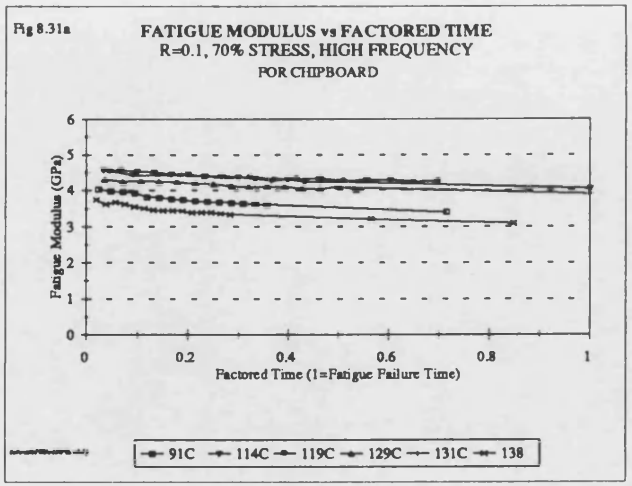
Fig 8.31a
FATIGUE MODULUS vs FACTORED TIME
R=0.1, 70% STRESS, HIGH FREQUENCY
FOR CHIPBOARD
Fatigue Modulus (GPa)
Factored Time (1=Fatigue Failure Time)
91C 114C 119C 129C 131C 138

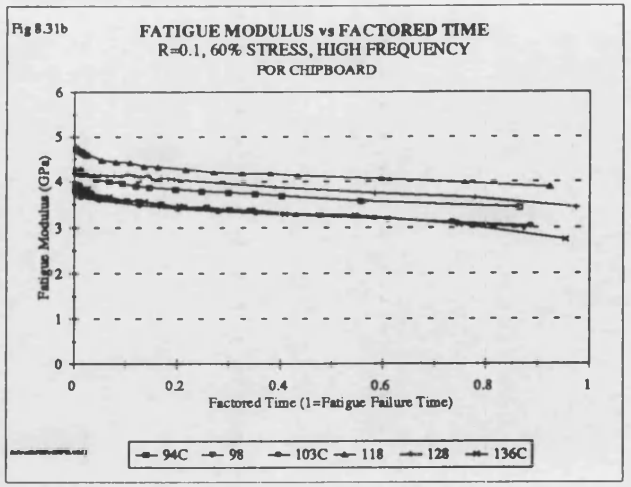
Fig 8.31b
FATIGUE MODULUS vs FACTORED TIME
R=0.1, 60% STRESS, HIGH FREQUENCY
FOR CHIPBOARD
Fatigue Modulus (GPa)
Factored Time (1=Fatigue Failure Time)
94C 98 103C 118 128 136C

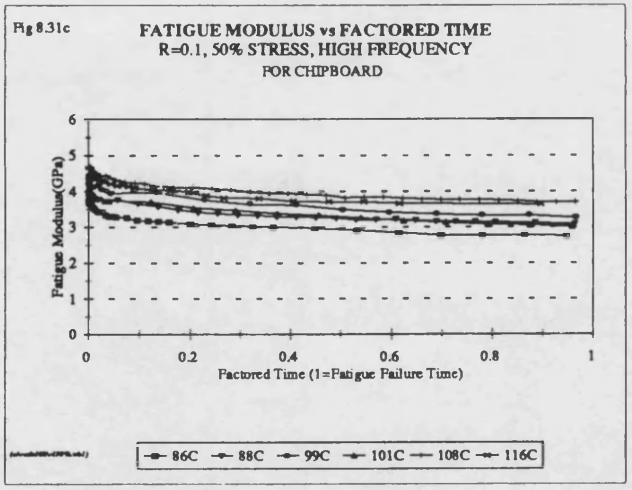
Fig 8.31c
FATIGUE MODULUS vs FACTORED TIME
R=0.1, 50% STRESS, HIGH FREQUENCY
FOR CHIPBOARD
Fatigue Modulus(GPa)
Factored Time (1=Fatigue Failure Time)
86C 88C 99C 101C 108C 116C

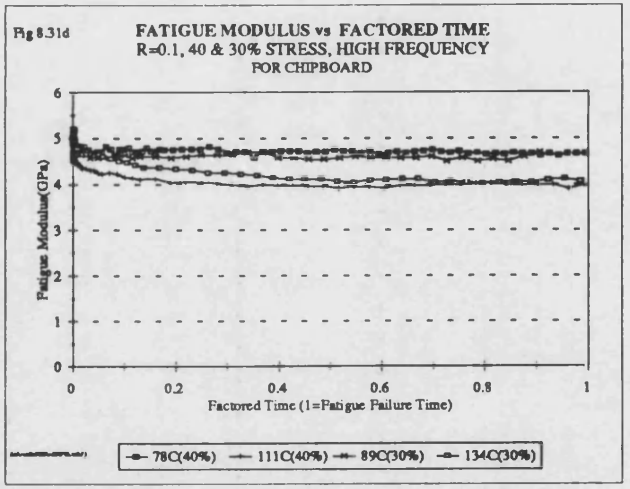
Fig 8.31d
FATIGUE MODULUS vs FACTORED TIME
R=0.1, 40 & 30% STRESS, HIGH FREQUENCY
FOR CHIPBOARD
Fatigue Modulus(GPa)
Factored Time (1=Fatigue Failure Time)
78C(40%) 111C(40%) 89C(30%) 134C(30%)

Fig 8.32a

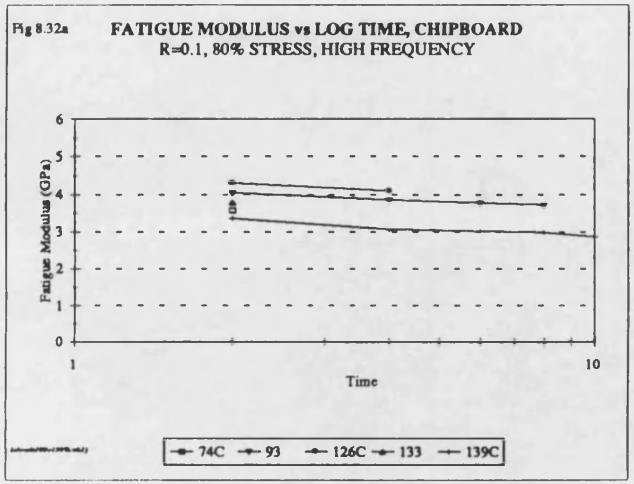

Fig 8.32b

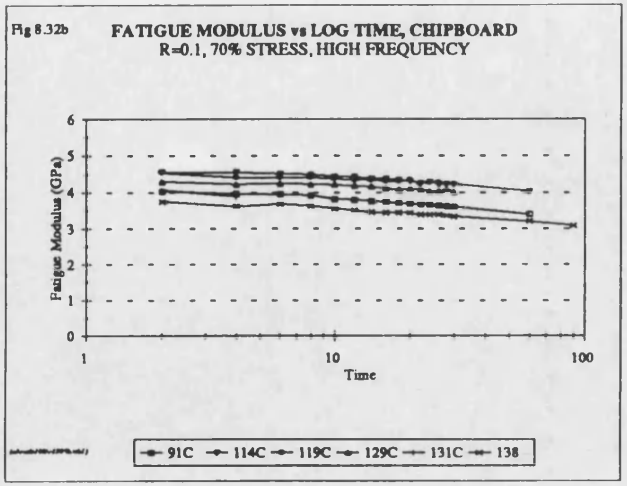

Fig 8.32c

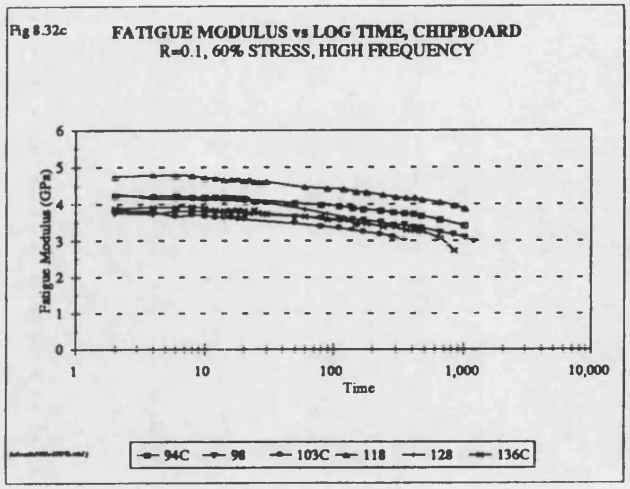

Fig 8.32d

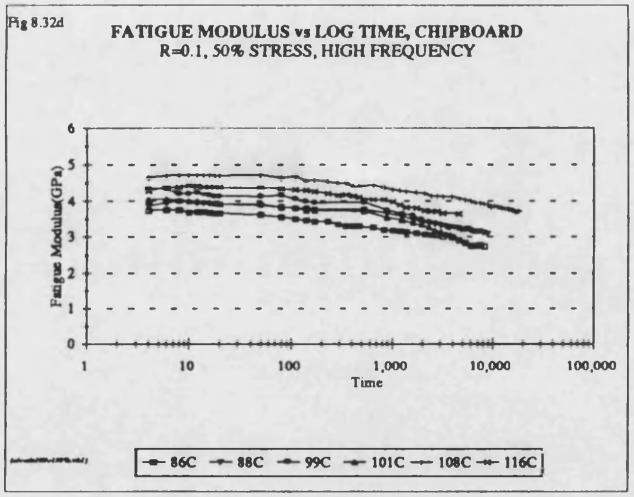

Fig 8.32e

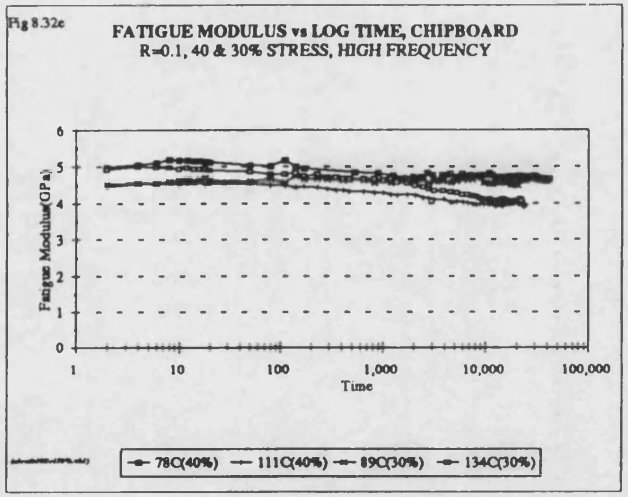

Discussion

The fatigue modulus is a more appropriate measure of sample stiffness than the dynamic modulus because it takes account of the creep occurring in the fatigue samples. The design parameters for wood based panels used as flooring are based on the duration of load, or on the deflection/creep of the panels. For this reason a stiffness measurement that accounts for the deflection is particularly appealing.

Figure 8.23a shows that the initial median fatigue moduli increase as the stress level is reduced from 80% down to 20%. This is an identical trend to that observed for the initial median dynamic moduli versus stress level because the first fatigue modulus value for each sample tested does not include any effects from creep occurring in the fatigue sample. The final median fatigue moduli, figure 8.23b, reduce as the stress level is reduced from 80% down to 60% then increase with reducing stress level from 50% down to 20% for the medium and the high frequency. The same trend is also observed for the median changes in the fatigue moduli, figure 8.23c. This is a feature of the test length and loop capture interval. At the high stress levels for the medium and high frequencies the initial loops are captured later than the first loading cycle as explained in section 8.6. This means that at the high stress levels the samples have already deflected considerably before the first data point was captured and so the changes in fatigue moduli before the samples fail are only relatively small. As the stress level is reduced, the initial deflections prior to the first data point reduce causing the changes in the fatigue moduli to increase with reducing stress level. The values plotted in figures 8.23a-c are also displayed in table 8.9.

For the low frequency loading the first hysteresis loops captured were either the very first loops or loops captured very soon after the first loop. The median final fatigue moduli were almost constant down to the 40% stress level for the low frequency testing. It seems therefore that the samples must be approaching failure when the fatigue moduli reduce to about 3 GPa. However, due to the variability in sample strengths, this cannot be concluded, particularly when table 8.9 and the plots showing individual tests, figures 8.24a-e, 8.25a-e and 8.26a-e, are examined. This trend is also confused because the fatigue moduli results for the low frequency testing at the 40, 30 and 20% stress levels are different to the fatigue moduli for the medium and high frequencies at the same stress levels. It is unlikely that the low frequency results are at fault because all three tests agree with each other and the loop captures for lower frequencies were generally superior to those for the higher frequencies. A higher proportion of the samples tested at the 50% stress level failed at the low frequency compared to failures at the higher frequencies and the fatigue life fell as the frequency

reduced. Since decreasing the frequency reduces the fatigue life it seems reasonable that the fatigue runout samples were more damaged at the low frequencies than those at the medium and high frequencies.

It can be seen from figures 8.24a-e, 8.25a-e and 8.26a-e that at low frequencies the fatigue moduli decrease at all the stress levels tested throughout each test. Figures 8.26a-e and 8.27a-e show that the fatigue moduli decrease in three stages. The fatigue moduli decrease rapidly at first due to the initial elastic deflections of the samples that were observed in the plots of microstrain, figures 8.12a-f, 8.13a-f and 8.14a-f. Then the decrease is at a fairly uniform slower rate for the main part of the tests. The third and final stage is only shown by a few of the samples where there is an increased rate of decrease towards the end of the tests as in figure 8.27d. The decreases in fatigue moduli for low frequency loading are almost linear when plotted with respect to $\log_{(10)}$ time for all the stress levels and the gradients are similar for different samples tested at the same stress level.

For the medium frequency loading, figures 8.27a-e, 8.28a-e and 8.29a-e, and for the high frequency loading, figures 8.30a-e, 8.31a-d and 8.32a-e, the fatigue moduli decrease throughout testing for all samples tested at the 80, 70 60 and 50% stress levels. This again is a three stage process as observed for the low frequency testing when plotted with respect to time and to factored time. The plots of fatigue moduli versus $\log_{(10)}$ time for the medium and high frequencies are not as close to linear as for the low frequency. At these higher frequencies the rate of decrease becomes greater as the tests progress.

The plots of fatigue moduli versus factored time show all the same features as the plots versus time. They also show that the trends in fatigue modulus as a function of factored time between different samples tested at the same stress level and frequency were very similar. The use of fatigue moduli instead of dynamic moduli produces more pronounced stiffness changes and smooths out many of the irregularities seen in the dynamic moduli plots for all three frequencies. The decreases observed for the fatigue moduli are greater than those for the dynamic moduli and are shown by the median changes in the fatigue moduli in figure 8.23c and table 8.9 compared to the median changes in the dynamic moduli in figure 8.16c and table 8.8.

The fatigue moduli measured by Hacker (1995) for khaya-epoxy wood laminates loaded in tension at R=0.1 remained fairly constant throughout testing and then decreased dramatically at the end of the tests. This was attributed to the formation of

large splinters in the wood, a phenomenon that could not occur in chipboard because the wood has been broken down into small chips. Hacker (1995) used the gradient of the initial fatigue modulus to predict the fatigue life for laminates loaded in compression at R=10 but the gradient for laminates loaded at R=0.1 in tension was found to be too shallow for this technique.

Fatigue life prediction models based on residual stiffness have been proposed by Yang *et al* (1992) and Lee *et al* (1993) for composite materials fatigue loaded in tension. Residual stiffness has an advantage over residual strength as a tool for life prediction because unlike the residual strength it can be measured non-destructively.

8.9 Hysteresis Loop Areas

The hysteresis loop area is the total energy dissipated in the sample during an individual loading and unloading cycle and is explained in section 6.6. Figures 8.33a-c show the median initial, median final and the median change in hysteresis loop areas respectively for chipboard at all three frequencies as a function of changing the stress level. Once again, median values have been plotted to reduce confusion caused by strength variations within individual sets of samples.

Table 8.10 provides a numerical summary of the median hysteresis loop areas for all the fatigue samples tested, at all stress levels, for all three frequencies. This table displays the median initial, median final and the median change in hysteresis loop areas. Also included are the ranges of the initial loop area, final loop area and the change in the loop areas for the different samples tested at each stress level for each frequency. The initial hysteresis loop areas are the first captured loop areas and the final loop areas are the last captured. They are not usually the true first and last values as explained in section 8.6. Again at the 80% stress level at low frequency the second hysteresis loop has been considered as the starting point for the tests because the first loading cycle begins at zero stress, not one tenth of the peak stress, as required for an R ratio of 0.1 and unclosed loops were captured. The second loop was also used for the high frequency tests at 30% stress as the maximum and minimum stresses were not obtained by the time the first hysteresis loop was captured. The two samples tested at 50% stress at low frequency which had moved on the rollers were again excluded from the median values.

Figures 8.34a-e, 8.37a-e and 8.40a-e show the hysteresis loop areas as a function of time for all the samples tested at the 80, 70, 60, 50, 40, 30 and 20% stress levels for the low, medium and high frequencies respectively. This allows direct comparisons to be made between the samples tested at the same and at different stress levels. Time is plotted on the X axis and varies greatly as it represents the duration of the tests. Because the tests are of greatly different time duration these figures have also been plotted with respect to factored time and are included as figures 8.35a-e, 8.38a-e and 8.41a-d for the low, medium and high frequencies respectively. Again a graph for the 80% stress level for high frequency loading has not been plotted with respect to factored time due to the short duration of the tests. All of the graphs have been plotted with the hysteresis loop area ranging from 0-8 kJ/m^3 on the Y axis. When the hysteresis loops were captured, there was a concentration of data points at the beginning of the tests, so the loop areas have also been plotted with respect to $\log_{(10)}$

time to remove the confusion produced by the clustering of data points close to the Y axis.

Fig. 8.33a MEDIAN INITIAL HYSTERESIS LOOP AREA FOR CHIPBOARD LOADED AT R=0.1

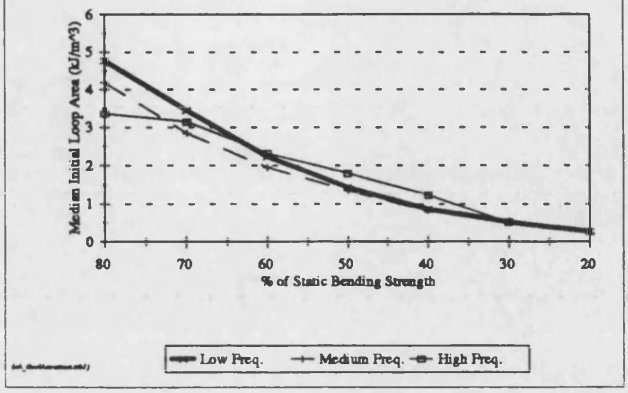

Fig. 8.33b MEDIAN FINAL HYSTERESIS LOOP AREA FOR CHIPBOARD LOADED AT R=0.1

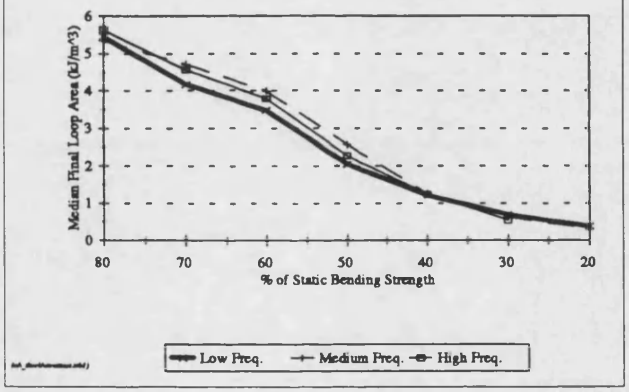

Fig. 8.33c MEDIAN CHANGES IN HYSTERESIS LOOP AREA FOR CHIPBOARD LOADED AT R=0.1

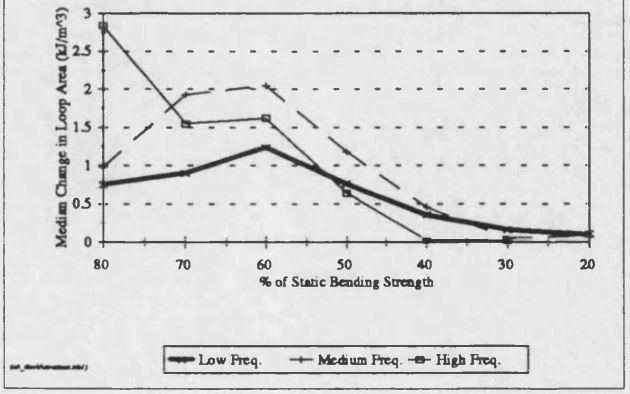

Table 8.10 Median hysteresis loop areas for chipboard tested at R=0.1, at low, medium and high frequencies.

Stress Level	Median Initial Hysteresis Loop Area kJ/m^3	Median Final Hysteresis Loop Area kJ/m^3	Median Change in Hysteresis Loop Area kJ/m^3	Range of Initial Hysteresis Loop Area kJ/m^3	Range of Final Hysteresis Loop Area kJ/m^3	Range of Change in Hysteresis Loop Area kJ/m^3
LOW FREQUENCY, R=0.1						
80%	4.78	5.46	0.75	4.35-5.00	4.90-6.03	0.21-1.65
70%	3.45	4.17	0.90	2.69-3.78	3.77-4.97	0.47-1.25
60%	2.24	3.48	1.24	1.97-2.48	3.17-3.60	0.74-1.45
50%	1.43	2.05	0.76	1.12-1.88	1.87-2.26	(-0.01)-0.86
40%	0.86	1.22	0.36	1 Sample	1 Sample	1 Sample
30%	0.53	0.69	0.16	1 Sample	1 Sample	1 Sample
20%	0.27	0.37	0.10	1 Sample	1 Sample	1 Sample
MEDIUM FREQUENCY, R=0.1						
80%	4.19	5.36	0.98	3.01-4.86	4.30-7.41	0.87-2.55
70%	2.85	4.72	1.93	2.09-3.66	3.89-7.06	1.58-3.40
60%	1.95	4.00	2.05	1.78-2.51	3.51-4.67	1.45-2.89
50%	1.35	2.57	1.18	1.24-1.43	2.23-2.78	0.87-1.54
40%	0.81	1.27	0.46	1 Sample	1 Sample	1 Sample
30%	0.56	0.62	0.05	1 Sample	1 Sample	1 Sample
20%	0.23	0.31	0.08	1 Sample	1 Sample	1 Sample
HIGH FREQUENCY, R=0.1						
80%	3.36	5.64	2.84	2.71-3.56	3.71-6.40	2.32-2.92
70%	3.15	4.56	1.55	2.27-3.89	4.03-5.51	1.16-1.78
60%	2.32	3.79	1.62	2.01-2.64	3.20-4.74	0.57-2.37
50%	1.80	2.28	0.64	1.56-2.12	1.95-2.75	0.16-0.79
40%	1.23	1.25	0.03	2 Samples	2 Samples	2 Samples
30%	0.52	0.54	0.02	2 Samples	2 Samples	2 Samples

Fig 8.34a

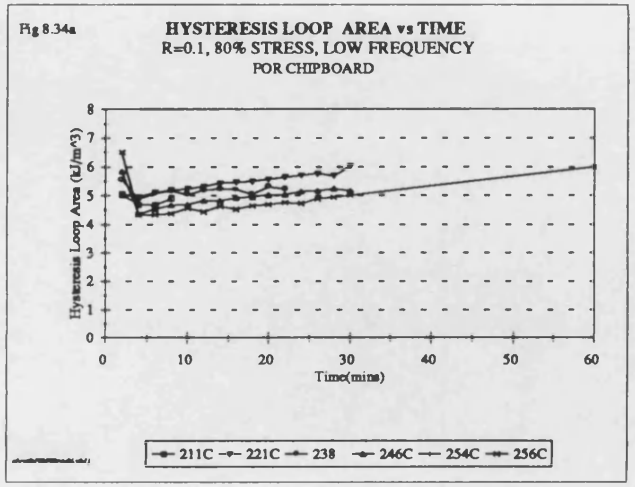

Fig 8.34b

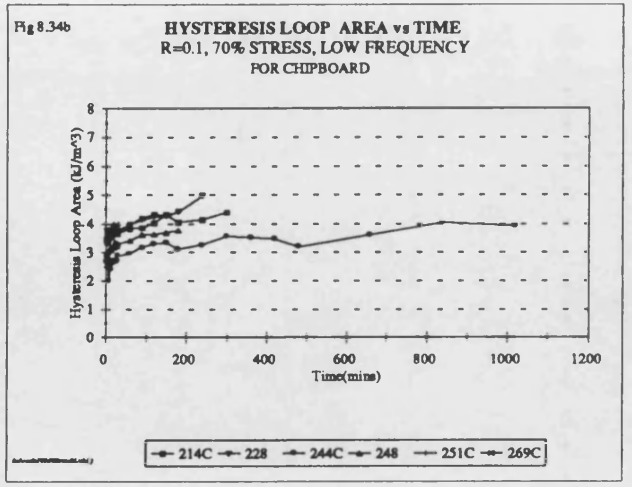

Fig 8.34c

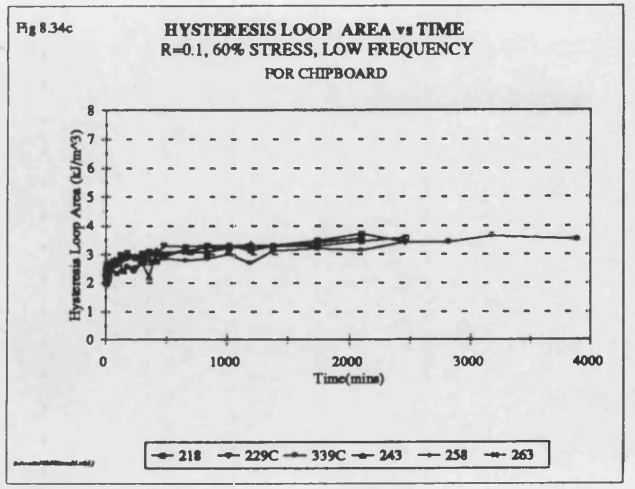

Fig 8.34d

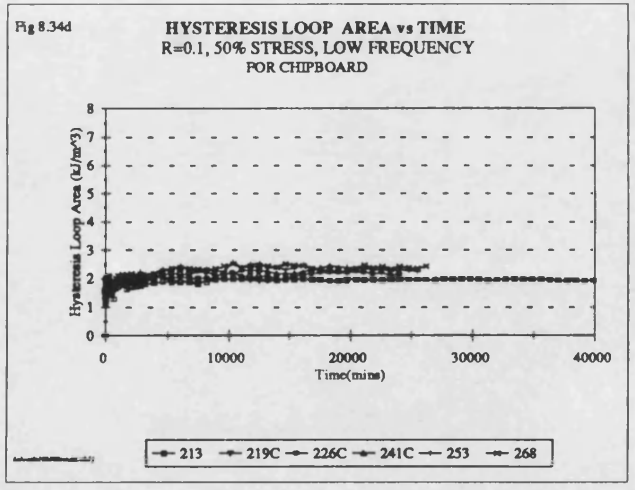

Fig 8.34e

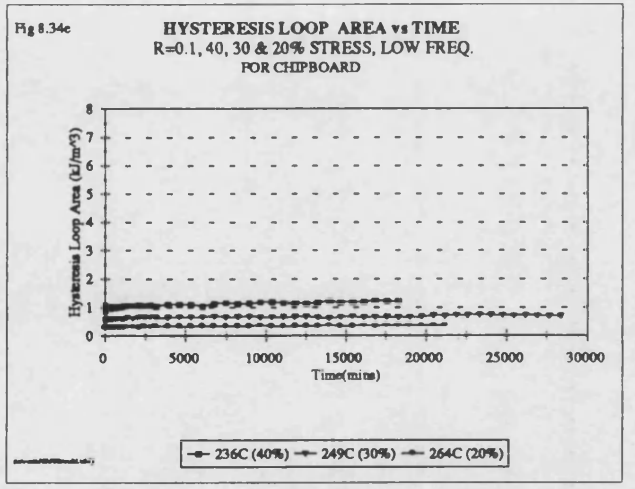

Fig 8.35a HYSTERESIS LOOP AREA vs FACTORED TIME
R=0.1, 80% STRESS, LOW FREQUENCY
FOR CHIPBOARD

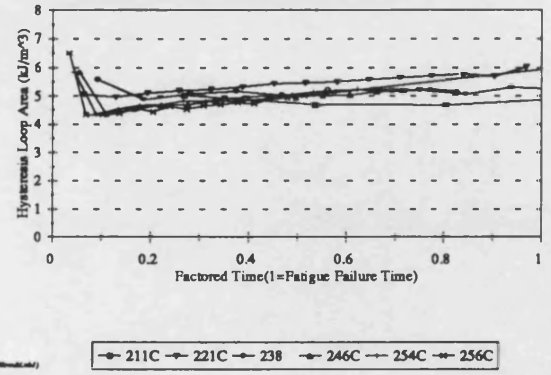

Fig 8.35b HYSTERESIS LOOP AREA vs FACTORED TIME
R=0.1, 70% STRESS, LOW FREQUENCY
FOR CHIPBOARD

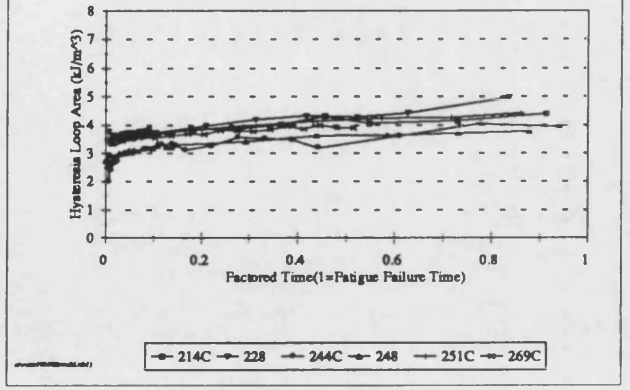

Fig 8.35c HYSTERESIS LOOP AREA vs FACTORED TIME
R=0.1, 60% STRESS, LOW FREQUENCY
FOR CHIPBOARD

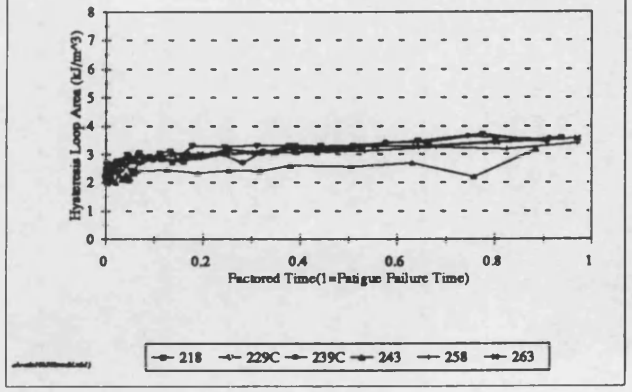

Fig 8.35d HYSTERESIS LOOP AREA vs FACTORED TIME
R=0.1 50% STRESS, LOW FREQUENCY
FOR CHIPBOARD

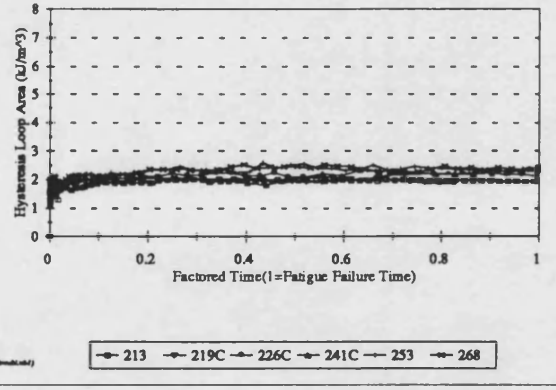

Fig 8.35e HYSTERESIS LOOP AREA vs FACTORED TIME
R=0.1, 40, 30 & 20% STRESS, LOW FREQ.
FOR CHIPBOARD

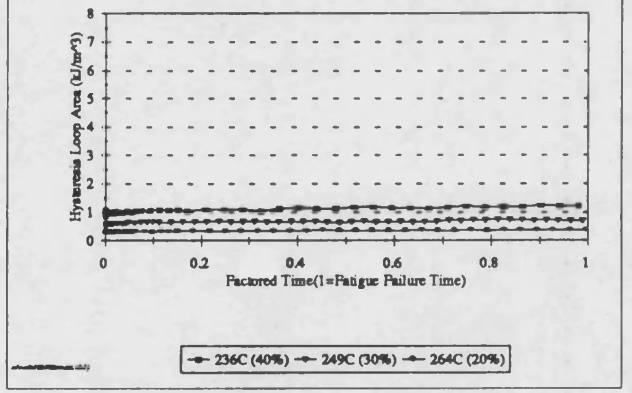

Fig 8.36a

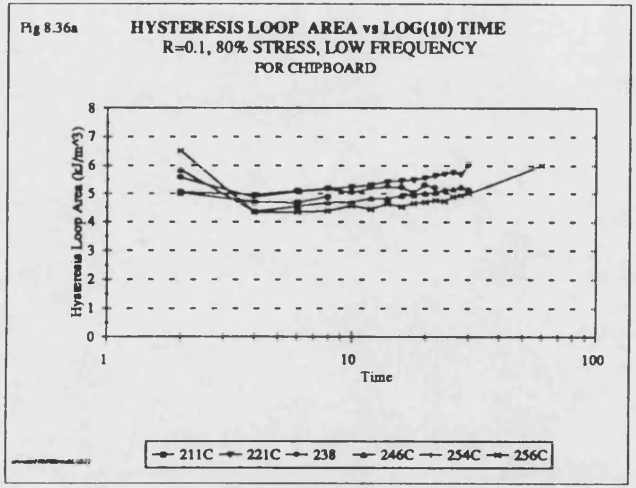

Fig 8.36b

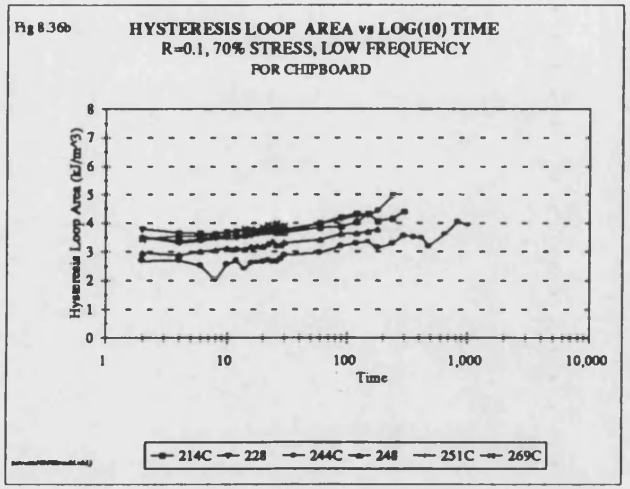

Fig 8.36c

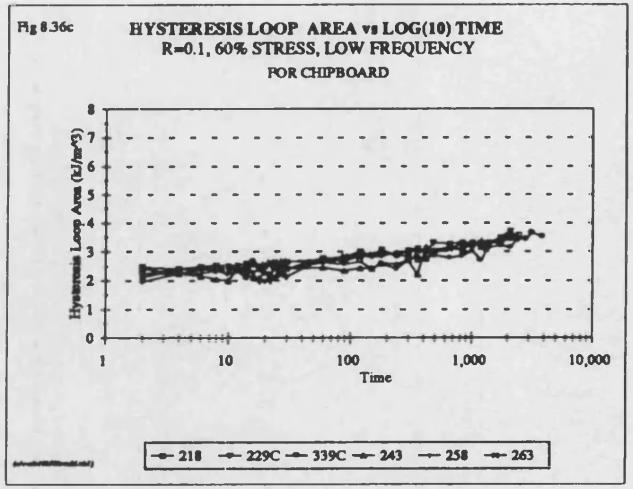

Fig 8.36d

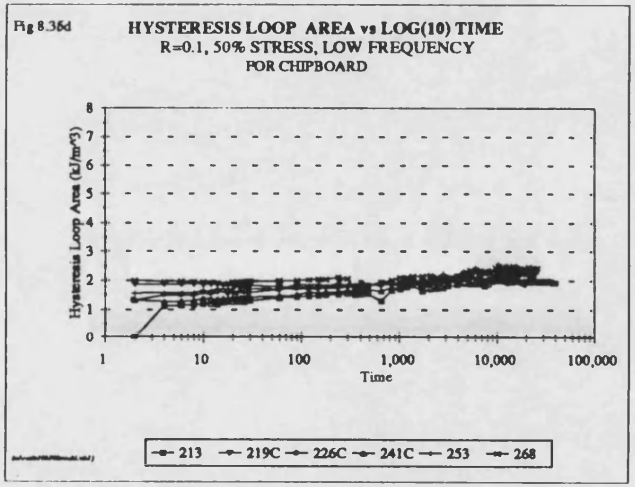

Fig 8.36e

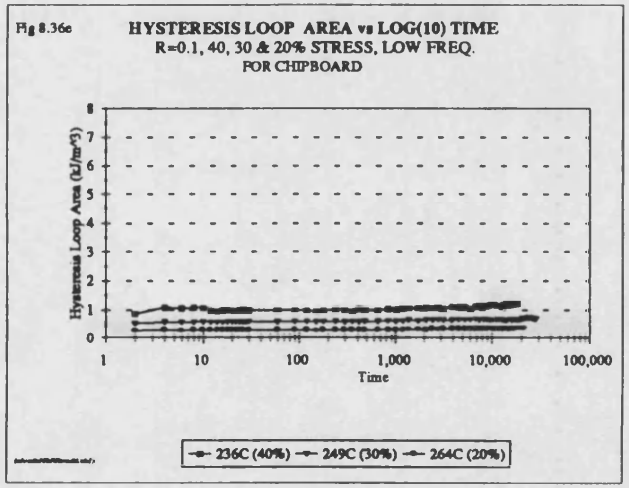

Fig 8.37a

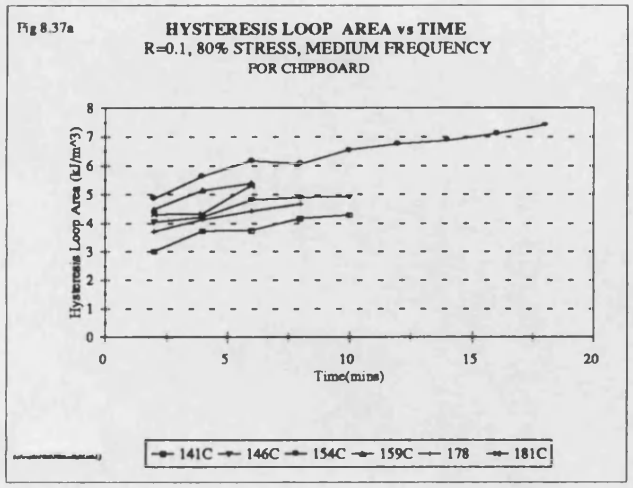

Fig 8.37b

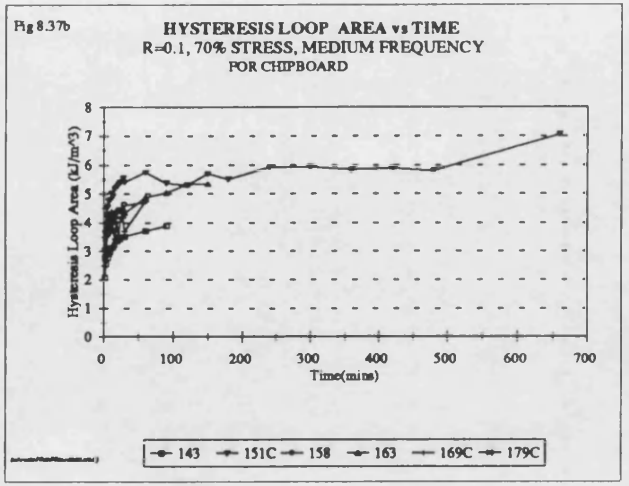

Fig 8.37c

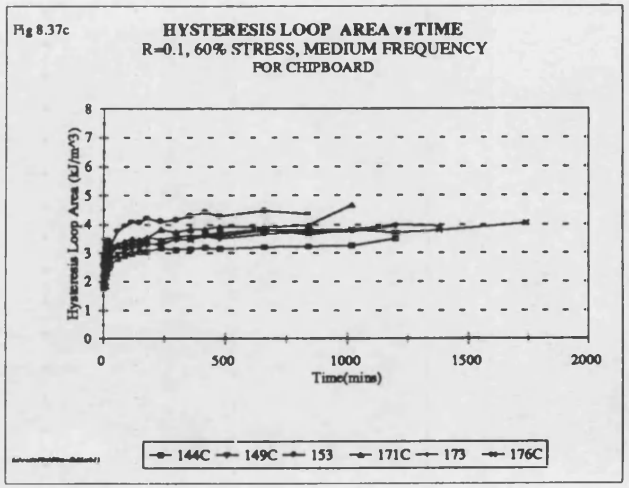

Fig 8.37d

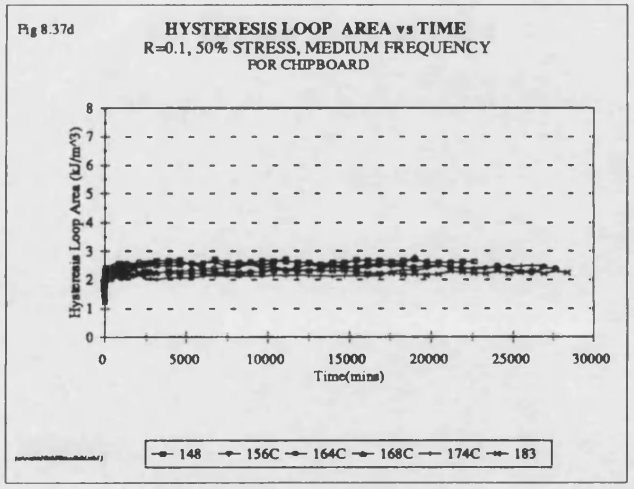

Fig 8.37e

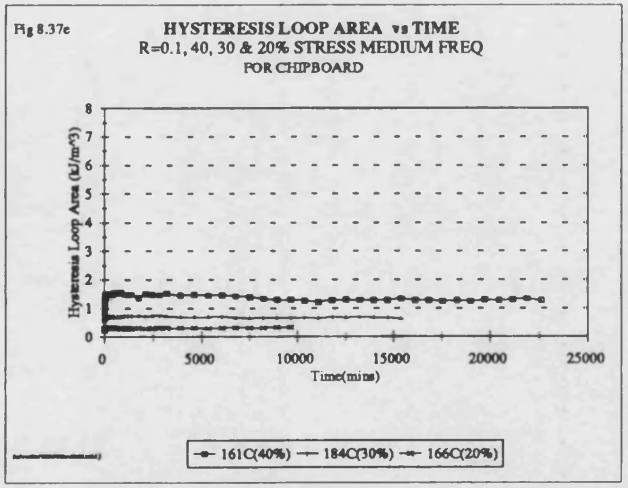

Fig 8.38a HYSTERESIS LOOP AREA vs FACTORED TIME
R=0.1, 80% STRESS, MEDIUM FREQUENCY
POR CHIPBOARD

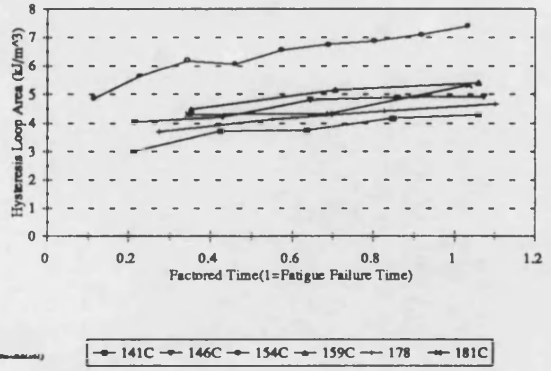

Fig 8.38b HYSTERESIS LOOP AREA vs FACTORED TIME
R=0.1, 70% STRESS, MEDIUM FREQUENCY
POR CHIPBOARD

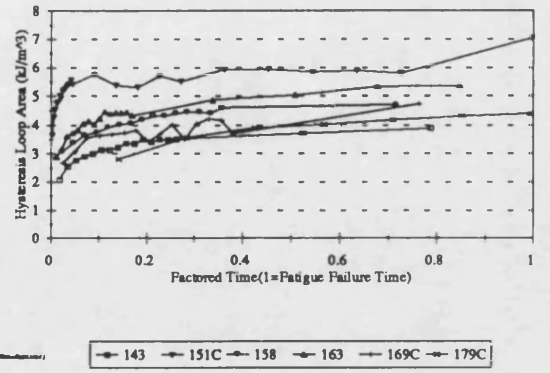

Fig 8.38c HYSTERESIS LOOP AREA vs FACTORED TIME
R=0.1 60% STRESS MEDIUM FREQUENCY
POR CHIPBOARD

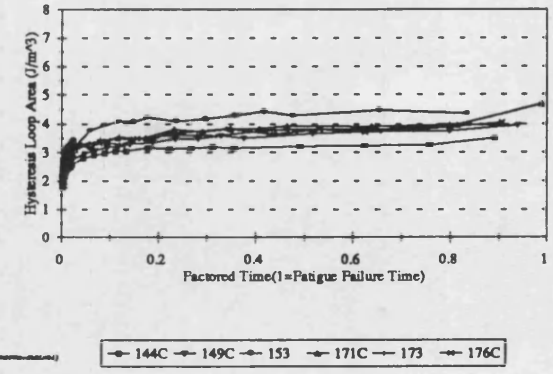

Fig 8.38d HYSTERESIS LOOP AREA vs FACTORED TIME
R=0.1, 50% STRESS, MEDIUM FREQUENCY
POR CHIPBOARD

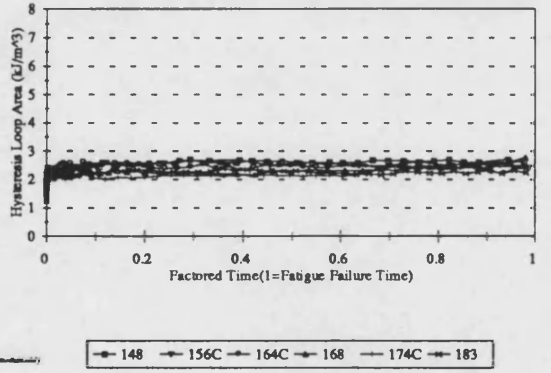

Fig 8.38e HYSTERESIS LOOP AREA vs FACTORED TIME
R=0.1, 40, 30 & 20% STRESS MEDIUM FREQ
POR CHIPBOARD

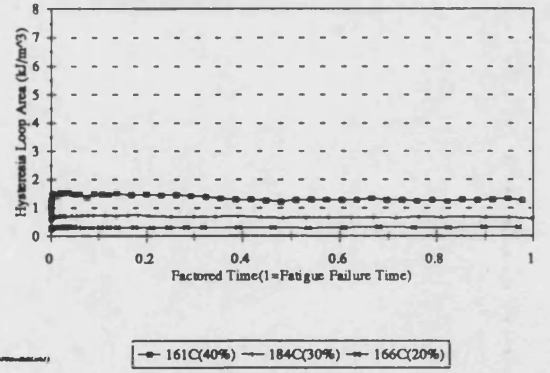

Fig 8.39a

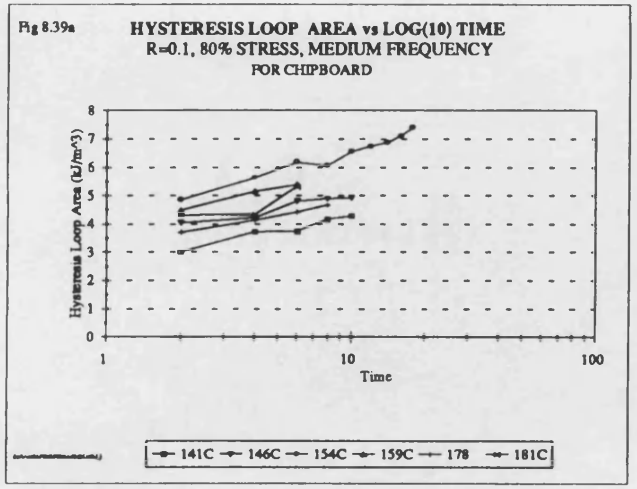

Fig 8.39b

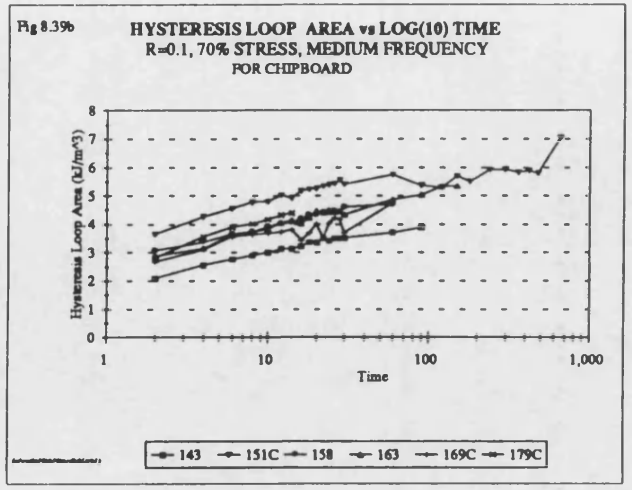

Fig 8.39c

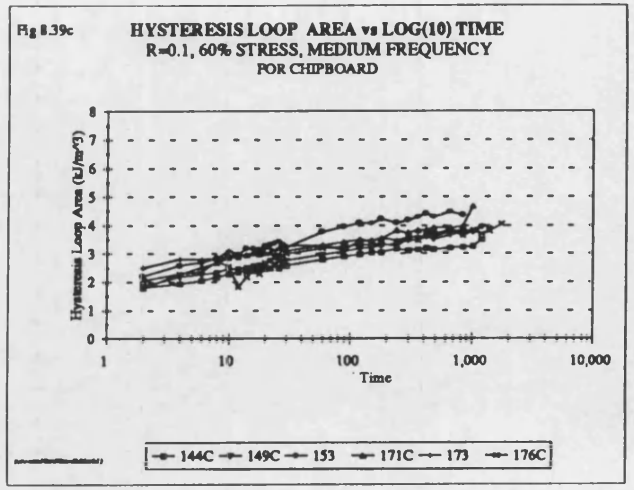

Fig 8.39d

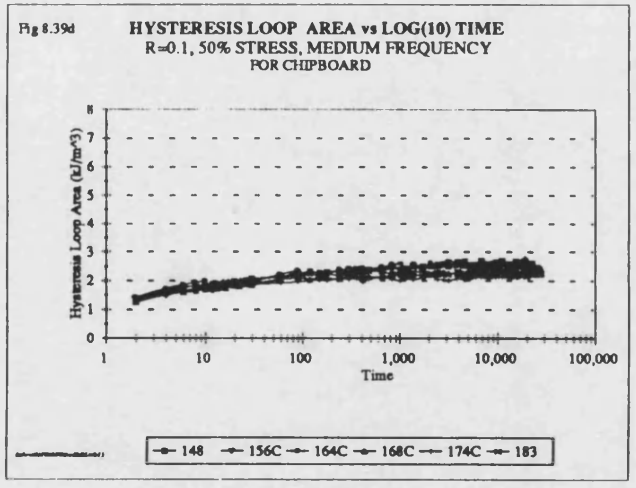

Fig 8.39e

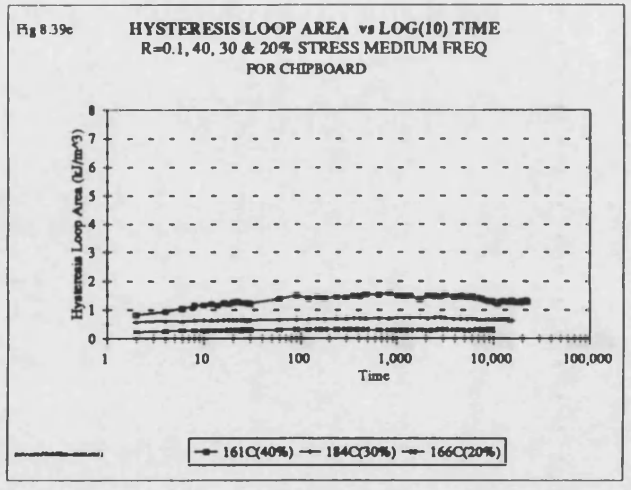

Fig 8.40a

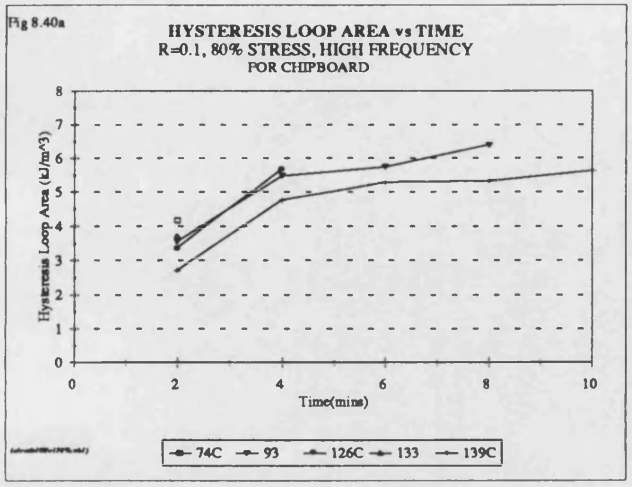

Fig 8.40b

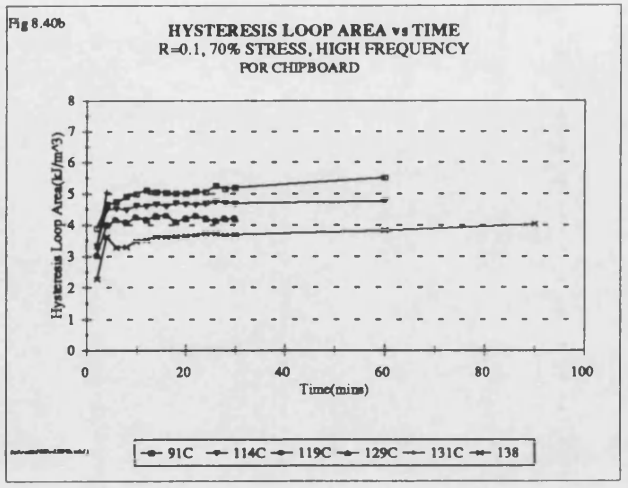

Fig 8.40c

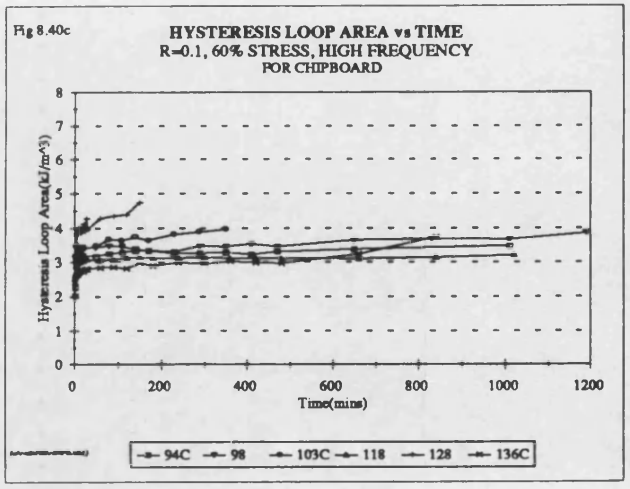

Fig 8.40d

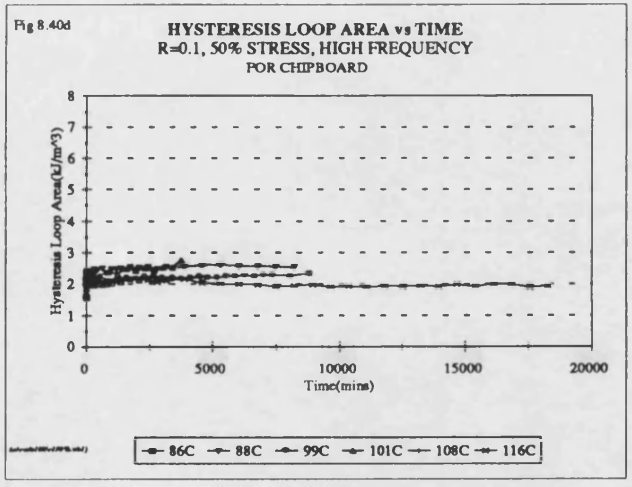

Fig 8.40e

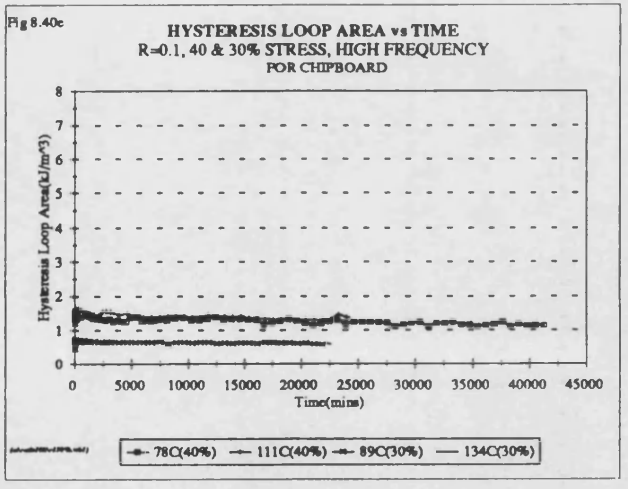

Fig 8.41a

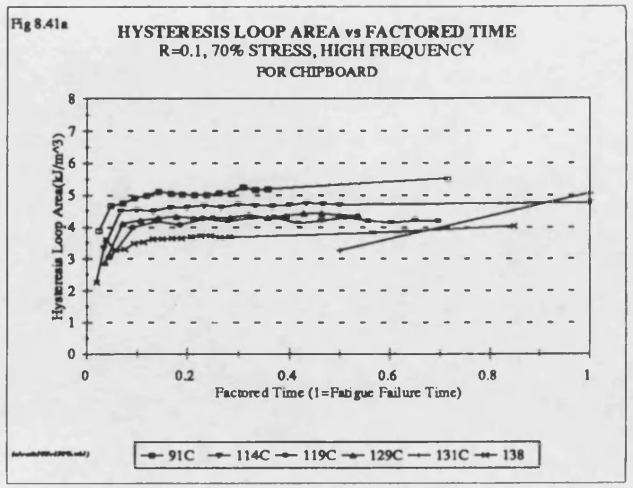

Fig 8.41b

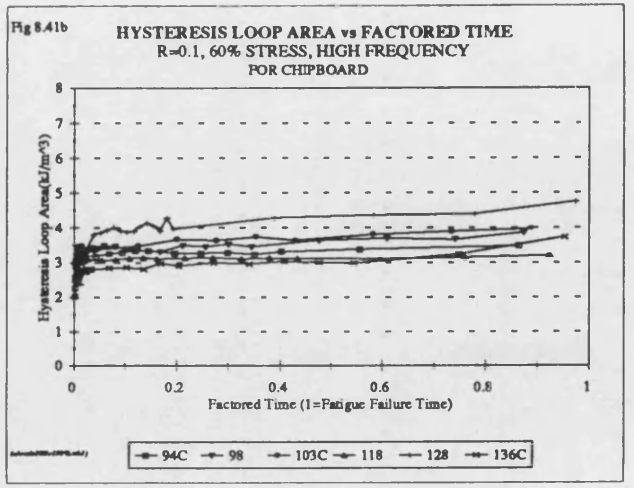

Fig 8.41c

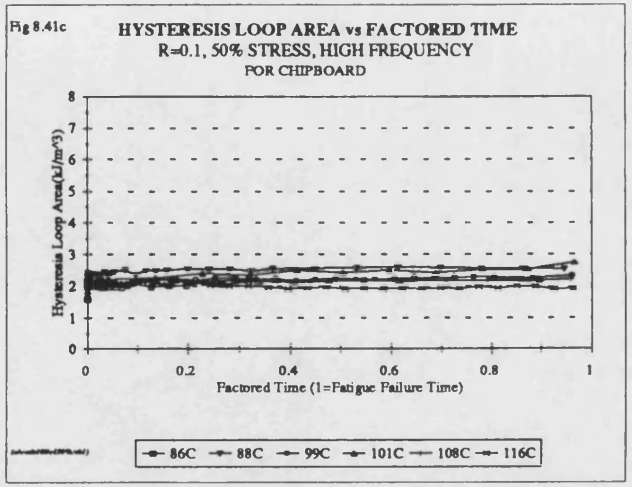

Fig 8.41d

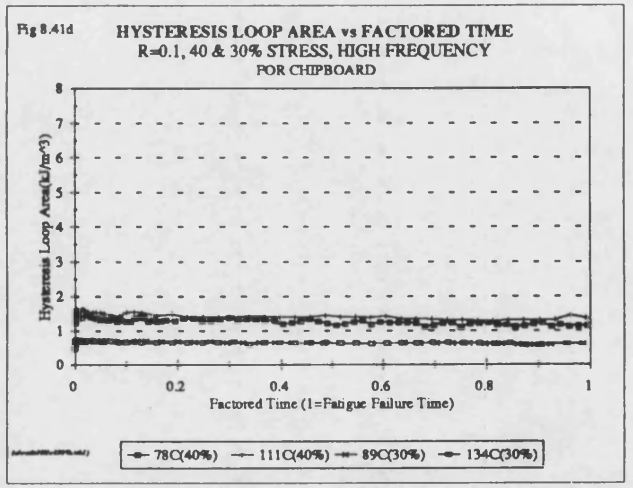

Fig 8.42a

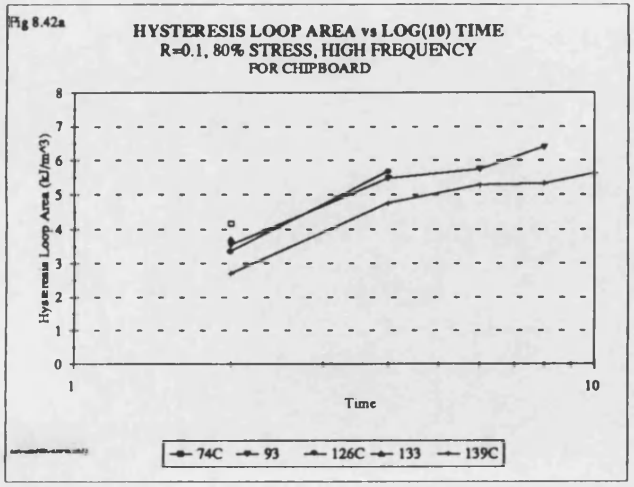

Fig 8.42b

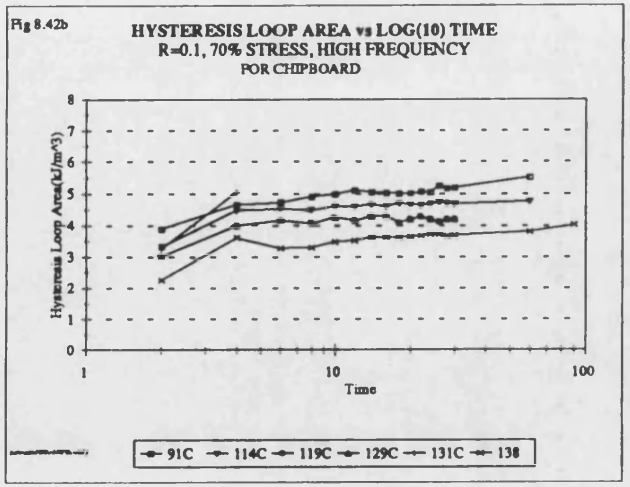

Fig 8.42c

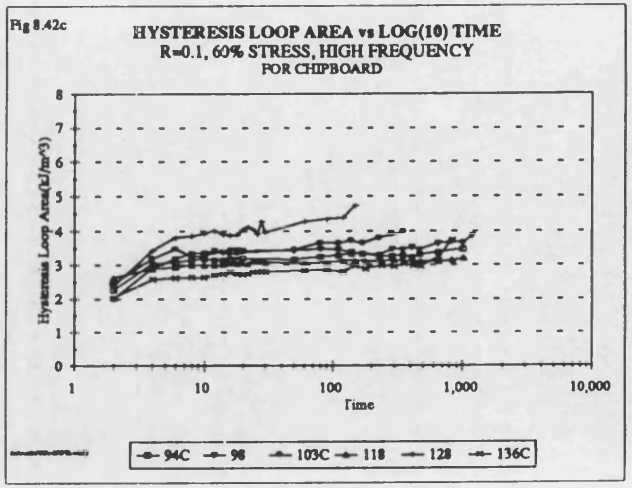

Fig 8.42d

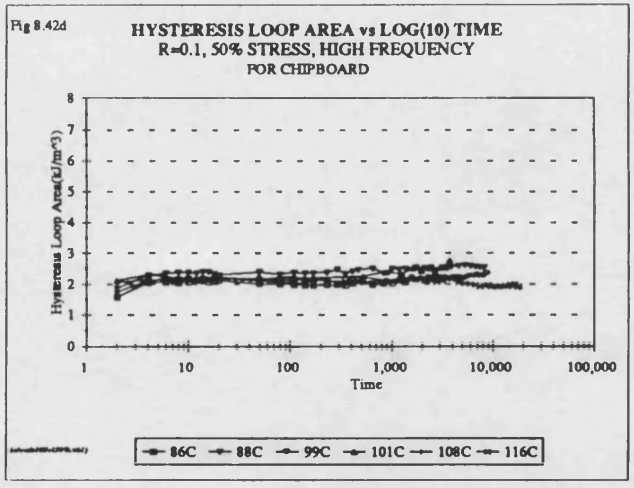

Fig 8.42e

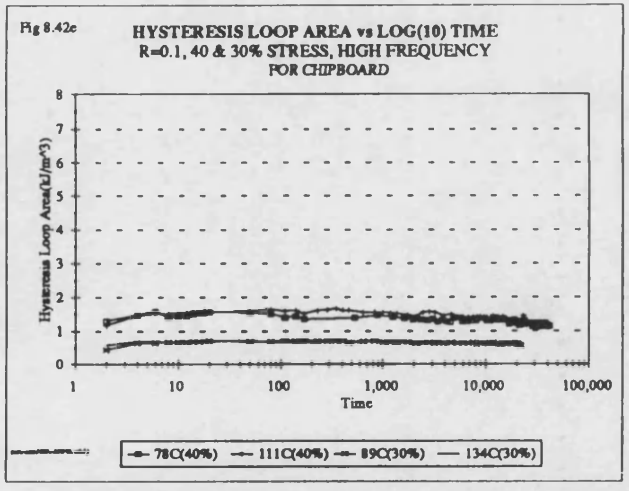

Discussion

The hysteresis loop areas are a result of the lag between the load being applied to the sample and the strain being produced in it. The formulae for calculating the surface stresses and strains are provided in Appendix 1A. The load applied to the sample is measured at the load cell. This was positioned between the upper set of rollers and the supporting frame, so this accurately measures the load on the sample. Equation 2 in Appendix 1A converts the load to the surface stress. The stress is greatest at the two outer surfaces and there is a neutral axis at the centre. The true centre point deflection measured by the transducer is used to calculate the surface strain.

The most important features seen in figures 8.33a-c and table 8.10 are that for all three frequencies the initial, final and the change in the median hysteresis loop areas decreases with decreasing stress level. Also there is no change in the loop areas as a result of changing the loading frequency. The three values, most importantly the changes in loop area tend towards zero below the 20% stress level. If there is no change in the hysteresis loop area from the start to the finish of testing then no damage is being produced in the sample and it will never fail. This suggests that there is a fatigue limit for chipboard at a stress level just below 20%, for all three loading frequencies which compliments the literature.

Tsai and Ansell (1990), and Kommers (1943) suggested that there is a fatigue limit for wood below the 25% stress level. Kyanka (1980) stated that the fatigue performance of particleboard is inferior to wood, so the fatigue limit for chipboard would occur at a stress level further below 25%. This was also supported by the findings of Kollman *et al* (1961) and Gillwald *et al* (1966).

At the 80% stress level, figure 8.34a, 8.35a and 8.36a for low frequency, figures 8.37a, 8.38a and 8.39a for medium frequency, and figures 8.40a, and 8.42a for high frequency there was a gradual increase in loop area up to failure for all the samples tested at all three frequencies. The initial high first cycle value for each sample at the low frequency at this stress level should be ignored because the cycle starts from zero stress, instead of from one tenth of the peak stress.

At the 70 and 60% stress levels, figures 8.34b-c, 8.35b-c, and 8.36b-c for low frequency loading, figures 8.37b-c, 8.38b-c and 8.39b-c for medium frequency loading, and figures 8.40b-c, 8.41a-b and 8.42b-c for high frequency, the hysteresis loop area increased in three stages as found by Bonfield *et al* (1993). At first there is a rapid increase due to the relatively large deflection produced by the initial elastic deflection.

This is followed by a slower progressive increase, then a final rapid increase leading to failure, also observed for wood loaded in bending (Bonfield *et al* 1993) and for wood laminates loaded axially (Hacker 1995). The third stage was only observed for a few of the samples. One sample tested at the 80% stress level also exhibited this final stage. This shows that damage builds up rapidly during initial cycling and then continues to increase at a slower rate, then there is a rapid increase leading to sample failure. This was very similar for all three frequencies except no third stage was observed for the high frequency results. A similar trend is observed at the 50% stress level, figures 8.34d, 8.35d and 8.36d for low frequency, 8.37d, 8.38d and 8.39d for medium frequency, and figures 8.40d, 8.41c and 8.42d for high frequency. At the 50% stress level for all three frequencies there is an initial rapid increase followed by a very gradual increase up to failure as the damage to the samples takes longer to occur or no further increase takes place. The small increase in loop area demonstrated that very little damage is being produced in the samples and explains the long fatigue lives. This corresponds with the fatigue modulus data where there was a slow but continuous decrease in fatigue modulus throughout testing after an initial rapid decrease.

At the lowest stress levels 40, 30 and 20%, for low and medium frequencies, and 40 and 30% for high frequency, following a very small initial increase there was no further increase in the hysteresis loop area. These trends are shown in figures 8.34e, 8.35e and 8.36e for low frequency, figures 8.37e, 8.38e and 8.39e for medium frequency, and figures 8.40e, 8.41d, and 8.42e for high frequency.

The plots of hysteresis loop area versus factored time show that the curves for the change in loop area for samples tested at the same stress level are very similar, once the time axes are standardized. It can be seen that the samples that failed at short lives had similar loss mechanisms to others at the same stress level but they became damaged more rapidly. The reduction in hysteresis loop area with decreasing stress level agrees with the previous results of Hacker (1991) and Thompson *et al* (1994).

8.10 Axial Testing

Bending tests impose tensile and compressive stresses on chipboard samples simultaneously. This section of work used axial loading in an attempt to discover the relative contributions to the fatigue failure of structural grade chipboard loaded in bending from tension and compression. The tensile and compressive strengths of the chipboard were determined initially and used to set the stress levels for the fatigue tests. Damage to the samples was evaluated using stress versus strain hysteresis loop capture.

8.10.1 Experimental Detail for Axial Testing

Axial tests were performed on eight samples from one cross-section of chipboard Panel 6. All the samples were pre-conditioned prior to testing in the same manner as for the tests in bending. The samples used for the tensile static and fatigue tests were cut to produce necked "dog bone" shaped samples 330 mm long, figure 8.43. A large radius of curvature was used for the region between 50 mm wide gripped section and the reduced, 18 mm thick, gauge length to minimise the possibility of failure at the grips.

Figure 8.43 Axial (necked) test specimen.

Preliminary trials concluded that it was not necessary to bond aluminium end tabs to the samples, as is sometimes required for the axial testing of some solid woods where crushing occurs at the grips. The loads imposed on chipboard were considerably lower than those required to test solid wood and so a lower gripping pressure was used. The static and fatigue compression tests were performed on samples that were not necked prior to testing and were of the same dimensions as the samples used for all the bending tests.

All the static and fatigue tests were performed using a four column, 200 kN capacity, Mayes servo hydraulic fatigue machine that was NAMAS calibrated. Sinusoidal, constant amplitude loads were applied to the samples, as for the bending fatigue tests. The tension/tension fatigue test was performed at R=0.1 and the compression/compression test was performed at R=10. The R ratio of 10 is the compressive equivalent of R=0.1 as shown in figure 8.44.

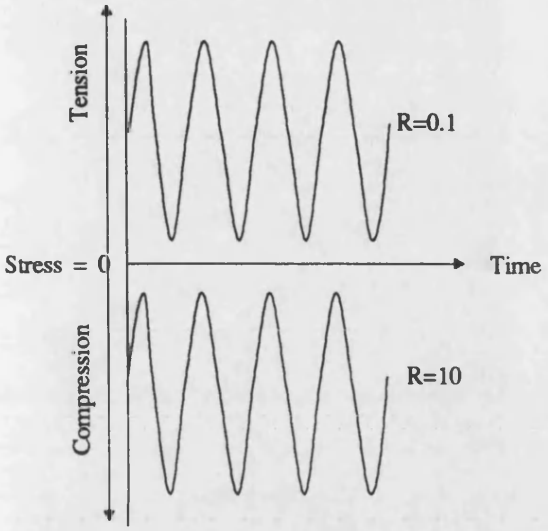

Figure 8.44 The R ratios used for the axial fatigue testing of chipboard.

The tensile fatigue test was performed at 0.5 Hz and the compressive fatigue test at 0.08 Hz to allow the software to capture the hysteresis loops. The strain for the fatigue tests was measured using a clip gauge with knife edge blades. These were located into small steel grooved tabs attached to the gauge length of the samples using "Araldite Rapide" [see Hacker (1995)]. The tabs located the clip gauge to the sample and prevented the knife edges from damaging the surfaces of the samples. The gauge was calibrated prior to testing. The stress versus strain hysteresis loops were calibrated by Hacker using a specialised nCode software package. During testing the relative humidity was maintained at ~65% by enclosing containers of saturated sodium nitrite solution in with the fatigue samples.

The machine was operated in load control using a Dartec M9500 controller similar to that used to control the Dartec 0.5 kN fatigue machine but driven by a personal computer. Load control was not as accurate as for the bending tests due to the excessive capacity of the testing machine used. However, this was the only available machine able to capture stress versus strain hysteresis loops for axial testing, as well as being capable of gripping the fatigue samples.

The eight samples tested were as shown in table 8.11.

Table 8.11 Samples tested.

Sample	Type of Test	Comments
207	Fatigue - compression, 50% stress	
207C	Static - compression	
208	Fatigue - compression, 50% stress	Loop capture failed
208C	Static - compression	
209	Static - tension (necked sample)	Failure load not captured
209C	Static - tension (necked sample)	Failed in necked region
210	Fatigue - tension (necked sample)	
210C	Static - tension (necked sample)	Failed in the necked region

8.10.2 Axial Static Strengths

The axial static strengths of four samples were obtained, two loaded in compression and two loaded in tension. The results of these four tests are shown in table 8.12.

Table 8.12 Axial static strengths.

Sample	Type of Test	Width mm	Thickness mm	Failure Load kN	Failure Stress MPa
207C	Compression	49.8	17.9	14.0	15.8
208C	Compression	50.1	17.9	14.2	15.8
209C	Tension	17.3	17.9	2.8	9.0
210C	Tension	18.4	17.9	3.0	9.1

8.10.3 Axial Fatigue Results

Two samples were fatigue tested, one in compression/compression at R=10 and one in tension/tension at R=0.1. It was not possible to test a larger number of samples because the machines were only available for a short time. The results of these two fatigue tests are shown in table 8.13.

Table 8.13 Axial fatigue results.

Sample	Type of Test	Width mm	Thickness mm	Stress Level	Number of Cycles
207	Compression	49.4	17.9	50%	75 000
210	Tension	19.0	17.9	50%	34 678

8.10.4 Hysteresis Loop Parameters

The hysteresis loop parameters for the two fatigue tests are shown in figures 8.45a to 8.49b. The first and last hysteresis loops captured for sample 210 fatigued in tension/tension and for sample 207 fatigued in compression/compression, both at 50% stress levels are shown in figures 8.45a and 8.45b respectively. The microstrains produced in these samples by the fatigue loading are shown with respect to the number of loading cycles in figures 8.46a and 8.46b respectively. The applied stresses imposed on the samples to produce the strains are shown in figures 8.47a and 8.47b respectively and clarify the unexpected reduction in the microstrain close to the end of the test for sample 210. The changes in the hysteresis loop areas due to the tension/tension and compression/compression fatigue loading of the two samples are presented in figures 8.48a and 8.48b respectively. Finally the dynamic moduli for the two samples are shown in figures 8.49a and 8.49b respectively.

Fig 8.45a

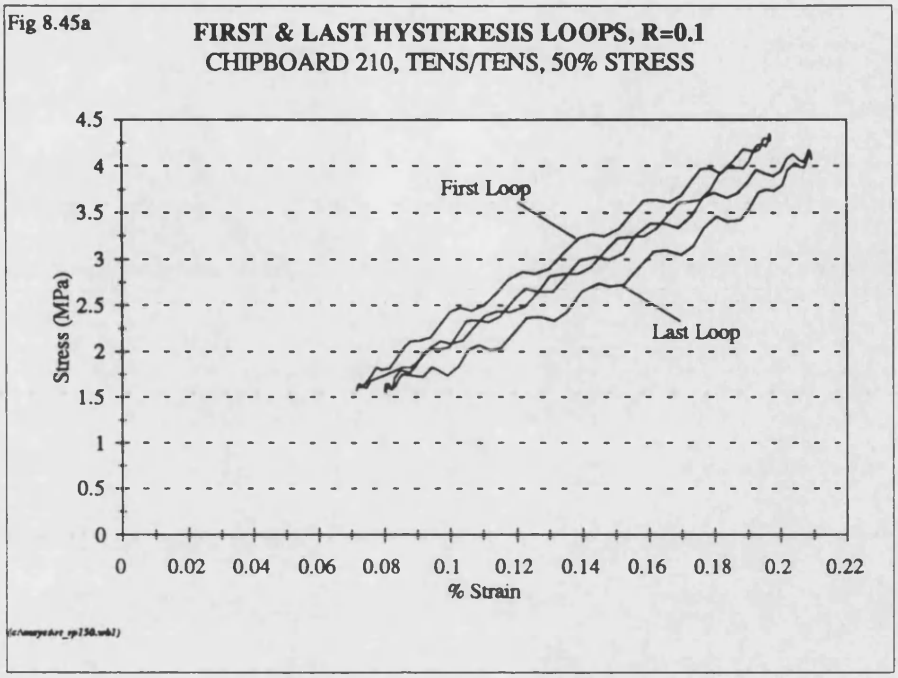

Fig 8.45b

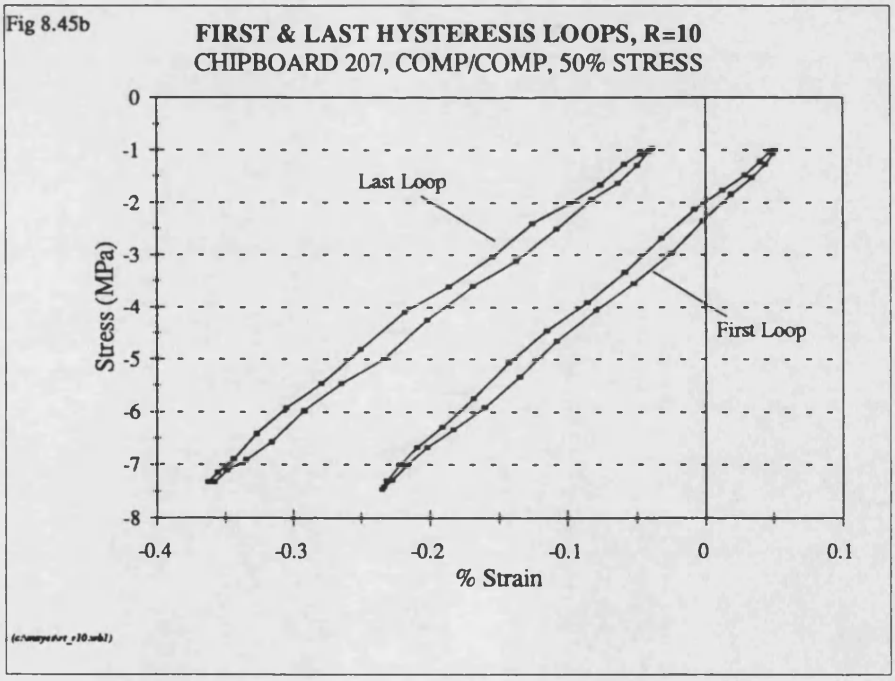

Fig 8.46a

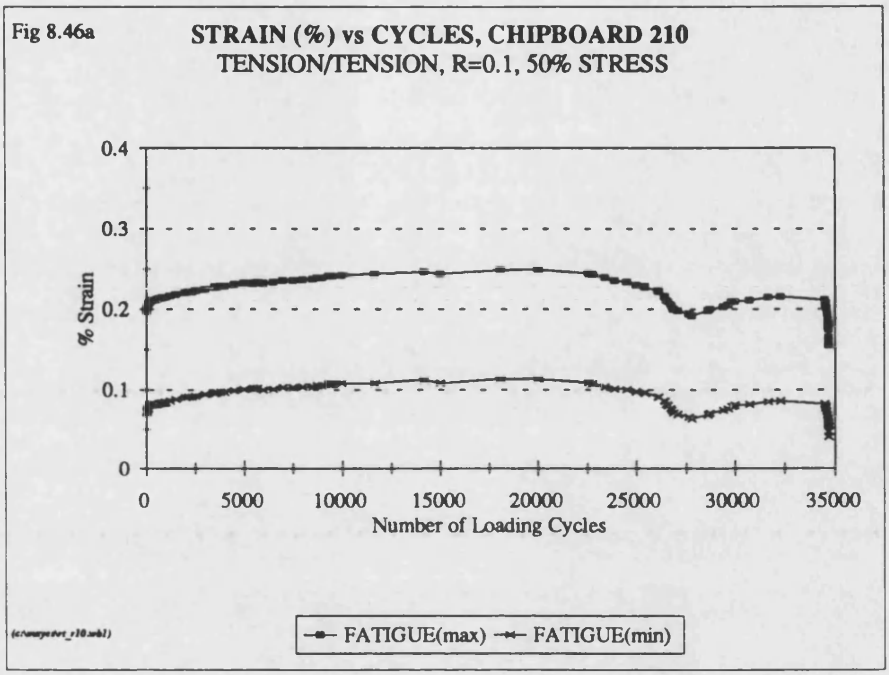

Fig 8.46b

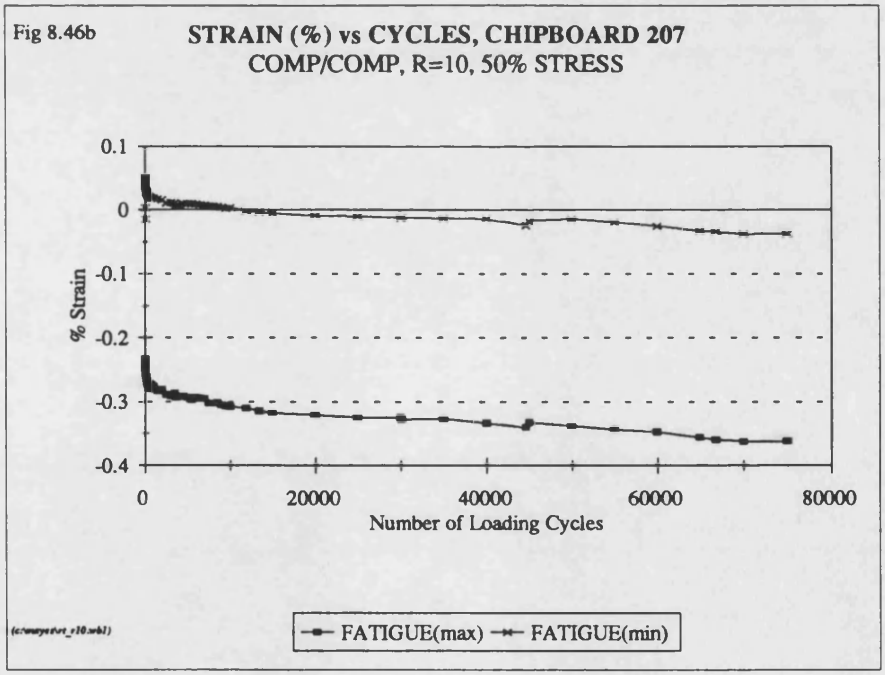

Fig 8.47a

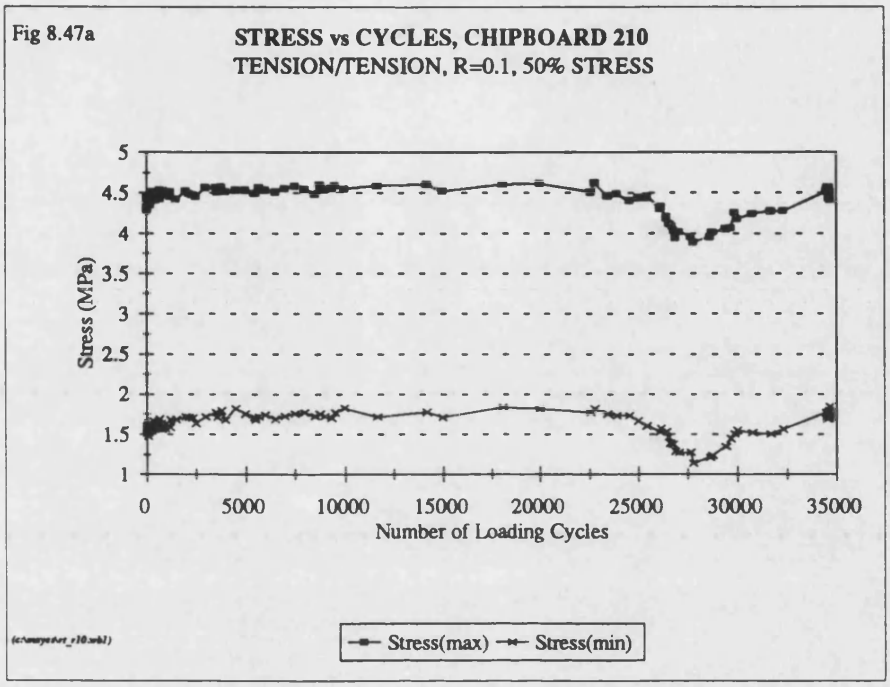

Fig 8.47b

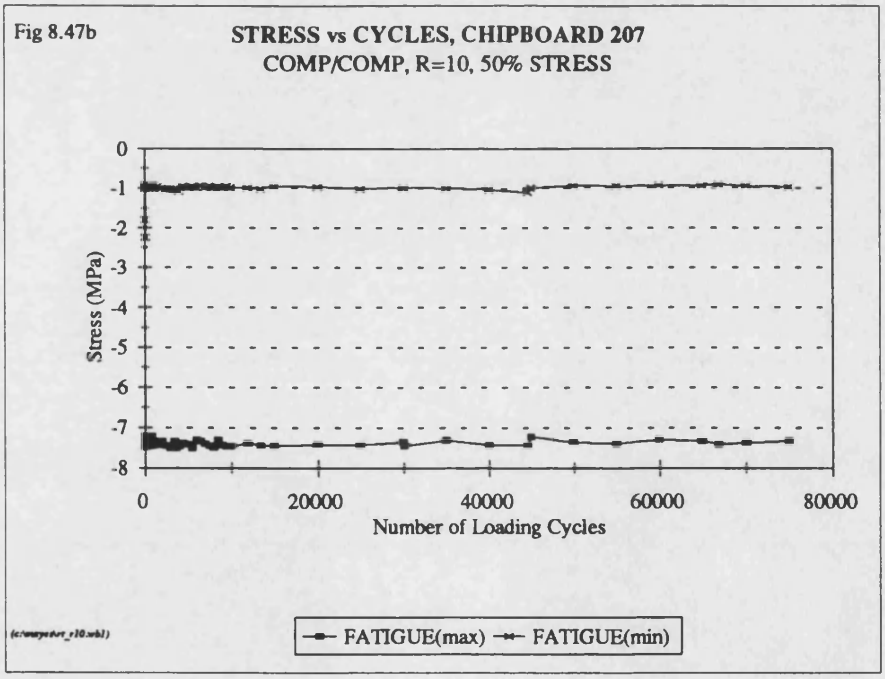

Fig 8.48a

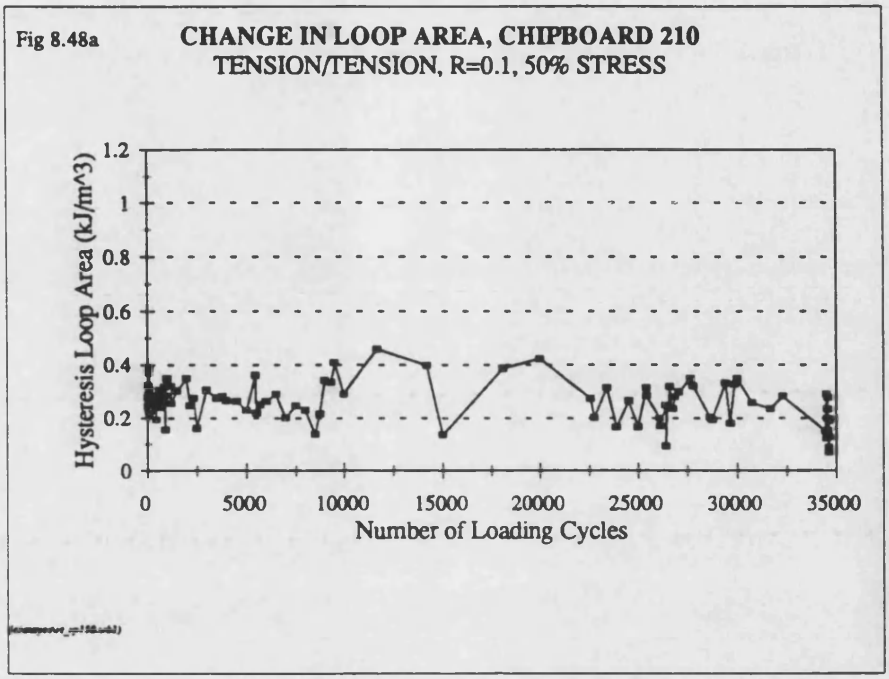

Fig 8.48b

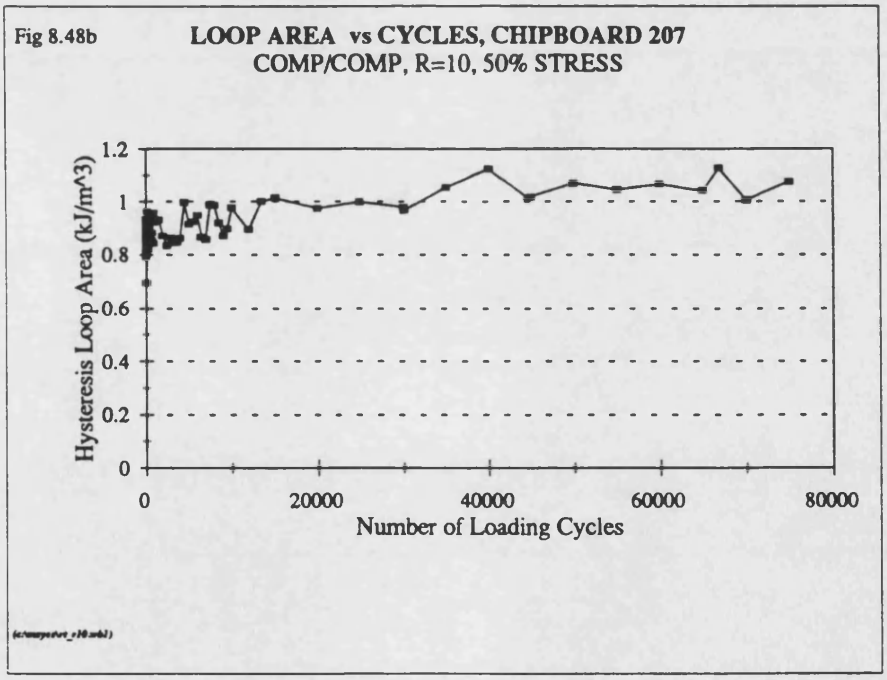

Fig 8.49a **DYNAMIC MODULUS vs TIME, CHIPBOARD 210**
TENS/TENS, R=10, 50% STRESS

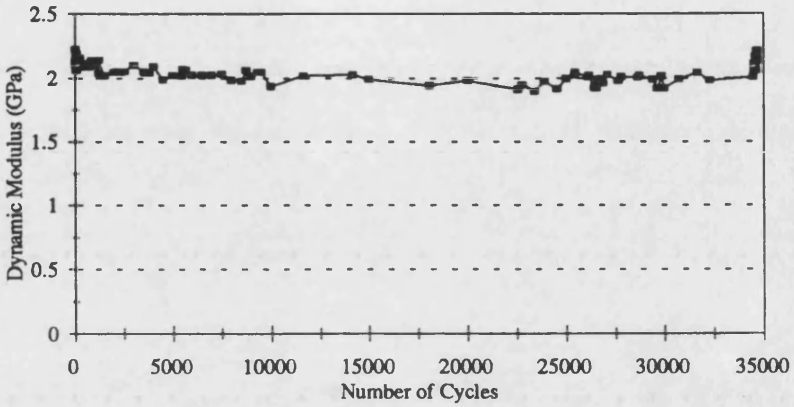

Fig 8.49b **DYNAMIC MODULUS vs TIME, CHIPBOARD 207**
COMP/COMP, R=10, 50% STRESS

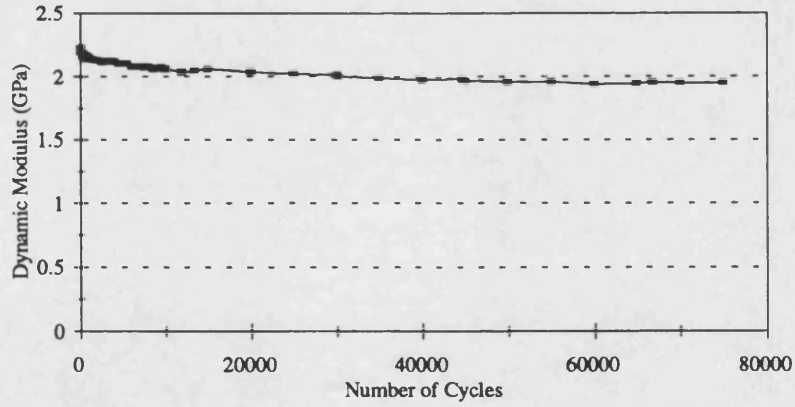

Discussion

Only a small number of samples were statically tested axially. These comprised only two samples for each condition (tension and compression) and were tested primarily to allow the stress levels to be set for the fatigue tests. However, the strength values for the two compressive and the two tensile tests were extremely close to each other and agreed with the literature. The compressive strength was greater than the tensile strength in the ratio of 1.7:1. This is an important finding because it is opposite to solid wood and this is not apparent from most of the literature. Wood is considerably stronger in tension than it is in compression, the magnitude of the difference depending upon the wood species. If wood loaded in bending fails it is generally assumed that the wood fails on the compressive side although this is not always physically obvious. In contrast, when chipboard is loaded in bending, it fails on the tensile side. The only publications reporting relative strengths show the compressive strength to be greater than the tensile strength in the ratio 1.65:1 TRADA (1992) and 1.64:1 in BS5669 part 2 (1989) for grade C5 structural grade chipboard.

The first and last hysteresis loops captured for the sample loaded in tension/tension, figure 8.45a, are wavy. This is a manifestation of the same problem that was reported in section 6.4 for the Dartec fatigue machine and is also reported by Hacker (1995) for the fatigue testing of wood laminates. The load applied to the sample by the Dartec machine proved to be sinusoidal but the measurement of the load was wavy due to the load cell changing direction. The last hysteresis loop is further to the right for both tests showing that tensile creep has occurred in the sample. However, the area of the loop does not appear to have increased. The loops for the compression/compression test, figure 8.45b, are bigger than those for the tension/tension test. This is clearer from the plots of hysteresis loop area versus time referred to later in this discussion.

The strains produced by loading in tension were slightly lower than those produced by loading in compression, figure 8.46a and 8.46b, implying that the compressive loading is the more damaging mode. The plot for the tensile loading shows an unexpected dip towards the end of the test. This was explained by plotting the stresses applied in the tests. It is clear from figure 8.47a that the dip in strain was produced by a dip in the stress applied. The reason for this reduction in the stress is not certain but was probably due to the machine failing to load control accurately. The compressive strains increased progressively throughout the test while the applied stress remained fairly constant, figure 8.47b.

The hysteresis loop areas for the tension/tension fatigue loading of sample 210 are slightly erratic due to the wavy hysteresis loops captured but appear to remain almost constant or decrease slightly as the number of loading cycles increased. The loop areas for the compression/compression fatigue test were considerably higher and increase throughout testing showing that the sample is being damaged. This implies that it is the compressive component that is likely to be primarily responsible for failure in bending fatigue. It must be remembered that the magnitude of the compression loop areas will be greater because the stress range is bigger. This results from using normalised, percentage stress values to set up the fatigue tests with the static strength in compression being greater than the tensile strength. However, the greater stress range for the compressive test does not account completely for the magnitude of the difference between the hysteresis loop areas. The compression samples were wider than the tensile samples because they were not necked but this is irrelevant to the loop areas because they are measured per unit volume of the samples. The loop areas indicate that the compressive side of a bending fatigue sample would suffer more damage than the tensile side. This is contradicted because the compression fatigue sample did not fail, unlike the tensile one, so it seems unlikely that the failure would be produced on the compressive side. Instead it is probable that damage accumulates on the compressive side of the samples causing the neutral axis to shift from the centre of the sample upwards towards the tensile side producing a tensile failure.

The dynamic moduli for the samples tested under the two loading regimes both decrease slightly throughout the fatigue tests, figures 8.49a and 8.49b. This demonstrates that the samples become less stiff as they are damaged. The tensile sample shows a rapid increase at the end of the test possibly due to internal friction heating and drying the sample as found by Bond (1994).

To derive strong conclusions in this area of work a comprehensive set of tests would be required, possibly including the use of thermal imaging in the same manner as Bond (1994). However, these results provide a useful insight into the relative contributions of the tensile and the compressive components of the load to the development of damage in bending, for static and fatigue loading of chipboard. McNatt and Werren (1975) produced S-N plots for axial tension/tension and interlaminar shear fatigue loading of particleboard and found the fatigue performances to be very similar. However testing in compression/compression was not performed.

8.11 Interim Conclusions 2

1) The fatigue performance of chipboard A, evaluated in this thesis, was very similar to the performance of chipboard B, tested previously, despite the initial appearance of the S-N plot, figure 8.1a.

2) Fatigue testing at R=0.1 slightly reduced the fatigue life of chipboard compared to testing at R=0.25 and agreed with the constant life diagram produced by Thompson *et al* (1994).

3) Reducing the test frequency by one and then two orders of magnitude causes chipboard to fail at shorter fatigue lives compared to testing at the same stress level at higher loading frequencies. This means that the frequency of loading must be accounted for when designing for fatigue loading of chipboard.

4) The linear regression lines fitted to the fatigue data pass close to the static strengths for all three frequencies.

5) Plotting the residuals demonstrated that a straight line fit is appropriate to the captured fatigue data.

6) The use of normalised stresses and side-matched sets of samples reduced the scatter of the captured fatigue life data for all three loading frequencies.

7) It appears that fatigue loading does not reduce the strength of chipboard until close to the point of failure. Significant strength reductions were not observed for runout samples tested at stress levels below 50%.

8) The creep, maximum fatigue and minimum fatigue microstrains are unaffected by changing the loading frequency and all three microstrains decrease with decreasing stress level.

9) The final creep microstrain prior to the third rapid stage that leads to failure (the critical strain) remains fairly constant at about 3800 between 80 and 50% stress levels. This indicates that failure may be strain dependent.

10) Fatigue and creep microstrains both increase as three stage processes.

11) Creep loaded samples only failed before fatigue loaded samples at the highest stress levels tested. Fatigue loading produced greater deflections than creep loading for the 70-50% stress levels. At the 40% stress level this changes and creep loading produces greater deflections than fatigue loading.

12) Dynamic moduli were unaffected by changing the loading frequency.

13) There is only a small change in the magnitude of the dynamic moduli as a result of reducing the stress level, and it increases slightly as the stress level is reduced from 80% down to 20% for all three frequencies.

14) At stress levels above 40% the dynamic moduli decrease slightly as a result of fatigue loading.

15) Dynamic moduli increase slightly as a result of fatigue loading at low stress levels, 40% and below, for the medium and high frequencies which is also reported in the literature.

16) Fatigue moduli decrease throughout all tests from 80% down to the 50% stress level and to a greater extent than the dynamic moduli. Some samples demonstrated three stage decreases in the fatigue moduli. At lower stress levels, (40-20%) for medium and high frequencies, fatigue moduli remained almost constant after the initial decrease.

17) Changes in fatigue moduli for different samples tested at the same stress level were very similar and many of the irregularities seen in the dynamic moduli are smoothed out.

18) Hysteresis loop areas were unaffected by the loading frequency and increased in three stages.

19) The magnitude of the median initial, median final and the median change in the hysteresis loop area reduced as stress level was reduced, tending towards zero below the 20% stress level. This predicts that there is a fatigue limit for chipboard just below the 20% stress level and this is supported by the literature.

20) Above the 50% stress level the loop areas increase throughout testing for all samples tested. Below this stress level there is very little or no increase in area after the initial rise implying that no damage is produced in the sample.

21) Reducing the frequency of fatigue loading reduced the scatter/variability of the fatigue life data.

22) Chipboard loaded axially was stronger in compression than in tension in the ratio of 1.7:1 which is the opposite of wood.

23) Axial loading in tension/tension produced lower strains than for loading in compression/compression implying that compression is the more damaging of the two loading modes.

24) Hysteresis loop areas captured for axial compression loading were greater than those for axial tensile loading, again indicating that compression is the more damaging of the two loading modes. However, it is likely that in bending fatigue the compression damage shifts the neutral axis leading to eventual tensile failure.

25) Axial dynamic moduli decreased as a result of both tensile and compressive fatigue loading.

9.0 STATIC TESTING OF OSB AND MDF

9.1 Static Test Results

Static tests on OSB and MDF at the medium loading rate of 0.864 kN/s were performed on samples cut from (8' x 8') panels denoted 1 and 2 for both materials. These MDF panels were larger than the chipboard panels providing seven cross-sections of twenty two samples per panel instead of seven cross-sections of ten samples. These were separated into side-matched sets of four samples. The loading rate of 0.864 kN/s is equivalent to 12 MPa/s, the rate of application of stress applied in all the medium frequency fatigue tests.

Seventy samples from OSB Panel 1, one hundred and twenty four from OSB Panel 2, seventy from MDF Panel 1 and one hundred and fifty four from MDF Panel 2 were tested to failure in four point bending, to determine the bending strengths. The samples from OSB Panel 1 and MDF Panel 1 comprised six cross-sections of outside samples from matched sets, together with one entire cross-section of twenty two samples. Those for OSB Panel 2 comprised two cross-sections of outside samples and five entire cross-sections and those for MDF Panel 2 comprised all seven entire cross-sections.

Table 9.1 shows the results for the one hundred and ninety four OSB samples and the two hundred and twenty four MDF samples statically loaded to failure. Also included are the corresponding results for the fifty chipboard samples tested at the same loading rate, also reported in Chapter 7. This allows the mean bending strengths and their standard deviations, the mean difference within matched sets of four samples and the strength ranges for the three materials to be compared. The mean strength, density and specific strength of all the samples statically tested to failure at the medium loading rate for OSB, chipboard and MDF are shown in figures 9.1a-c respectively.

Figures 9.2a-c and 9.3a-c are histograms showing the strength distributions for Panel 1, Panel 2 and both panels combined for OSB and MDF respectively. The strengths of the outside samples from the matched sets of four and entire cross-sections of OSB panels 1 and 2 are shown in their relative positions in figures 9.4a-d and 9.5a-e. The same is plotted for MDF in figures 9.6a-d and 9.7a-g.

The materials are categorised by the size of the constituent particles. The particle dimensions are not important since all that is required is a ranking order. The particles are referred to as large, medium and small, for OSB, chipboard and MDF respectively.

Table 9.1 Bending strength data for OSB, chipboard and MDF tested at the medium loading rate.

1	Loading rate (kN/s)	OSB 0.864 kN/s (Medium Rate)					Chipboard 0.864 kN/s (Medium Rate)					MDF 0.0864 kN/s (Medium Rate)				
2	Panel Number	OSB 1		OSB 2		OSB 1&2	CB 5		CB 6		CB 5 & 6	MDF 1		MDF 2		MDF 1&2
3	Samples Tested	Total	X	Total	X	Total	Total	X	Total	X	Total	Total	X	Total	X	Total
4	Number of samples	70	22	124	22	194	28	--	22	10	50	70	22	154	22	224
5	Mean Bending Strength (MPa)	28.3	26.4	27.6	26.5	27.9	21.1	--	20.9	21.6	21.0	43.7	43.8	49.8	51.3	47.9
6	SD from Mean (MPa)	4.2	4.2	3.7	2.9	3.9	2.2	--	1.5	0.7	1.9	2.2	1.7	3.1	2.1	4.0
7	SD as % of Mean BS	14.7	15.7	13.5	10.8	14.0	10.4	--	7.1	3.2	9.0	5.1	3.8	6.3	4.1	8.4
8	Mean Diff. Matched Sets (%)	15.3	27.6	11.4	6.5	14.5	3.8	--	3.2	3.0	3.6	4.0	4.3	N/A	6.0	4.3
9	SD from the Mean Diff. (%)	11.2	15.4	12.5	4.7	11.8	1.9	--	1.4	N/A	1.71	3.5	4.4	N/A	4.3	3.6
10	(8) excluding out of bound sets	5.5	N/A	2.9	5.1	4.8	N/A	--	N/A	N/A	N/A	3.4	2.8	N/A	3.9	3.4
11	SD of (10) %	2.1	N/A	3.2	3.2	2.6	N/A	--	N/A	N/A	N/A	2.3	2.4	N/A	2.7	2.4
12	Strength Range (MPa) Min	18.6	20.2	17.8	22.4	17.8	18.0	--	17.8	20.6	17.8	37.5	40.2	38.9	46.1	37.5
	Max	36.6	34.0	37.9	33.5	37.9	26.4	--	23.3	22.5	26.4	48.2	46.7	55.9	54.1	55.9
13	Strength Range (MPa)	18.0	13.8	20.1	11.0	20.1	8.4	--	5.5	1.9	8.6	10.7	6.5	17.0	8.0	18.4

Notes:-

CB = Chipboard

X = Cross section of each panel consisting of 10 samples for chipboard and 22 samples for OSB and MDF.

BS = Bending Strength

SD = Standard Deviation.

Mean Diff. Matched Sets of Four = the mean difference in strength between the outside two samples of each set of four when tested to failure.

Out of bound sets were those where the difference between the static strengths of the outside two samples was greater than 10.5% of the mean strength obtained from those two samples. This resulted in 33 sets of OSB samples, no sets of chipboard samples and 5 sets of MDF samples being excluded.

A cross section of chipboard Panel 5 was not statically tested to failure as the samples were required for dynamic tests.

3/7 of Panel 6 was not tested and is stored in the conditioning cupboard in case the samples are needed at a later date.

Fig. 9.1a BENDING STRENGTHS, MEDIUM LOADING RATE FOR OSB, CHIPBOARD AND MDF

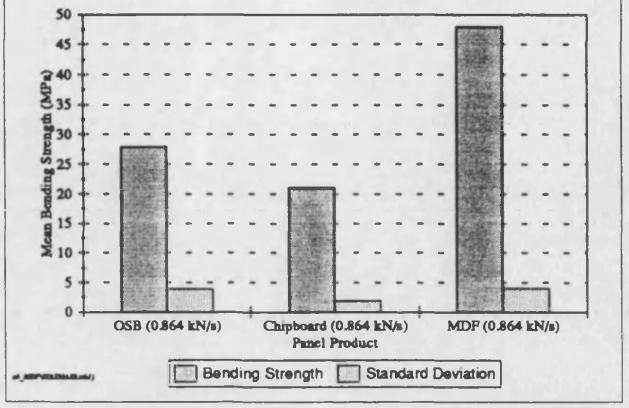

Fig. 9.1b DENSITIES FOR OSB, CHIPBOARD AND MDF TESTED AT THE MEDIUM LOADING RATE

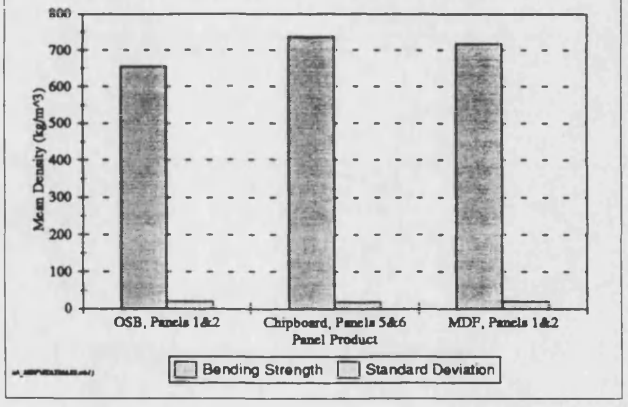

Fig. 9.1c SPECIFIC STRENGTH, MEDIUM LOADING RATE FOR OSB, CHIPBOARD AND MDF

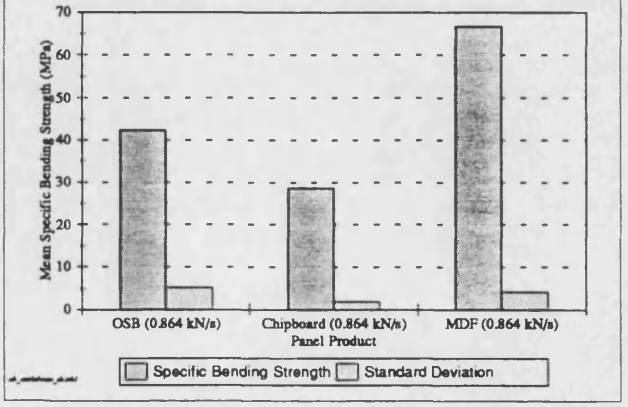

Fig 9.2a

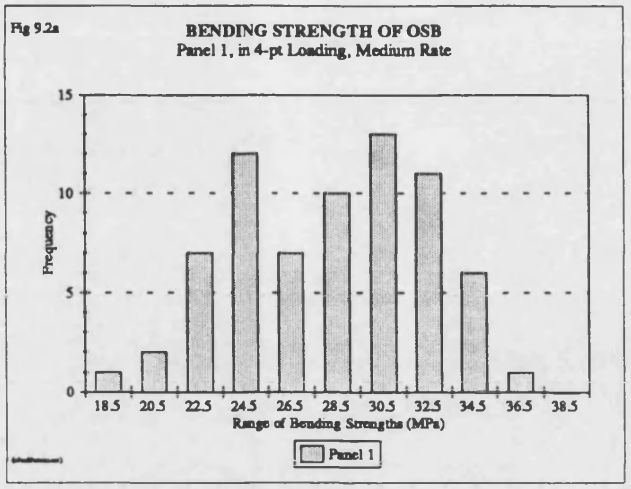

Fig 9.2b

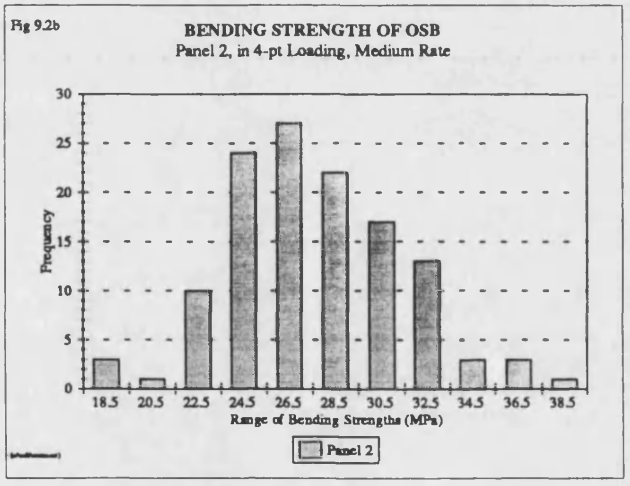

Fig 9.2c

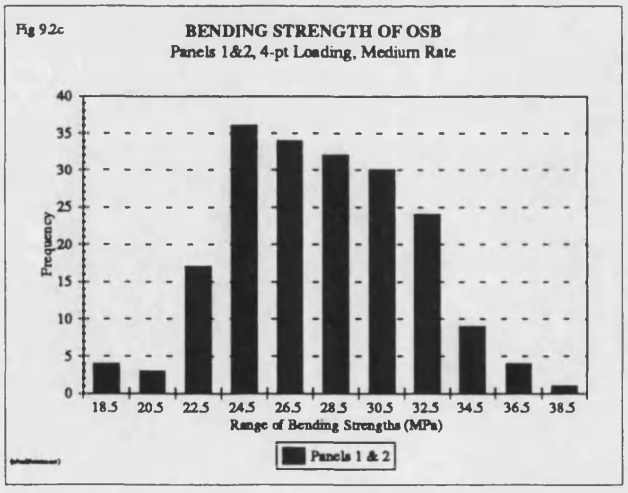

Fig 9.3a

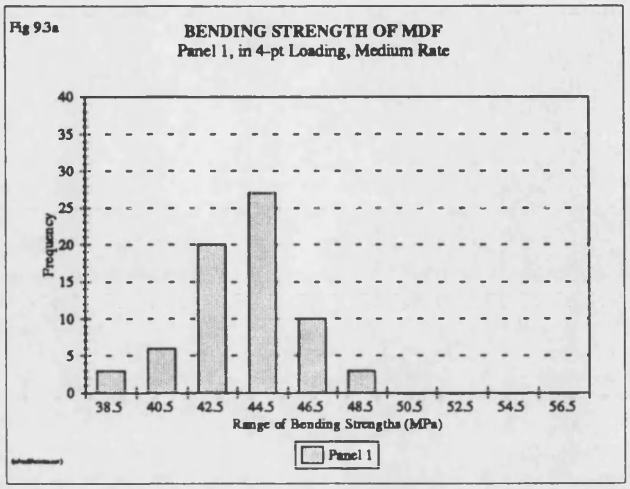

Fig 9.3b

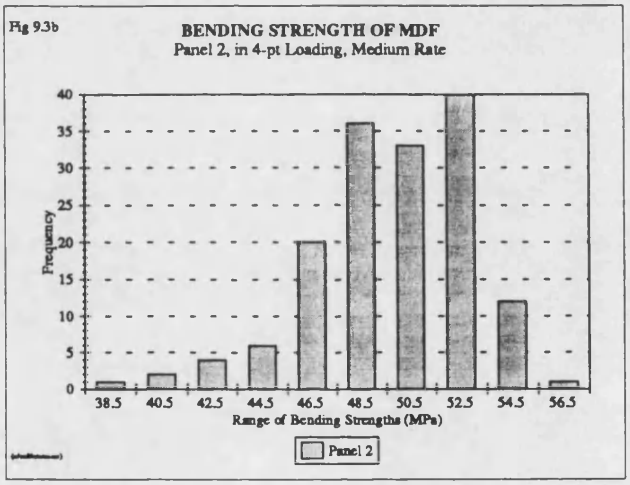

Fig 9.3c

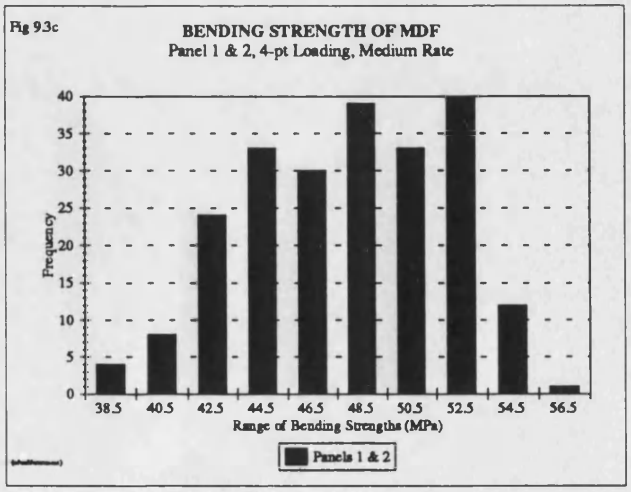

Fig 9.4a

BENDING STRENGTH OF OSB

Panel 1a, Outside Samples, Medium Rate

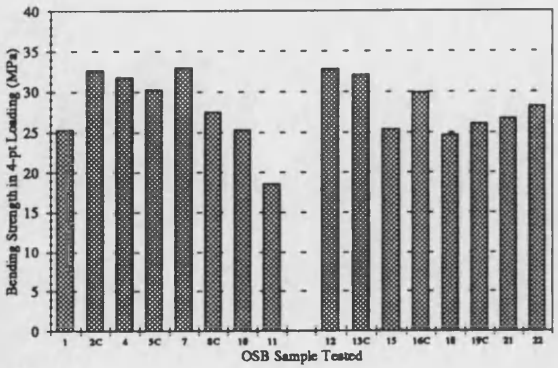

Fig 9.4b

BENDING STRENGTH OF OSB

Panel 1b, Cross-Section, Medium Rate

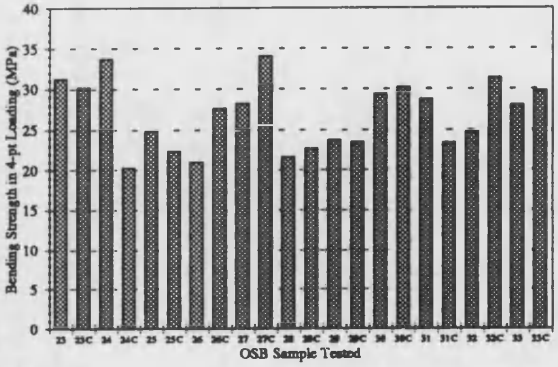

Fig 9.4c

BENDING STRENGTH OF OSB

Panel 1c, Outside Samples, Medium Rate

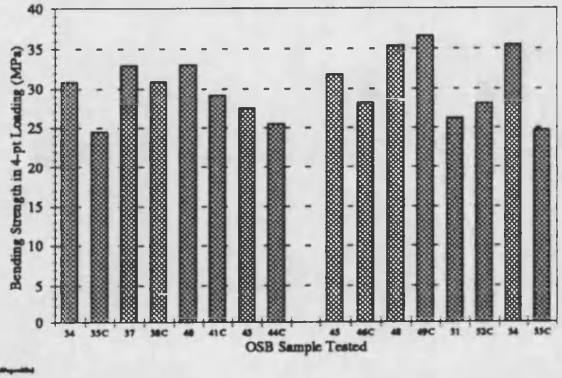

Fig 9.4d

BENDING STRENGTH OF OSB

Panel 1d, Outside Samples, Medium Rate

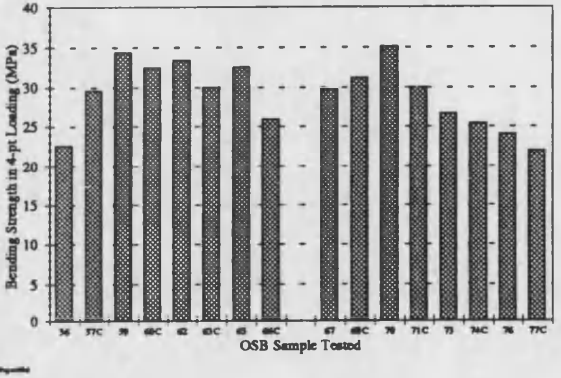

Fig 9.5a

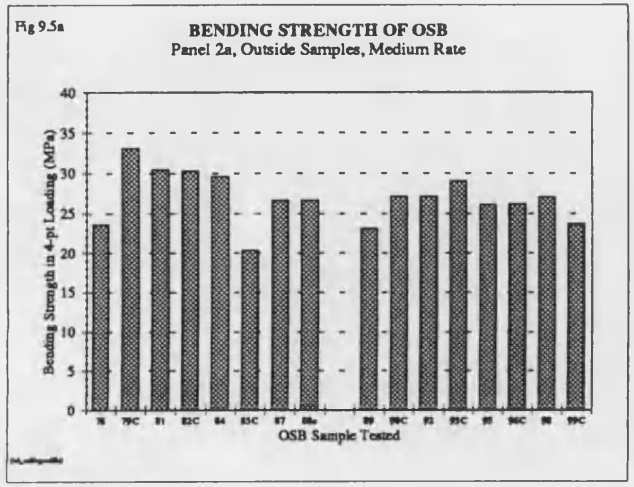

Fig 9.5b

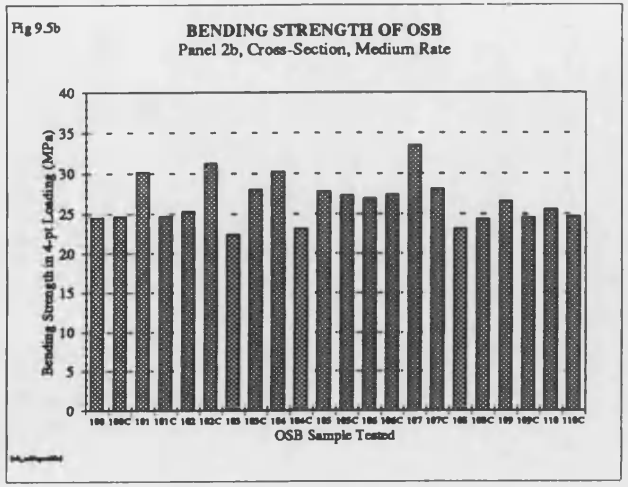

Fig 9.5c

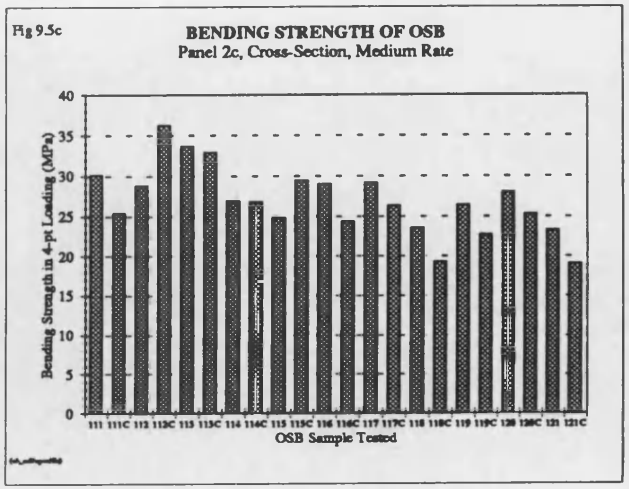

Fig 9.5d

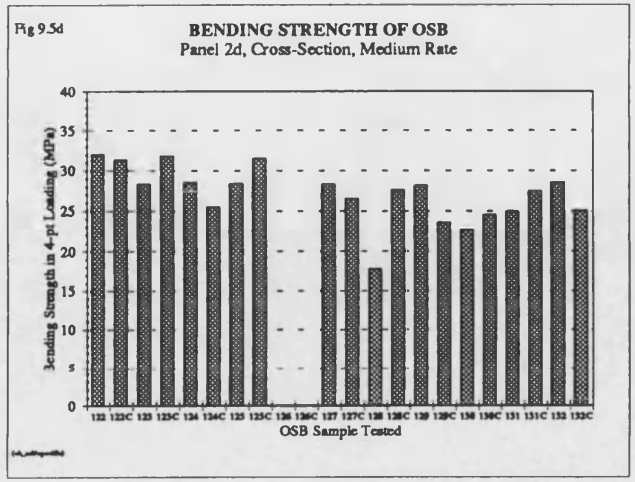

Fig 9.5e

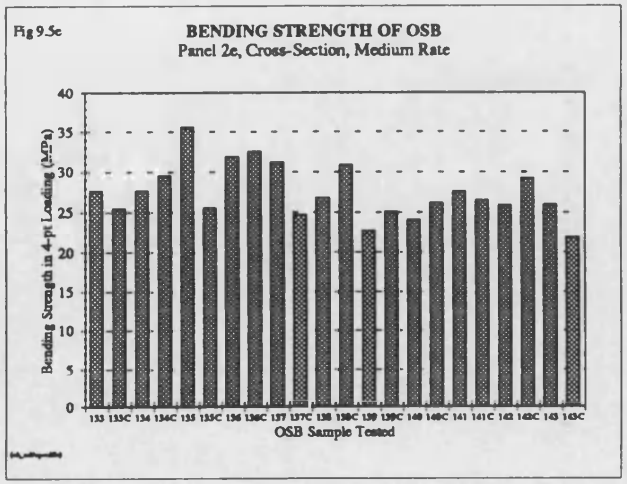

Fig 9.5f

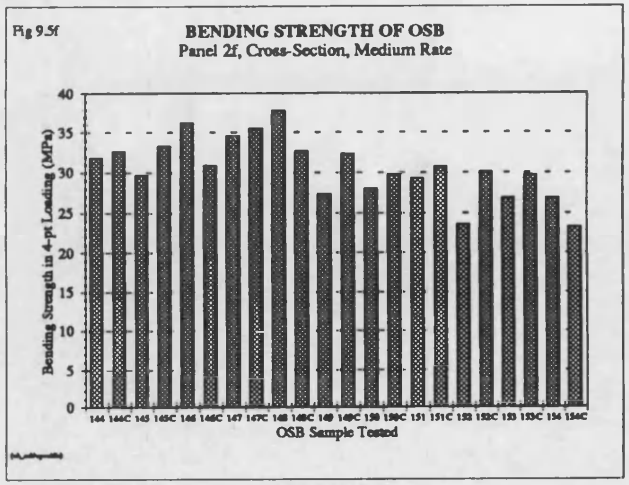

Fig 9.6a

BENDING STRENGTH OF MDF
Panel 1a, Outside Samples, Medium Rate

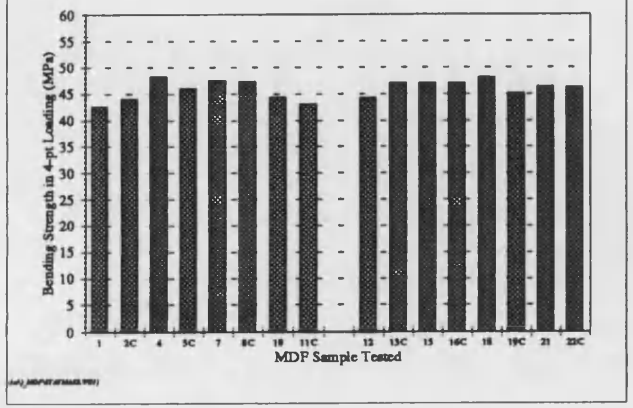

Fig 9.6b

BENDING STRENGTH OF MDF
Panel 1b, Cross-Section, Medium Rate

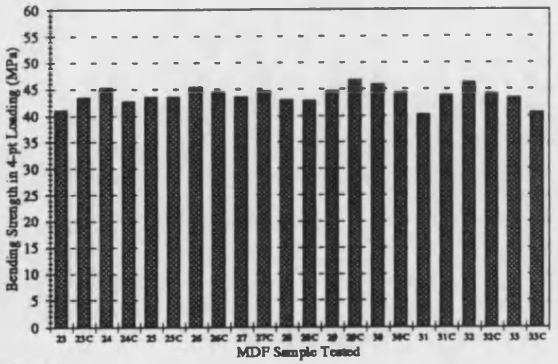

Fig 9.7a

BENDING STRENGTH OF MDF
Panel 2a, Cross-Section, Medium Rate

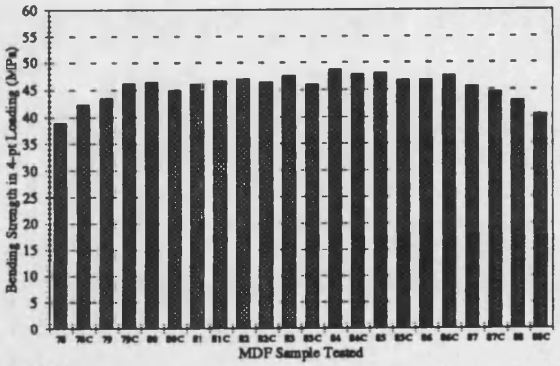

Fig 9.6c

BENDING STRENGTH OF MDF
Panel 1c, Outside Samples, Medium Rate

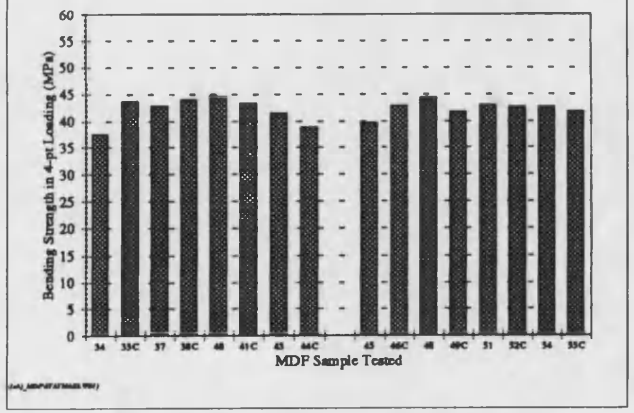

Fig 9.6d

BENDING STRENGTH OF MDF
Panel 1d, Outside Samples, Medium Rate

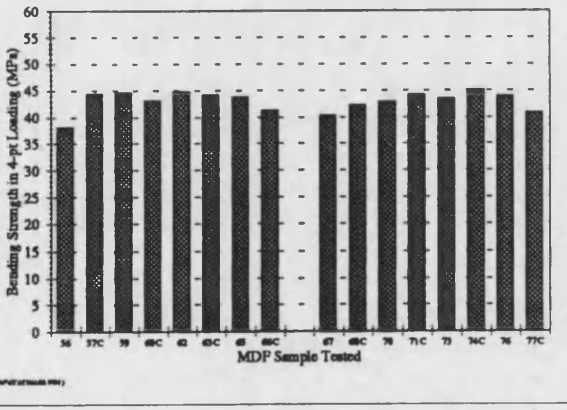

Fig 9.7b

BENDING STRENGTH OF MDF
Panel 2b, Cross-Section, Medium Rate

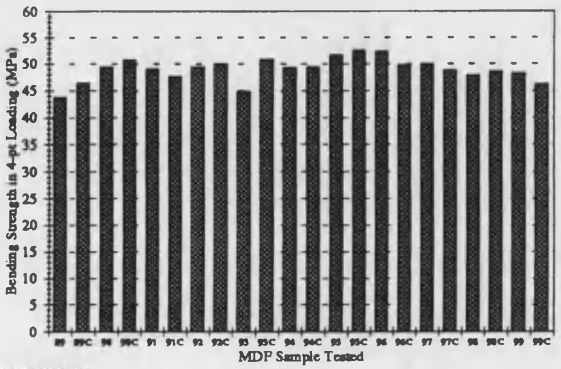

Fig 9.7c

BENDING STRENGTH OF MDF
Panel 2c, Cross-Section, Medium Rate

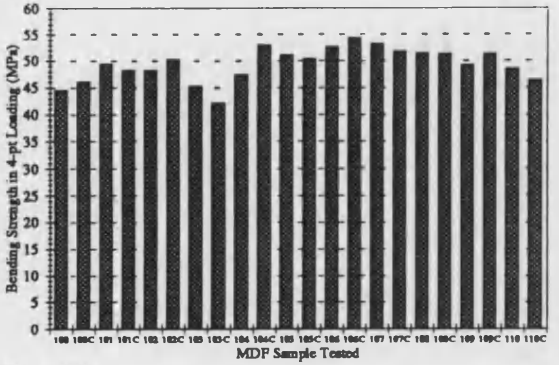

Fig 9.7d

BENDING STRENGTH OF MDF
Panel 2d, Cross-Section, Medium Rate

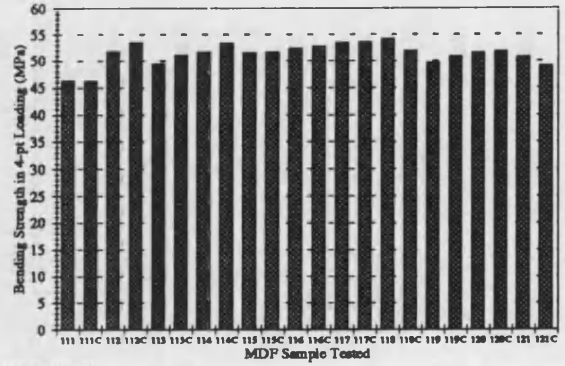

Fig 9.7e

BENDING STRENGTH OF MDF
Panel 2e, Cross-Section, Medium Rate

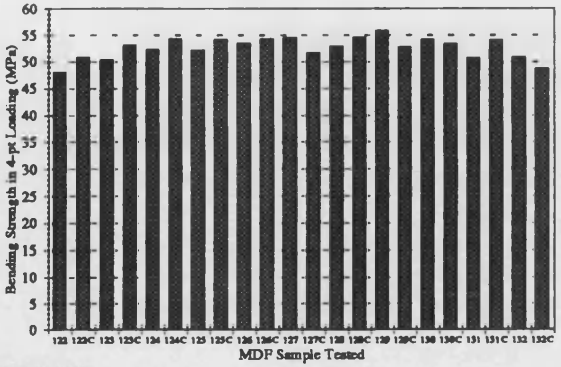

Fig 9.7f

BENDING STRENGTH OF MDF
Panel 2f, Cross-Section, Medium Rate

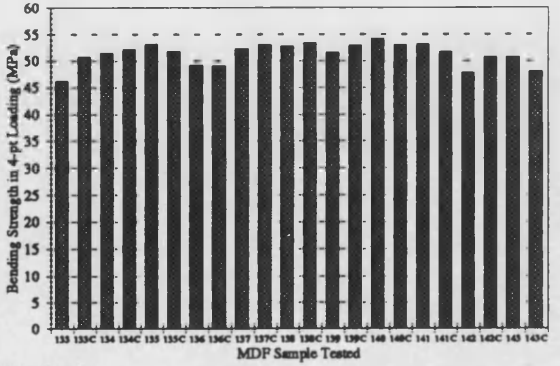

Fig 9.7g

BENDING STRENGTH OF MDF
Panel 2g, Cross-Section, Medium Rate

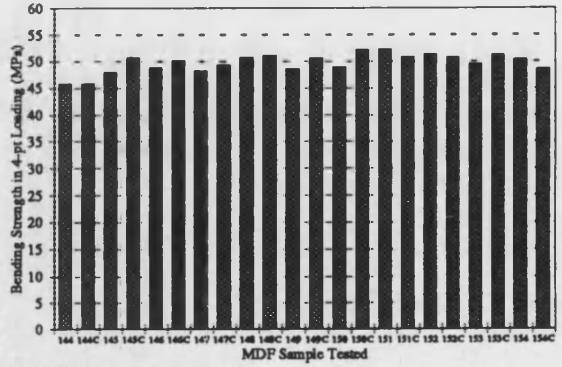

Discussion

It is clearly demonstrated in figure 9.1a and table 9.1 that the strength of MDF was significantly greater than that of OSB and chipboard. The mean strengths were 27.9 MPa for OSB, 21.0 MPa for chipboard and 47.9 MPa for MDF. The measured strengths for MDF were considerably greater than indicated in the Wood Panel Products Federation Folder, "The Facts on Board" (1994). The strengths did not correlate with the constituent particle size which reduced from OSB to chipboard to MDF. The relative strengths were in the ratio of 1.32:1:2.28 as the particle size decreased. Despite the high strength of MDF compared to the other two materials, the use of MDF as a structural material will be limited by its deflection under load, which is far greater than the other two materials, and is evaluated in Chapter 10.

The densities for the three materials and their standard deviations are compared in figure 9.1b and were similar for all three materials. Chipboard was the densest material, then MDF and finally OSB. The values were 656 ±19 kg/m^3 for OSB, 736 ±18 kg/m^3 for chipboard and 717 ±19 kg/m^3 for MDF. These values did not correlate with the constituent particle size either but agreed with the literature (WPPF 1994).

The mean specific strengths for the three materials are compared in figure 9.1c and the trend is the same as that for the strengths. The mean specific strengths ± the standard deviations were 42.4 ±5.2 MPa for OSB, 28.6 ±1.95 MPa for chipboard and 66.7 ±4.1 MPa for MDF. Again there is no direct correlation with the constituent particle size.

The distributions of the sample strengths for OSB Panel 1, figure 9.2a, appear to be normally distributed. Those for Panel 2 and both panels combined, figures 9.2b and 9.2c, appear to be normally distributed or slightly skewed to the left. The strength of chipboard has been demonstrated as being normally distributed and, because only an indication of the relative strengths and variability is required, normality will be assumed for the purposes of this discussion. In the distribution plots for MDF, figures 9.3a-c, the strengths for Panel 1, figure 9.3a, appear to be normally distributed. Those for Panel 2 and both panels combined, figures 9.3b and 9.3c, appear normally distributed or slightly skewed to the right. To simplify the analysis and to allow the three sets of results to be compared the same assumption has been used for this data. Figures 9.3a and 9.3b also show that most the samples from MDF Panel 2 were stronger than those from OSB Panel 1, demonstrating that there are strength variations between different Panels, as well as within individual panels.

The standard deviations from the mean strengths are shown in figure 9.1a. This was greatest for OSB which is also clearly demonstrated in table 9.1, row seven which shows the standard deviations as a percentage of the mean strength. The standard deviations were 14.0% for OSB, 9.0% for chipboard and 8.4% for MDF. This gives a general trend for the variability within panels, for samples of the dimensions tested here, decreasing as the size of the constituent wood particles decreases.

Of great importance to the fatigue testing is the variability in strengths within side-matched sets of four samples shown in table 9.1, row eight. This shows the mean difference between outside paired samples to be 14.5% for OSB, 3.6% for chipboard and 4.3% for MDF. (The difference is taken as the mean strength of each pair minus the lower of the two strengths.) The values show that the strength variability within side-matched sets of OSB samples is far greater than the variability of chipboard and MDF which were both very similar. This is also demonstrated for OSB by figures 9.4a-d and 9.5a-f, and for MDF by figures 9.6a-d and 9.7a-g. The strengths for the side-matched OSB samples are considerably more random than those for the MDF. Equivalent figures for chipboard were presented in section 7.2 and were similar to those for MDF.

Excluding the out of bounds sets (see section 7.2), the differences reduced to 4.8% for OSB, 3.6% for chipboard (this value is unchanged because no sets were out of bounds) and 3.4% for MDF. The greater variability for OSB introduces a large error when the strengths of the outside samples from matched sets of four are used to set the stress levels for the fatigue and creep tests since it is assumed that the variability within sets is lower than that within the panels.

The implication of the strength variation for OSB is demonstrated in figures 9.4a-d for Panel 1 and figures 9.5a-f for Panel 2. These should be compared to figures 9.6a-d and 6.7a-g for MDF. In figures 9.4a, c and d for OSB Panel 1, and figure 9.5a for OSB Panel 2, each pair of adjacent columns on the plots represents the outside samples from matched sets of four samples and there are large differences in height between the adjacent columns. This represents a large strength difference, but if the difference between the strengths of the outside two samples was greater 10.5% of their mean strength, then that set was not used to set up fatigue and creep tests. Therefore these differences do not create a problem when matched sets of four samples are tested in fatigue and creep loading because the out of bounds sets are never used. However, the high percentage of sets that had to be excluded meant that significant time was expended measuring and testing those samples that could then not be used. The

strength differences that produce a problem for estimating stress levels in the fatigue and creep testing are those between side-matched samples. This can be seen in figure 9.4.b for Panel 1 and figures 9.5b-f for Panel 2. For example, if samples 32, 32C, 33 and 33C in figure 9.4b were considered as a matched set of four samples, the strength of sample 32C would be expected to be close to the mean strength measured from the outside two samples, 32 and 33C. This is clearly not the case and excessive scatter in the fatigue data is likely. If this sample was tested at the 60% stress level calculated from the strengths of the outside two samples, it would in fact be loaded at less than 50% of its own strength.

Figures 9.6a-d and 9.7a-g demonstrate that the MDF panels suffer from edge effects, i.e. the samples at the ends of each cross-section are consistently weaker than those in the centre. This edge effect must contribute to the level of variation reported for the MDF panels. If the edge samples were eliminated then the variability for MDF would be slightly lower than for chipboard. Edge effects were not apparent for OSB or chipboard.

The range of strengths encountered for OSB was 20.1 MPa, which is 72% of the mean for all the strengths, this was 8.6 MPa, 41.0% of the mean for chipboard and 18.4 MPa, 38.4% of the mean strength for MDF again demonstrating the large variability for the OSB samples. The large range of strengths for OSB must be considered when considering the fatigue data. Since the scatter of strengths is large both within the entire OSB panels and in the localised matched sample sets it is difficult to see how this situation could be improved upon. The only possibility is to test wider samples because the particle size for OSB is large with respect to the width of samples presently used. An increase in sample width would not conform with the extensive tests performed to date, so this was not really a viable option unless embarking on a new work programme.

Only the strength variability correlated to particle size. However, the particles in OSB were frequently almost as wide as the test samples. It is probable that if wider samples were tested then this variability would be reduced but to what extent is uncertain. Width effects are presently being evaluated at BRE but the results are not available at this stage. An investigation and literature review of the relationship between small-specimen and large panel bending tests on structural wood based panels is presented by McNatt *et al* (1984 and 1990). In general terms it is concluded that large panels yielded lower strengths and higher stiffness values than those for small specimens.

However, specimen width is not considered to affect the strength but it is possible that this only becomes a factor when the particle size approaches the specimen width.

The chipboard, OSB and MDF were chosen to be of equivalent grades (or as close as possible) but particle size is far from the only parameter which causes property differences between them. The reason the results do not correlate to the size of the constituent particles may be due to other variables such the resin type, resin content, wood species and the manufacturing process.

9.2 Interim Conclusions 3

1) The mean strength of all the MDF samples tested, 47.9 MPa, was greater than that for the OSB samples, 27.9 MPa, which was greater than that for the chipboard samples, 21.0 MPa. There was no correlation between strength and the constituent particle size.

2) The mean densities for the three panel products decreased in the following order, chipboard>MDF>OSB. There was no correlation between density and the constituent particle size.

3) Strength variability between samples was greatest for OSB, then chipboard and finally MDF. This means that strength variability for samples of the dimensions tested decreased as the constituent particle size was decreased. This was both for variability within the panels and within side-matched sets of samples.

4) The use of side-matched sets of samples reduced the variability between samples for chipboard and MDF, but not for OSB.

5) MDF suffered from edge effects, i.e. the samples at the edges of the panels were weaker than those at the centre of the panels. This was not the case for chipboard and OSB.

10.0 FATIGUE IN OSB AND MDF

In this chapter the fatigue performances of OSB, chipboard and MDF are compared for loading at medium frequency, at R=0.1. This includes the use of stress versus strain hysteresis loop capture as a non-interuptive method of measuring damage accumulation in the materials. The creep deflections for parallel side-matched samples were again captured and are compared for the three materials. The hysteresis loop parameters evaluated for chipboard loaded at the three different frequencies are also evaluated for OSB and MDF. Part of Chapter 10 evaluates whether there is a correlation between the size of the constituent wood particles and the fatigue performance of wood based panel products.

10.1 S-N Results

Figures 10.1, 10.2 and 10.3 are S-N plots comparing the fatigue lives for OSB, chipboard and MDF. The data for the three materials was collected from testing at R=0.1, at medium frequency. In figure 10.1 the number of fatigue loading cycles is plotted against the percentage stress level with the static data excluded. In all cases the fatigue samples and the side-matched static samples used to obtain the 100% stress values were tested at a loading rate of 0.864 kN/s. Figure 10.2 shows essentially the same data but the static data has been included in the regression analysis and forces the three fitted lines to converge towards the quarter cycle loading point at the 100% stress level. Figure 10.3 presents the raw stress data in MPa (not normalised into percentage stress levels) because the strength of the OSB samples was found to be considerably more variable than that for the chipboard and MDF. Least squares linear regression has been applied to all the sets of data for the three plots. Runout samples were excluded from the regression analysis in every case. The regression analysis was performed in the same manner as reported in Chapter 8.

The fatigue lives (cycles to failure) for medium frequency testing of OSB, chipboard and MDF are provided in tables 10.1 and 10.2. Table 10.1 provides a comparison between the mean sample lives for each stress level for the three materials. Runouts have been included in the table at the allotted 10^6 loading cycles for medium frequency testing but were excluded when calculating the mean values.

Table 10.2 is similar to table 10.1 but compares the median lives for each stress level for the three materials instead of the mean lives. Again median values are used to prevent unusually high or low values from adversely influencing the data analysis. This is particularly appropriate for OSB because of the highly variable results obtained.

The equations for the regression lines and their respective correlation coefficients in the normalised plots, figures 10.1 and 10.2, were as follows:

For figure 10.1:

OSB tested at R=0.1 at medium frequency, static and runout data excluded.

1) $\text{Log}(N) = -0.125(S) + 11.62 \qquad r^2 = 0.61$

Chipboard tested at R=0.1 at medium frequency, static and runout data excluded.

2) $\text{Log}(N) = -0.119(S) + 11.76 \qquad r^2 = 0.96$

MDF tested at R=0.1 at medium frequency, static and runout data excluded.

3) $\text{Log}(N) = -0.083(S) + 8.79 \qquad r^2 = 0.92$

For figure 10.2:

OSB tested at R=0.1 at medium frequency, static data included, runout data excluded.

1) $\text{Log}(N) = -0.117(S) + 11.14 \qquad r^2 = 0.92$

Chipboard tested at R=0.1 at medium frequency, static included, runout data excluded.

2) $\text{Log}(N) = -0.132(S) + 12.62 \qquad r^2 = 0.99$

MDF tested at R=0.1 at medium frequency, static included, runout data excluded.

3) $\text{Log}(N) = -0.110(S) + 10.44 \qquad r^2 = 0.99$

The equations for the regression lines and their respective correlation coefficients for the raw stress data (MPa), figure 10.3, were as follows:

OSB tested at R=0.1 at medium frequency, static data and runout data excluded.

$$Log(N) = -0.470(S) + 12.23 \qquad r^2 = 0.72$$

Chipboard tested at R=0.1 at medium frequency, static data and runout data excluded.

$$Log(N) = -0.360(S) + 8.89 \qquad r^2 = 0.60$$

MDF tested at R=0.1 at medium frequency, static data and runout data excluded.

$$Log(N) = -0.186(S) + 8.69 \qquad r^2 = 0.88$$

In order to enhance the value of these results for use in design applications the lower bounds of the 95% confidence limits are plotted for all three materials in figure 10.4a. There is 97.5% confidence that the true population mean for each material occurs above this line.

Fig. 10.1

S-N PLOT FOR CHIPBOARD, OSB AND MDF

R=0.1, AT MEDIUM FREQUENCY

(Static data and runout data excluded from the regression analysis)

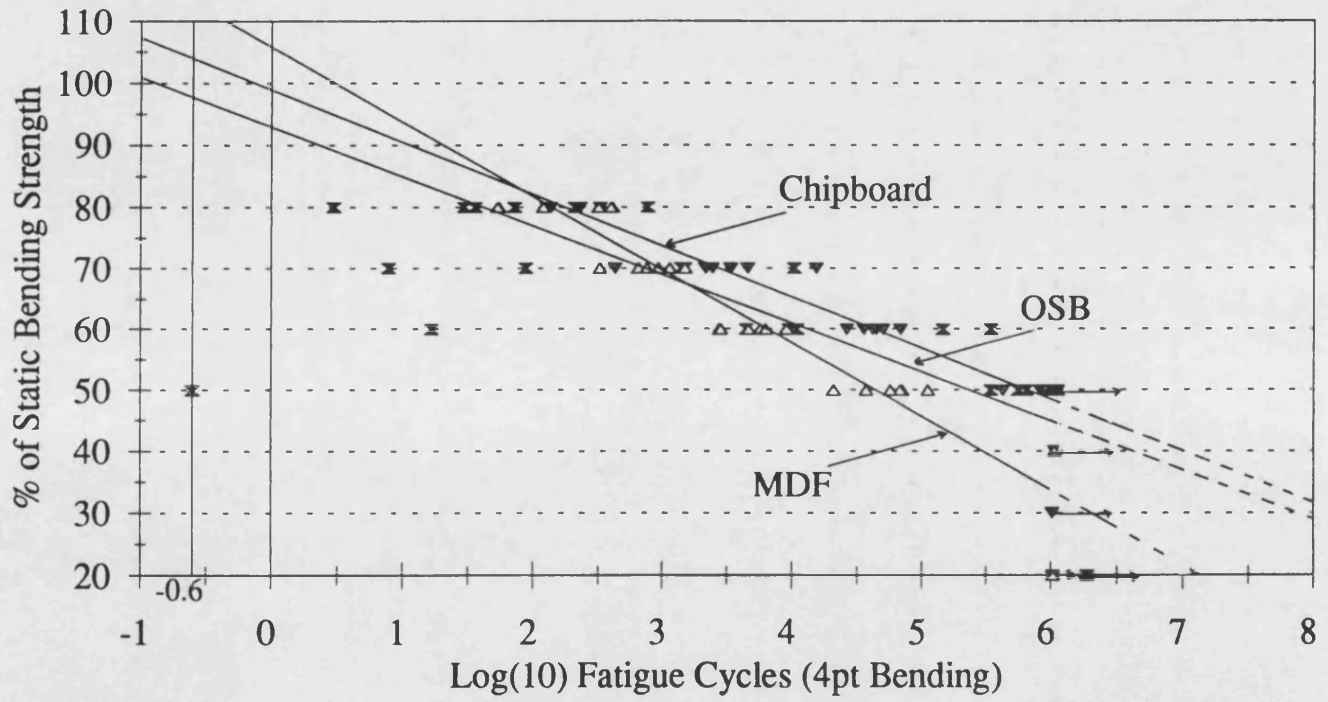

▼ Chipboard Log(N)=-0.119(S)+11.76 ⧗ OSB Log(N)=-0.125(S)+11.62

△ MDF Log(N)=-0.083(S)+8.79

(C:_mdf\SN.wb1)

Fig. 10.2

S-N PLOT FOR CHIPBOARD, OSB AND MDF

R=0.1, AT MEDIUM FREQUENCY

(Static data included and runout data excluded from the regression analysis)

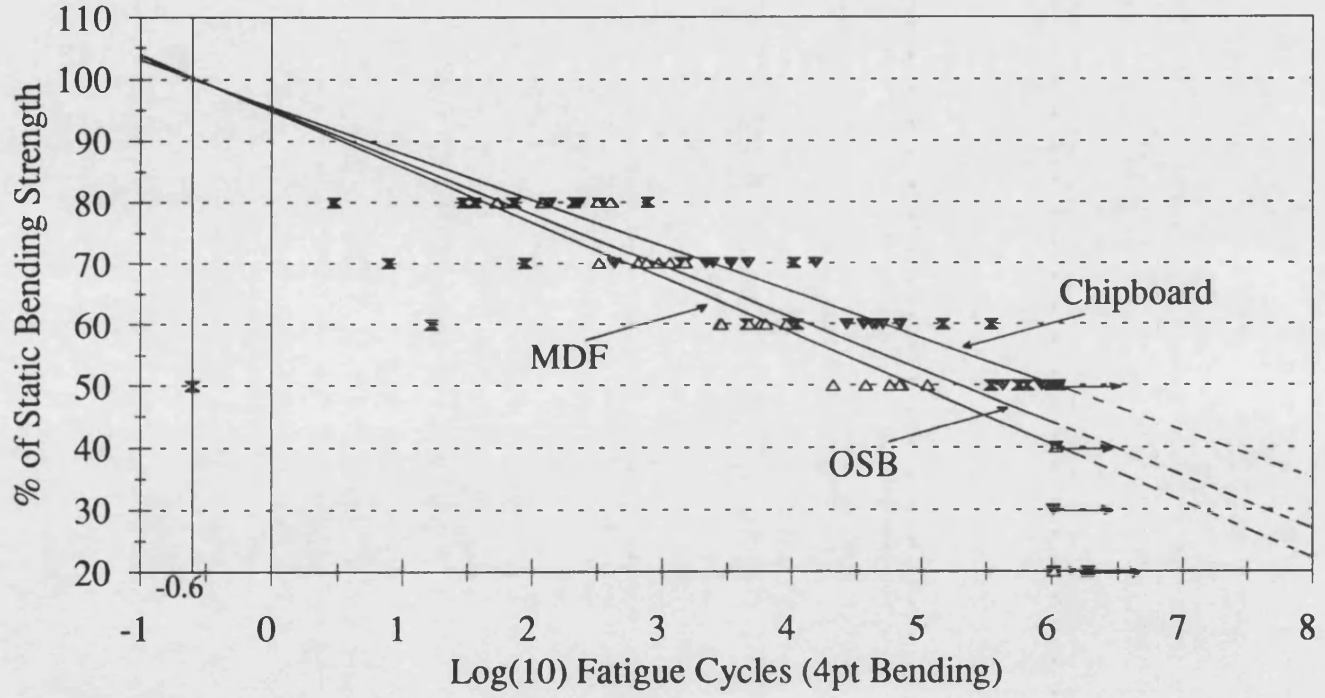

Fig. 10.3

S-N PLOT FOR CHIPBOARD, OSB AND MDF

4pt BENDING, R=0.1, MEDIUM FREQUENCY

(Static data and runout data excluded from the regression analysis)

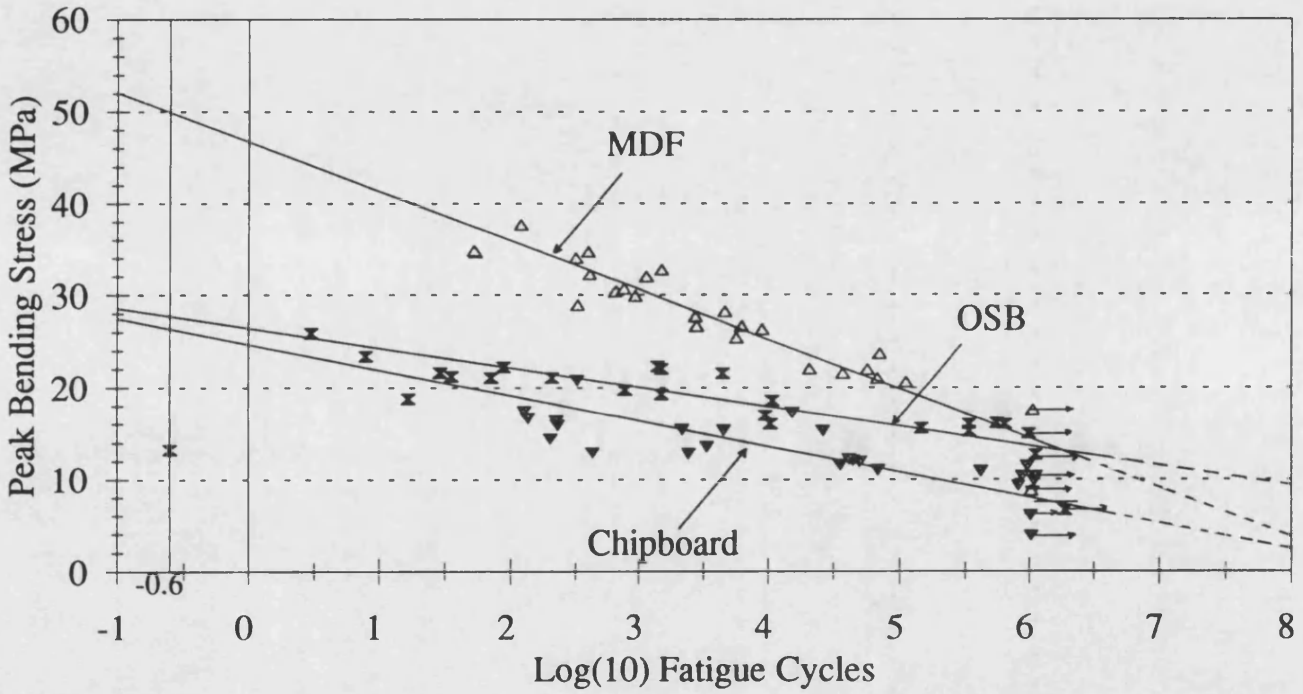

(C:_MDF\SN.WB1)

Table 10.1 Mean fatigue lives for OSB, Chipboard and MDF: The effect of particle size.

	OSB (0.864 kN/s)		CHIPBOARD (0.864 kN/s)			MDF (0.864 kN/s)		
Particle Size	**Large**		**Medium**			**Small**		
Stress Level	Mean Fatigue life ± Standard Deviation (No of Cycles)	Fraction of Samples Failed	Mean Fatigue Life ± Standard Deviation (No of Cycles)	Fraction of Samples Failed	Increased Life Compared to OSB (Multiplied by)	Mean Fatigue Life ± Standard Deviation (No of Cycles)	Fraction of Samples Failed	Increased Life Compared to Low Freq. (Multiplied by)
80%	188 ± 295	6/6	212 ± 75	6/6	**1.1**	228 ± 171	6/6	**1.2**
70%	2 485 ± 3 923	6/6	4 731 ± 5 375	6/6	**1.9**	887 ± 405	6/6	**0.4**
60%	86 659 ± 139 931	6/6	44 737 ± 14 632	6/6	**0.5**	5 222 ± 2 368	6/6	**0.1**
50%	388 565 ± 286 581	4/6	784 587 ± 242 185	4/6	**2.0**	60 808 ± 31 161	6/6	**0.2**
40%	None Tested	NA	1 000 000(Runout)	0/1	NA	1 000 000(Runout)	0/1	NA
30%	None Tested	NA	1 000 000(Runout)	0/1	NA	None Tested	NA	NA
20%	1000 000(Runout)	0/1	1 000 000(Runout)	0/1	NA	1 000 000(Runout)	0/1	NA

NA = applies to those conditions where few or no samples failed for the duration of the tests.
Means calculated from failed samples only.

Table 10.2 Median fatigue lives for OSB, chipboard and MDF: The effect of particle size.

	OSB (O.864 kN/s)		CHIPBOARD (O.864 kN/s)			MDF (O.864 kN/s)		
Particle Size	**Large**		**Medium**			**Small**		
Stress Level	Sample Lives (Cycles) and **Median Life (M)**	Fraction of Samples Failed	Sample Lives and **Median Life (M)**	Fraction of Samples Failed	Increased Life Compared to OSB (Multiplied by)	Sample Lives and **Median Life (M)**	Fraction of Samples Failed	Increased Life Compared to OSB (Multiplied by)
80%	3,30,36,73,213,771 **M = 55**	6/6	130,139,202,228, 236,334 **M = 215**	6/6	**3.9**	54,55,120,322, 403,415 **M = 221**	6/6	**4.0**
70%	8,89,1 422,1 509, 1 520,103 364 **M = 1 467**	6/6	436,2 183,2 457,3 359, 4 616,15 336 **M = 2 908**	6/6	**2.0**	330,660,763,925, 1 146,1 499 **M = 844**	6/6	**0.6**
60%	17,4 515,9 604, 11 070,146 533, 348 217 **M = 10 337**	6/6	26 352,35 629,41 938, 44 558,50 554,69 393 **M = 43 248**	6/6	**4.2**	2 771,2 834,4 687, 5 711,6 278,9 054 **M = 5 199**	6/6	**0.5**
50%	0.25,350 572, 563 222,640 466, 1 076 016+, 1 129 700+ **M = 601 844**	4/6	431 184,837 667, 895 045,974 452, 108 8931+,1 123 401+ **M = 934 749**	4/6	**1.6**	20 920,37 059, 57 049,68 143, 70 484,111 191 **M = 62 596**	6/6	**0.1**
40%	None Tested	NA	1075351+	0/1	NA	1 079 538+	0/1	NA
30%	None Tested	NA	1019403+	0/1	NA	None Tested	NA	NA
20%	1 916 050+	0/1	1043001+	0/1	NA	1 029 800+	0/1	NA

NA = applies to those conditions where few or no samples failed for the duration of the tests.
+ denotes a runout samples.

Fig. 10.4

95% CONFIDENCE INTERVALS, MEDIUM FREQ.
CHIPBOARD, OSB, & MDF AT R=0.1

(Static data and runout data excluded from the regression analysis)

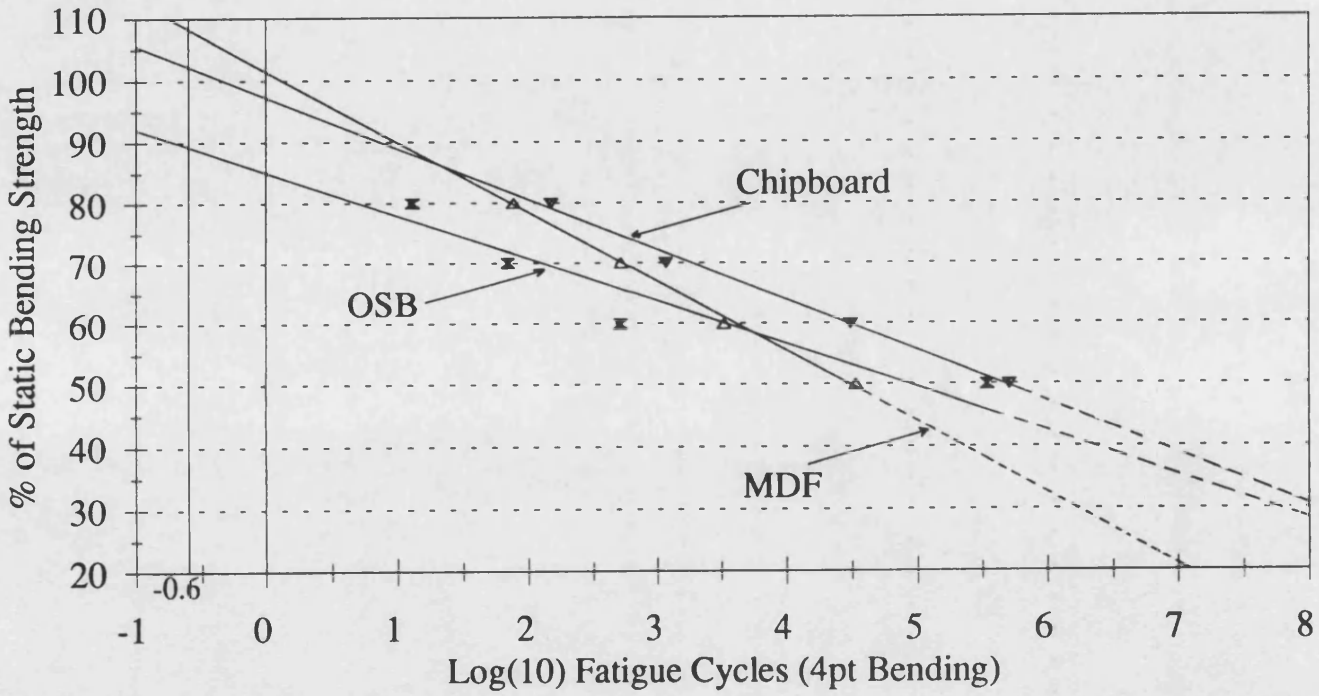

Discussion

The three sets of data and the regression lines plotted enable the fatigue response of the three materials to be compared. All testing was performed using the identical loading configuration and test methodology. The fatigue and static tests were performed at the same loading rates and only the number of data points included in the regression analysis at the 50% stress level is different. One OSB sample failed on the first loading cycle and was excluded. This sample failed at below 50% of the strength predicted from its side-matched partners and was therefore not a representative sample for the 50% stress level. This does, however, highlight once again the huge variations between the strengths of the OSB samples tested. Three data points for the 50% stress level were included in the regression analyses for OSB, compared with four points for chipboard and six points for MDF.

The three S-N plots should be considered separately. The first two plots, figures 10.1 and 10.2, compare the fatigue performances of the three materials relative to their own strengths whereas figure 10.3 compares the ultimate difference between them in terms of the applied stresses (MPa).

Considering figure 10.1 first, it can be seen that the OSB has an inferior fatigue performance to the chipboard, relative to its own strength, although the magnitude of this difference decreases with decreasing stress level. MDF has a considerably worse fatigue performance than both materials and this difference increases as the stress level reduces. The regression lines for OSB and chipboard converge as the stress level is reduced so it is probable that there would be very little, if any, difference in their fatigue lives at design stresses. However, the OSB data was by far the most varied and the regression line had a correlation coefficient of only 0.61 compared to 0.96 for chipboard and 0.92 for MDF, so this conclusion must be viewed with caution. However, tables 10.1 and 10.2 reinforce this conclusion if the changes in fatigue lives relative to OSB are compared. The regression line for MDF has a considerably steeper gradient than for OSB and chipboard and so the comparative fatigue life would be even lower at design stress levels. There was limited literature comparing the fatigue performance of wood based panels. Kyanka (1980) reported that, relative to its own strength, particleboard is inferior to wood and laminated wood loaded in fatigue. This was also reported by Kollman and Krech (1961), and by Gillwald (1966).

Figure 10.2 shows the same information as figure 10.1 but with the static strength data included. This plot reinforces the ranking that, when normalised relative to the static strengths, chipboard has the best fatigue performance, followed by OSB and then

MDF. Including the static data in the regression analysis significantly improved the correlation coefficient for the OSB but only serves to obscure its variability in performance. This plot would not predict the true magnitude to which the fatigue performance of MDF decreases relative to OSB and chipboard at low stress levels. The plot would overestimate the fatigue life unless confidence boundaries were computed. The fatigue life did not correlate with the constituent particle size unlike reported for creep loading in the literature where the propensity to creep increases as the constituent particle size is reduced (Dinwoodie and Bonfield 1995). However, for wood based panel products there will always be an overlap between good brands of the one panel type and poorer brands of another. This is an inherent difficulty in evaluating panel products and increases the need for considerable research into the properties of these materials.

Tables 10.1 and 10.2 are both based on the data shown in figures 10.1 and 10.2 because percentage stress levels are more appropriate than absolute stress values (MPa) for comparing the relative lives of the three materials. Both tables are similar and distinguish between the three materials by particle size. The exact size of the particles is academic, as explained in Chapter 9, since all that is required is a broad ordering of the three materials. The median values in table 10.2 are more appropriate for comparing the lives of chipboard and MDF with those for OSB, compared with the mean values in table 10.1 because of the large variability for OSB. Clearly chipboard has the greatest fatigue life, then OSB and then MDF and there is no correlation with the constituent particle size.

These conclusions are, however, challenged by the results of figure 10.3 for absolute stress values which show that MDF has a fatigue performance superior to that of OSB which in turn is superior to that of chipboard. The magnitude of the superiority of MDF over OSB and chipboard decreases as the peak applied stress is reduced. Also the superiority of OSB over chipboard increases as the stress level is reduced. This means, for example, that designing for a fatigue life of 10^5 cycles using the 50% probability of failure fitted regression lines, MDF could be loaded at about 20 MPa, OSB at 15 MPa and chipboard at only 10 MPa. So it can be concluded, based on the peak applied stress (MPa), that the fatigue performance of MDF is superior to OSB, which is superior to chipboard. However, the regression line for MDF is much steeper than those for OSB and chipboard. Designing for very long fatigue lives the performance of the three materials is very similar, as was found by Tsai (1987) for different wood species. Above 10^8 cycles, MDF would have the worst fatigue performance of the three materials.

The mean strength for all the MDF samples loaded to failure was 228% greater than that for the chipboard and 35% higher than that for OSB, so the trend for the fatigue lives based on applied stresses is to be expected. The results are a reflection of the relative static strengths and do not correlate to the size of the constituent wood particles.

From the correlation coefficients of the regression lines it can be seen that using matched sets of four samples reduces the spread of the fatigue life data for chipboard and MDF but it does not for OSB. The regression line for OSB in figure 10.1 intersects the 1/4 cycle point ($Log_{(10)}$ N = -0.6) at 97.78% of the ultimate stress, the line for the chipboard intersects at 103.92% and that for MDF intersects at 113.13%. Both the values for OSB and chipboard are close to the 100% stress value showing that the static tests are closely related to the regression lines fitted to the fatigue data for these materials. However, for MDF it appears that the static results are not so closely related to the fatigue results. It is likely that the S-N line for MDF should be a more pronounced S shaped than for OSB and chipboard. The correlation coefficients show that the fit of the regression line for OSB improves when the matched sets of four samples are not used and agrees with the variability in the static data highlighted in Chapter 9. Since variability also plays a significant role in designing with different materials the lower bound of the 95% confidence intervals are plotted in figures 10.4 to account for the variability in the measured fatigue lives.

The ranking of the fatigue performances for the three materials normalised by the static strengths is unaltered by plotting the lower 95% confidence intervals. Chipboard remains superior to OSB which is superior to MDF. However, the performance of OSB is reduced relative to the other two materials due to the strength variability between samples.

The fatigue results reported in this section do not take account of the relative deflections/creep performances of the three materials. Building materials are not generally subjected to high cycle fatigue loading and design is generally limited by deflection/creep under load. However, designing floors for a 50 year life when subjected to pedestrian/fork lift truck motion, supporting vibrating machinery or when used in sports hall floors are just a few examples of fatigue loading.

10.2 Runouts

Samples were designated as runouts after 10^6 loading cycles for OSB and MDF loaded at medium frequency and tests were then stopped in accordance with the procedure for chipboard tested at medium frequency (see section 8.4). The surviving samples (runouts) and their side-matched creep partners were again statically tested to determine their residual bending strengths. This allowed the strength changes resulting from fatigue and creep loading of the three different materials to be compared.

Twenty five samples of OSB and twenty six of MDF were tested at R=0.1, at medium frequency. Out of these three OSB samples and two MDF samples survived beyond the 10^6 loading cycles required for a runout. Two of the surviving OSB samples were tested at the 50% stress level but all the six of the MDF samples tested at 50% the stress level failed. The third OSB runout was tested at 20% stress level. The two MDF runouts were tested at the 40% and 20% stress levels. All the runouts were stored in the conditioning cupboard until the respective section of testing was complete and then the residual strengths were measured.

The residual strengths for the OSB and MDF runouts together with their side-matched creep partners are shown in tables 10.3 and 10.4 respectively. One of the OSB creep partners loaded at the 50% stress level, sample O-83C, had failed but none of the MDF creep partners failed within the duration of the fatigue runout tests.

Table 10.3 Residual bending strengths of OSB runout samples and their side-matched creep partners (medium frequency loading) at R=0.1.

Fatigue Sample	R ratio	Stress Level %	Width mm	Thickness mm	Failure Load kN	Residual Strength MPa	Strength Change %
O-18C	0.1	50	50.2	18.8	2.200	27.90	+10.0
O-83	0.1	50	50.3	18.6	2.690	34.78	+16.3
O-61C	0.1	20	50.1	18.5	2.635	34.58	+4.9

Creep Sample		Stress Level %	Width mm	Thickness mm	Failure Load KN	Residual Strength MPa	Strength Change %
O-19	NA	50	50.2	18.9	2.361	29.62	+16.8
O-83C	NA	50	NA	NA	NA	NA	NA
O-62	NA	20	50.2	18.6	1.6558	21.45	-34.9

Table 10.4 Residual bending strengths of MDF runout samples and their side-matched creep partners (medium frequency loading) at R=0.1.

Fatigue Sample	R ratio	Stress Level %	Width mm	Thickness mm	Failure Load kN	Residual Strength MPa	Strength Change %
M-42	0.1	40	50.4	18.2	2.446	32.97	-22.2
M-10C	0.1	20	50.5	17.9	3.126	43.47	-0.5

Creep Sample		Stress Level %	Width mm	Thickness mm	Failure Load kN	Residual Strength MPa	Strength Change %
M-42C	NA	40	50.5	17.9	3.309	46.01	+8.5
M-11	NA	20	50.6	17.9	3.155	43.79	+0.2

Discussion

The residual strength results for OSB presented in table 10.3 are inconclusive. The residual strengths of the fatigue loaded samples increased by between 4.9 and 16.3%. For the creep loaded samples, the strength changes ranged from a decrease of 34.9%, to an increase of 16.8%. Unfortunately due to the excessive variability in the original static strengths for OSB these results are all within the natural spread of the data.

There are only two sets of residual strength results for MDF. The strength of the fatigue runout tested at the 40% stress level showed a decrease of over 20% whilst the side-matched creep partner showed an increase of 8.5%. The result for the fatigue sample represents a significant strength reduction unlike the increase for its creep partner, which was within the spread of the data. The fatigue and creep samples tested at 20% stress both show negligible strength changes of less than 1% and represent no change in strength.

Although the small number of residual strengths measured makes it impossible to draw firm conclusions, the results do agree with those for chipboard at the medium and low frequencies presented in section 8.4. The only difference is that no significant strength reductions were observed below 50% for chipboard whereas there was a reduction for MDF at the 40% stress level. This is in agreement with the S-N results, see section 8.1, which showed the normalised regression line for MDF to be considerably steeper than for chipboard. It is reasonable to assume from the S-N plot, figure 10.1, that greater fatigue damage would be produced at lower stress levels for MDF than for chipboard.

10.3 Stress versus Strain Hysteresis Loops (First and Last)

Figures 10.5a-c show the first and last hysteresis loops captured by the FDAS for a sample of OSB tested at medium frequency, at R=0.1, at each of the stress levels 70, 50 and 20%. Figures 10.6a-c show the same plots for representative MDF samples tested under the same conditions and stress levels. Equivalent plots for chipboard were presented in section 8.5 and the details regarding this type of plot are explained in that section.

One example of a screen-dumped loop capture produced by the dot matrix printer during the testing for OSB and one for MDF are included as figures 10.7 and 10.8 respectively. The equivalent plot for chipboard was included as figure 8.7 in section 8.5.

Discussion

The hysteresis loops reduce in size with decreasing stress level for both OSB and MDF because smaller stresses produce smaller strains, as was the case for chipboard. In each test for OSB and MDF the last loop increases in area and moves to a greater microstrain compared to the first loop as occurred for chipboard. This shows that damage has been produced in the sample and therefore the energy dissipated per cycle of loading has increased and creep has occurred.

The magnitudes of the loops shown for OSB and chipboard are similar, with the stress range for OSB slightly greater than for chipboard due to the higher strength of OSB. However, the strength of MDF was considerably greater than that for OSB and chipboard, so the stress range in the plots for MDF, figures 10.6a-c, is considerably greater resulting in larger hysteresis loops.

In figures 10.5a and 10.5b, for OSB fatigue loaded at 70 and 50% stress levels, the gradient of the last loop has reduced compared to the first loop indicating that the stiffness has reduced. This is discussed in depth in the following sections of this chapter along with the other loop parameters.

The negative microstrain values in figures 10.5b and 10.5c are explained in section 10.4.

Fig. 10.5a **FIRST & LAST CAPTURED HYSTERESIS LOOPS**
OSB TESTED AT R=0.1, 70% STRESS

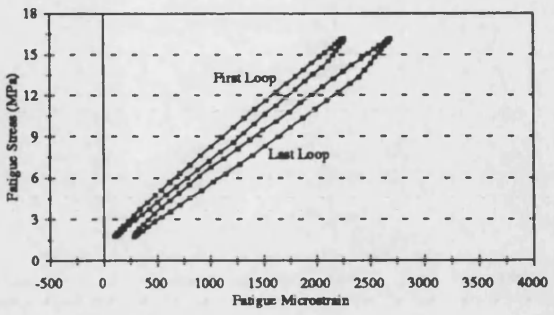

Fig. 10.5b **FIRST & LAST CAPTURED HYSTERESIS LOOPS**
OSB TESTED AT R=0.1, 50% STRESS

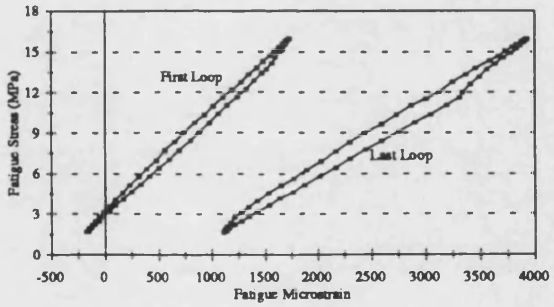

Fig. 10.5c **FIRST & LAST CAPTURED HYSTERESIS LOOPS**
OSB TESTED AT R=0.1, 20% STRESS

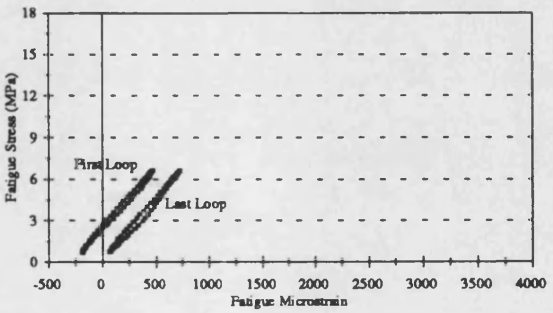

Fig. 10.6a **FIRST & LAST CAPTURED HYSTERESIS LOOPS**
MDF TESTED AT R=0.1, 70% STRESS

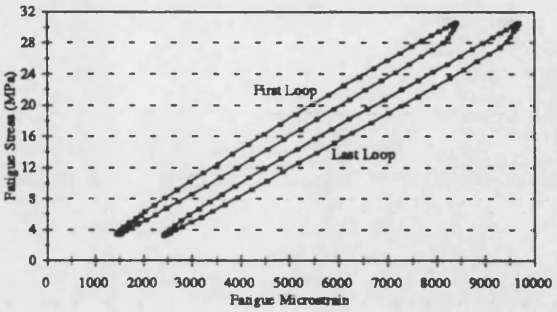

Fig. 10.6b **FIRST & LAST CAPTURED HYSTERESIS LOOPS**
MDF TESTED AT R=0.1, 50% STRESS

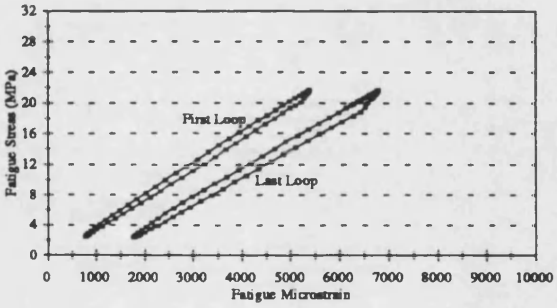

Fig. 10.6c **FIRST & LAST CAPTURED HYSTERESIS LOOPS**
MDF TESTED AT R=0.1, 20% STRESS

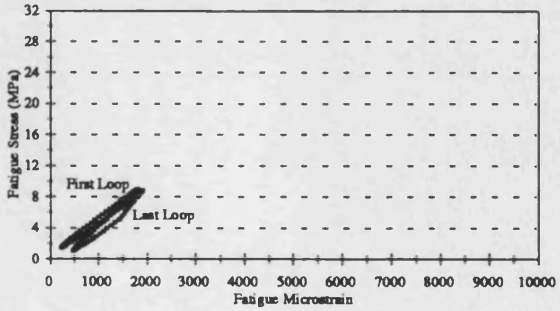

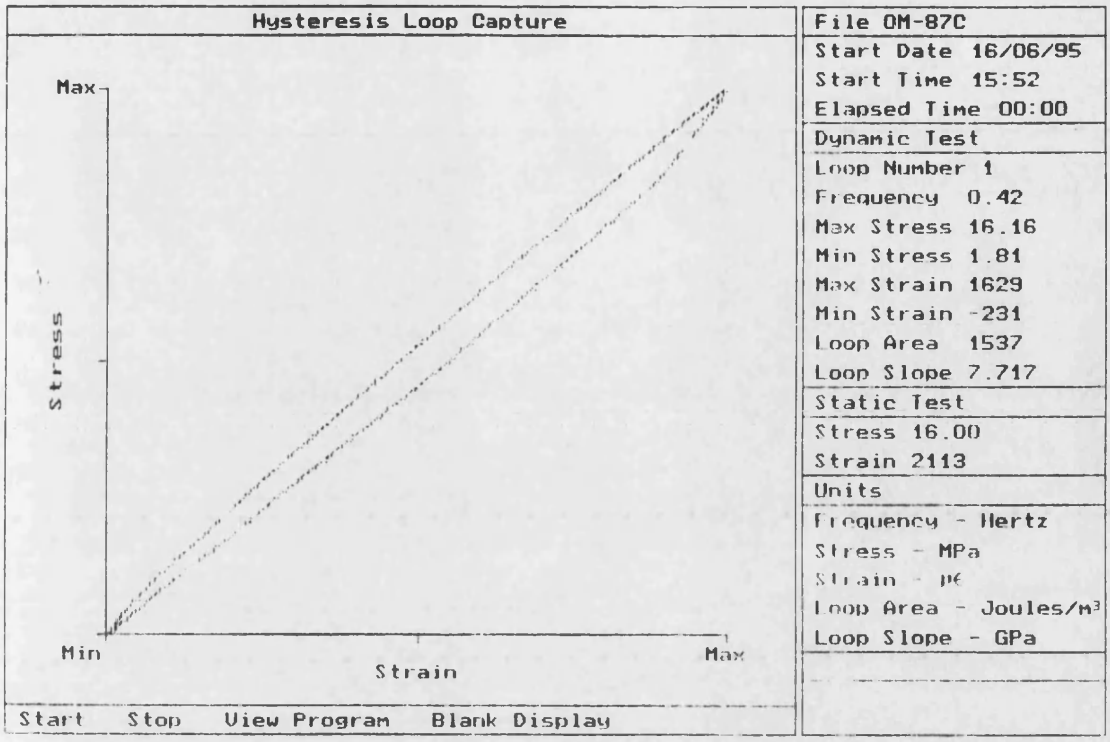

Fig 10.7 Hysteresis loop captured for medium frequency loading of OSB at the 60% stress level, at R=0.1.

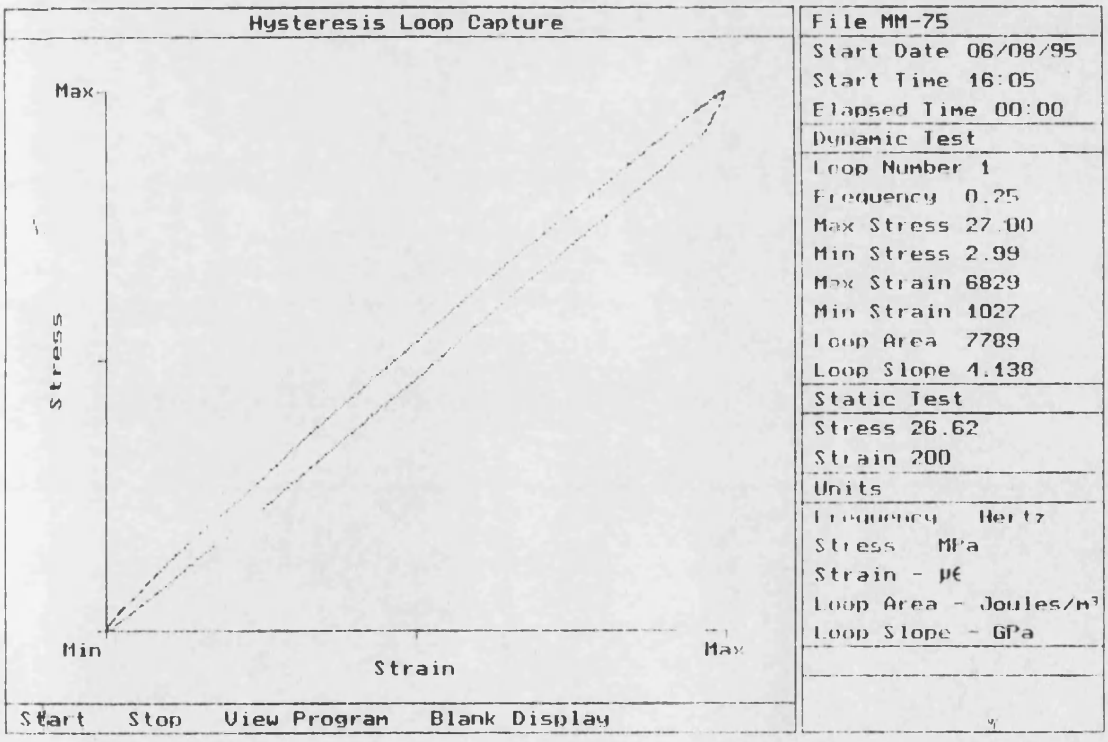

Fig 10.8 Hysteresis loop captured for medium frequency loading of MDF at the 60% stress level, at R=0.1.

10.4 Creep and Fatigue Deflections

The maximum and minimum fatigue microstrains for the fatigue samples, and the creep microstrains for the side-matched creep partners were recorded during OSB and MDF tests exactly as for the medium frequency testing of the chipboard (see chapter 6 and section 8.6). Once again the first and last captured loops do not correspond with the very first and the very last loading cycles. For OSB and MDF the first loop was captured after four to ten loading cycles, for chipboard loaded at medium frequency this was after thirty to sixty loading cycles. The last loop captures were again subject to the restraints explained in section 8.6 which result in the tertiary stage of deflection in fatigue and creep rarely being recorded.

For OSB and MDF tested at medium frequency, at R=0.1, six samples of each material were tested at the 80, 70, 60 and 50% stress levels. One sample was tested at the 40% stress level for MDF and for both materials one sample was tested at the 20% stress level. At these low stress levels replicates were not tested because the samples were runouts and did not fail, so further tests would have required excessive machine time.

Figures 10.9a-c, 10.10a-c and 10.11a-c show the median initial, median final and median changes in the microstrains for OSB, chipboard and MDF, plotted with respect to stress level, reducing from 80% to 20%. Figures 10.9a-c show the median microstrain trends for the samples loaded in creep. Figures 10.10a-c show the median maximum microstrains for the fatigue loaded samples, with the peak stress applied to the sample and figures 10.11a-c show the median minimum microstrains for the fatigue loaded samples, with 10% of the peak stress applied to the sample.

Table 10.5 shows the median values for the initial, final and change in microstrain for the creep samples, and the maximum and minimum initial, final and change in microstrain for the fatigue samples for OSB, chipboard and MDF. The ranges of values for the initial and final microstrains for the fatigue and creep samples are shown in table 10.6 providing an indication of the spread of the data.

Figures 10.12a-e and 10.13a-f show the three microstrains plotted as a function of time, for representative tests performed at each stress level for OSB and MDF respectively. The figures for OSB have been plotted with Y axes showing microstrain from 0 to 6000 while those for MDF are from 0 to 12000. This allows the creep, maximum fatigue and minimum fatigue microstrains to be compared between samples at all the stress levels tested for each material. Figures 8.13a-f, in section 8.6 show the equivalent plots for chipboard.

Fig 10.9a

MEDIAN INITIAL CREEP MICROSTRAIN
OSB, CHIPBOARD & MDF, R=0.1 MED. FREQ.

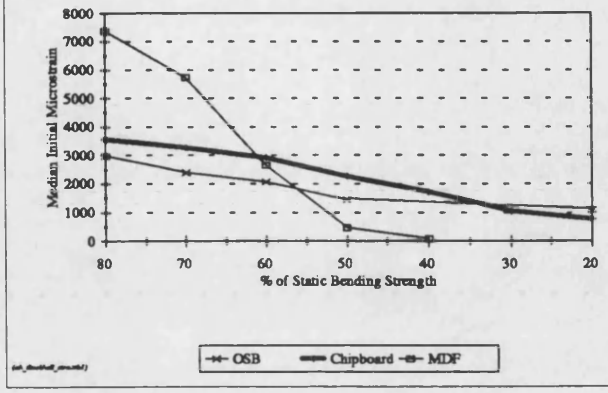

Fig 10.9b

MEDIAN FINAL CREEP MICROSTRAIN
OSB, CHIPBOARD & MDF, R=0.1 MED. FREQ.

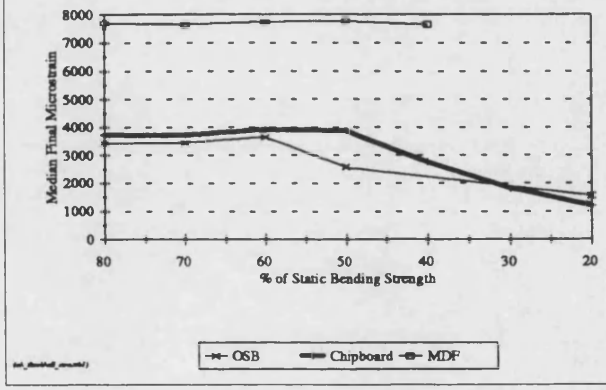

Fig 10.9c

MEDIAN CREEP MICROSTRAIN CHANGE
OSB, CHIPBOARD & MDF, R=0.1 MED. FREQ.

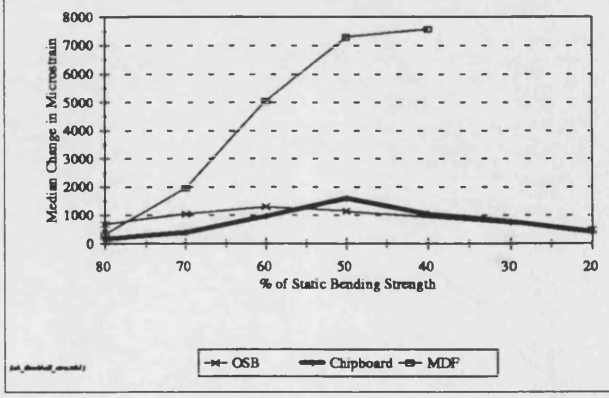

Fig 10.10a MEDIAN INITIAL MAX FATIGUE MICROSTRAIN
OSB, CHIPBOARD & MDF, R=0.1 MED. FREQ.

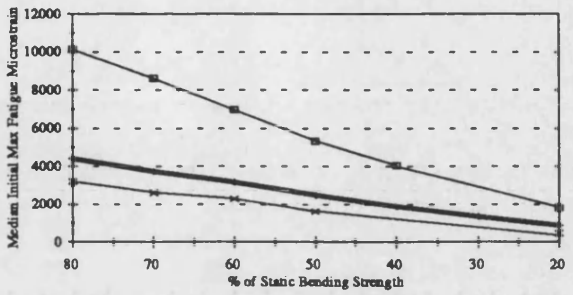

Fig 10.10b MEDIAN FINAL MAX FATIGUE MICROSTRAIN
OSB, CHIPBOARD & MDF, R=0.1 MED. FREQ.

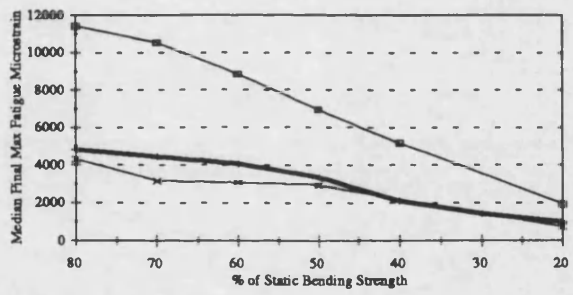

Fig 10.10c MEDIAN CHANGE, MAX FATIGUE MICROSTRAIN
OSB, CHIPBOARD & MDF, R=0.1 MED.FREQ.

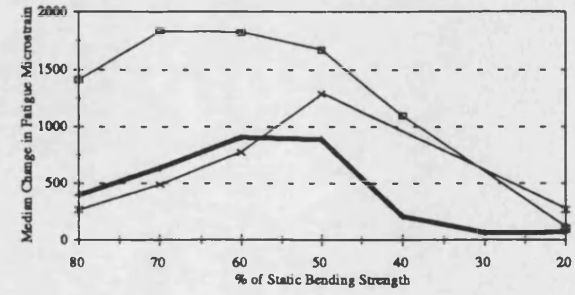

Fig 10.11a MEDIAN INITIAL MIN FATIGUE MICROSTRAIN
CHIPBOARD, OSB & MDF, R=0.1 MED. FREQ.

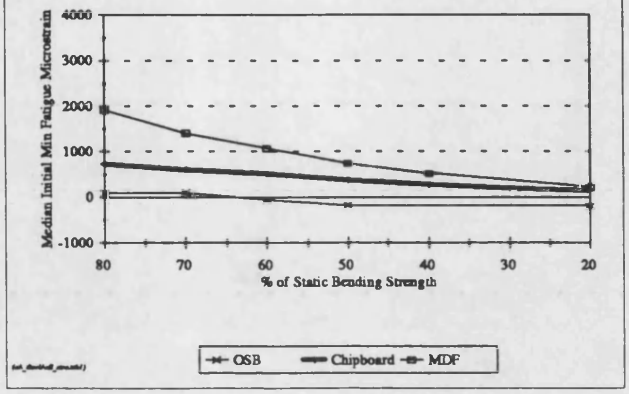

Fig 10.11b MEDIAN FINAL MIN FATIGUE MICROSTRAIN
OSB, CHIPBOARD & MDF, R=0.1 MED. FREQ.

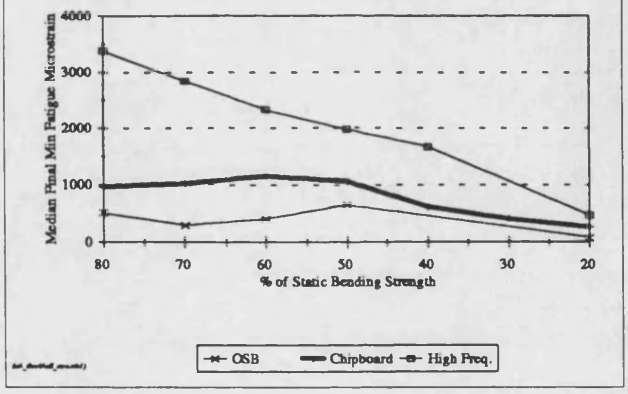

Fig 10.11c MEDIAN CHANGE, MIN FATIGUE MICROSTRAIN
OSB, CHIPBOARD & MDF, R=0.1 MED. FREQ.

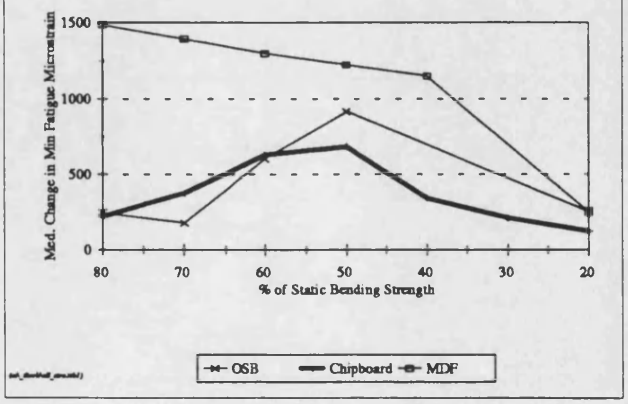

Table 10.5 Median creep and fatigue microstrains for OSB, chipboard and MDF tested at R=0.1, at medium frequency.

Stress Level	Initial Median Creep Microstrain	Final Median Creep Microstain	Median Change in Creep Microstrain	Initial Median Max Fatigue Microstrain	Final Median Max Fatigue Microstrain	Median Change in Max Fatigue Microstrain	Initial Median Min Fatigue Microstrain	Final Median Min Fatigue Microstrain	Median Change in Min Fatigue Microstrain
OSB, Medium Frequency, R=0.1									
80%	2990	3477	686	3207	4312	267	93	511	248
70%	2399	3432	1034	2627	3174	489	99	293	177
60%	2075	3642	1294	2303	3074	774	-58	407	601
50%	1441	2591	1148	1623	2961	1288	-174	656	916
20%	1079	1546	467	465	734	269	-195	65	260
Chipboard, Medium Frequency, R=0.1									
80%	3573	3729	168	4405	4840	393	736	972	221
70%	3284	3706	392	3746	4471	635	605	1018	374
60%	2926	3913	960	3177	4078	904	518	1158	626
50%	2285	3867	1593	2490	3379	890	384	1064	684
40%	1725	2775	1050	1898	2109	211	273	617	344
30%	1061	1821	760	1367	1429	62	201	411	210
20%	775	1188	413	901	971	70	139	264	125
MDF, Medium Frequency, R=0.1									
80%	7374	7698	324	10147	11440	1410	1915	3381	1487
70%	5735	7648	1956	8633	10534	1831	1409	2843	1395
60%	2653	7740	5044	6976	8859	1821	1078	2328	1298
50%	466	7777	7284	5349	6946	1670	746	1972	1225
40%	98	7661	7563	4071	5168	1097	517	1668	1151
20%	-15	1249	1264	1802	1911	109	225	473	248

Table 10.6 The range of creep microstrains, and fatigue microstrains for OSB, chipboard and MDF loaded at medium frequency, at R=0.1.

Stress Level	Initial Creep Microstrain	Final Creep Microstrain	Initial Maximum Fatigue Microstrain	Final Maximum Fatigue Microstrain	Initial Minimum Fatigue Microstrain	Final Minimum Fatigue Microstrain
OSB, MEDIUM FREQUENCY, R=0.1						
80%	2167-3336	2734-3942	1891-4134	2158-5298	(-235)-393	(-113)-1134
70%	1513-3429	2438-4033	2309-3174	2407-3368	50-172	(-82)-328
60%	1759-3038	2053-4289	1629-3587	2403-3743	(-231)-(-32)	276-563
50%	655-1869	1803-4012	1144-1732	1931-3929	(-364)-(-48)	186-1102
20%	1079	1546	465	734	-195	65
CHIPBOARD, MEDIUM FREQUENCY, R=0.1						
80%	3392-3580	3535-3786	4032-4816	4311-5321	660-815	792-1103
70%	2796-3640	3676-3904	3402-4032	3830-4708	539-784	800-1188
60%	2585-3215	3644-3919	3014-3281	3698-4443	455-613	955-1320
50%	2023-2796	3768-3928	2416-2531	3099-3635	310-450	929-1328
40%	1725	2775	1898	2109	273	617
30%	1061	1821	1367	1429	201	411
20%	775	1188	901	971	139	264
MDF, MEDIUM FREQUENCY, R=0.1						
80%	7151-7597	7568-7827	9602-10946	11372-11851	1753-2291	3039-3878
70%	4637-5974	7231-7769	8173-8789	9315-11046	1382-1531	2276-3345
60%	3066-3081	7525-7807	6673-7416	8437-9232	994-1166	2279-2557
50%	380-667	7030-7896	5267-5485	6526-7540	699-780	1615-2101
40%	98	7661	4071	5168	517	1668
20%	-15	1249	1802	1911	225	473

Fig 10.12a

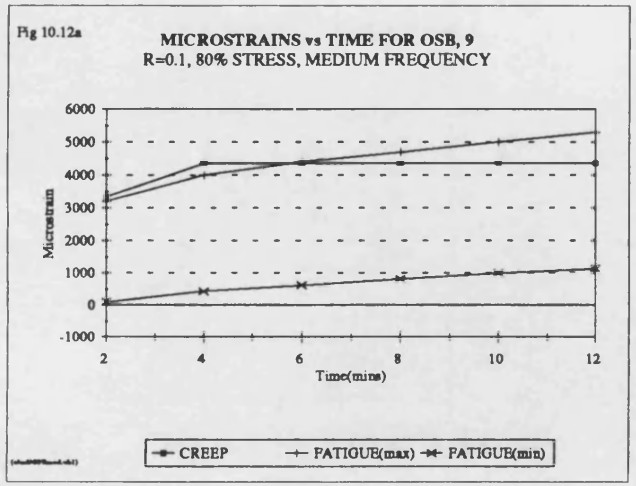

Fig 10.12b

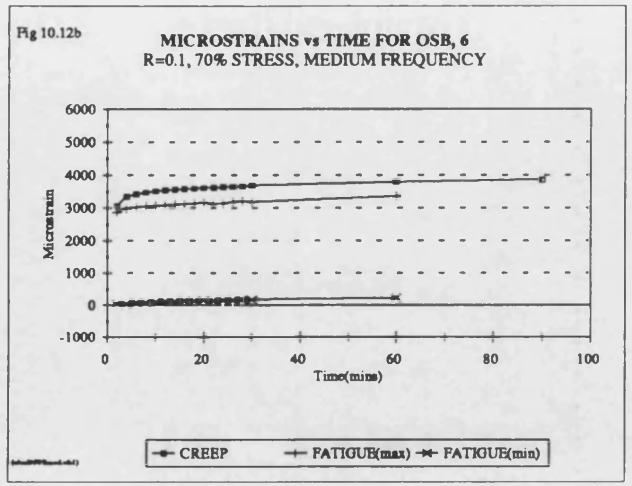

Fig 10.12c

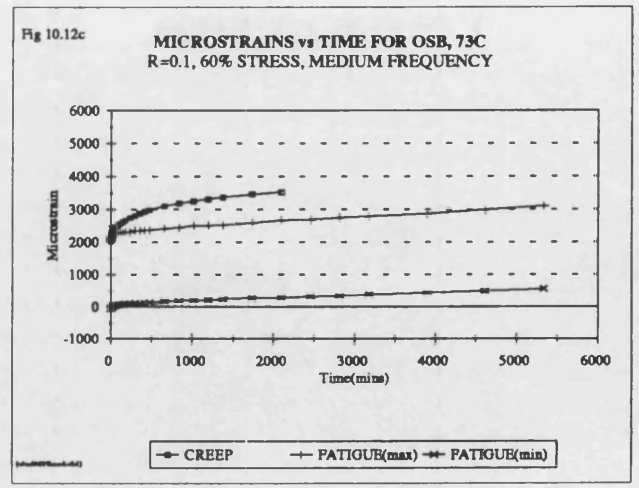

Fig 10.12d

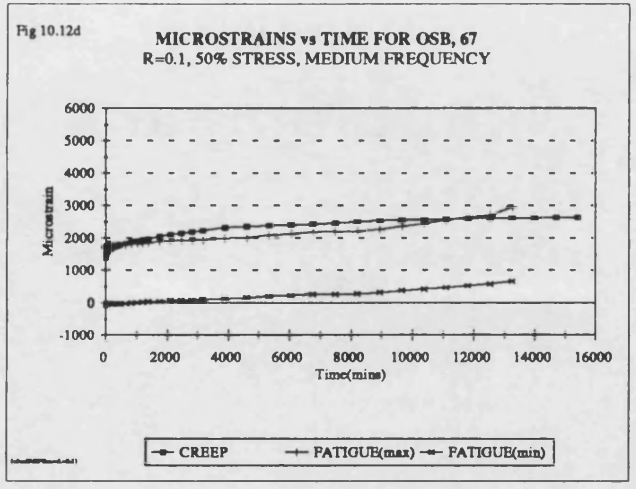

Fig 10.12e

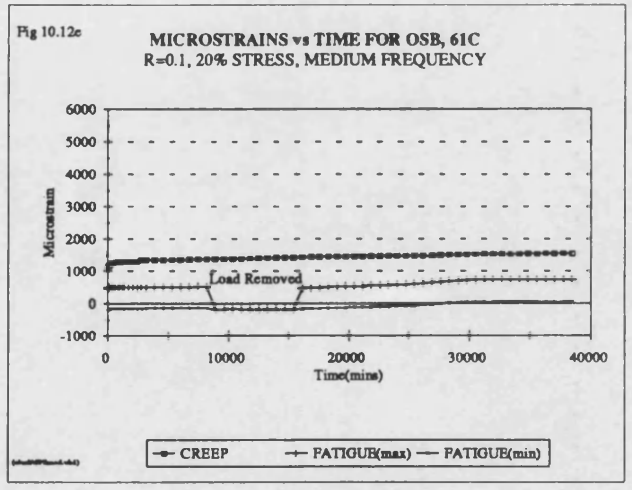

Fig 10.13a

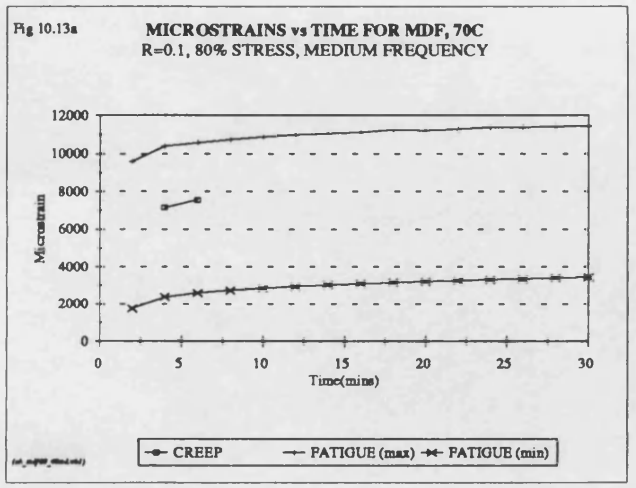

Fig 10.13b

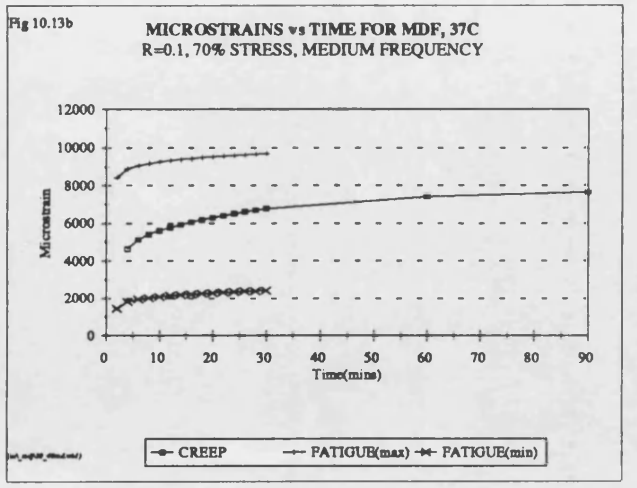

Fig 10.13c

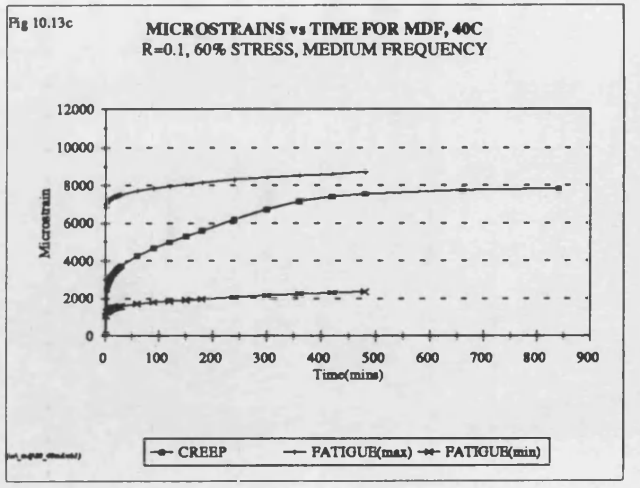

Fig 10.13d

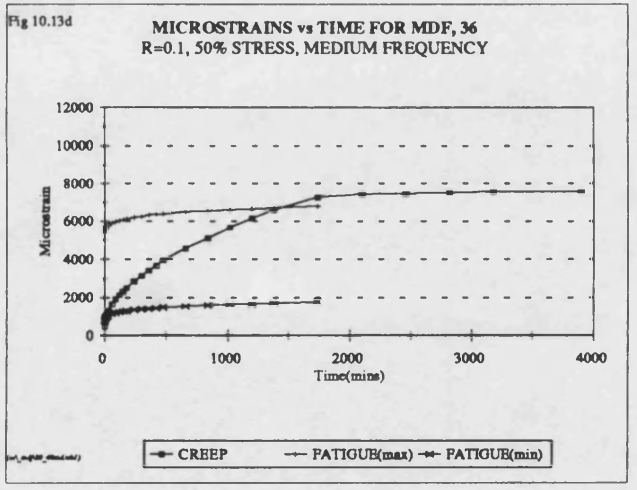

Fig 10.13e

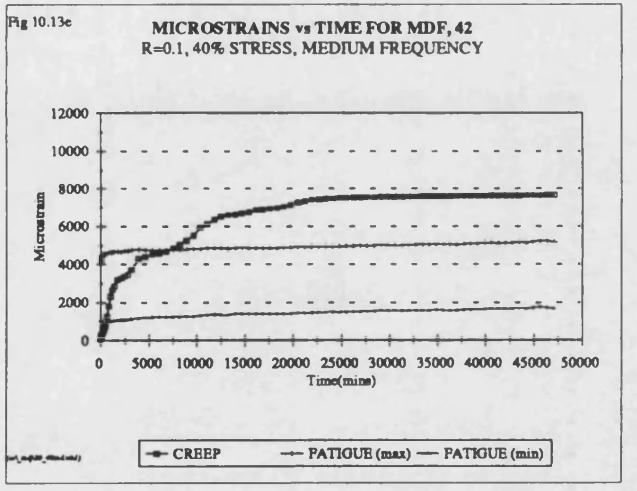

Fig 10.13f

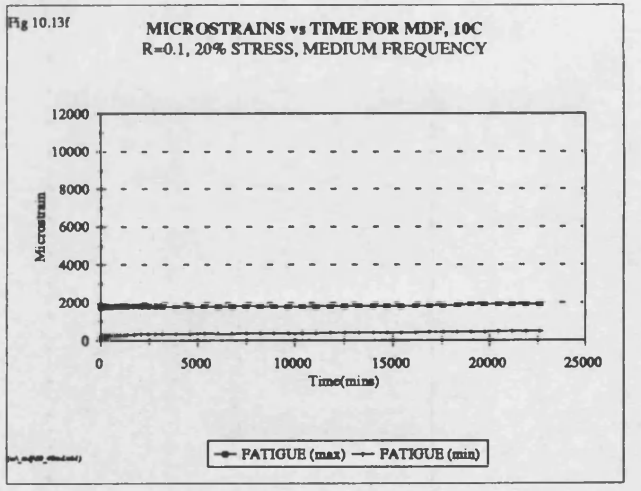

Discussion

In figures 10.9a-c the changes in the microstrains for the creep loaded samples with respect to reducing level of applied stress are compared for the OSB, chipboard and MDF. In all three plots the values and trends for OSB and chipboard are very similar but are different to those for MDF. One reason for this is that the MDF tested was considerably stronger than the OSB and chipboard, so the equivalent percentage stress levels for MDF are at considerably higher stresses. In addition the constituent particles in the MDF are fibres which are smaller than the particles in OSB and chipboard. It is generally accepted (Dinwoodie and Bonfield 1995) that the smaller the constituent particles, the more susceptible the wood based panel is to creep. It is plausible that the magnitude of the deflections is dependent upon particle size because the values for OSB are generally slightly lower than those for chipboard. This agrees with the literature in that there is an increased propensity to creep as the particle size is reduced. The initial creep microstrains, figure 10.9a, reduce in magnitude with reducing stress level for all three materials, with those for MDF decreasing to a greater extent. This shows that decreasing the loads applied to both materials reduces the resulting instantaneous deflections. The final creep microstrains, figure 10.9b, are almost constant from the 80%, down to the 50% stress level and then decrease down to the 20% stress level. None of the samples tested at below the 50% stress level had failed so this implies that, within the duration of the tests performed, the creep failure point for panel products occurs at a critical strain which is dependent upon the material. The critical strain is the transition between the gradual second stage of deflection and the final rapid stage leading to failure. The transition occurs at roughly 0.4% strain for OSB and chipboard, and at roughly 0.75% strain for MDF. The decrease below the 50% stress level is purely because none of these samples had failed by the end of testing. The creep curve for MDF loaded at 20% stress is missing because there was a fault with the transducer and no data was captured.

The changes in the creep microstrains, figure 10.9c, are a reflection of the initial microstrain values. The most important feature is that there are only very small increases in the creep microstrains at the lowest stress levels for OSB and chipboard, i.e. approaching design stresses. However, the deflection for MDF were still large at the 40% stress level and the MDF deflections were generally far greater than for the other two materials. This presents a misleading impression for the MDF, again this is because the data has been normalised by using percentage stress levels. The mean bending strength of the MDF was more than twice that for the chipboard. If the microstrains for MDF loaded at the 30% stress level are compared to those for chipboard loaded at the 60% stress level the resulting deflections are very similar. This

means that the performance of two materials is very similar but that chipboard fails at a considerably lower stains. This view will be consolidated when the dynamic and fatigue moduli are discussed in sections 10.5 and 10.6 respectively.

The plots for the maximum fatigue microstrains, figures 10.10a-c, show similar trends to those for the creep samples. Again there is a negative correlation between particle size and the initial microstrains for all three materials, figure 10.10a. This is also true for the final maximum fatigue microstrains, figure 10.10b. The initial and final microstrains for all three materials decrease with decreasing stress level from 80% down to 20%. As for the creep samples the magnitude of the deflections for MDF loaded in fatigue are considerably greater than for OSB and chipboard. Also the extent of the decrease is greater for MDF than for OSB and chipboard. This agrees with the fatigue lives shown in the S-N plot for the three materials, figure 10.3 in section 10.1. The change in the maximum fatigue microstrains was very similar for OSB and chipboard but that for MDF was considerably greater although the difference decreased as the stress level was reduced. Once again this shows that decreasing the applied load reduces the resulting deflection. However, it must again be considered that the primary reason for the MDF samples deflecting twice a much as the other two materials is because twice the load has been applied. The changes in the maximum fatigue microstrains, figure 10.10c, are very small at the lowest stress levels as were the creep microstrains. This implies that at design stress levels there is virtually no difference between the three materials. However, this would require verification by testing a suitable population of samples at low stress levels which would be time consuming and expensive.

The plots showing the minimum fatigue microstrains with respect to reducing level of stressing, for the three materials, figures 10.11a-c, show essentially the same features as figures 10.10a-c for the maximum fatigue microstrains. Although the microstrain values are lower.

OSB does not have a uniform surface, unlike chipboard and MDF. This introduces a large possibility for error when measuring the centre point deflections. This was not a problem for all the OSB samples tested but does account for any sudden drastic changes in values caused by the transducer probe moving off the edge of a wood chip. There is also a possibility of the OSB wood chip that the transducer probe is contacting bowing out from the surface, since it is on the compressive side of the sample, producing an unrealistic reduction in the measured microstrain. The problem of the uneven surface of the OSB samples is highlighted by the values for the initial

fatigue microstrains in tables 10.5 and 10.6. Both tables show negative values for the initial fatigue microstrains. These values should be positive and of the order of 0 to 1000 depending upon the stress level. Due to their uneven surfaces the OSB samples do not lie completely flat on the lower rollers until the load is applied and so all the microstrain values are between 0 and 1000 lower than they should be. Also, the OSB data was too varied to justify looking at whether the fatigue or the creep sample failed first since it is not known with any degree of confidence whether they were initially loaded at the same stress level or not. This disrupts the negative correlation between particle size and deflection but the material with the smallest particles still demonstrated by far the greatest deflections relative to its own strength, so the correlation is still loosely appropriate.

The representative graphs, for all the stress levels tested for OSB, figures 10.12a-e, are enclosed but will not be discussed at length, since they are subject to all the errors detailed above. However, because the median values shown in table 10.5 and plotted in figures 10.9a-c, 10.10a-c and 10.11a-c eliminate the effects of any extreme values they can be considered as representative values for OSB. These values must still be considered as providing general trends, not as exact numbers. The problems encountered with OSB show that the measurement of true centre point deflection is possibly not the best method of measuring the strains for OSB, at least not for samples of the dimensions tested in this research. However, if strain gauges were used as an alternative method of strain measurement these would also be subject to similar errors.

The equivalent plots for chipboard tested at medium frequency are figures 8.13a-f in section 8.6 and these are discussed in that section. Figures 10.13a-f are representative plots for MDF at each of the stress levels tested. There is a vast difference between the time axes since they are a measure of the life of the samples. For MDF sample life has already been considered in the S-N results in section 10.1.

In all six MDF tests at the 80% stress level, represented by figure 10.13a, the fatigue sample failed after the creep sample. However, the maximum fatigue microstrain was always significantly greater than the creep microstrain, when the creep sample survived long enough for it to be captured. This is the same as was observed for the chipboard. At the 70% stress level, represented by figure 10.13b, the maximum fatigue microstrain was above the creep microstrain for the duration of all six tests. However, the fatigue sample failed after the creep sample in four out of the six tests. This is again similar to the results for chipboard although the magnitude of the differences between the fatigue and creep microstrains was greater for MDF.

With the stress level reduced to 60%, represented by figure 10.13c the creep microstrain begins at values much lower than the fatigue microstrain but increases at a greater rate becoming very close to the maximum fatigue microstrain. This was the case for all six of the tests at this stress level although the fatigue sample failed first in five out of the six tests. At this stress level for the chipboard the creep microstrains exceeded the maximum fatigue microstrains in some cases indicating that the differences between cyclic and creep loading is greater for MDF than for chipboard.

At the 50% stress level, represented by figure 10.13d, the creep microstrain begins considerably lower than the fatigue microstrain but increases rapidly in comparison to the maximum fatigue microstrain and exceeds it. This occurred in all six of the tests at this stress level. Although the strain in the creep samples was greater than for the fatigue samples, none of the six creep samples failed but all of the fatigue samples failed. This agrees with the observation for chipboard made by Thompson *et al* (1994) that at all but the highest stress levels it is the static component of the load that produces the deflection but the cyclic component is more damaging and causes sample failure. However, the deflections of the MDF creep samples are excessive compared to OSB and chipboard. When removed from the creep rig the MDF samples were severely deformed and were "banana shaped" in appearance. Although this does not account for the higher loading of the MDF samples.

At the lowest stress levels of 40 and 20%, represented by figures 10.13e and 10.13f the trend continues. The creep microstrain at the 40% stress level begins below the maximum fatigue microstrain but rapidly exceeds it and then levels off at a considerably higher value than the maximum fatigue microstrain. As mentioned previously, the microstrain curve for the 20% stress level test was not captured. At the 40 and 20% stress levels the maximum fatigue microstrain curves are flatter following the initial elastic deflection. Fatigue deformation is slow but not non existent, as it was for chipboard. So if there is a fatigue limit for MDF it would be at a lower stress level than that for chipboard and probably OSB. This agrees with the steeper fitted regression line in the S-N plot for MDF in section 10.1.

In general the creep and fatigue microstrains reduce in magnitude as the stress level is reduced, as for chipboard. Also the maximum fatigue microstrain curves flatten out with reducing stress level as less deformation is taking place. The creep samples fail first at the highest stress level only but the fatigue loading is more damaging than creep loading down to approximately 50% stress where the fatigue cycling produces significantly less deformation than the creep loading. The results are very similar to

those for chipboard but the magnitude of the microstrains for MDF are far greater, as are the differences between loading in creep and fatigue.

10.5 Dynamic Moduli

The dynamic moduli were measured for the OSB and MDF samples during fatigue testing as for chipboard. These measurements were determined from the same loop captures as the microstrains values and are subject to the same limitations on the first and last measurements. The number of data points at each stress level is also the same as for the microstrain values (see section 10.4).

Figures 10.14a-c show the median initial, median final and median changes in the dynamic moduli with respect to reducing stress level for OSB, chipboard and MDF. The data plotted in these figures is displayed in table 10.7 which also includes the range of initial and final moduli measured for the different samples tested at each stress level to provide an indication of the variability.

Figures 10.15a-e and 10.17a-f show the dynamic moduli as a function of time for OSB and MDF respectively, for all the samples tested at the 80, 70, 60, 50, 40 and 20% stress levels, tested at R=0.1, at medium frequency. Time is plotted on the X axis and once again varies greatly because it represents the duration of the tests. These figures have also been plotted with respect to factored time and are included as figures 10.16a-e and 10.18a-f for OSB and MDF respectively. All the graphs for OSB have been plotted with dynamic moduli ranging from 0-10 GPa on the Y axis while for MDF this was plotted from 0-6 GPa.

Equivalent plots for the dynamic moduli of chipboard loaded at R=0.1, at medium frequency were included as figures 8.19a-e and 8.20a-e in section 8.7.

Fig 10.14a

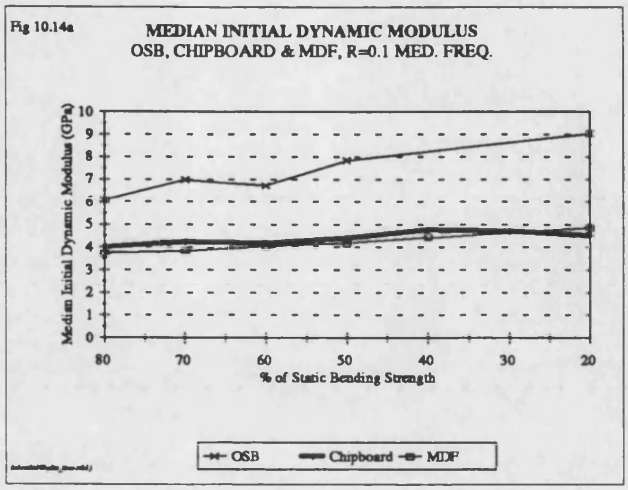

Fig 10.14b

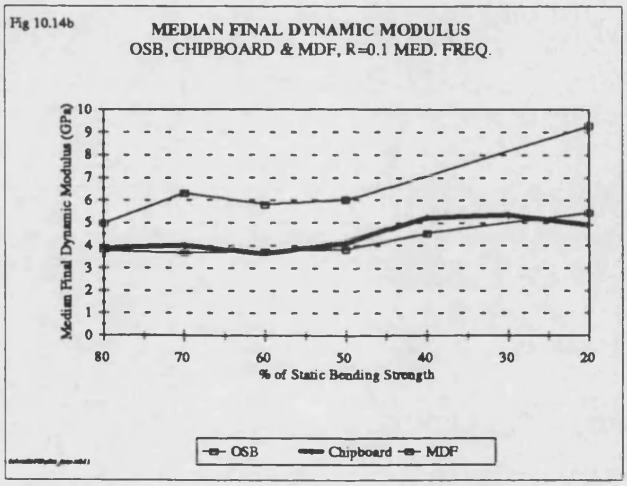

Fig 10.14c

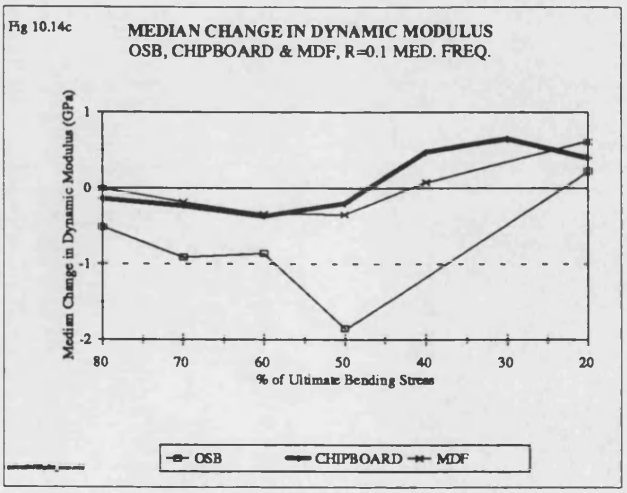

Table 10.7 Median dynamic moduli for OSB, chipboard and MDF tested at R=0.1, at medium frequency.

Stress Level	Median Initial Dynamic Modulus GPa	Median Final Dynamic Modulus GPa	Median Change in Dynamic Modulus GPa	Range of Initial Dynamic Moduli GPa	Range of Final Dynamic Moduli GPa	Range of Change in Dynamic Modulus GPa
OSB, Medium Frequency, R=0.1						
80%	6.06	4.97	-0.51	5.17-8.33	4.55-7.84	0.49-1.52
70%	6.97	6.31	-0.91	6.63-8.98	5.95-8.07	0.65-1.13
60%	6.71	5.81	-0.86	4.63-7.94	5.48-7.22	0.49-2.13
50%	7.84	6.00	-1.85	7.49-8.38	5.07-7.57	0.54-2.60
20%	9.05	9.28	+0.23	1 Sample	1 Sample	1 Sample
Chipboard, Medium Frequency, R=0.1						
80%	4.02	3.89	-0.14	3.59-4.84	3.50-4.43	(-0.09)-(-0.15)
70%	4.23	4.01	-0.23	3.51-4.87	3.29-4.43	(-0.17)-(-0.44)
60%	4.18	3.65	-0.37	3.61-4.86	3.26-4.55	(-0.27)-(-0.65)
50%	4.41	4.13	-0.20	3.90-4.87	3.58-4.64	(-0.13)-(-0.42)
40%	4.76	5.23	+0.47	1 Sample	1 Sample	1 Sample
30%	4.71	5.36	+0.65	1 Sample	1 Sample	1 Sample
20%	4.53	4.93	+0.40	1 Sample	1 Sample	1 Sample
MDF, Medium Frequency, R=0.1						
80%	3.73	3.77	0	3.59-4.09	3.64-4.13	(-0.08)-(+0.16)
70%	3.84	3.68	-0.18	3.74-4.13	3.53-3.93	(-0.12)-(-0.22)
60%	4.04	3.75	-0.34	3.83-4.45	3.52-4.14	(-0.20)-(-0.41)
50%	4.18	3.85	-0.35	4.11-4.59	3.64-4.18	(-0.22)-(-0.55)
40%	4.45	4.53	+0.08	1 Sample	1 Sample	1 Sample
20%	4.84	5.45	+0.61	1 Sample	1 Sample	1 Sample

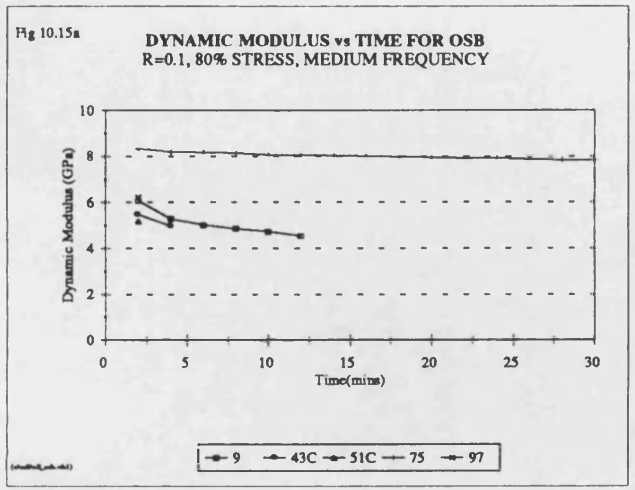
Fig 10.15a
DYNAMIC MODULUS vs TIME FOR OSB
R=0.1, 80% STRESS, MEDIUM FREQUENCY
Dynamic Modulus (GPa)
Time(mins)
9
43C
51C
75
97

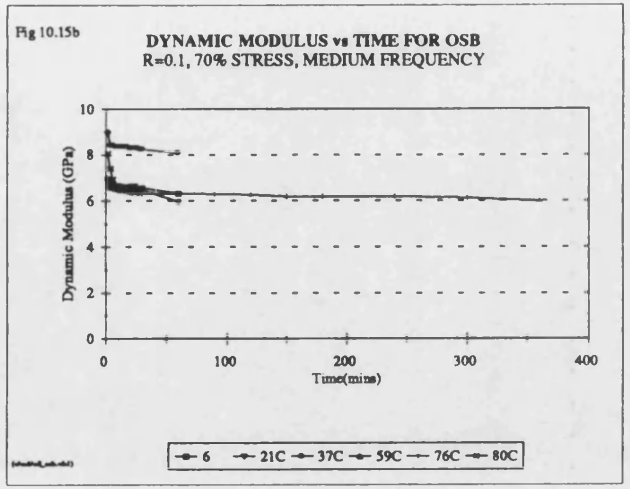
Fig 10.15b
DYNAMIC MODULUS vs TIME FOR OSB
R=0.1, 70% STRESS, MEDIUM FREQUENCY
Dynamic Modulus (GPa)
Time(mins)
6
21C
37C
59C
76C
80C

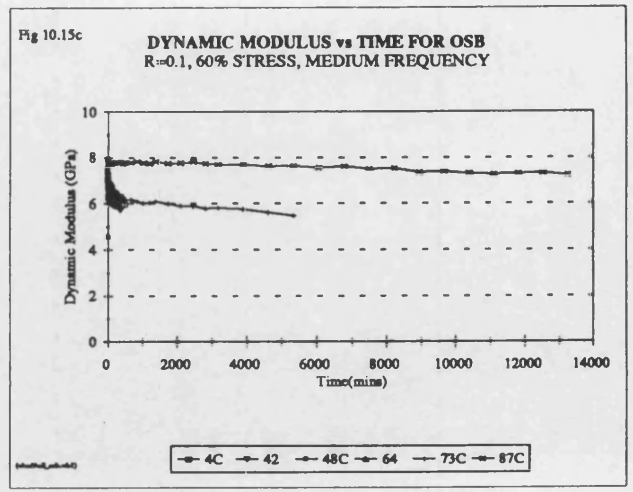
Fig 10.15c
DYNAMIC MODULUS vs TIME FOR OSB
R=0.1, 60% STRESS, MEDIUM FREQUENCY
Dynamic Modulus (GPa)
Time(mins)
4C
42
48C
64
73C
87C

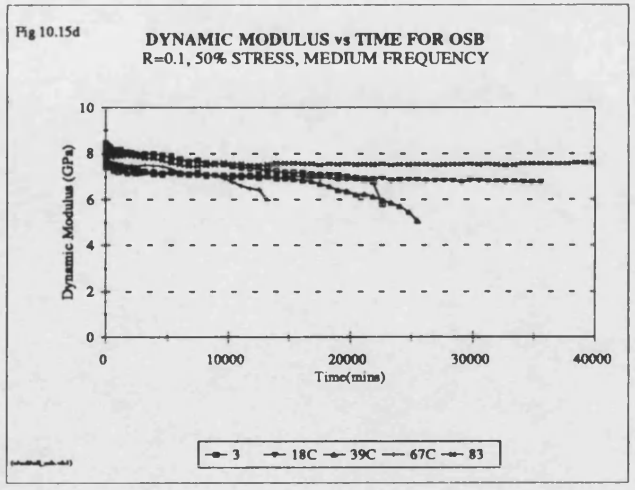
Fig 10.15d
DYNAMIC MODULUS vs TIME FOR OSB
R=0.1, 50% STRESS, MEDIUM FREQUENCY
Dynamic Modulus (GPa)
Time(mins)
3
18C
39C
67C
83

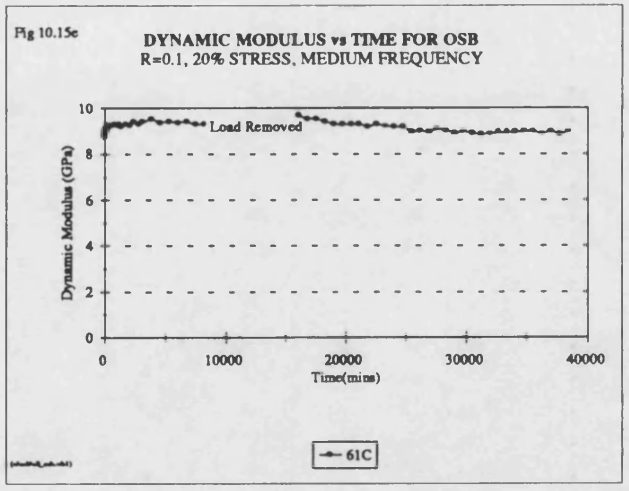
Fig 10.15e
DYNAMIC MODULUS vs TIME FOR OSB
R=0.1, 20% STRESS, MEDIUM FREQUENCY
Load Removed
Dynamic Modulus (GPa)
Time(mins)
61C

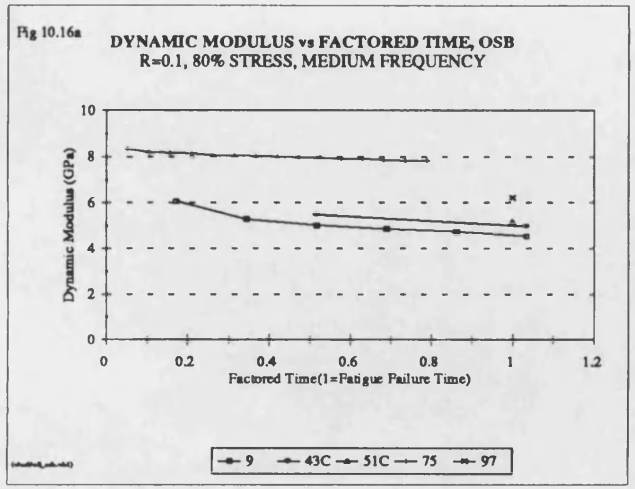
Fig 10.16a
DYNAMIC MODULUS vs FACTORED TIME, OSB
R=0.1, 80% STRESS, MEDIUM FREQUENCY
Dynamic Modulus (GPa)
Factored Time(1=Patigue Failure Time)
9
43C
51C
75
97

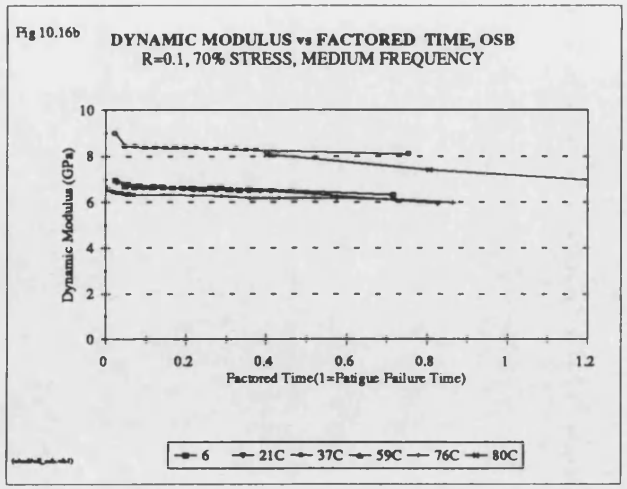
Fig 10.16b
DYNAMIC MODULUS vs FACTORED TIME, OSB
R=0.1, 70% STRESS, MEDIUM FREQUENCY
Dynamic Modulus (GPa)
Factored Time(1=Patigue Failure Time)
6
21C
37C
59C
76C
80C

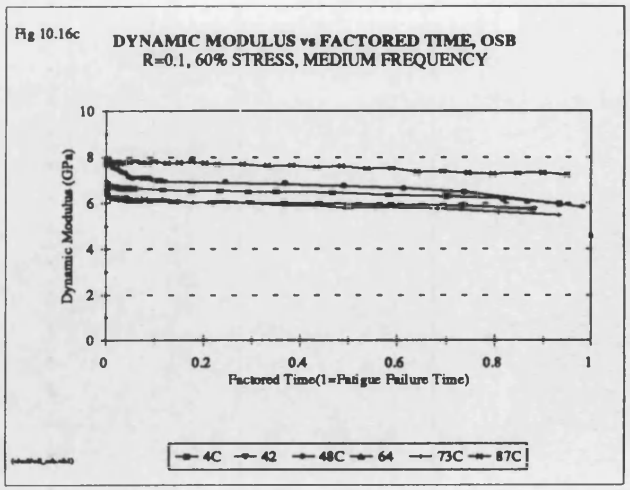
Fig 10.16c
DYNAMIC MODULUS vs FACTORED TIME, OSB
R=0.1, 60% STRESS, MEDIUM FREQUENCY
Dynamic Modulus (GPa)
Factored Time(1=Patigue Failure Time)
4C
42
48C
64
73C
87C

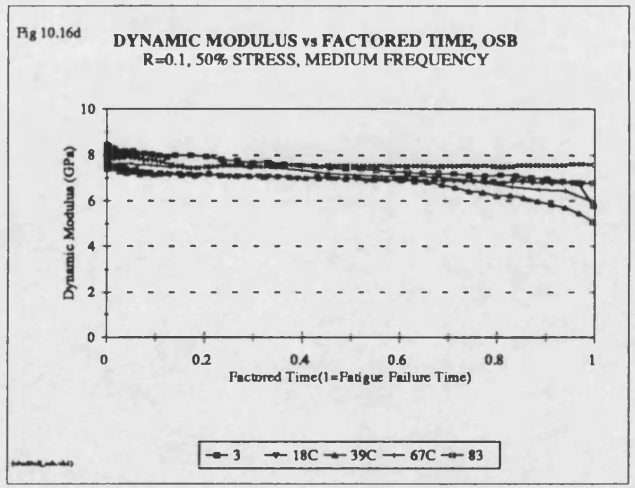
Fig 10.16d
DYNAMIC MODULUS vs FACTORED TIME, OSB
R=0.1, 50% STRESS, MEDIUM FREQUENCY
Dynamic Modulus (GPa)
Factored Time(1=Patigue Failure Time)
3
18C
39C
67C
83

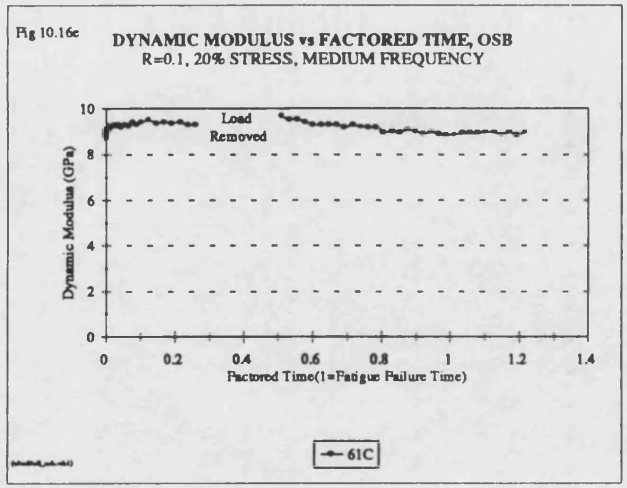
Fig 10.16e
DYNAMIC MODULUS vs FACTORED TIME, OSB
R=0.1, 20% STRESS, MEDIUM FREQUENCY
Load
Removed
Dynamic Modulus (GPa)
Factored Time(1=Patigue Failure Time)
61C

Fig 10.17a

DYNAMIC MODULUS vs TIME FOR MDF
R=0.1, 80% STRESS, MEDIUM FREQUENCY

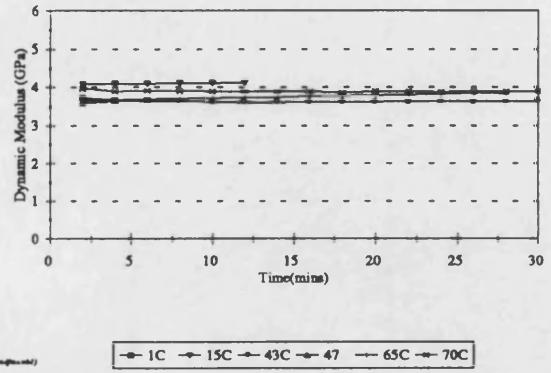

Fig 10.17b

DYNAMIC MODULUS vs TIME FOR MDF
R=0.1, 70% STRESS, MEDIUM FREQUENCY

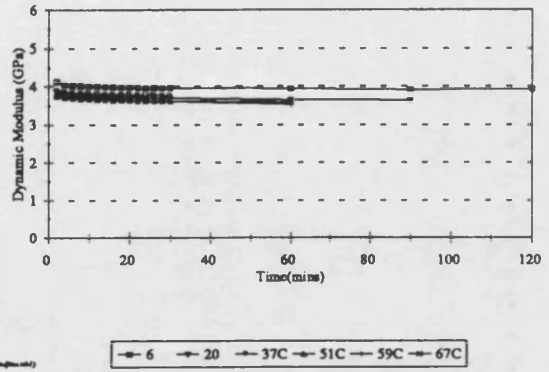

Fig 10.17c

DYNAMIC MODULUS vs TIME FOR MDF
R=0.1, 60% STRESS, MEDIUM FREQUENCY

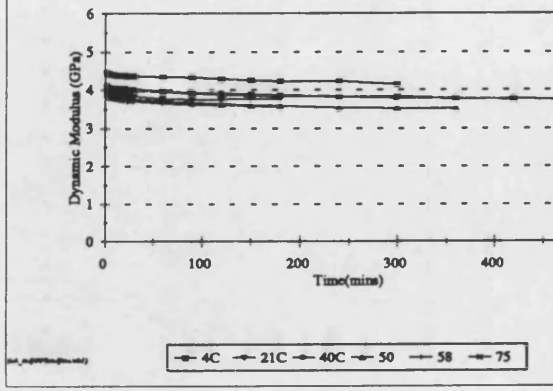

Fig 10.17d

DYNAMIC MODULUS vs TIME FOR MDF
R=0.1, 50% STRESS, MEDIUM FREQUENCY

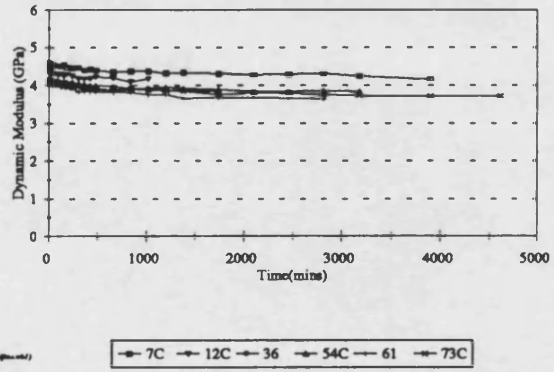

Fig 10.17e

DYNAMIC MODULUS vs TIME FOR MDF
R=0.1, 40% STRESS, MEDIUM FREQUENCY

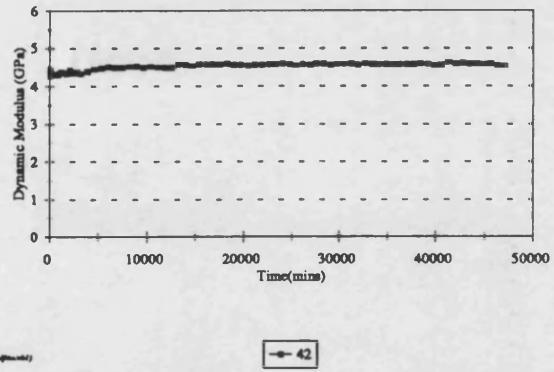

Fig 10.17f

DYNAMIC MODULUS vs TIME FOR MDF
R=0.1, 20% STRESS, MEDIUM FREQUENCY

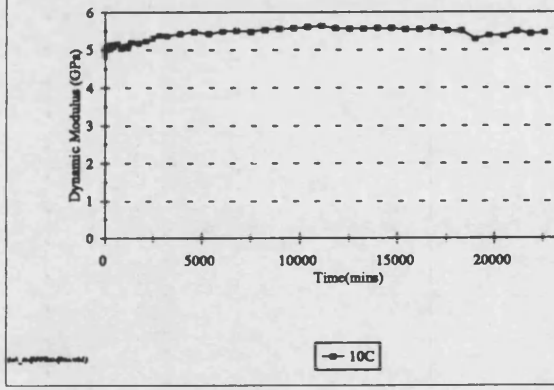

Fig 10.18a DYNAMIC MODULUS vs FACTORED TIME, MDF
R=0.1, 80% STRESS, MEDIUM FREQUENCY

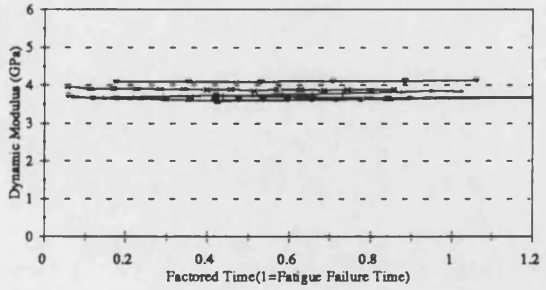

Fig 10.18b DYNAMIC MODULUS vs FACTORED TIME, MDF
R=0.1, 70% STRESS, MEDIUM FREQUENCY

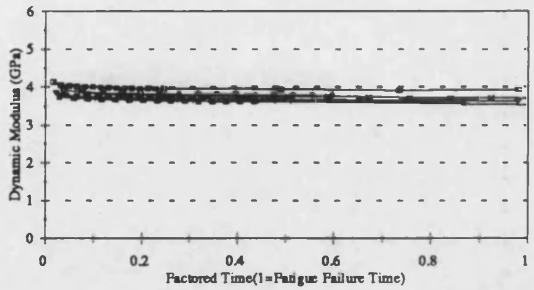

Fig 10.18c DYNAMIC MODULUS vs FACTORED TIME, MDF
R=0.1, 60% STRESS, MEDIUM FREQUENCY

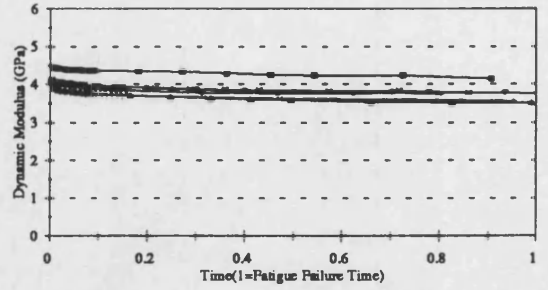

Fig 10.18d DYNAMIC MODULUS vs FACTORED TIME, MDF
R=0.1, 50% STRESS, MEDIUM FREQUENCY

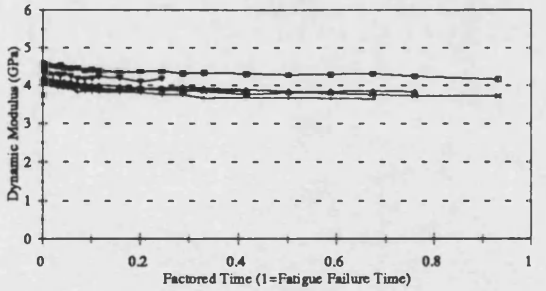

Fig 10.18e DYNAMIC MODULUS vs FACTORED TIME, MDF
R=0.1, 40% STRESS, MEDIUM FREQUENCY

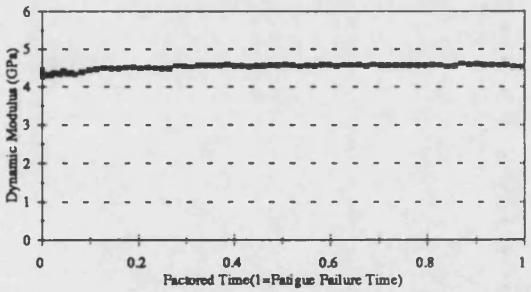

Fig 10.18f DYNAMIC MODULUS vs FACTORED TIME, MDF
R=0.1, 20% STRESS, MEDIUM FREQUENCY

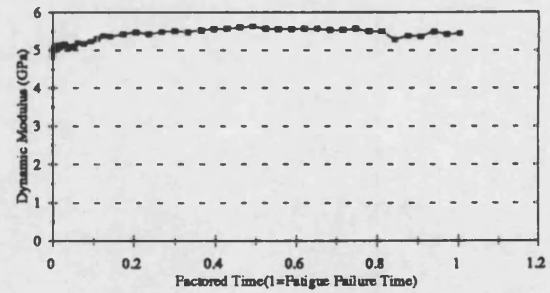

Discussion

Median values for the initial dynamic moduli, figure 10.14a and table 10.7, were very similar for chipboard and MDF but were significantly higher for OSB. The dynamic moduli increased slightly at lower stress levels, passing from 80% to 20%, for all three materials and increased to a greater extent for OSB. The increases occur because as the stress level is reduced less damage is produced by the initial fatigue cycles and the samples remain stiffer with less deflection produced.

The median final dynamic moduli, figure 10.14b and table 10.7, were fairly constant between the 80 and 50% stress levels for all three materials. The values for MDF and chipboard were again very similar and those for OSB were considerably higher. Below the 50% stress level the median final dynamic moduli increased with reducing stress level. However, none of these samples had failed so the moduli would probably have decreased prior to the failure of these samples. Both the initial and the final values for the dynamic moduli were higher for OSB and MDF than the representative values provided in the literature (WPPF PD/15, 1992), as was found for chipboard loaded at all three frequencies (section 8.7).

The median changes in dynamic moduli decreased for all three materials between the 80 and 50% stress levels and the decrease accelerated as the stress level was reduced towards 50%. Below the 50% stress level the magnitude of the decrease reduced and became an increase at the lowest stress levels. Again the changes observed were very similar for chipboard and MDF but were larger for OSB.

The OSB tested was significantly stiffer than the chipboard and MDF. However, in any evaluation of panel products it is important to remember that the panels tested are representative of an individual manufacturer's product. There will always be a considerable variation in properties for panels of the same material and grade particularly when produced by different manufacturers, from different wood species using different resins etc.

The stiffness of the MDF might have been expected to be considerably lower than that for chipboard due to the very large deflections produced in the MDF samples. However, the deflections in the MDF samples were produced by applying considerably larger stresses than those applied to chipboard and OSB. This means that MDF has a very similar stiffness to chipboard but can sustain larger strains before failure is produced. It is possible that the finer structure (smaller particles) of MDF posses a larger internal surface area and contains many smaller less critical flaws than chipboard

allowing it to strain to a greater extent. In the literature OSB is considered to be stiffer than chipboard, which is considered to be stiffer than MDF (WPPF PD/15, 1992).

There was no correlation between the magnitude of the dynamic moduli and the constituent particle size. However, in the literature the bending moduli are said to decrease with decreasing particle size (WPPF PD/15, 1992).

The dynamic modulus data for the OSB samples, figures 10.15a-e and 10.16a-e, is clearly more varied than that for the chipboard, figures 8.19a-e and 8.20a-e, and for the MDF, figures 10.17a-f and 10.18a-f (summarised in table 10.7). The variations result from the wide scatter in the strengths of the side-matched OSB samples and the large particle size compared to the widths of the samples. The moduli data for OSB is, however, less varied than the associated microstrain values. The dynamic modulus is an average stiffness and is not affected by the initial minimum fatigue microstrain having incorrect negative values resulting from the samples levelling out on the rollers when the load is applied. There is still the risk of wood chips bowing on the underside of the samples, affecting the modulus values, but the median values quoted are a reasonable representation of the dynamic stiffness of the OSB fatigue samples.

The dynamic moduli trends plotted with respect to time and factored time for the MDF samples were very similar to those for the chipboard samples. To examine the change in the dynamic moduli during individual tests it is clearer to look at the plots with respect to factored time, figures 10.16a-e and 10.18a-e, for OSB and MDF respectively rather than the plots with respect to time, where the data is compacted close to the Y axis.

At the 80% stress level for OSB, figures 10.15a and 10.16a, there is a definite decrease in dynamic moduli throughout testing for the three samples where there was sufficient data to observe a trend. This is the same as for all six chipboard samples tested at the medium frequency, although the values are significantly higher for OSB. There was no change in the dynamic moduli at this stress level for MDF, figures 10.17a and 10.18a.

With the stress level reduced to 70, 60 and 50%, figures 10.15b-d and 10.16b-d for OSB, the dynamic moduli continue to decrease throughout testing for all samples tested as was the case for the chipboard samples. This was also the case for MDF, figures 10.17b-d and 10.18b-d. There were considerable decreases in the dynamic moduli towards the end of the tests for the 50% stress level for OSB, and there were similar decreases for the 60% stress level but to a lesser extent. This decrease did not

occur (or possibly was just not captured) in the chipboard and MDF. The reason this occurred in the OSB samples may be a due to a weakening of the samples or it may be due to the underside of the samples splitting and deflecting the transducer probe, thus producing an exaggerated reading, but this seems unlikely when the hysteresis loop areas in section 10.7 are considered.

The 40, 30 and 20% stress level for the medium frequency testing of chipboard (section 8.7) showed that the dynamic moduli increased at first and then remained almost constant for the duration of the tests. This implied that the samples were not significantly damaged by the continuous fatigue loading. This seemed reasonable as the samples survived the allotted 10^6 loading cycles resulting in runouts. The tests were stopped in each case and no failures occurred. This also agreed with the creep microstrain curves that showed the microstrain not to have increased after the initial elastic deformation. The dynamic modulus for the 30% stress level test on chipboard at medium frequency showed a continuous increase throughout the test. This meant that the sample became stiffer throughout the test. This sample also survived to become a runout sample. The dynamic moduli trends for MDF tested at the 40 and 20% stress levels are very similar to those for chipboard but the increases observed are slightly lower at 40% stress level and slightly higher at the 20% level. These results are inconclusive because the runout results and the normalised S-N plot indicated that MDF was damaged by applying lower stress levels than chipboard.

There was only one result for OSB tested below the 50% stress level and that is for the 20% stress level. This sample showed no change in dynamic modulus for the majority of the tests. It was only after the machine had tripped out resulting in the load being removed for several days that the dynamic modulus reduced. It is considered that this may be due to the LVDT relocating rather than a real effect, but this is not certain.

10.6 Fatigue Moduli

The fatigue moduli were calculated for all the OSB and MDF samples fatigue tested using the stress and strain values from the captured hysteresis loops. The fatigue modulus incorporates the changing stiffness and creep strain of the sample during a fatigue test (see section 6.6). The limitations on the first and last data points are the same as for the microstrains (see section 10.4).

Figures 10.19a-c show the effect of changing stress level upon the median initial, median final and the median changes in the fatigue moduli respectively for OSB, chipboard and MDF. Table 10.8 provides a numerical summary of the data plotted in figures 10.19a-c and shows the ranges of fatigue moduli for each material at each stress level tested as an indication of variability.

Figures 10.20a-e and 10.23a-f show the fatigue moduli for OSB and MDF respectively tested at R=0.1, at medium frequency plotted as a function of time for all the samples tested at the 80, 70, 60, 50, 40 and 20% stress levels. All the graphs for OSB are plotted with the fatigue modulus scale from 0-10 GPa on the Y axis and those for MDF are plotted from 0-6 GPa to allow direct comparisons to be made between the different stress levels. Time is plotted on the X axis and varies greatly as it represents the duration of the tests.

These figures have been re-plotted twice using factored time as the X axis and then $\log_{(10)}$ time. These are included as figures 10.21a-e and 10.22a-e for OSB, and figures 10.24a-f and 10.25a-f for MDF. These plots provide a better comparison between tests of greatly different time duration compared to those plotted with respect to time. The equivalent plots for chipboard are included in section 8.8 as figures 8.27a-e, 8.28a-e and 8.29a-e.

Fig 10.19a

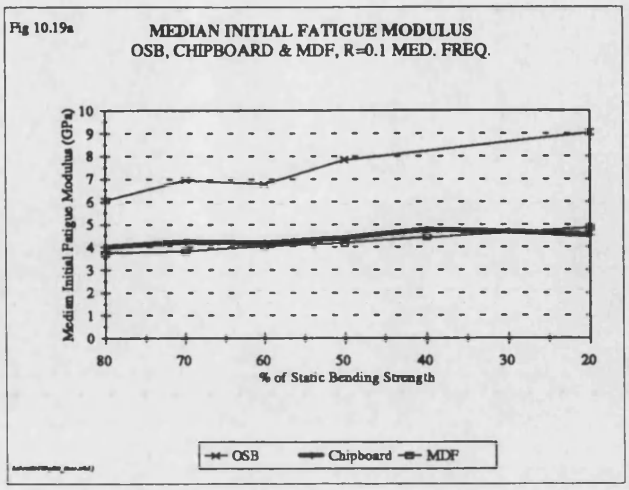

Fig 10.19b

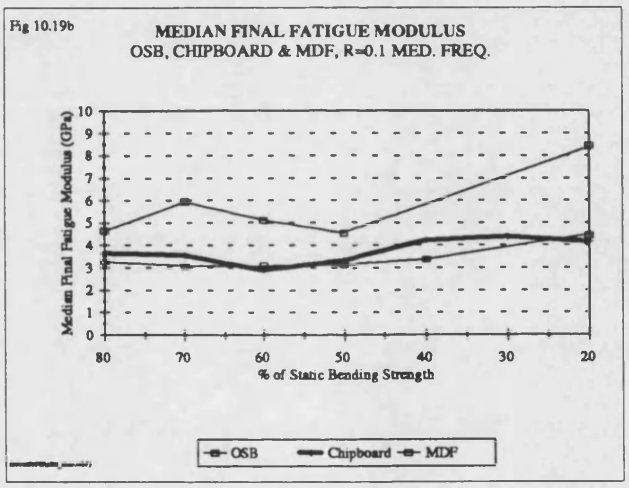

Fig 10.19c

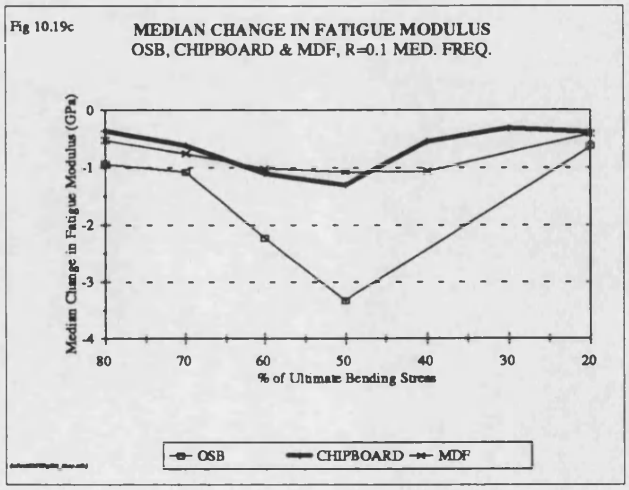

Table 10.8 Median fatigue moduli for OSB, chipboard and MDF tested at R=0.1, at medium frequencies.

Stress Level	Median Initial Fatigue Modulus GPa	Median Final Fatigue Modulus GPa	Median Change in Fatigue Modulus GPa	Range of Initial Fatigue Moduli GPa	Range of Final Fatigue Moduli GPa	Range of Change in Fatigue Modulus GPa
OSB, Medium Frequency, R=0.1						
80%	6.06	4.64	-0.94	5.14-8.33	3.62-7.39	(-0.84)-(-2.44)
70%	6.97	5.93	-1.08	6.60-8.08	5.46-8.59	(-0.39)-(-1.08)
60%	6.71	5.10	-2.23	4.63-7.99	4.43-5.30	(-1.22)-(-2.23)
50%	7.84	4.51	-3.33	7.49-8.43	3.48-5.55	(-2.58)-(-4.02)
20%	9.05	8.43	-0.63	1 Sample	1 Sample	1 Sample
Chipboard, Medium Frequency, R=0.1						
80%	4.02	3.65	-0.37	3.59-4.84	3.25-4.03	(-0.31)-(-0.81)
70%	4.23	3.57	-0.62	3.51-4.87	2.91-3.73	(-0.48)-(-1.14)
60%	4.18	2.91	-1.10	3.61-4.86	2.63-3.86	(-0.73)-(-1.42)
50%	4.41	3.35	-1.30	3.90-4.87	2.69-3.41	(-1.46)-(-1.09)
40%	4.76	4.21	-0.55	1 Sample	1 Sample	1 Sample
30%	4.70	4.38	-0.32	1 Sample	1 Sample	1 Sample
20%	4.53	4.15	-0.38	1 Sample	1 Sample	1 Sample
MDF, Medium Frequency, R=0.1						
80%	3.73	3.26	-0.53	3.59-4.09	3.11-3.64	(-0.09)-(-0.77)
70%	3.84	3.08	-0.76	3.74-4.13	2.94-3.30	(-0.55)-(-1.01)
60%	4.04	3.10	-1.02	3.83-4.45	2.91-3.39	(-0.82)-(-1.06)
50%	4.18	3.15	-1.08	4.11-4.59	2.92-3.50	(-0.90)-(-1.29)
40%	4.45	3.38	-1.07	1 Sample	1 Sample	1 Sample
20%	4.84	4.43	-0.41	1 Sample	1 Sample	1 Sample

Fig 10.20a

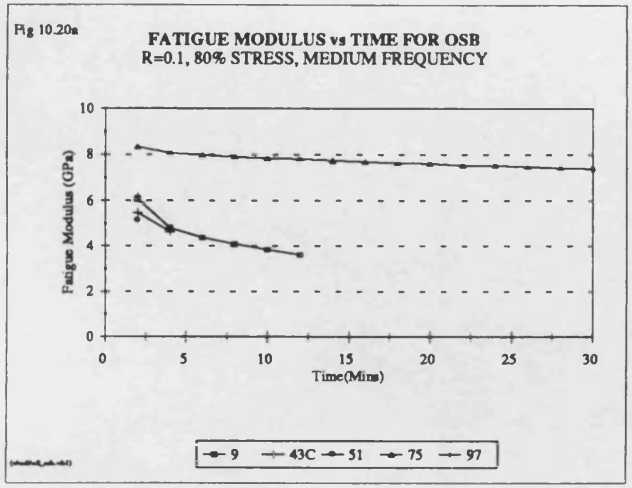

Fig 10.20b

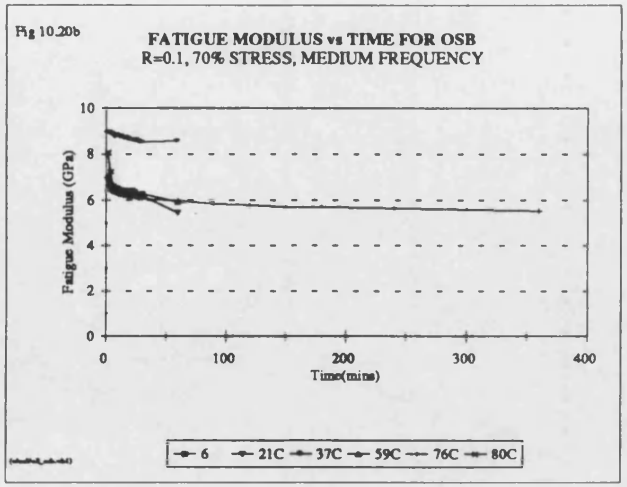

Fig 10.20c

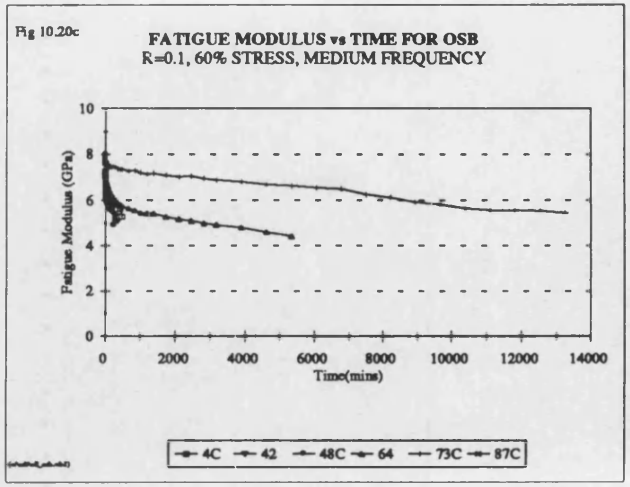

Fig 10.20d

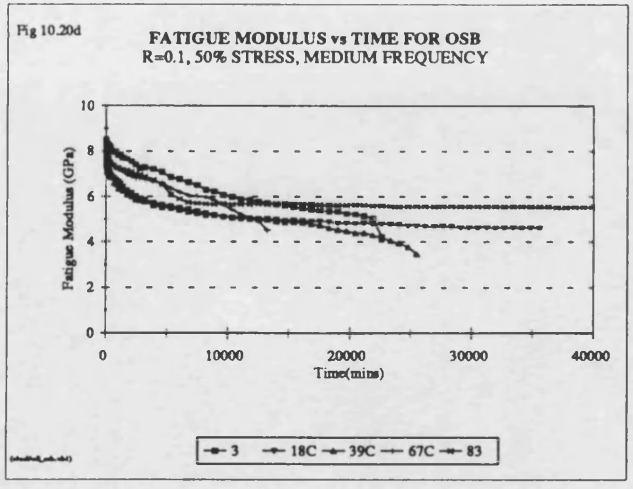

Fig 10.20e

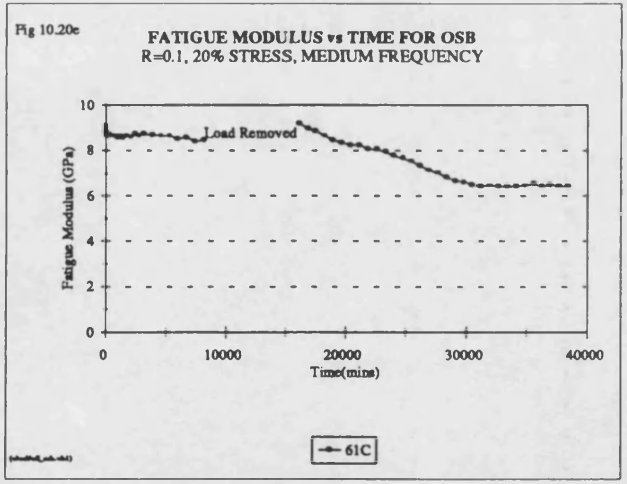

Fig 10.21a

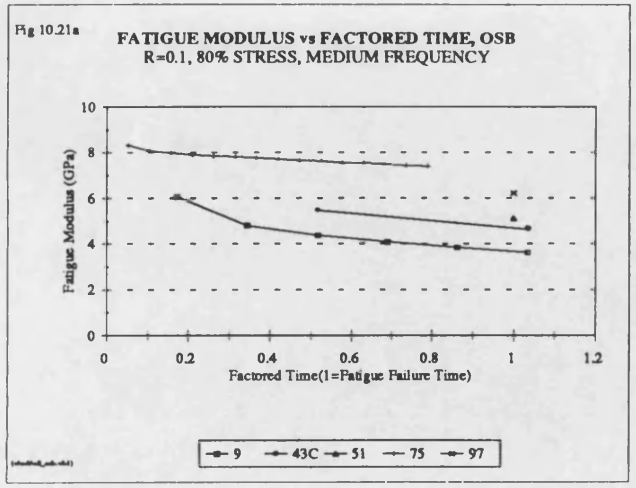

Fig 10.21b

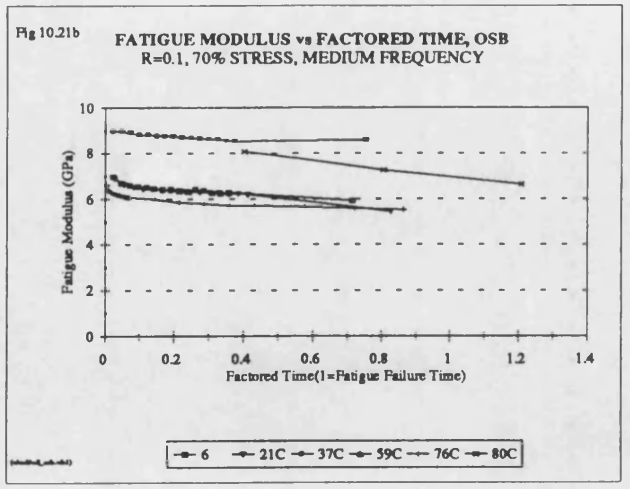

Fig 10.21c

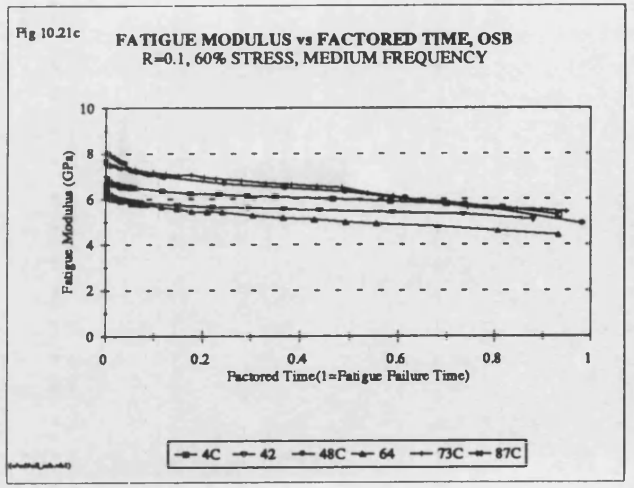

Fig 10.21d

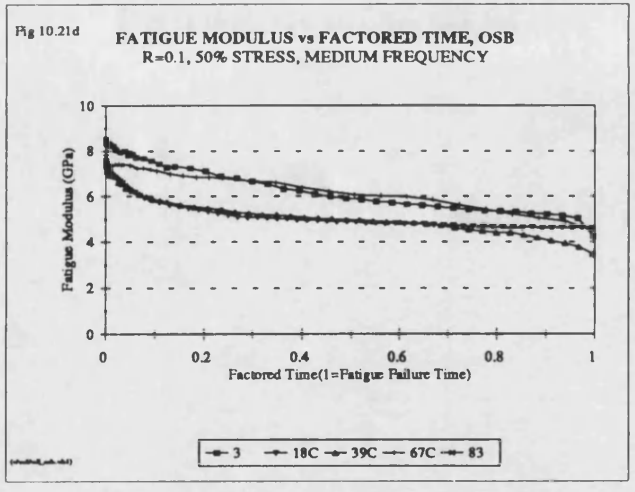

Fig 10.21e

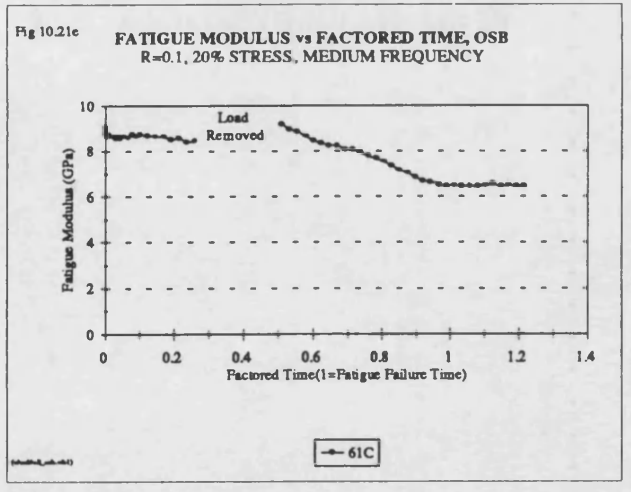

Fig 10.22a

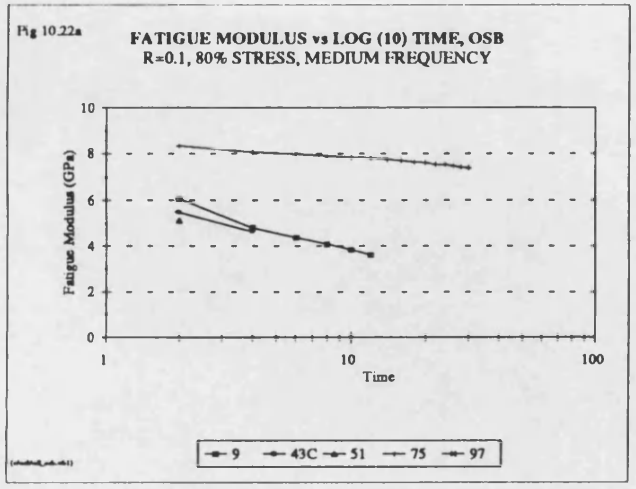

Fig 10.22b

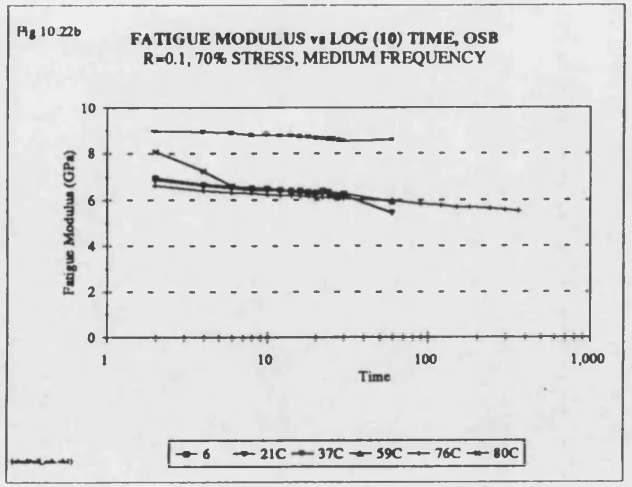

Fig 10.22c

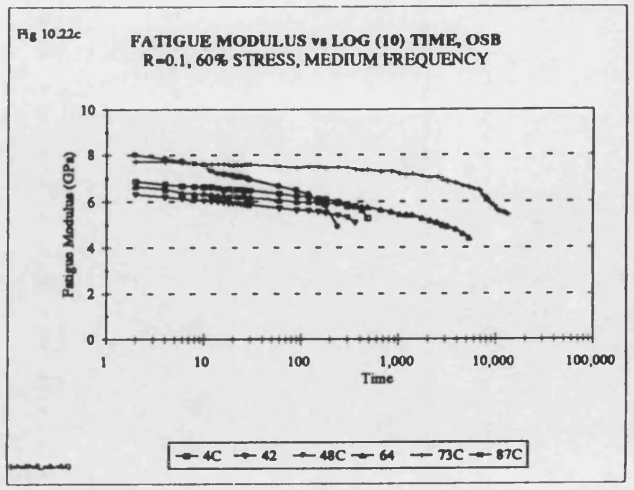

Fig 10.22d

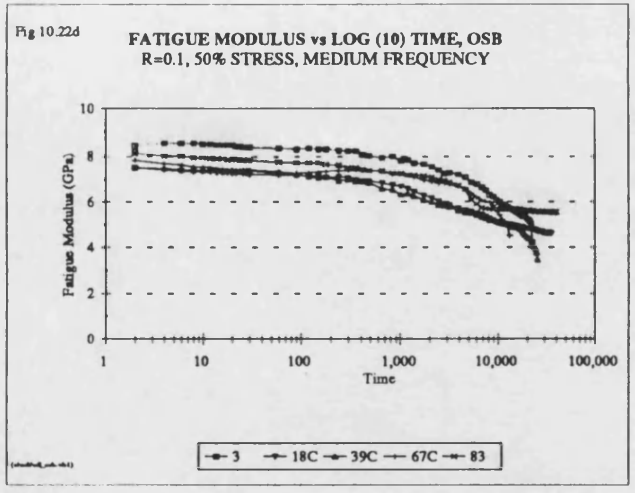

Fig 10.22e

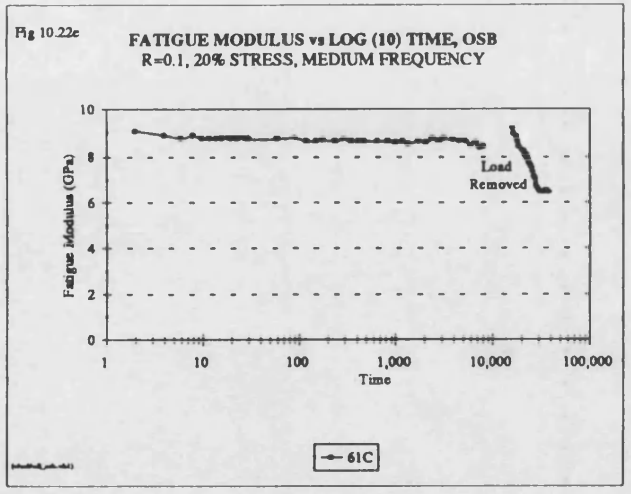

Fig 10.23a

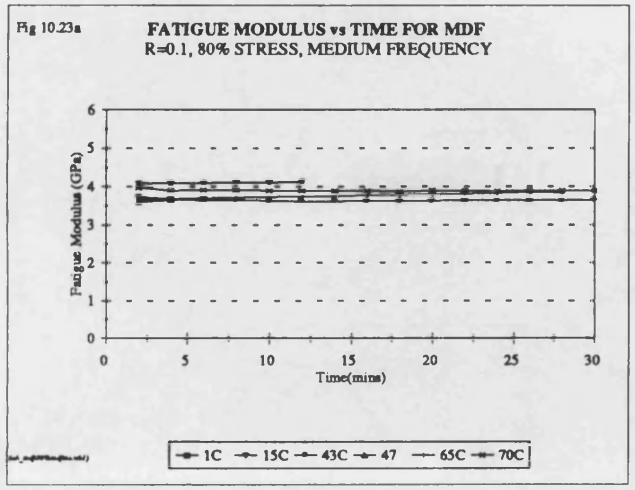

Fig 10.23b

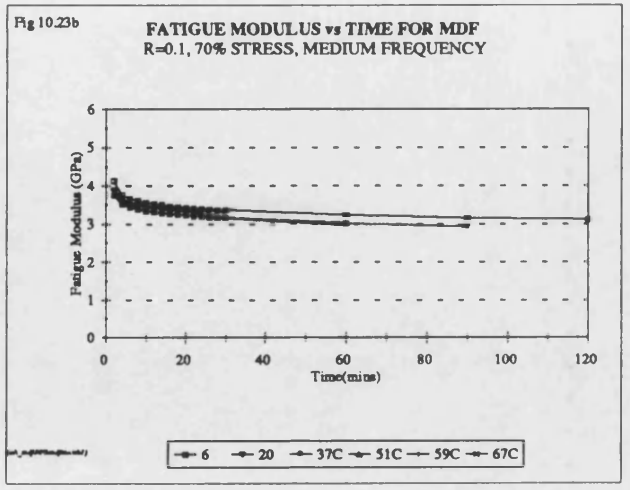

Fig 10.23c

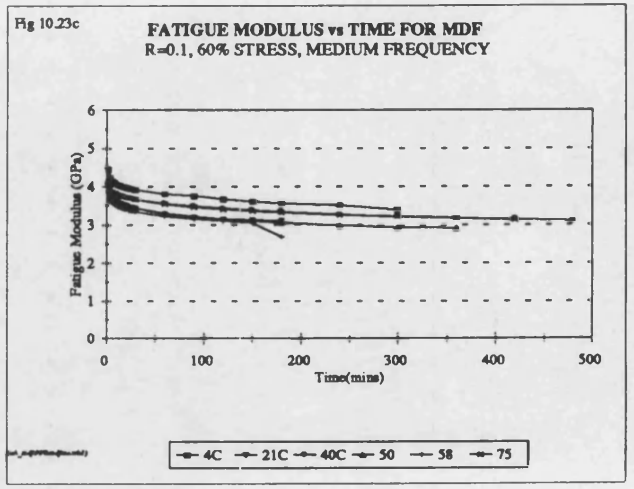

Fig 10.23d

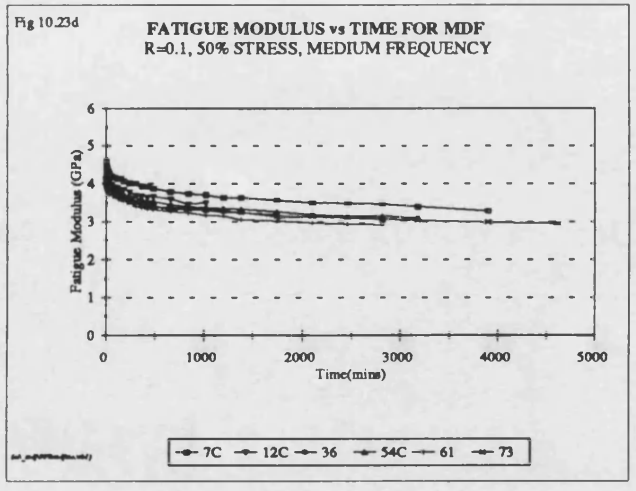

Fig 10.23e

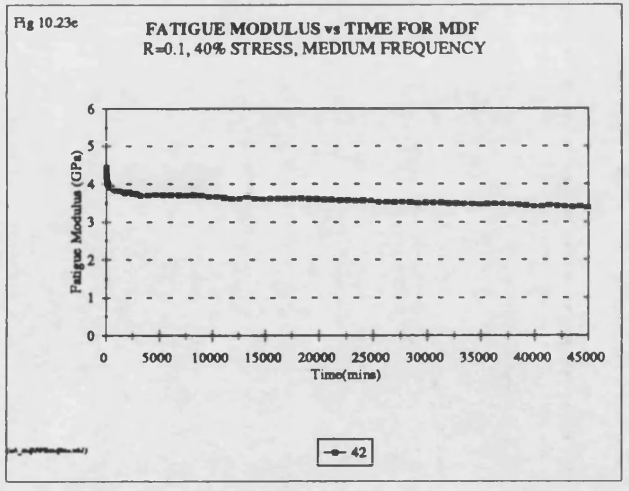

Fig 10.23f

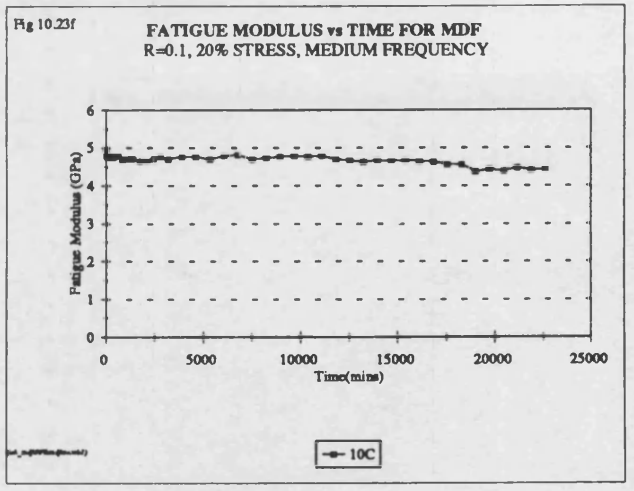

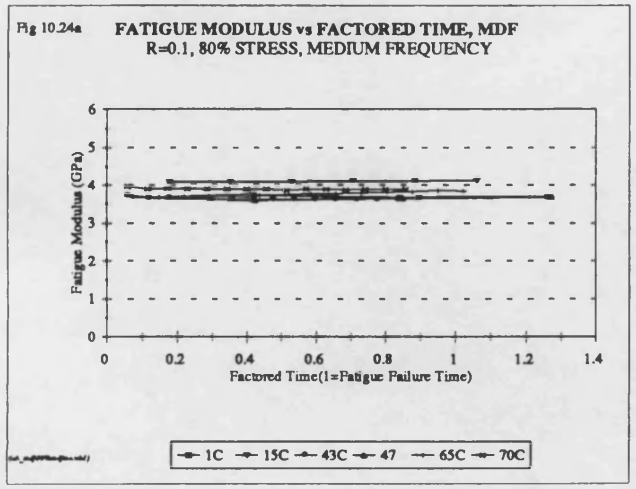
Fig 10.24a
FATIGUE MODULUS vs FACTORED TIME, MDF
R=0.1, 80% STRESS, MEDIUM FREQUENCY
Fatigue Modulus (GPa)
Factored Time(1=Patigue Pailure Time)
1C
15C
43C
47
65C
70C

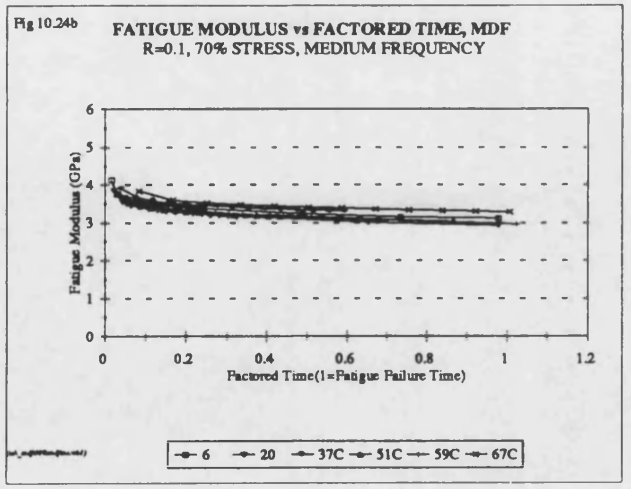
Fig 10.24b
FATIGUE MODULUS vs FACTORED TIME, MDF
R=0.1, 70% STRESS, MEDIUM FREQUENCY
Fatigue Modulus (GPa)
Factored Time(1=Patigue Pailure Time)
6
20
37C
51C
59C
67C

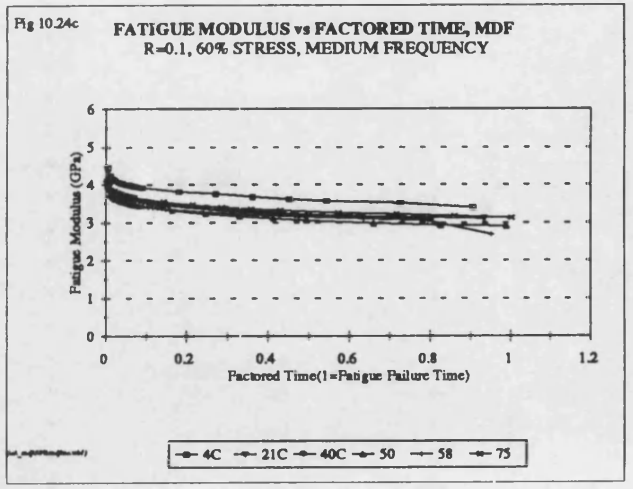
Fig 10.24c
FATIGUE MODULUS vs FACTORED TIME, MDF
R=0.1, 60% STRESS, MEDIUM FREQUENCY
Fatigue Modulus (GPa)
Factored Time(1=Patigue Pailure Time)
4C
21C
40C
50
58
75

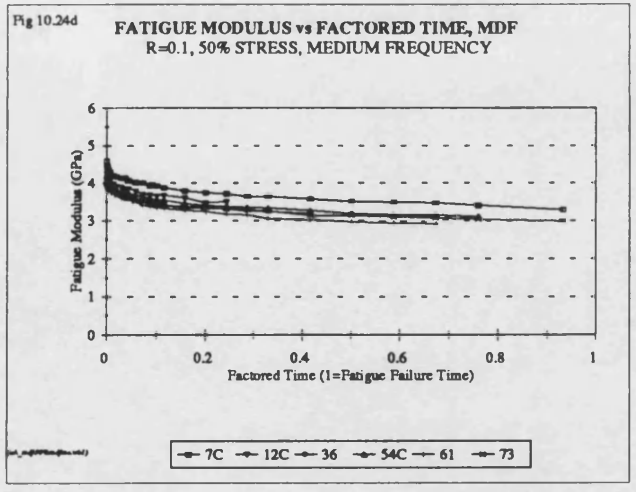
Fig 10.24d
FATIGUE MODULUS vs FACTORED TIME, MDF
R=0.1, 50% STRESS, MEDIUM FREQUENCY
Fatigue Modulus (GPa)
Factored Time (1=Patigue Pailure Time)
7C
12C
36
54C
61
73

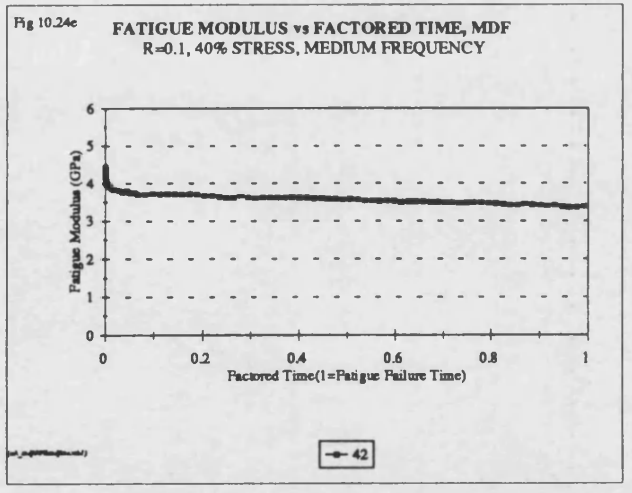
Fig 10.24e
FATIGUE MODULUS vs FACTORED TIME, MDF
R=0.1, 40% STRESS, MEDIUM FREQUENCY
Fatigue Modulus (GPa)
Factored Time(1=Patigue Pailure Time)
42

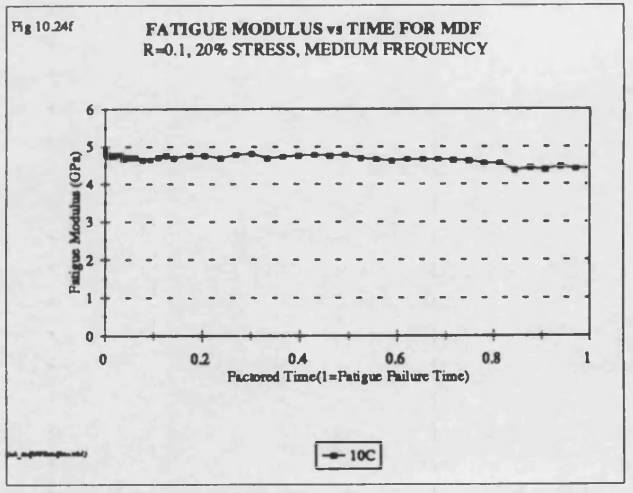
Fig 10.24f
FATIGUE MODULUS vs TIME FOR MDF
R=0.1, 20% STRESS, MEDIUM FREQUENCY
Fatigue Modulus (GPa)
Factored Time(1=Patigue Pailure Time)
10C

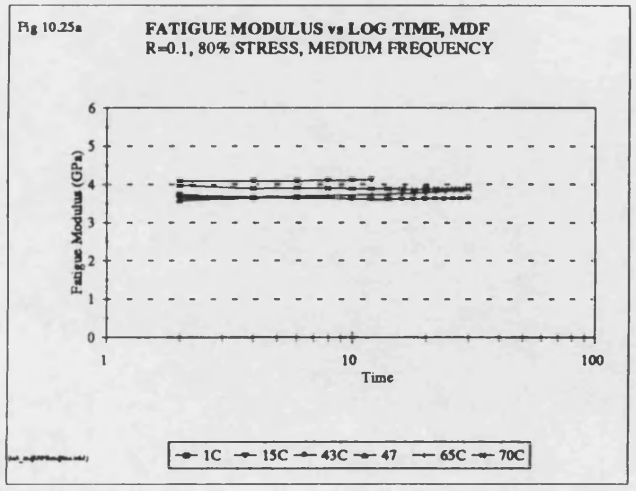
Fig 10.25a
FATIGUE MODULUS vs LOG TIME, MDF
R=0.1, 80% STRESS, MEDIUM FREQUENCY
Fatigue Modulus (GPa)
Time
1C 15C 43C 47 65C 70C

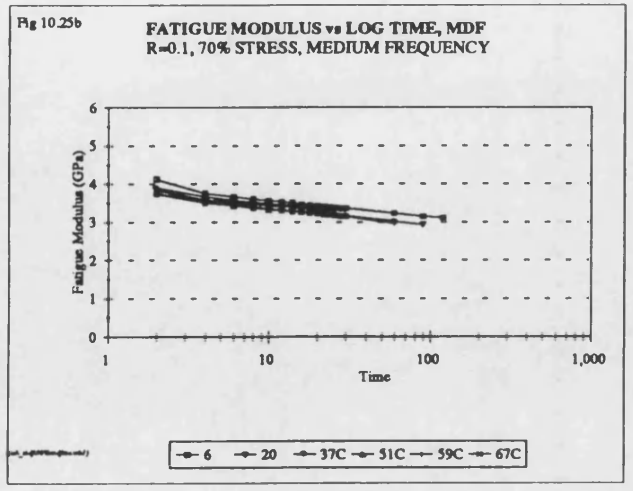
Fig 10.25b
FATIGUE MODULUS vs LOG TIME, MDF
R=0.1, 70% STRESS, MEDIUM FREQUENCY
Fatigue Modulus (GPa)
Time
6 20 37C 51C 59C 67C

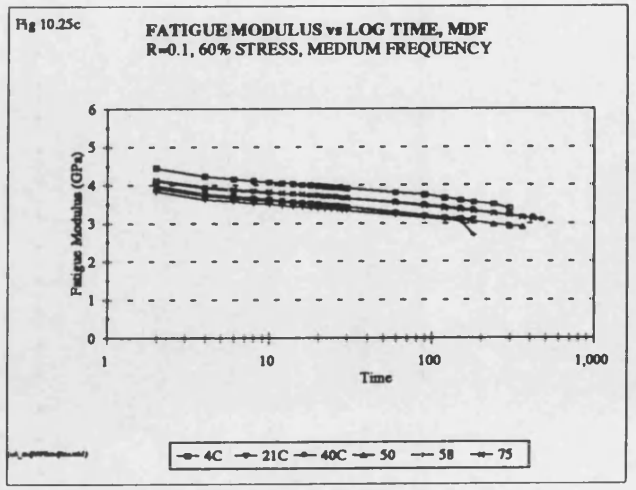
Fig 10.25c
FATIGUE MODULUS vs LOG TIME, MDF
R=0.1, 60% STRESS, MEDIUM FREQUENCY
Fatigue Modulus (GPa)
Time
4C 21C 40C 50 58 75

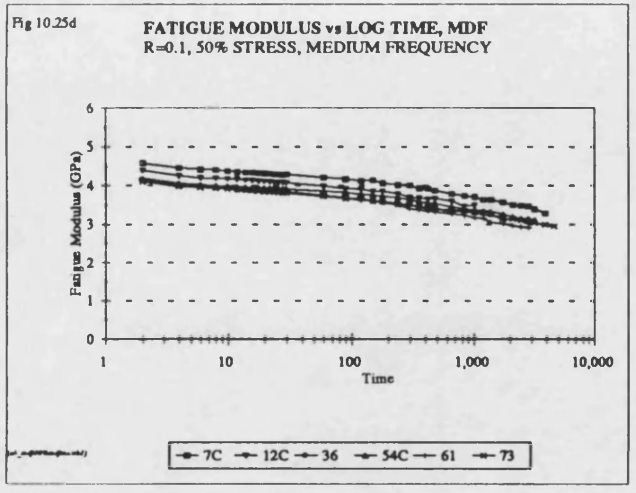
Fig 10.25d
FATIGUE MODULUS vs LOG TIME, MDF
R=0.1, 50% STRESS, MEDIUM FREQUENCY
Fatigue Modulus (GPa)
Time
7C 12C 36 54C 61 73

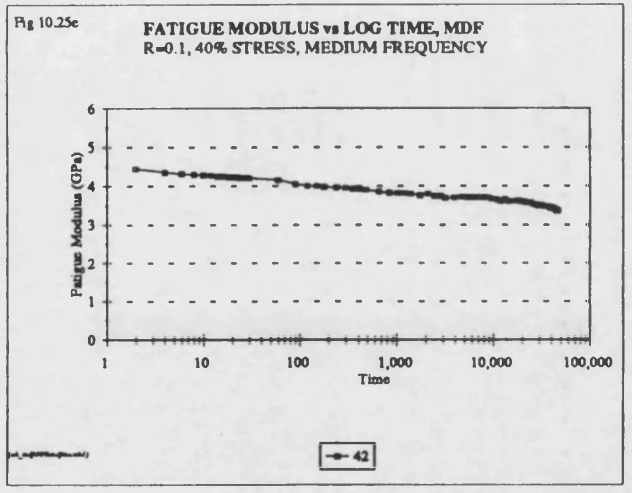
Fig 10.25e
FATIGUE MODULUS vs LOG TIME, MDF
R=0.1, 40% STRESS, MEDIUM FREQUENCY
Fatigue Modulus (GPa)
Time
42

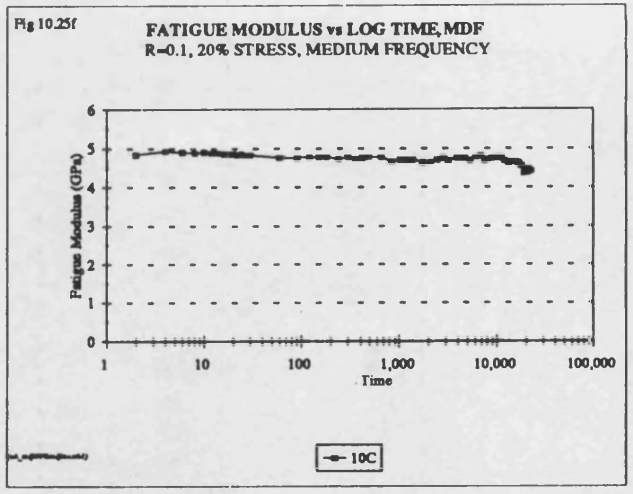
Fig 10.25f
FATIGUE MODULUS vs LOG TIME, MDF
R=0.1, 20% STRESS, MEDIUM FREQUENCY
Fatigue Modulus (GPa)
Time
10C

Discussion

The median initial fatigue moduli for OSB, chipboard and MDF, figure 10.19, are identical to the median initial dynamic moduli, figure 10.14a, because the initial loop captures are not affected by the strain in the samples (see section 10.5).

Figure 10.19b shows that the median final fatigue moduli are roughly constant with decreasing stress level from 80% down to 50% stress and then increase as the stress level is reduced further for all three materials. The reason the median final fatigue moduli remain roughly constant between the 80 and 50% stress levels is because these values represent failed samples and the critical strains remained roughly constant for all three materials. When the stress level is reduced to stress levels below 50% level the samples may be a long time away from failure or even an infinite time away, so the fatigue modulus is unlikely to have reduced to any great extent. This is also reflected in the median changes in the fatigue moduli. As was the case for the dynamic moduli the values for chipboard and MDF were very similar and those for OSB were significantly higher. The changes in the fatigue moduli were greater for OSB than for chipboard and MDF. Again the variability between the samples was greater for OSB than for chipboard and MDF for the fatigue moduli.

The decreases observed for the fatigue moduli are greater than those for the dynamic moduli because of the creep component. This is shown by the changes in the median dynamic moduli and the median fatigue moduli in table 10.7 (section 10.5) and table 10.8 respectively, and in figure 10.14c (section 10.5) and figure 10.19c.

As occurred with the dynamic moduli the decreases in the fatigue moduli for MDF may have been expected to have been greater than for the other two materials. However, again the large deflections were produced by applying larger stresses.

There is a definite decrease in the fatigue moduli for OSB throughout testing for all the samples tested for the stress levels 80% down to 20%, figures 10.20a-e, 10.21a-e and 10.22 a-e. This was also the case for MDF, figures 10.23a-f, 10.24a-f and 10.25a-f.

The decrease in fatigue modulus for OSB is a three stage process when plotted with respect to time and factored time, particularly at the 50% stress level figures 10.20e and 10.21e, but appears only to have two stages in the $\log_{(10)}$ plots. There is an initial relatively rapid decrease, that is followed by a more gradual, almost linear stage, until close to failure. The third stage is only exhibited by a few samples. However, this third stage is quite rapid, leading to failure and so would only rarely be captured by the

FDAS. The third stage was only observed for one of the MDF samples loaded at the 60% stress level, figure 10.23c. Similar trends were observed for the medium frequency testing of chipboard (see section 8.8). The decreases towards the end of the OSB tests for the 60 and 50% stress level tests were greater than those for chipboard and MDF but it is possible this may be caused by bowing of the wood chips on the underside of the samples.

When plotted with respect to $\log_{(10)}$ time the fatigue moduli for MDF decrease almost linearly unlike OSB and chipboard which both displayed more rapid decreases towards the end of the tests.

10.7 Hysteresis Loop Areas

The hysteresis loop area (see section 6.6) was determined at every loop capture for all the OSB and MDF samples fatigue tested as for chipboard. The first and last values are subject to the same limitations as the microstrain and moduli values.

Figure 10.26a shows the effect of reducing the stress level from 80% down to 20% on the median initial and median final hysteresis loop areas. Due to the magnitude of the hysteresis loop area values for MDF the equivalent data for MDF has been plotted separately as figure 10.26b. The median changes in the hysteresis loop areas for all three materials with the stress level reducing from 80% down to 20% are plotted in figure 10.26c. The data plotted for the three materials in figures 10.26a-c is presented in table 10.9 together with the range of values for the initial, final and change in the hysteresis loop areas for all the samples tested at each stress level. This provides an indication of the spread of values for different samples tested at the same stress level.

Figures 10.27a-e and 10.30a-f show the hysteresis loop area as a function of time for OSB and MDF respectively for all the tests performed at R=0.1, at medium frequency at the 80, 70, 60, 50 and 20% stress levels. As was the case for the dynamic moduli, fatigue moduli and microstrain plots the X axes vary greatly due to the length of the tests. The plots of hysteresis loop area for OSB are all plotted with identical Y axis from 0-8 kJ/m^3 while those for MDF are plotted from 0-25 kJ/m^3 to allow direct comparisons to be made between the results for different stress levels.

These figures have all been re-plotted twice with factored time and then $\log_{(10)}$ time as the X axis instead of time. These are included as figures 10.28a-e and 10.29a-e for OSB, and figures 10.31a-f and 10.32a-f for MDF. These plots once again make it possible to compare the results of different tests, at the same or different stress levels, where there was a large difference between the time duration of the tests.

Fig 10.26a

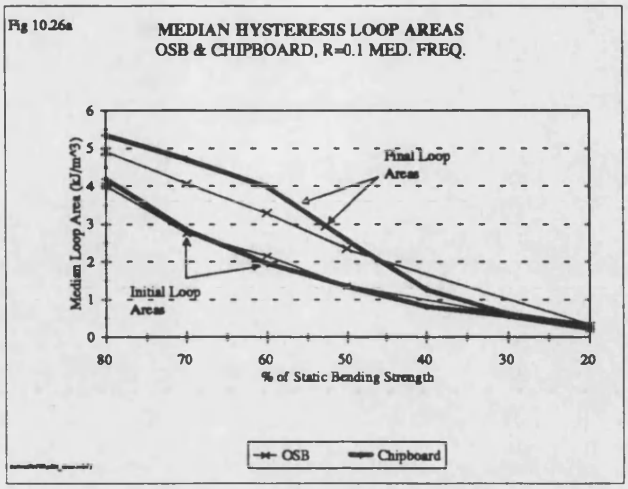

Fig 10.26b

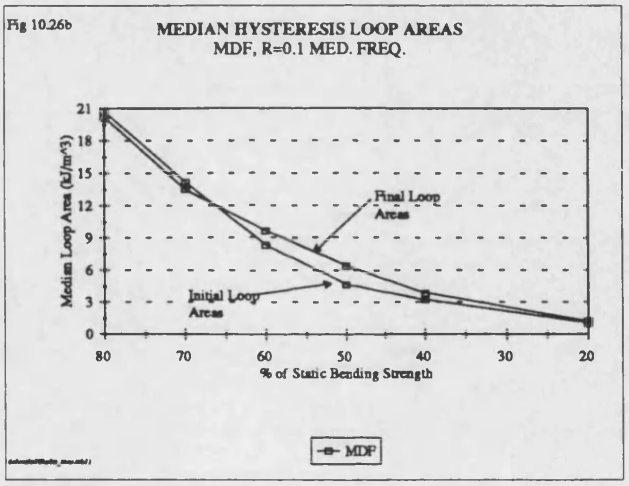

Fig 10.26c

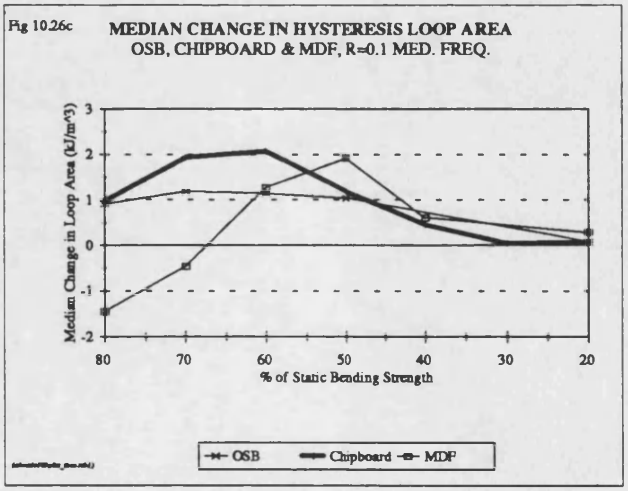

Table 10.9 Median hysteresis loop areas for OSB, chipboard and MDF tested at R=0.1, medium frequencies.

Stress Level	Median Initial Hysteresis Loop Area kJ/m^3	Median Final Hysteresis Loop Area kJ/m^3	Median Change in Hysteresis Loop Area kJ/m^3	Range of Initial Hysteresis Loop Area kJ/m^3	Range of Final Hysteresis Loop Area kJ/m^3	Range of Change in Hysteresis Loop Area kJ/m^3
OSB, Medium Frequency, R=0.1						
80%	4.01	4.92	0.91	2.15-5.32	2.84-7.23	1.72-3.22
70%	2.76	4.07	1.18	1.71-4.75	2.49-4.59	1.10-1.49
60%	2.16	3.29	1.14	1.54-4.57	1.87-5.69	0.33-3.94
50%	1.36	2.35	1.03	0.84-1.39	1.28-2.98	0.20-1.60
20%	0.22	0.30	0.07	1 Sample	1 Sample	1 Sample
Chipboard, Medium Frequency, R=0.1						
80%	4.19	5.36	0.98	3.01-4.86	4.30-7.41	0.87-2.55
70%	2.85	4.72	1.93	2.09-3.66	3.89-7.06	1.58-3.40
60%	1.95	4.00	2.05	1.78-2.51	3.51-4.67	1.45-2.89
50%	1.35	2.57	1.18	1.24-1.43	2.23-2.78	0.87-1.54
40%	0.81	1.27	0.46	1 Sample	1 Sample	1 Sample
30%	0.56	0.62	0.05	1 Sample	1 Sample	1 Sample
20%	0.23	0.31	0.08	1 Sample	1 Sample	1 Sample
MDF, Medium Frequency, R=0.1						
80%	20.71	20.19	-1.45	18.32-25.25	17.90-22.37	(-3.0)-(1.44)
70%	14.22	13.51	-0.46	12.15-16.36	11.67-16.79	(-0.34)-(-0.94)
60%	8.36	9.66	1.27	7.63-9.48	8.49-10.87	0.40-1.93
50%	4.70	6.46	1.92	4.22-5.46	5.97-8.09	0.51-4.02
40%	3.22	3.82	0.60	1 Sample	1 Sample	1 Sample
20%	0.97	1.26	0.29	1 Sample	1 Sample	1 Sample

Fig 10.27a

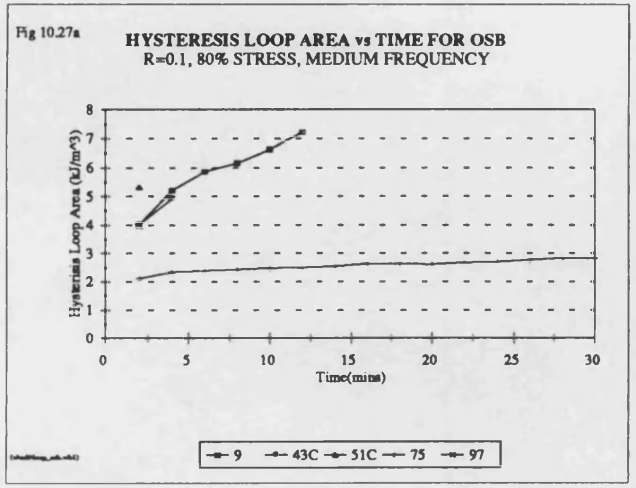

Fig 10.27b

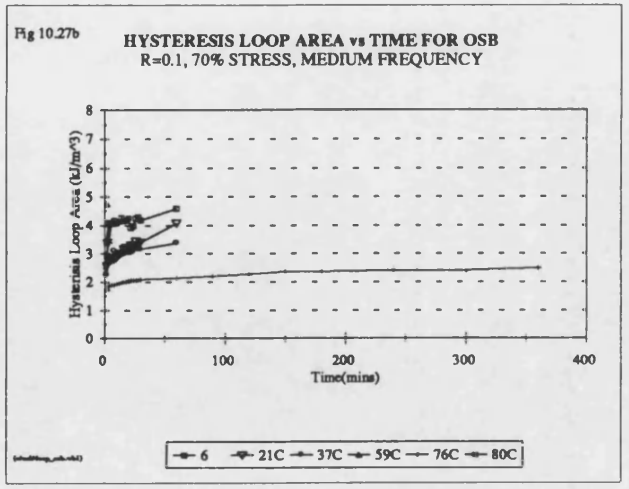

Fig 10.27c

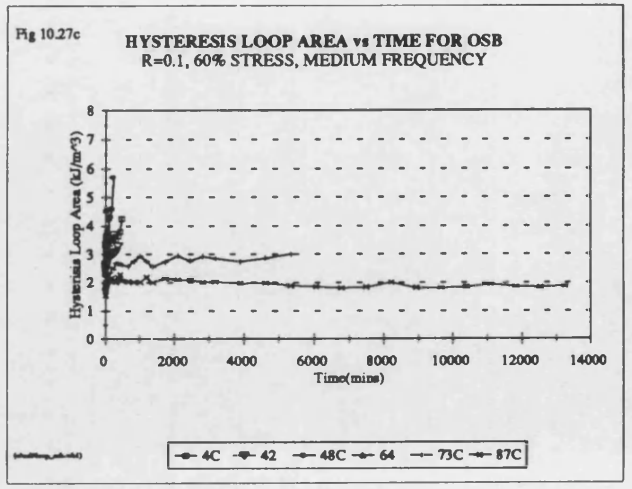

Fig 10.27d

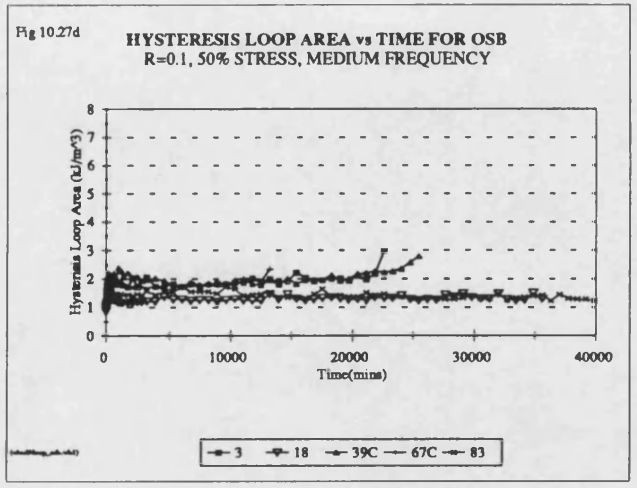

Fig 10.27e

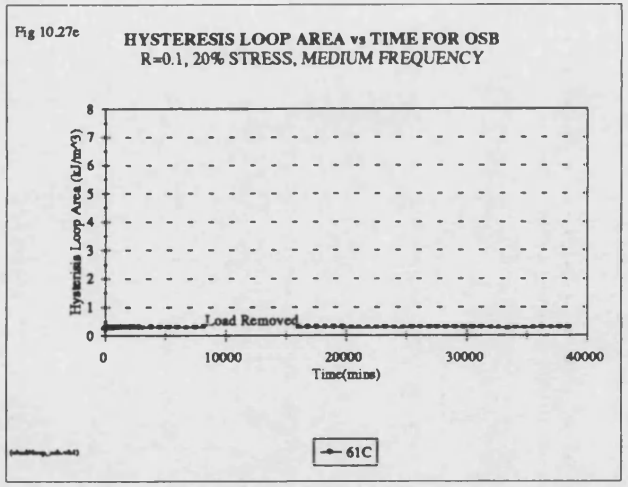

Fig 10.28a

LOOP AREA vs FACTORED TIME, OSB
R=0.1, 80% STRESS, MEDIUM FREQUENCY

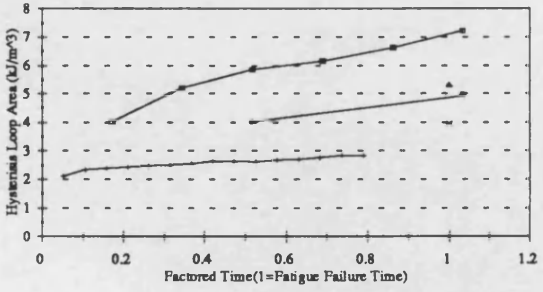

Fig 10.28b

LOOP AREA vs FACTORED TIME, OSB
R=0.1, 70% STRESS, MEDIUM FREQUENCY

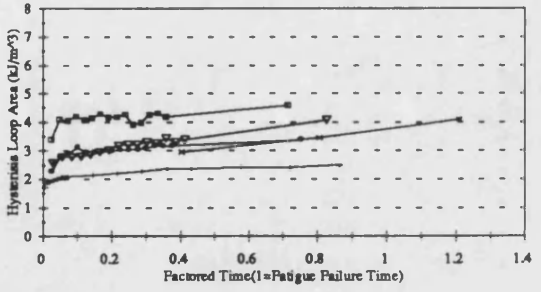

Fig 10.28c

LOOP AREA vs FACTORED TIME, OSB
R=0.1, 60% STRESS, MEDIUM FREQUENCY

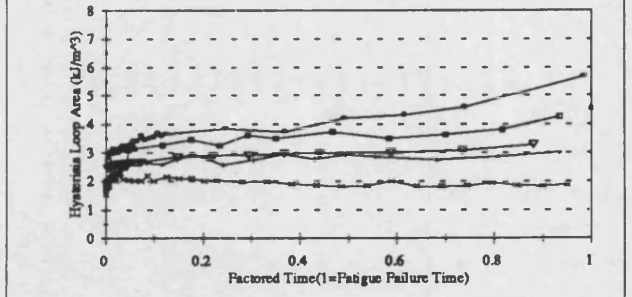

Fig 10.28d

LOOP AREA vs FACTORED TIME, OSB
R=0.1, 50% STRESS, MEDIUM FREQUENCY

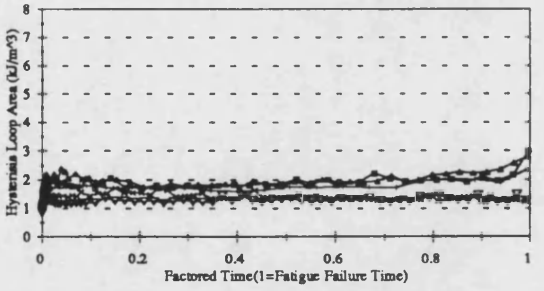

Fig 10.28e

LOOP AREA vs FACTORED TIME, OSB
R=0.1, 20% STRESS, MEDIUM FREQUENCY

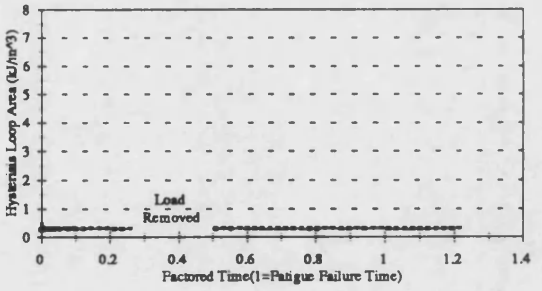

Fig 10.29a

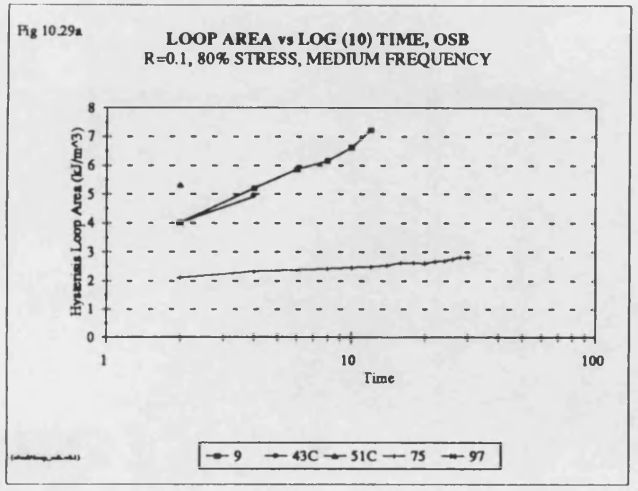

Fig 10.29b

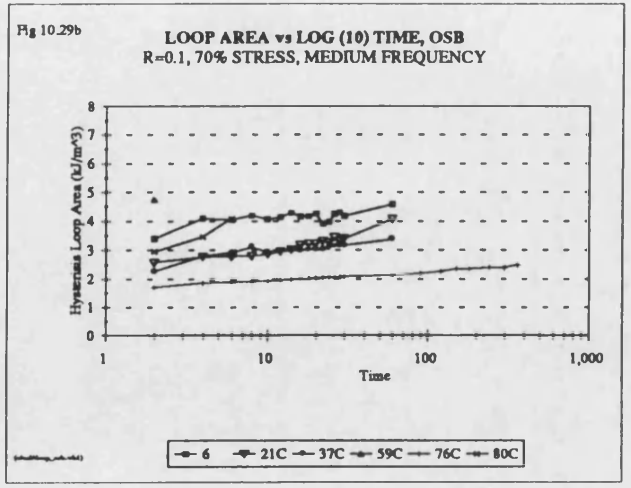

Fig 10.29c

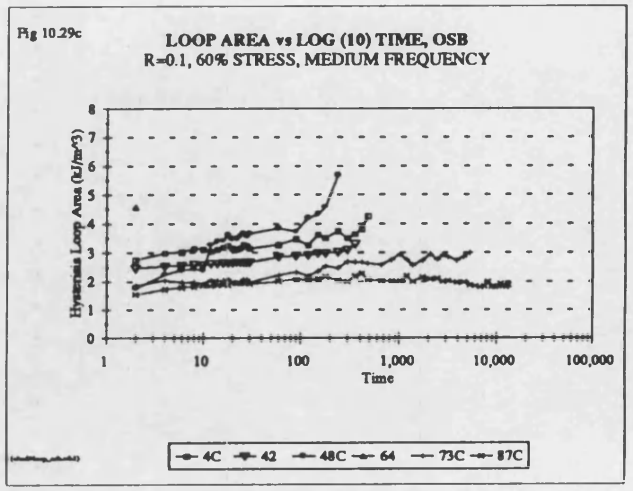

Fig 10.29d

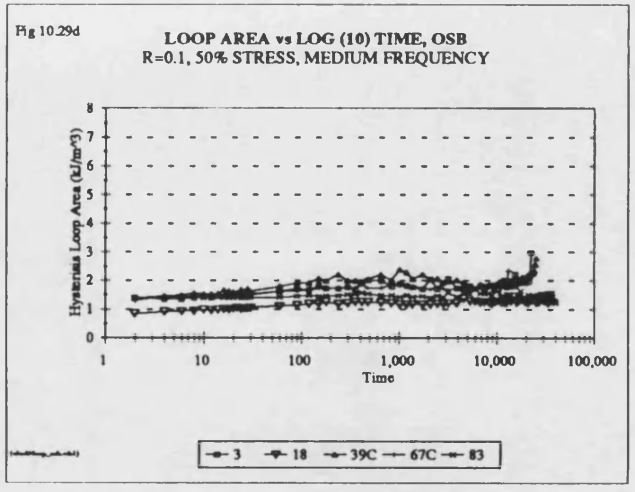

Fig 10.29e

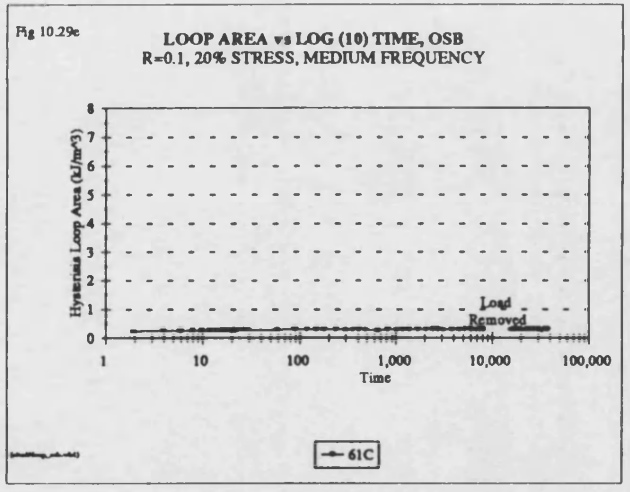

Fig 10.30a

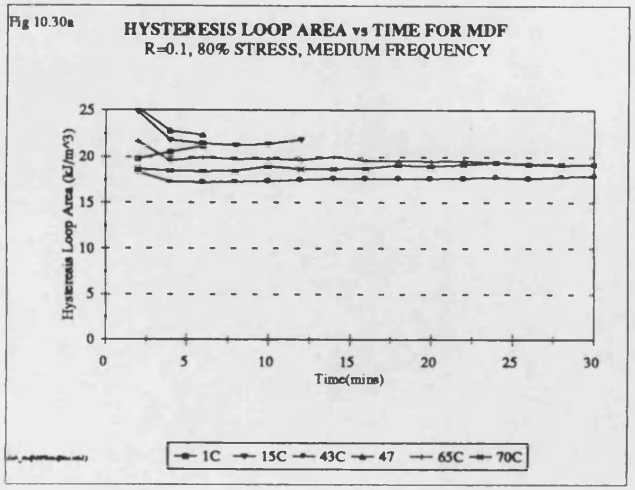

Fig 10.30b

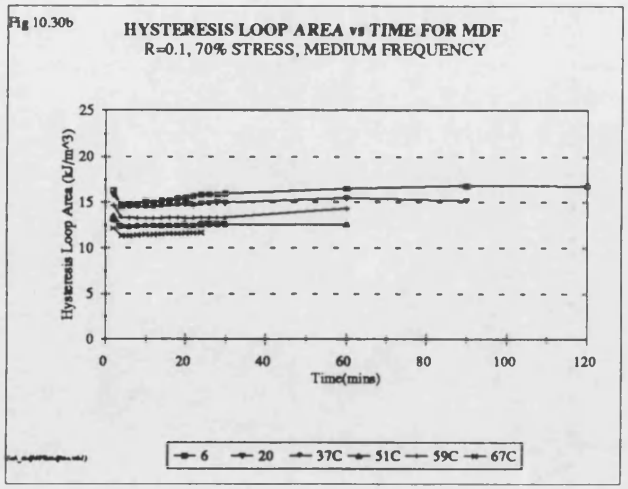

Fig 10.30c

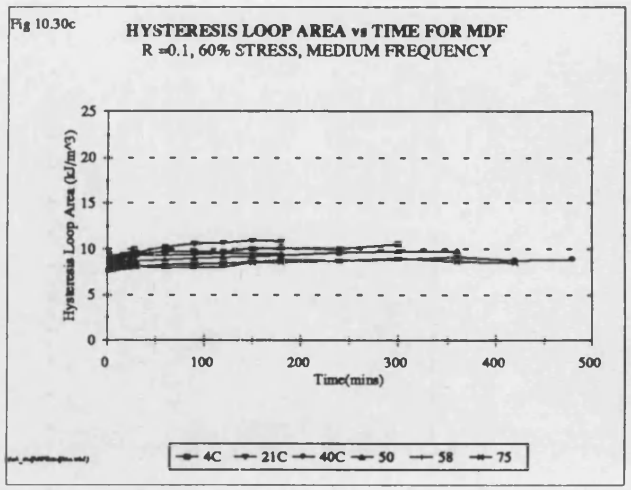

Fig 10.30d

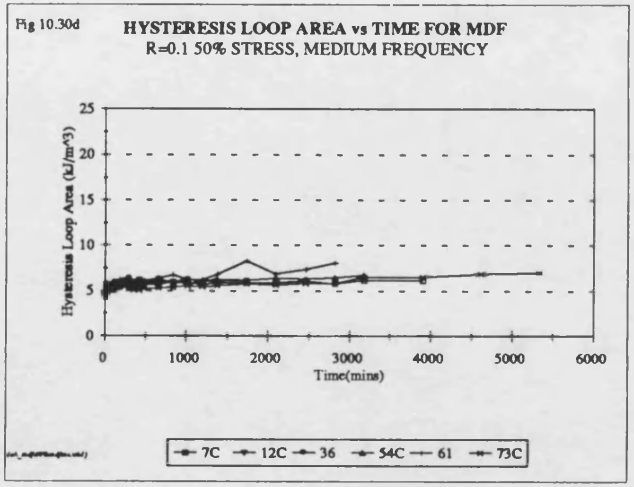

Fig 10.30e

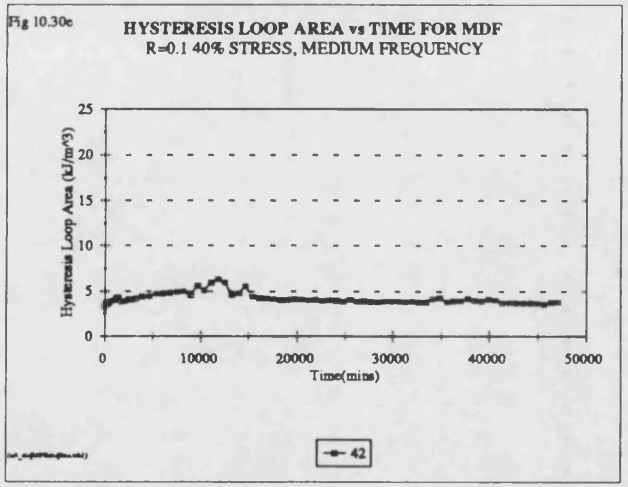

Fig 10.30f

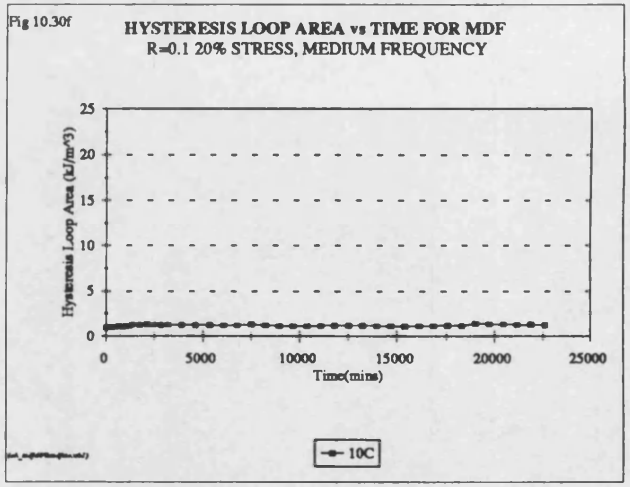

Fig 10.31a

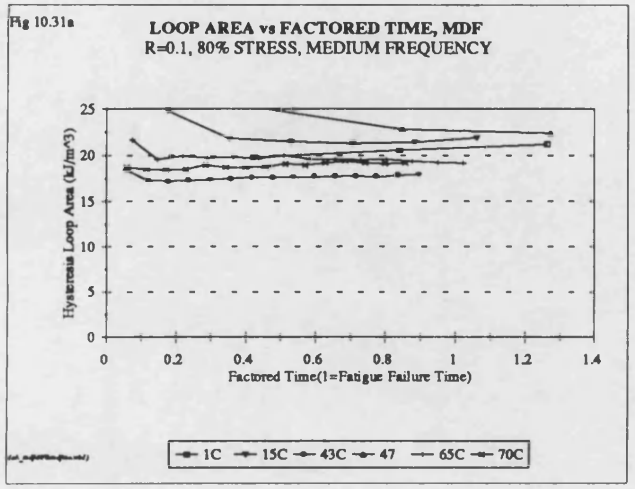

Fig 10.31b

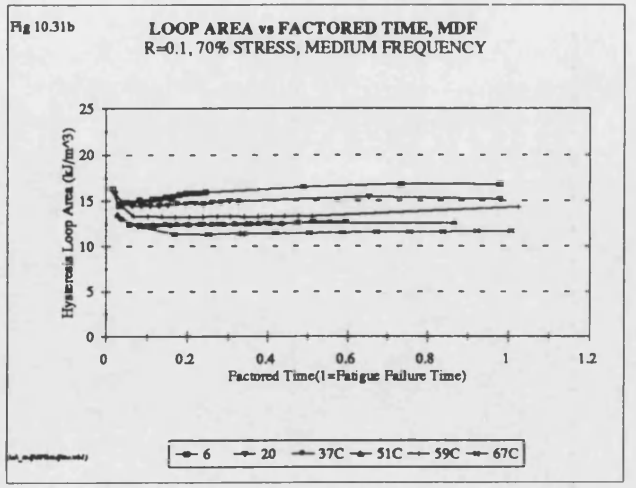

Fig 10.31c

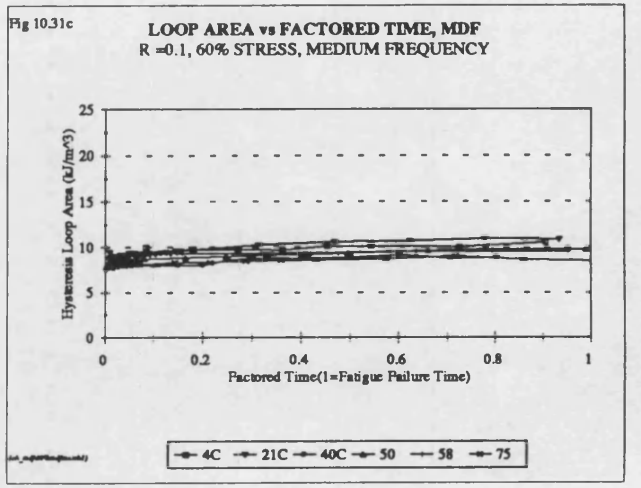

Fig 10.31d

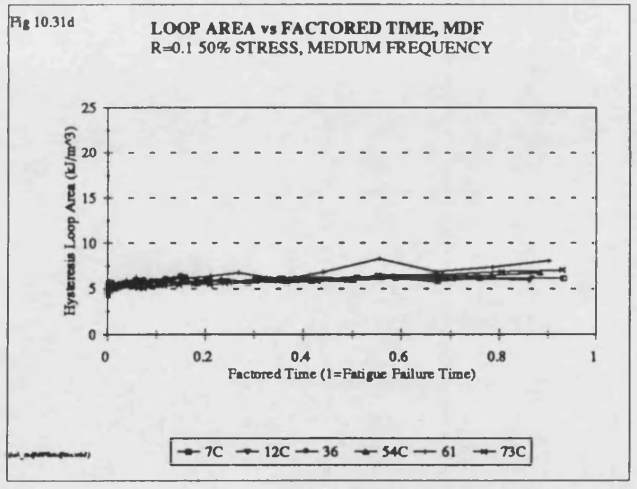

Fig 10.31e

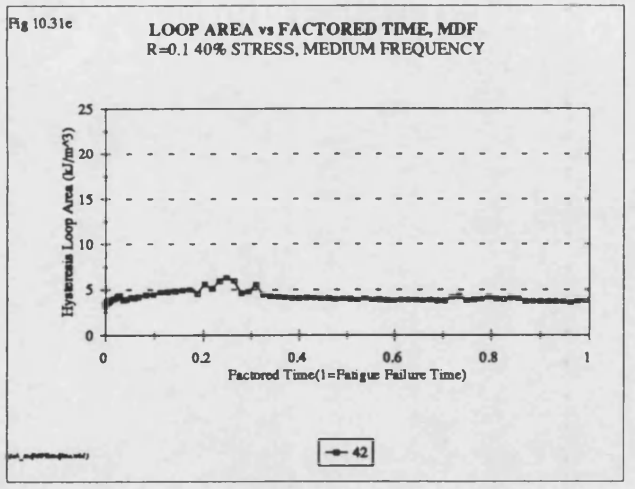

Fig 10.31f

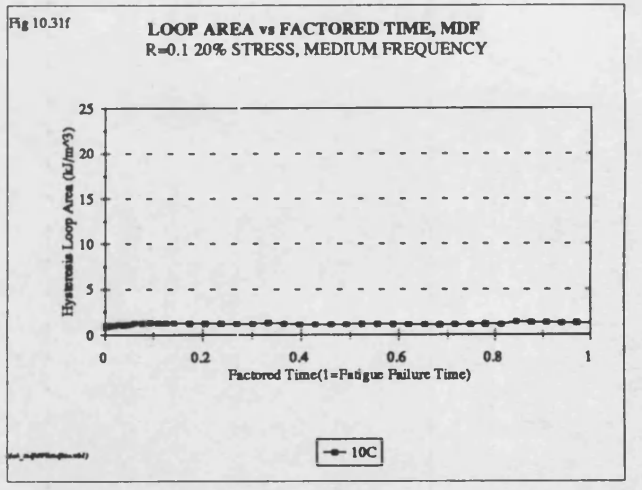

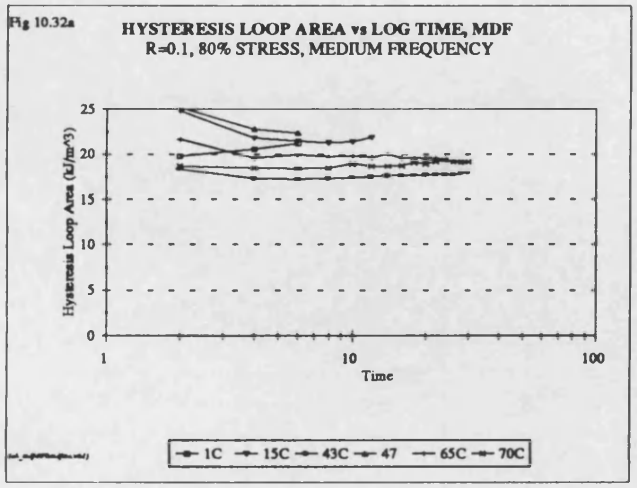
Fig 10.32a
HYSTERESIS LOOP AREA vs LOG TIME, MDF
R=0.1, 80% STRESS, MEDIUM FREQUENCY
Hysteresis Loop Area (kJ/m^3)
Time
1C 15C 43C 47 65C 70C

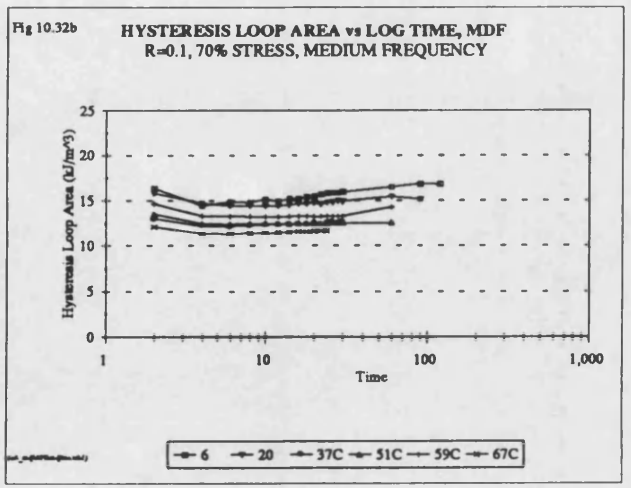
Fig 10.32b
HYSTERESIS LOOP AREA vs LOG TIME, MDF
R=0.1, 70% STRESS, MEDIUM FREQUENCY
Hysteresis Loop Area (kJ/m^3)
Time
6 20 37C 51C 59C 67C

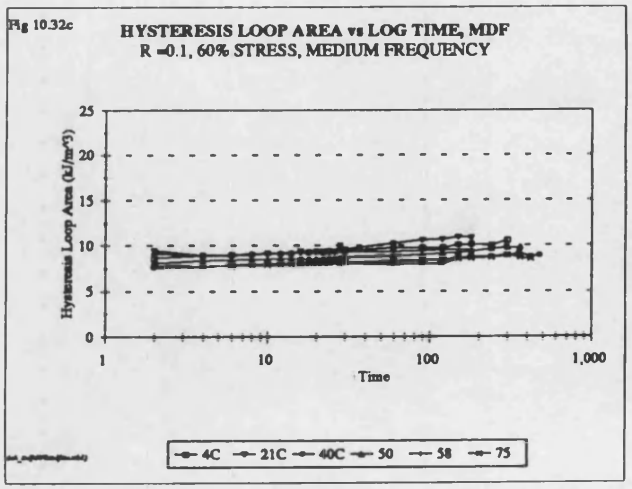
Fig 10.32c
HYSTERESIS LOOP AREA vs LOG TIME, MDF
R =0.1, 60% STRESS, MEDIUM FREQUENCY
Hysteresis Loop Area (kJ/m^3)
Time
4C 21C 40C 50 58 75

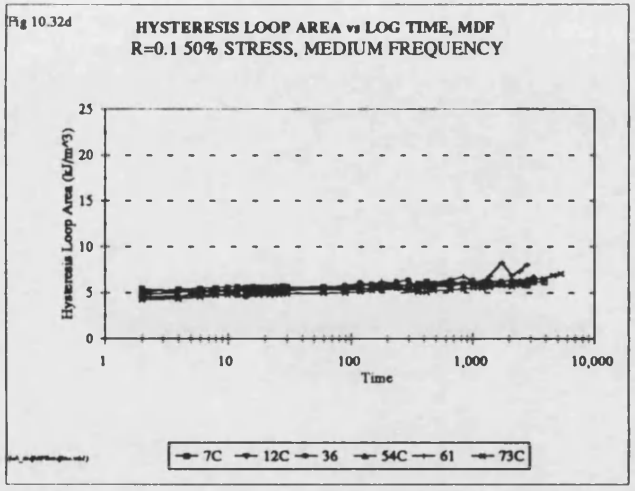
Fig 10.32d
HYSTERESIS LOOP AREA vs LOG TIME, MDF
R=0.1 50% STRESS, MEDIUM FREQUENCY
Hysteresis Loop Area (kJ/m^3)
Time
7C 12C 36 54C 61 73C

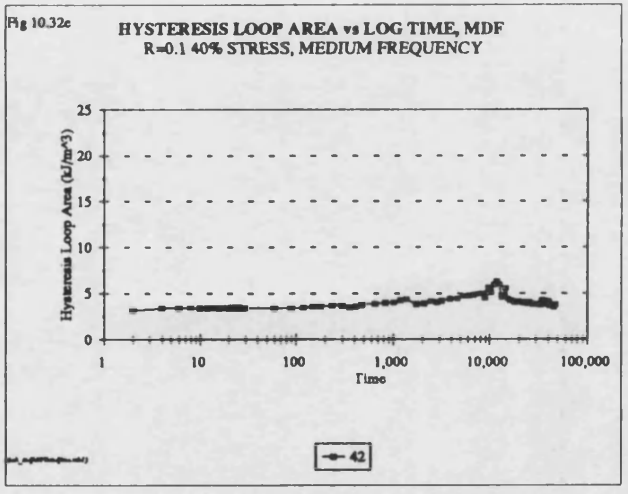
Fig 10.32e
HYSTERESIS LOOP AREA vs LOG TIME, MDF
R=0.1 40% STRESS, MEDIUM FREQUENCY
Hysteresis Loop Area (kJ/m^3)
Time
42

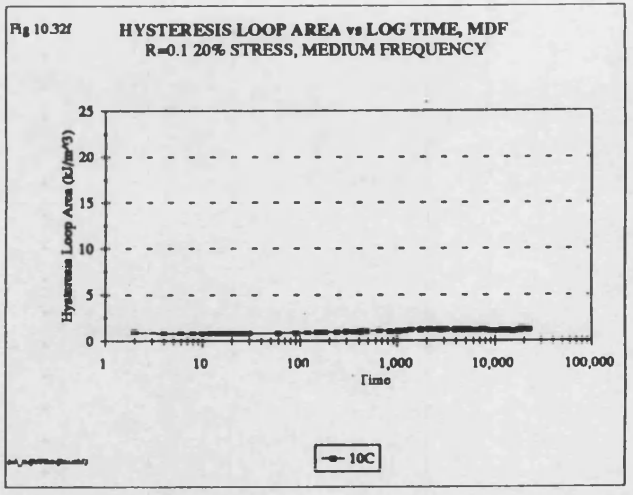
Fig 10.32f
HYSTERESIS LOOP AREA vs LOG TIME, MDF
R=0.1 20% STRESS, MEDIUM FREQUENCY
Hysteresis Loop Area (kJ/m^3)
Time
10C

Discussion

Figure 10.26a shows the median initial and median final hysteresis loop areas for all the stress levels tested for OSB and chipboard. The magnitude of the initial and final loop areas decreases with decreasing stress level for both materials. Considering that the OSB is considerably stiffer than chipboard and the stresses imposed on it are on average 35% higher than those applied to the chipboard the loop areas are very close. This shows that cyclic loading produces a similar quantity of damage per loading cycle on both OSB and chipboard when loaded at the same percentage stress level. This reinforces the similarity between the two materials on the normalised S-N plot, figure 10.1.

The hysteresis loop areas for MDF were considerably larger than those for OSB and chipboard, up to five times greater for equivalent stress levels, table 10.9. However, the magnitude of the difference between the values for MDF and the other two materials reduces as the stress level is reduced. The median initial and median final hysteresis loop areas, however, show similar trends to those for OSB and chipboard, decreasing with decreasing stress level. One reason why the magnitudes of the loop areas for MDF are so much greater than for the other two materials is because the stresses applied to the samples were greater but these were only twice as high. This could mean that the MDF samples are damaged more rapidly than the other OSB and chipboard. This is also supported by the normalised S-N plot, figure 10.1, where the MDF samples have an inferior fatigue performance to the other two materials loaded at the equivalent percentage stress levels. The increased loop areas may also be caused by MDF having a much larger internal surface area due to the considerably smaller constituent particle size. This may increase the materials capacity to absorb energy. The magnitude of the loop areas for MDF is, however, exaggerated because when higher stresses are applied the increase in loop area is not directly proportional to the increased stress due to the shape of the loops captured. The true increase is roughly proportional to the increase in the applied stress squared.

The loop area values for MDF at the 80 and 70% stress levels must be treated with caution because the high stresses caused slight indentations on the surfaces of the samples (bedding in) and the deflections were very large and will have caused an error in the applied stress due to angle of the sample's neutral axis to the inner support. However, this does not appear to have affected the moduli.

The most important feature seen in figures 10.26a and 10.26b is that for all three materials the difference between the median initial and the median final loop areas

decreases with decreasing stress level. This difference tends towards zero below but close to the 20% stress level. This was also found previously for chipboard exposed to high and low frequency loading. If there is no change in the hysteresis loop area from the start to the finish of testing then no damage is being produced in the sample and it will never fail. This predicts that there is a fatigue limit for both OSB and chipboard at a stress level below 20%. Considering the S-N results together with the loop areas it is likely that the fatigue limit for MDF is also below the 20% stress level but slightly lower than that for OSB and chipboard.

Figure 10.26c shows the median changes in the hysteresis loop areas as a result of fatigue cycling for all stresses tested for the three materials. These values also decrease as stress is decreased from 60% down to 20% for OSB and chipboard. The values for MDF decreased below the 50% stress level. They also show that the change in loop area approaches zero just below the 20% stress level for all three materials as observed in figures 10.26a and 10.26b. The hysteresis loop area trends for chipboard were very similar regardless of the test frequency (section 8.9).

At the 80 and 70% stress levels for OSB, figures 10.27a-b, 10.28a-b and 10.29a-b there is a progressive increase in the loop area up to failure, as was observed for the chipboard. At the 60 and 50% stress levels, figures 10.27c-d, 10.28c-d and 10.29c-d this is a three stage process. There is a rapid initial increase, followed by an almost linear more gradual increase and ending with a rapid final stage leading to failure, which was not captured for the chipboard. The damage builds up rapidly during initial cycling and then continues to increase at a slower rate and then there is a rapid increase leading to failure of the sample. This agrees with the fatigue modulus data where there was a slow but continuous decrease in the fatigue modulus throughout testing after an initial rapid decrease. At the 20% stress level, figure 10.27e, 10.28e and 10.29e there is almost no increase in loop area implying that little or no damage was inflicted on the fatigue sample.

The loop areas for MDF at the 80 and 70% stress levels, figures 10.30a-b, 10.31a-b and 10.32a-b must be treated with caution due to the magnitude of the deflections and the surface indentions but the initial values were very high regardless of the possible errors. At the 60 and 50% stress levels, figures 10.30c-d, 10.31c-d and 10.32c-d the loop areas increase throughout testing and at the 50% stress level the loop area increases as a three stages as for OSB and chipboard. At the 40 and 20% stress level, figures 10.30e-f, 10.31e-f and 10.32e-f there is little or no increase in the loop areas

implying that the samples are not damaged. However, for the 40% stress level this contradicts the residual strength measured (see section 10.2).

10.8 Interim Conclusions 4

1) Normalised with respect to the static strengths, the fatigue performance of chipboard was superior to that of OSB, although the two materials have very similar performances at low stress levels. Normalised with respect to the static strengths, the fatigue performance of MDF was inferior to both materials and at lower stress levels the fatigue performance deteriorated to a greater extent. There was no correlation between the fatigue lives and the constituent particle size for the three materials.

2) Considered with respect to the applied stress (MPa), the fatigue performance of MDF was superior to that of OSB which was superior to that of chipboard. However, as the stress was reduced and the resulting fatigue lives extended, the difference between the three materials reduced. At low stresses the performances of the three materials were quite similar. Fatigue life was again not correlated to the constituent particle size.

3) The use of side-matched sets of samples reduced the spread of the measured fatigue lives for chipboard and MDF but not for OSB.

4) The static strengths were closely related to the linear regression lines fitted to the fatigue lives for chipboard and OSB but not for MDF.

5) The residual strengths for OSB were impossible to interpret due to the excessive scatter in the original strengths. There was a significant reduction in the residual strength for MDF after being fatigue loaded at the 40% stress level. This indicated that MDF was fatigue damaged at lower percentage stress levels than chipboard which agreed with the S-N results. However, this does not account for the stresses applied to MDF being higher for equivalent stress levels.

6) Creep and fatigue microstrains for OSB and MDF decreased with reducing stress level in the same manner as for chipboard.

7) The creep rate reduced for the maximum fatigue microstrain curves as the stress level was reduced for OSB and MDF in the same manner as for chipboard.

8) Creep samples failed before the fatigue samples at the highest stress levels tested only. This trend was reversed at the lower stress levels.

9) The creep and fatigue microstrains were both considerably higher for MDF than for OSB and chipboard. However, the use of normalised stresses resulted in considerably higher stresses being imposed on the MDF samples.

10) The microstrains at individual stress levels were more varied for OSB than for chipboard and MDF.

11) The difference between the maximum fatigue microstrains and the creep microstrains for side-matched samples was greater for MDF than for OSB and chipboard.

12) The median initial dynamic moduli were very similar for chipboard and MDF which were both lower than for OSB. The dynamic moduli reduced with reducing stress level for all three materials.

13) The median final dynamic moduli were almost constant for failed samples.

14) The dynamic moduli for chipboard and MDF were very similar despite the large deflections for MDF.

15) The magnitude of the dynamic moduli did not correlate with the constituent particle size, contradicting the literature.

16) The dynamic moduli at individual stress levels were more varied for OSB than for chipboard and MDF.

17) The dynamic moduli decreased throughout testing for all three materials between the 70 and 50% stress levels. The decreases were always small.

18) Dynamic moduli decreased in three stages (this was not captured for MDF).

19) Below the 40% stress level there was very little or no decrease in the dynamic modulus for all three materials, indicating that very little or no damage occurred.

20) The median final fatigue moduli decreased with decreasing stress level for failed samples for all three materials.

21) The fatigue moduli for chipboard and MDF were very similar, those for OSB were considerably greater. At individual stress levels the fatigue moduli were more varied for OSB than for chipboard and MDF.

22) The fatigue moduli decreased throughout testing for all three materials at all stress levels. Three stage decreases were observed for OSB, chipboard and MDF.

23) The magnitude of the decreases in the dynamic moduli were always less than for the fatigue moduli.

24) The initial and final hysteresis loop areas decreased with reducing stress level for all three materials.

25) The magnitude of the hysteresis loop areas were very similar for OSB and chipboard, showing that the damage produced per loading cycle was similar. The loop areas for MDF were far greater but this was expected because the loop area will be approximately proportional to the square of the stress range.

26) The median initial, median final and median changes in the hysteresis loop areas reduced with decreasing stress level for all three materials. The change in loop area tended towards zero for all three materials at a stress level just below 20%. No increase in the hysteresis loop areas indicates that no damage has occurred. This indicated that all three materials have fatigue limits at just below 20% stress with the fatigue limit for MDF slightly lower than those for OSB and chipboard.

27) Three stage increases in the hysteresis loop areas were observed for all three materials.

28) The hysteresis loop area trends for individual samples tested at 40% stress and below showed little or no increase in the hysteresis loop areas. Again this indicates that little or no damage has occurred.

11.0 MAJOR CONCLUSIONS

1) Increasing the loading rate the for static testing of chipboard increased the bending strengths and strength variability slightly.

2) The use of side-matched samples and normalised stresses reduced the scatter of the fatigue life data and hysteresis loop parameters for chipboard and MDF but not for OSB. All the properties measured for OSB were more variable than those for chipboard and MDF.

3) Reducing the test frequency by one and then two orders of magnitude causes chipboard to fail at shorter fatigue lives compared to testing at the same stress level at higher loading frequencies.

4) The linear regression lines fitted to the fatigue data pass close to the static strengths for chipboard loaded at all three frequencies and for OSB loaded at medium frequency but not for MDF loaded at medium frequency.

5) The creep microstrains, maximum fatigue microstrains, minimum fatigue microstrains, dynamic moduli, fatigue moduli and hysteresis loop areas for chipboard are virtually unaffected by changing the loading frequency.

6) The median initial, median final and median changes in the hysteresis loop areas reduced with decreasing stress level for OSB and MDF loaded at medium frequency, and for chipboard at all three frequencies. The change in loop area tended towards zero for OSB and MDF and for chipboard regardless of frequency at a stress level just below 20%. This indicated that all three materials have fatigue limits at just below 20% stress with the fatigue limit for MDF slightly lower than those for OSB and chipboard. The fatigue limit for chipboard was unaffected by the loading frequency.

7) Reducing the frequency of fatigue loading reduced the scatter/variability of the fatigue life data.

8) The limited data collected indicated that chipboard loaded axially was stronger in compression than in tension in the ratio of 1.7:1 which is the opposite of wood. Axial loading in tension/tension produced lower strains and higher hysteresis loop areas than for loading in compression/compression implying that compression is the more damaging of the two loading modes.

hysteresis loop areas than for loading in compression/compression implying that tension is the more damaging of the two loading modes.

9) The bending strengths measured for the three panel products decreased as follows, MDF>OSB>chipboard.

10) The mean densities for the three panel products decreased in the following order, chipboard>MDF>OSB.

11) The constituent particle size did not correlate with the bending strength, density, fatigue lives (normalised or not), dynamic moduli, fatigue moduli and hysteresis loop areas. The only correlation was with the strength variability.

12) Normalised with respect to the static strengths, the fatigue performance of chipboard was superior to that of OSB, although the two materials have very similar performances at low stress levels. The fatigue performance of MDF was inferior to both materials and at lower stress levels the fatigue performance deteriorated to a greater extent.

13) Considered with respect to the applied stress (MPa), the fatigue performance of MDF was superior to that of OSB which was superior to that of chipboard. However, as the stress was reduced and the resulting fatigue lives extended, the difference between the three materials reduced. At low stresses the performances of the three materials was quite similar.

14) Creep and fatigue microstrains for OSB and MDF loaded at medium frequency and for chipboard loaded at all frequencies decreased with reducing stress level.

15) The dynamic moduli and fatigue moduli for chipboard and MDF were very similar despite the large deflections for MDF while those for OSB were considerably higher.

16) In general the dynamic moduli and fatigue moduli reduced throughout testing for OSB and MDF, and for chipboard at all three frequencies. The magnitude of the decreases reducing with decreasing stress level. Fatigue moduli decreased further than the dynamic moduli due to the underlying creep. Simultaneously the hysteresis loop areas increase throughout testing with the magnitude of the loop areas decreasing with decreasing stress level.

12.0 IMPLICATIONS OF CONCLUSIONS

a) Chipboard subjected to fatigue loading must use fatigue stress and not creep stress design parameters.

b) Using design stresses from creep results to predict fatigue lives at the same peak stress level is likely overestimate the life of the material.

c) Fatigue design parameters for chipboard must account for the frequency of the fatigue loading. This will affect the life of the material significantly.

d) The lower the frequency of the fatigue loading the lower the number of cycles required to break the material.

e) The relative properties of OSB, chipboard and MDF are highlighted in figure 12.1: Chipboard and MDF are very similar in stiffness but MDF can sustain far higher stresses and strains than chipboard. OSB is stiffer than both chipboard and MDF and OSB will sustain similar strains to chipboard. This means that OSB is the best material where stiffness is of prime importance but if damage tolerance is required then MDF is superior.

It must, however, be remembered that these results do not consider the long term duration of load performances of the three panels. These results are also representative of a single manufacturer's brand of each panel type.

Fig 12.1

FIRST CAPTURED HYSTERESIS LOOPS FOR
OSB, CHIPBOARD & MDF, 70% STRESS,
R=0.1

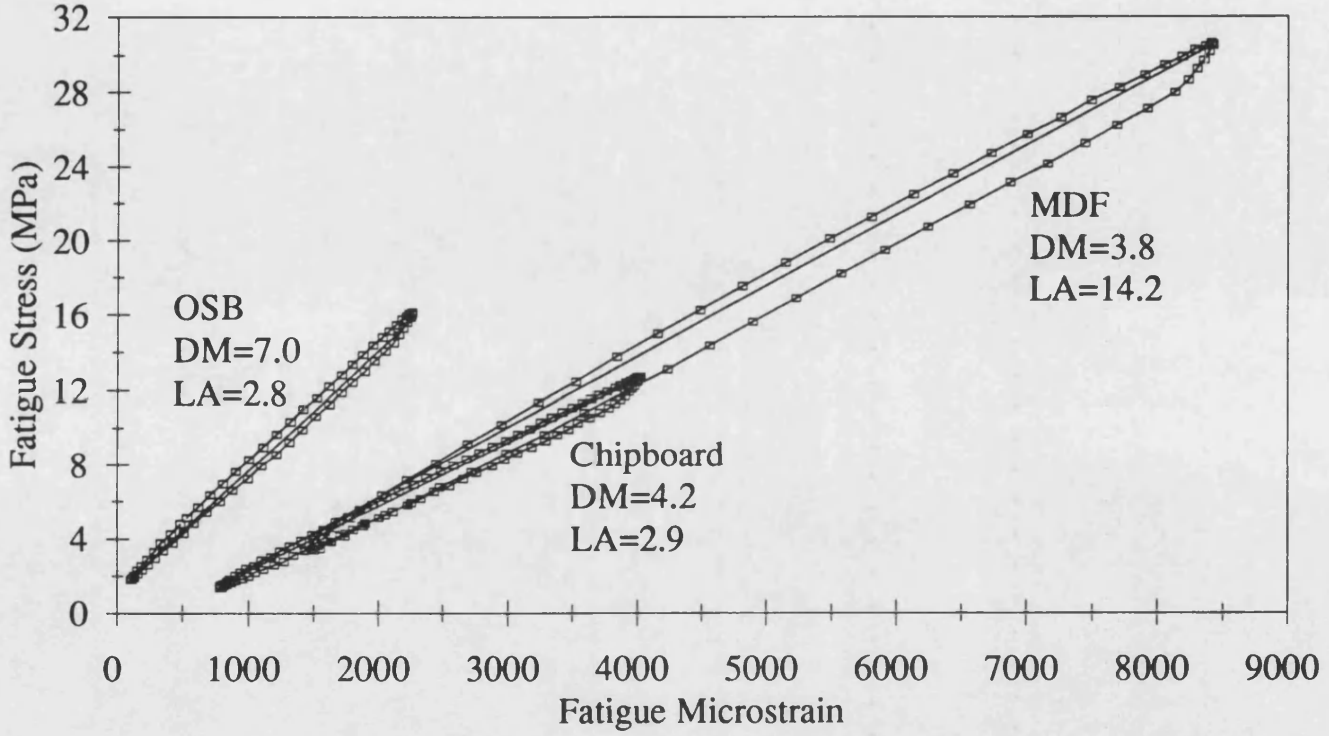

DM = Median Dynamic Modulus (GPa) LA = Median Loop Area (J/m^3)
(Median values are from six tests for each material)

(C:\OSB\1_LASTT.WB1)

13.0 REFERENCES

Anderson, J. (1995). Past, present and future for OSB. Institute of Wood Science 40th Anniversary Conference. Swallow Royal Hotel, Bristol, UK. 28 - 30th April 1995.

Andriamitantsoa, L. A. (1995). Creep. STEP Lecture A19. STEP/EUROFORTECH - an initiative under the EU Comett Programme.

Ansell, M.P. and Bonfield, P.W. (1990). High frequency cyclic loading of chipboard. First Progress Report. Prepared for the Building Research Establishment. University of Bath Internal Report.

Ansell, M.P. (1983). Layman's guide to fatigue. Wind Energy Conservation, Ed Gault, J.M. Mechanical Engineering Publications Ltd., London, pp. 39-54.

Armstrong, L.D. and Grossman, P.U.A. (1972). The behaviour of particleboard and hardboard beams during moisture cycling. Wood Sci. and Tech. Vol. 6, No. 2, pp. 128-137.

Ashby, M.F. and Jones, D.R.H. (1986). Engineering Materials 2: An introduction to microstructures and design. Pergamon Press.

Bender, D.A., Taylor, S.E. and Swinnea, J.W. (1988). Load rate adjustment for tensile proof testing of southern pine 2 by 10's. Forest Prod. J. Vol. 38, No. 6, pp. 26-30.

Bennett, J.P. (1993). A suite of programs for creep modelling. Bath University, School of Mathematical Sciences - Private Memorandum.

Bodig, J and Jayne, B.A. (1982). Mechanics of wood and wood composites. Van Nostrand Reinhold Co. Inc., New York.

Bond, I.P. (1994). The fatigue design of commercial wood composite wind turbine blades. PhD. Thesis, University of Bath.

Bonfield, P.W., Dinwoodie, J.M., Paxton, B.H. and Mundy, J.S. (1995). Slow cyclic fatigue of chipboard. Proceedings of COST508 Wood Mechanics Workshop on Mechanical Properties of Panel Products.

Bonfield, P.W., Hacker, C.L., Ansell, M.P. and Dinwoodie, J.M. (1994a). Fatigue and creep of chipboard. Part 1: Fatigue at R=0.01. Wood Sci. and Tech. Vol. 28, No. 6, pp. 423-435.

Bonfield, P.W., Dinwoodie, J.M., Paxton, B.H. and Mundy, J.S. (1994b). Creep in wood-based board materials. Proceedings of the Pacific Timber Engineering Conference. Gold Coast, Australia.

Bonfield, P.W., Dinwoodie, J.M., Ansell, M.P. and Hacker, C.L. (1993). Damage quantification of wood and wood-based products via stress-strain hysteresis loop capture. Proceedings of COST508 Wood Mechanics Workshop on Failure and Plasticity in Wood.

Bonfield, P.W. (1991). Fatigue evaluation of wood laminates for the design of wind turbine blades. PhD. Thesis, University of Bath.

BRE Digest 323 (1992b). Selecting wood-based panel products. The Building Research Establishment, Garston, Watford.

BRE Digest 373 (1992a). Wood chipboard. The Building Research Establishment, Garston, Watford.

BRE Information Paper IP 12/91, (1991). Fibre building board: types and uses. The Building Research Establishment, Garston, Watford.

BRE Information Paper IP 5/86, (1986). Waferboard and OSB. The Building Research Establishment, Garston, Watford.

BS1142 (1989). Fibre building boards, Part 2: mediumboard and hardboard.

BS5268 (1987). Part 2: Domestic flooring and flat roof decking.

BS 5669 (1989). British standard for particleboard. British Standards Institution.

BS8201 (1987). Code of practice for flooring of timber, timber products and wood based panel products.

Clad, W. and Schmidt-Helleraue, Ch. (1981a). (Abstract only in English). Fatigue testing of particleboard 1: test results of industrially manufactured particleboard. Holz als Roh-und Werkstoff. Vol. 39, pp. 217-222.

Clad, W. and Schmidt-Helleraue, Ch. (1981b). (Abstract only in English). Fatigue testing of particleboard 2: supplementary tests. Holz als Roh-und Werkstoff. Vol. 39, pp. 241-248.

Clarke, P. (1991). Panel products - past present and future - developments. J. Inst. Wood Sci. Vol. 12, No. 4, pp.233-241.

Crane, F.A.A. and Charles, J.A. (1985). Selection and use of engineering materials. Butterworths.

D'Agostino, R. B. and Stephens, M. A. (1986). Goodness-of-fit techniques. Marcel Dekker, Inc., New York, USA.

Desch, H.E. and Dinwoodie, J.M. (1981). Timber its structure, properties and utilisation. 6th Edition. Macmillan Press Ltd.

Dinwoodie, J.M., Paxton, B.H., Bonfield, P.W. and Mundy, J.S. (1995). Fatigue and creep in chipboard. Part 2: the influence of slow cyclic fatigue on the creep behaviour of chipboard at a range of stress levels and moisture contents. Wood Sci. and Tech. Vol. 29, No. 1, pp. 64-76.

Dinwoodie, J.M. and Bonfield, P.W. (1995). Recent research on the rheological behaviour of wood based panels. Proceedings of COST 508 Wood Mechanics Workshop on mechanical properties of panel products. 22-23 March 1995.

Dinwoodie, J.M., Higgins, J.-A., Paxton, B.H., and Robson, D.J. (1992a). Creep in chipboard. Part 11: the effect of cyclic changes in moisture content on creep behaviour of a range of boards at different levels of stressing. Wood Sci. and Tech. Vol. 26, pp. 429-448.

Dinwoodie, J.M., Paxton, B.H., Higgins, J.-A. and Robson, D.J. (1992b). Creep in chipboard. Part 10: the effect of variable climate on the creep behaviour of a range of chipboards and one waferboard. Wood Sci. and Tech. Vol. 26, pp. 39-53.

Dinwoodie, J.M., Higgins, J.-A., Paxton, B.H. and Robson, D.J. (1991a). Creep in chipboard. Part 9: the effect of steady state moisture content, temperature and level of stressing on the components of creep deflection for a range of boards. Wood Sci. and Tech. Vol. 25, pp. 383-396.

Dinwoodie, J.M., Robson, D.J., Paxton, B.H. and Higgins, J.-A. (1991b). Creep in chipboard. Part 8: the effect of steady state moisture content, temperature and level of stressing on the relative creep behaviour and creep modulus of a range of boards. Wood Sci. and Tech. Vol. 25, No. 3, pp. 225-239.

Dinwoodie, J.M., Higgins, J.-A., Paxton, B.H. and Robson, D.J. (1991c). Quantifying, predicting and understanding the mechanism of creep in board materials. Proceedings of COST 508 Wood Mechanics Workshop on the Fundamental Aspects of Creep in Wood. March 20-21, 1991.

Dinwoodie, J.M. Higgins, J.-A., Robson, D.J. and Paxton, B.H. (1990a). Creep in Chipboard. Part 7: Testing the efficiency of models on 7-10 years data and evaluating optimum period of prediction. Wood Sci. and Tech. Vol. 24, pp. 181-189.

Dinwoodie, J.M. Higgins, J.-A., Paxton, B.H. and Robson, D.J. (1990b). Creep research on particleboard. 15 year's work at the UK Building Research Establishment. Holz als Roh-und Werkstoff. Vol. 48, pp. 5-10.

Dinwoodie, J.M. (1989). Wood: nature's cellular, polymeric fibre composite. The Institute of Metals.

Dinwoodie, J.M., Paxton, B.H., Pierce, C.B. and Aloysius, E.J. (1984). Quantification and prediction of creep in particleboard. In 42nd Meeting of the Technical Commission of the European Federation of Associates of Particleboard Manufacturers Reports and Discussions, pp. 79-94.

Dinwoodie, J.M. (1981). Timber: its nature and behaviour. Van Nostrand Reinhold Co. Inc., New York.

Foliente, G. (1994). Hysteresis characterisation and modelling of timber joints and structures. Proceedings of the Pacific Timber Engineering Conference. Gold Coast, Australia.

Freas, A.D. and Werren, F. (1959). Effect of repeated loading and salt-water immersion on flexural properties of laminated white oak. Forest Prod. J., Vol. 9, No. 2, pp. 100-103.

Fuller, F.B. and Oberg, T.T. (1943). Fatigue characteristics of natural and resin-impregnated, compressed, laminated woods. J. Aeronautical Sci. March 1943, pp. 81-85.

Gerhards, C.C. and Link, C.L. (1986). Effect of loading rate on the bending strength of Douglas-fir 2 by 4's. Forest Prod. J. Vol. 36, No. 2, pp. 63-66.

Gerhards, C.C., Marx, C.M, Green, D.W. and Evans, J.W. (1984). Effect of loading rate on the tensile strength of douglas-fir 2 by 6's. Forest Prod. J. Vol. 34, No. 4, pp. 23-26.

Gibson, E.J. (1992). Wood: a natural fibre reinforced composite. Metals and Materials. Vol. 8, No. 6, pp. 333-336.

Gillwald, W. (1966). Investigations on the fatigue resistance of multiple layer particleboard. (Abstract only in English). Int. J. of Fracture. (1980) Vol. 16 No. 6.

Gressel, P. (1984). Long term particleboard performance under load. In 42nd Meeting of the Technical Commission of the European Federation of Associates of Particleboard Manufacturers Reports and Discussions, pp. 62-78.

Griffiths, D.R. and Wickens, H.G. (1995). CEC Programme: Design stresses for OSB. University of Surrey tests and reduction of results. Proceedings of COST 508 Wood Mechanics Workshop on mechanical properties of panel products. 22-23 March 1995.

Grossman, P.A.U. and Nakai, T. (1987). Deflection of wood under intermittent loading. Part 2: Cycles of two days and fourteen minutes. Wood Sci. and Tech. Vol. 21, pp. 349-360.

Hacker, C.L. (1995). Fatigue damage in wood composites. PhD. Thesis, University of Bath.

Hacker, C.L. (1993). Damage accumulation in wood composites under fatigue loading. Second Year Report for the DOE, Contract No. E/5A/6111/2818. School of Materials Sci., University of Bath. (Internal Report).

Hacker, C.L. (1991). Fatigue and creep of structural grade chipboard. Final Year Project Report. School of Materials Sci., The University of Bath. (Internal Report).

Hall, H. and Haygreen, J. (1978). Flexural creep of 5/8-inch particleboard and plywood during 2 years of concentrated loading. Forest Prod. J. Vol. 28, No. 6 pp. 19-22.

Hammant, B. (1971). The use of 4-point loading to determine mechanical properties. Composites, Dec. 1971, pp. 246-249.

Ibuki, Y., Sasaki, H., Kawamoto, Maku, T. (1962). (Abstract only in English.) On the endurance of glue-laminated wood. The plane bending strength of glue-laminated wood. J. Jap. Soc. Test. Mater., Vol. 11, No. 101, pp. 103-109.

Imayana, N. and Matsumoto, T. (1970). (Abstract only in English.) Studies on the fatigue of wood. 1. Phenomenological study on the fatigue process. Mokuzai Gakkaishi (J. Jap. Wood Research Soc.), Vol. 20, No. 2, pp. 319-325.

Kajita, H., Mukudai, J. and Yano, H. (1991). Durability evaluation of particleboard by accelerated ageing tests. Wood Sci. and Tech. Vol. 25, pp. 239-249.

Kato, K., Suzuki, S. and Saito, F. (1990). (Abstract only in English.) Fatigue properties of particleboards 2. Effects of partial non-reversed loading on tensile fatigue properties. Mokuzai Gakkaishi (J. Japan Wood Research Soc.), Vol. 36, No. 12, pp. 1057-1062.

Kingston, R.S.T. and Budgen, B. (1972). Some aspects of the rheological behaviour of wood. Part 4: Non-linear behaviour at high stresses in bending and compression. Wood Sci. and Tech. Vol. 6, pp. 230-238.

Kliger, R. (1991). Creep and duration of load behaviour of board materials. Final Report. Department of Structural Engineering, Chalmers University of Tech., Sweden.

Kommers, W.J. (1943). The fatigue behaviour of wood and plywood subjected to repeated and reversed bending stresses. U.S. Forest Prod. Lab. Rep. No. 1327.

Kollman, F. and Krech, H. (1961). Fracture range and resistance of particleboard. (Abstract only in English). Int J. of Fracture. (1990). Vol. 16, No. 6, pp. 113-118.

Kyanka, G.H. (1980). Fatigue properties of wood and wood composites. International J. of Fracture. Vol. 16, No. 6, pp. 609-616.

Lee, L.J., Yang, J.N. and Sheu, D.Y. (1993). Prediction of fatigue life for matrix-dominated composite laminates. Comp. Sci. and Tech. Vol. 46, pp. 21-28.

Lewis, W.C. (1962). Fatigue resistance of quarter-scale bridge stingers in flexure and shear. U.S. For. Prod. Lab. Rep. No. 2236.

Lewis, C. (1960). Design considerations for fatigue in timber structures. J. of the Struct. Div. Proc. of ASCE., pp. 15-23.

Lyon, D.E. and Barnes, H.M. (1978). Time dependent properties of particleboard decking in flexure. Forest Prod. J. Vol. 28, No. 12, pp. 28-33.

Madsen, B. (1992). The structural behavior of timber. Timber Engineering LTD.

Maku, T. and Sasaki, H. (1963). (Abstract only in English.) The rotation bending fatigue strength of glued laminated wood. Mokuzai Kenkyu, No. 31 pp. 1-10.

McNatt, J.D., Wellwood, R.W. and Bach, L. (1990). Relationship between small-specimen and large panel bending tests on structural wood-based panels. Forest Prod. J. Vol. 40, No. 9, pp. 10-16.

McNatt, J.D. (1984). Static bending properties of structural wood-based panels: large panel versus small-specimen tests. Forest Prod. J. Vol. 34, No. 4, pp. 50-54.

McNatt, J.D. and Hunt, M.O. (1982). Creep of thick structural flakeboards in constant and cyclic humidity. Forest Prod. J. Vol. 32, No. 5, pp. 49-53.

McNatt, J.D. (1977). Research note: linear regression of fatigue data. Wood Sci. and Tech. Vol. 11, No. 1, pp. 39-41.

McNatt, J.D. and Werren, F. (1975). Fatigue properties of three particleboards in tension and interlaminar shear. Forest Prod. J. Vol. 26, pp. 45-48.

Mundy, J.S. (1993). Wood product usage figures. Private communication taken from FAO Timber Bulletin XLIV No. 9.

Nakai, T. and Grossman, P.U.A. (1983). Deflection of wood under intermittent loading. Wood Sci.and Tech.. Vol 17, pp. 55-67.

Owen, D.B. (1962). Handbook of statistical tables. Adison - Welsey Publishing Co. Inc., Massachusetts, pp. 318.

Park, J-Y. and Mataki, Y. (1990a). (Abstract only in English). Bending fatigue characteristics of particleboard under controlled deflection. Mokuzai Gakkaishi (J. Japan Wood Research Soc.), Vol. 36, No. 11, pp. 952-960.

Park, J-Y. and Mataki, Y.(1990b). (Abstract only in English). Behaviour of hysteresis energy in bending fatigue for particleboard. Mokuzai Gakkaishi (J. Japan Wood Research Soc.), Vol. 36, No. 11, pp. 961-968.

Pierce, C.B., Dinwoodie, J.M. and Paxton, B.H. (1986). Creep in chipboard. Part 6: time to failure analysis under steady state conditions. Wood Sci. and Tech. Vol. 20, pp. 281-292.

Pierce, C.B., Dinwoodie, J.M. and Paxton, B.H. (1985). Creep in chipboard. Part 5: an improved model for prediction of creep deflection. Wood Sci. and Tech. Vol. 19, pp. 83-91.

Robson, D.J. (1988). Creep in chipboard, an improved model of creep. BRE Note, File Number PR4/020.

Rotem, A. (1988). Residual strength after fatigue loading. Int. J. of Fatigue. Vol. 10, No. 1, pp. 27-31.

Rowntree, D. (1981). Statistics without tears - a primer for non-mathmaticians. Penguin.

Salmén, L. (1987). The effect of the frequency of a mechanical deformation on the fatigue of wood. J. of Pulp and Paper Sci. Vol. 13 (1), pp. 23-28.

Salmén, L., Tigerström, A. and Fellers, C. (1985). Fatigue of wood - characterisation of mechanical defibrillation. J. of Pulp and Paper Sci. Vol. 11 (3), pp. 68-73.

Schober, B. (1987). Studies of the effect of loading on creep behaviour of solid wood and particleboards. Holzechnologie Vol. 28, No. 1, pp. 13-16. (BRE Library translation No. LT89/13).

Sekhar, A.C., Sukla, N.K. and Gupta, V.K. (1963). A note on the fatigue properties of timber: effect of torsional stress and moisture content. J. Natn. Blbgs. Org., Vol. 8, No. 4, pp. 36-40.

Sekino, N. and Okuma, M. (1985). Performance over time of construction particleboard 1. Fatigue behaviour in bending. Mokuzai Gakkaishi (J. Japan Wood Research Soc.), Vol. 31, No. 10, pp. 801-806.

Sterr, R. (1963). Investigation on the fatigue strength of laminated wood beams. Holz. als Roh und Werkstoff, Vol. 21, No. 2, pp. 47-61, (Trans. No. 171. Canada. Dept. of For. For. Prod. Res. Branch.)

Suzuki, S. and Saito, F. (1988). Fatigue properties of particleboards 1. Effects of ageing on tensile properties parallel to the surface. Mokuzai Gakkaishi (J. Japan Wood Research Soc.), Vol. 34, No. 7, pp. 590-596.

Suzuki, S. and Saito, F. (1987). (Abstract only in English.) Effects of environmental factors on the properties of particleboard 1. Effects of temperature on bending properties. Mokuzai Gakkaishi (J. Japan Wood Research Soc.), Vol. 33, No. 4, pp. 298-303.

Suzuki, S. and Saito, F. (1986). Fatigue behaviour of particleboard in tension perpendicular to the surface 2. Effect of moisture content. Mokuzai Gakkaishi (J. Japan Wood Research Soc.), Vol. 32, No. 10, pp. 801-807.

Suzuki, S. and Saito, F. (1984). Fatigue behaviour of particleboard in tension perpendicular to the surface 1. Effects of resin type. Mokuzai Gakkaishi (J. Japan Wood Research Soc.), Vol. 30, No. 10, pp. 799-806.

Tanaka, A. and Suzuki, M. (1984). (Abstract only in English.) Bending fatigue strength of particleboard. Mokuzai Gakkaishi (J. Japan Wood Research Soc.), Vol. 30, No. 10 pp. 807-813.

Talreja, R. (1981). Estimation of Weibull parameters for composite material strength and fatigue life data. Fatigue of fibrous composite materials, ASTM 723, American Soc. for Test. and Mat., pp. 291-311.

Thompson, R.J.H., Bonfield, P.W., Hacker, C.L., Dinwoodie, J.M. and Ansell, M.P. (1994). Creep and fatigue of chipboard in flexure. Proceedings of the Pacific Timber Engineering Conference. Gold Coast Australia.

Thompson, R.J.H. (1992). Fatigue and creep characteristics of structural grade chipboard. Final Year Project Report. School of Materials Sci., The University of Bath. (Internal Report).

TRADA (1992). Wood information sheet, section 2/3, sheet 34. Structural grade chipboard. Timber Research and Development Association, High Wycombe, Buckinghamshire.

TRADA (1985a). Wood information sheet, section 2/3, sheet 23. Introduction to wood-based panel products. Timber Research and Development Association, High Wycombe, Buckinghamshire.

TRADA (1985b). Wood information sheet, section 2/3, sheet 23. Timber and wood-based sheet materials for floors. Timber Research and Development Association, High Wycombe, Buckinghamshire.

Tsai, K.T. and Ansell M.P. (1990). The fatigue properties of wood in flexure. J. of Mat. Sci., Vol. 25, pp. 865-878.

Tsai, K.T. (1987). An investigation into the fatigue properties of wood laminates for wind energy converter blade design. PhD Thesis, University of Bath.

Urakami, H. and Fukuyama, M. (1982). A rheological model of bending creep in wood with an analysis of model element constants (Translated from Japanese). Mokuzai Gakkaishi (J. Japan Wood Research Soc.), Vol. 28, No. 7, pp. 414-421.

Wood Panel Products Federation (WPPF) folder, "the facts on boards" (1994). Wood panel products information sheets:

WPPF Ref PD/6, medium density fibreboard (1994);
WPPF Ref PD/7, medium density fibreboard - moisture resistant (1994);
WPPF Ref PD/11, wood chipboard - type C1 (1992);
WPPF Ref PD/12, wood chipboard - type C1A (1992);
WPPF Ref PD/13, wood chipboard - type C2 (1992);
WPPF Ref PD/14, wood chipboard - type C3 (1992);
WPPF Ref PD/15, wood chipboard - type C4 (1992);
WPPF Ref PD/16, wood chipboard - type C5 (1992);
WPPF Ref PD/17, oriented strand board - type F1 (1992);
WPPF Ref PD/18, oriented strand board - type F2 (1992);
WPPF Ref AD/16, structural floor decking on joists (1994);

Weibull, W. (1952). Statistiacl design of fatigue experiments. J. of Applied Mechanics, Vol. 19, pp. 109-113.

Wöhler, M. (1867). "Wöhler's experiments on the strength of metals", Engineering, August 23.

Yang, J.N., Lee, L.J. and Sheu, D.Y. (1992). Modulus reduction and fatigue damage of matrix dominated composite laminates. Composite Struct. Vol. 21, pp. 91-100.

APPENDIX 1A: Surface Stress and Strain Calculations

The FDAS calculated and recorded the surface stresses and strains for the creep and fatigue samples for each hysteresis loop captured using the formulae below with the dimensions shown in figure A1.1.

$$\text{Strain} = 16(Ts * y)/[(2l + d) \times 1000000]$$

$$\text{Stress} = 3/4F*[(2l + d)/B_S * Ts^2] \times 1000$$

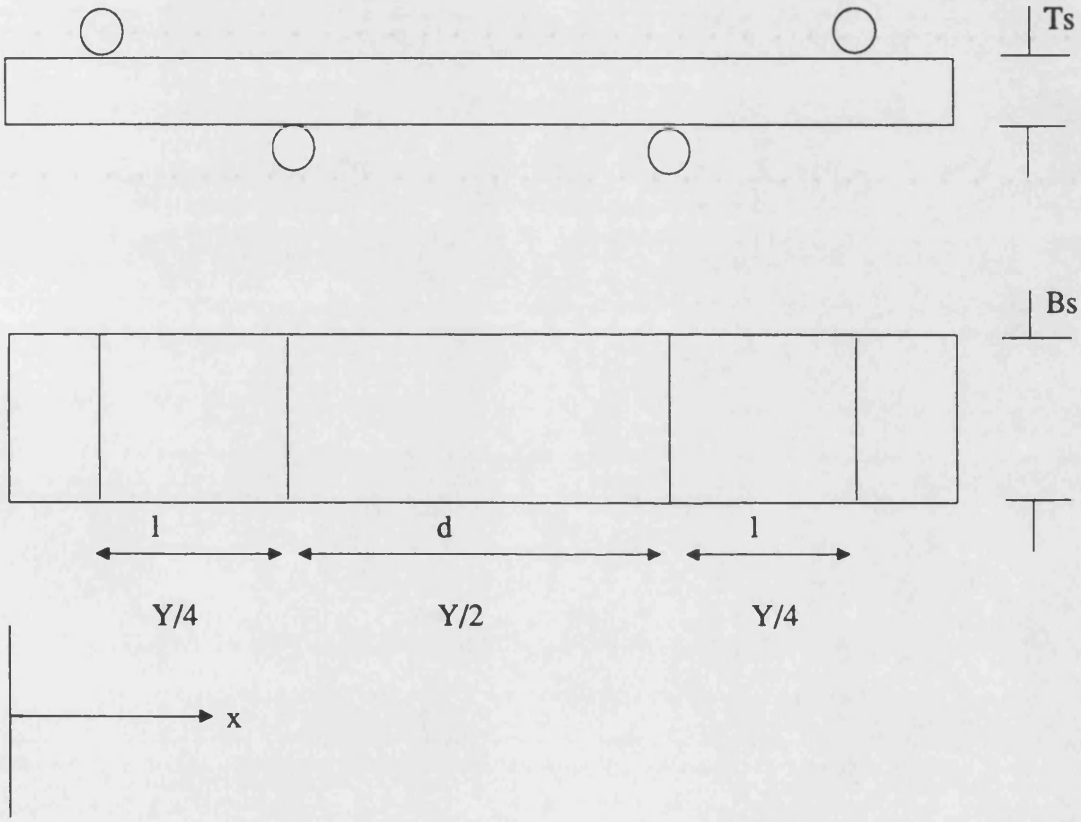

Fig A1.1 Sample dimensions.

l, Bs ,Ts, d, are all in mm.

y = measured deformation in mm.

F = measured force in kN.

Y = 300 mm, the distance between the outer supports.

APPENDIX 1B: Test Parameter Equations

The test programmes included in Appendix 3 were used to calculate the following parameters: maximum and minimum fatigue stresses; the maximum and minimum fatigue loads; the mean fatigue stress and mean load; the creep load and creep weight. The frequency was also calculated which is described in Appendix 2.

Variables	Input
Smax = max stress, MPa	Pult = % ultimate load
Smin = min stress, MPa	Smu = mean ultimate stress, MPa
Pmax = max load, kN	Bf = fatigue sample breadth (width), mm
Pmin = min load, kN	Tf = fatigue sample thickness, mm
Pmean = mean load, kN	Tc = creep sample thickness, mm
Pc = creep load, kN	Bc = creep sample breadth (width), mm
Wc = creep weight, kg	Ts = sample thickness, mm
	Bs = sample breadth, mm

1) Max stress = (mean ultimate stress) * (% ultimate load)

$$Smax = Smin * Pult$$

2) Min stress = (max stress) * (R ratio) where R=0.1 or 0.25

$$Smin = Smax * R$$

3) Max load applied to the fatigue sample to give the required max stress was calculated using the beam formulae. The dimensions are shown in figure A1.2.

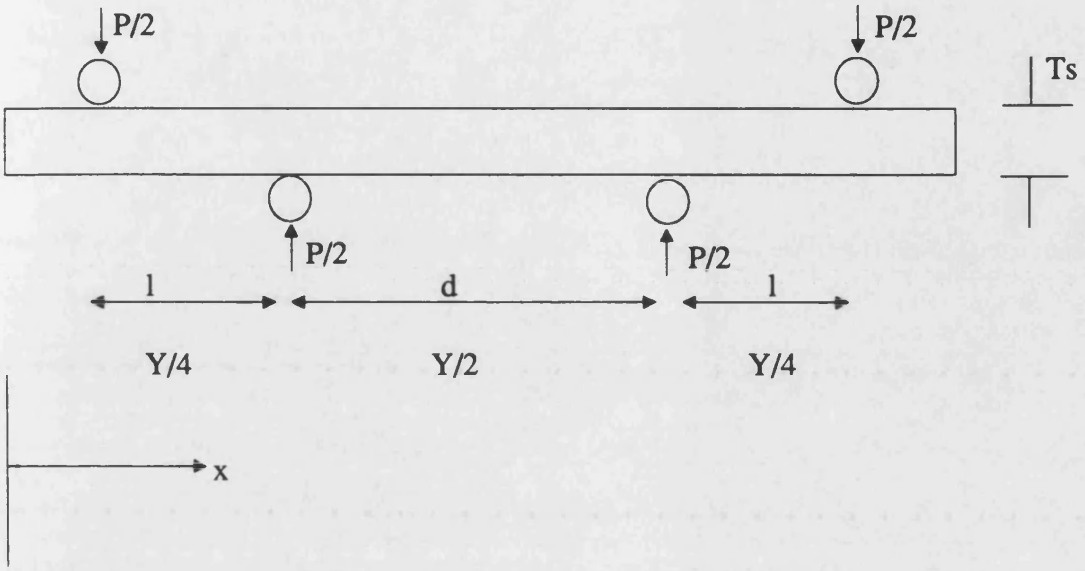

Fig A1.2 Sample loading configuration.

M = bending moment of central span

I = second moment of area

$$M = (P/2)x - P/2\,[x-(Y/4)] = (P/2) * (Y/4)$$

$$M = (Y * I)/8$$

$$Ss = (M * Y)/I$$

Ss = shear stress. Ss is a maximum at $\pm t/2$ (see figure A2)

$$I = (F * Ts^{3})/12$$

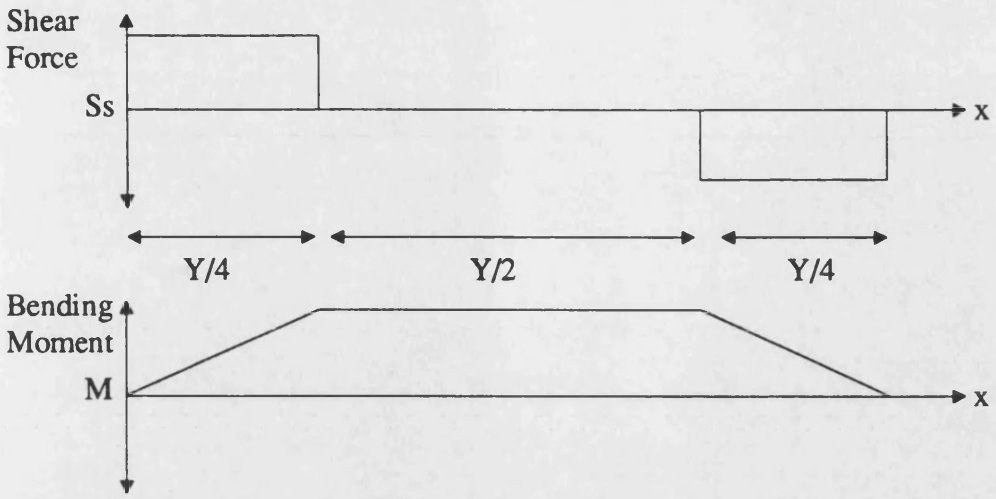

Fig. A1.3 Shear force and bending moment diagrams.

Span, Y = 300 mm

$$Smax = (3Y * I)/(4Bs * Ts^2)$$

Inserting Y = 300 mm and rearranging

$$I = (4Bs * Ts^2 * Smax)/900$$

4) Min load = (max load) * R where R = 0.25

$$Pmin = Pmax * R$$

5) Mean stress on sample

$$Smean = (Smax + Smin)/2$$

6) Mean load on sample

$$Pmean = (Pmax + Pmin)/2$$

7) Load applied to creep sample

$$Pc = (4Bc * Tc^2 * Smax)/900$$

8) Creep weight required

$$Wc = \frac{(\text{max load}) \text{ X } (\text{stress level})}{100 \text{ X } 9.81 \text{ X } 7} - 2.72$$

where 7 is the mechanical advantage of the lever arm.
The mass 2.72 kg comprises of:

1.00 kg - hanger
0.20 kg - hook and chain
1.52 kg - lever arm

9) The frequency of loading was calculated as shown in Appendix 2.

APPENDIX 2: RATE OF APPLICATION OF STRESS

All the fatigue tests for each loading configuration were performed at a constant rate of application of stress to minimise viscoelastic effects. To achieve this those tests with large stress amplitudes have to be performed at lower frequencies than those with small stress amplitudes. (The symbols were explained in Appendix 1.) The rates of application of stress were set at 1.2 MPa/s for low frequency testing, 12 MPa/s for medium frequency and 150 MPa/s for high frequency testing.

Using medium frequency loading as an example the frequency is determined using the rate of application of stress as follows:

Stress = (Rate of application of stress * Time) + Minimum Stress

$$S = 12t + Smin$$

at time $t = t/2$, $S = Smax$, so

$$Smax = 120(t/2) + Smin$$

rearranging for t,

$$t = 2(Smax - Smin)/12$$

$$f = 1/t = 12/[2(Smax-Smin)]$$

The triangular wave form below was used to calculate the average loading rate of the sinusoidal stress wave.

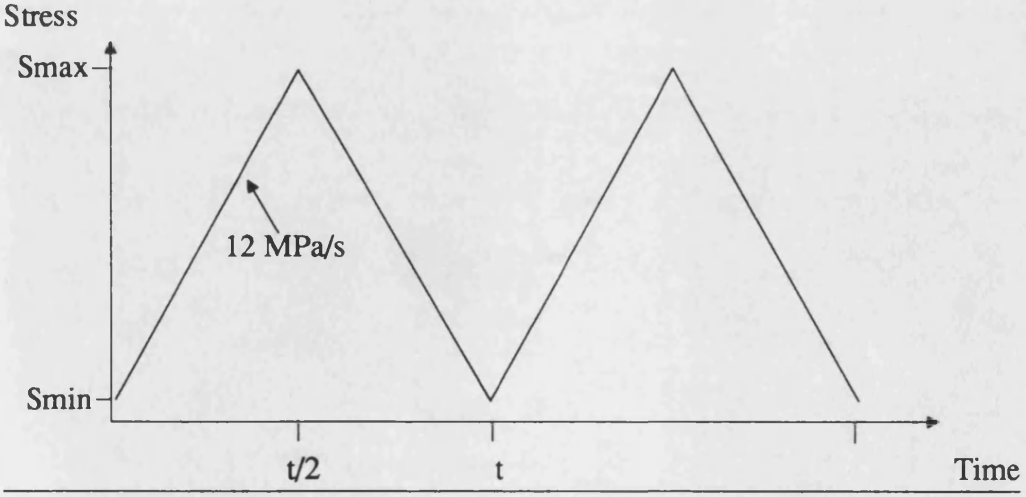

Fig. A2 Triangular Wave Form.

APPENDIX 3: Test Parameter Programmes

Low Frequency, R=0.1

```
10    REM R=0.1 1.2 MPa/s Calculations Programme
20    PRINT "R=0.1 1.2 MPa/s TEST VALUES PROGRAMME"
30    PRINT "Enter %, Mean Stress, Width, Thickness"
40    PRINT "and Width and Thickness for Creep Sample, R ratio"
50    INPUT Pult, Smu, Bf, Tf, Bc, Tc, R
60    LET Smax = Pult * Smu
70    LET Smin = R * Smax
80    LET Pmax = ( 4 * Bf * Tf * Tf * Smax ) / 900
90    LET Pmin = R * Pmax
100   LET Smean = ( Smax + Smin ) / 2
110   LET Pmean = (Pmax + Pmin) / 2
120   LET Pc = ( 4 * Bf * Tf * Tf * Smax ) / 900
130   LET Wc = ( Pc / 68.67 ) -2.72
140   LET f = .6 / ( Smax - Smin )
150   PRINT "Max Stress"; Smax; "MPa"
160   PRINT "Min Stress"; Smin; "MPa"
170   PRINT "Max Load"; Pmax; "N"
180   PRINT "Min Load"; Pmin; "N"
190   PRINT "Mean Stress"; Smean; "MPa"
200   PRINT "Mean Load"; Pmean; "N"
210   PRINT "Creep Load"; Pc; "N"
220   PRINT "Creep Weight"; Wc; "Kg"
230   PRINT "Frequency"; f; "Hz"
240   PRINT " "
250   GOTO 30
260   END
```

Medium Frequency, R=0.1

```
10    REM R=0.1 12 MPa/s Calculations Programme
20    PRINT "R=0.1 12 MPa/s TEST VALUES PROGRAMME"
30    PRINT "Enter %, Mean Stress, Width, Thickness"
40    PRINT "and Width and Thickness for Creep Sample, R ratio"
50    INPUT Pult, Smu, Bf, Tf, Bc, Tc, R
60    LET Smax = Pult * Smu
70    LET Smin = R * Smax
80    LET Pmax = ( 4 * Bf * Tf * Tf * Smax ) / 900
90    LET Pmin = R * Pmax
100   LET Smean = ( Smax + Smin ) / 2
110   LET Pmean = (Pmax + Pmin) / 2
120   LET Pc = ( 4 * Bf * Tf * Tf * Smax ) / 900
130   LET Wc = ( Pc / 68.67 ) -2.72
140   LET f = 6 / ( Smax - Smin )
150   PRINT "Max Stress"; Smax; "MPa"
160   PRINT "Min Stress"; Smin; "MPa"
170   PRINT "Max Load"; Pmax; "N"
180   PRINT "Min Load"; Pmin; "N"
190   PRINT "Mean Stress"; Smean; "MPa"
200   PRINT "Mean Load"; Pmean; "N"
210   PRINT "Creep Load"; Pc; "N"
220   PRINT "Creep Weight"; Wc; "Kg"
230   PRINT "Frequency"; f; "Hz"
240   PRINT " "
250   GOTO 30
260   END
```

High Frequency, R=0.1

```
10    REM R=0.1 150 MPa/s Calculations Programme
20    PRINT "R=0.1 150 MPa/s TEST VALUES PROGRAMME"
30    PRINT "Enter %, Mean Stress, Width, Thickness"
40    PRINT "and Width and Thickness for Creep Sample, R ratio"
50    INPUT Pult, Smu, Bf, Tf, Bc, Tc, R
60    LET Smax = Pult * Smu
70    LET Smin = R * Smax
80    LET Pmax = ( 4 * Bf * Tf * Tf * Smax ) / 900
90    LET Pmin = R * Pmax
100   LET Smean = ( Smax + Smin ) / 2
110   LET Pmean = (Pmax + Pmin) / 2
120   LET Pc = ( 4 * Bf * Tf * Tf * Smax ) / 900
130   LET Wc = ( Pc / 68.67 ) -2.72
140   LET f = 60 / ( Smax - Smin )
150   PRINT "Max Stress"; Smax; "MPa"
160   PRINT "Min Stress"; Smin; "MPa"
170   PRINT "Max Load"; Pmax; "N"
180   PRINT "Min Load"; Pmin; "N"
190   PRINT "Mean Stress"; Smean; "MPa"
200   PRINT "Mean Load"; Pmean; "N"
210   PRINT "Creep Load"; Pc; "N"
220   PRINT "Creep Weight"; Wc; "Kg"
230   PRINT "Frequency"; f; "Hz"
240   PRINT " "
250   GOTO 30
260   END
```

High Frequency, R=0.25

```
10    REM R=0.25 150 MPa/s Calculations Programme
20    PRINT "R=0.25 150 MPa/s TEST VALUES PROGRAMME"
30    PRINT "Enter %, Mean Stress, Width, Thickness"
40    PRINT "and Width and Thickness for Creep Sample, R ratio"
50    INPUT Pult, Smu, Bf, Tf, Bc, Tc, R
60    LET Smax = Pult * Smu
70    LET Smin = R * Smax
80    LET Pmax = ( 4 * Bf * Tf * Tf * Smax ) / 900
90    LET Pmin = R * Pmax
100   LET Smean = ( Smax + Smin ) / 2
110   LET Pmean = (Pmax + Pmin) / 2
120   LET Pc = ( 4 * Bf * Tf * Tf * Smax ) / 900
130   LET Wc = ( Pc / 68.67 ) -2.72
140   LET f = 60 / ( Smax - Smin )
150   PRINT "Max Stress"; Smax; "MPa"
160   PRINT "Min Stress"; Smin; "MPa"
170   PRINT "Max Load"; Pmax; "N"
180   PRINT "Min Load"; Pmin; "N"
190   PRINT "Mean Stress"; Smean; "MPa"
200   PRINT "Mean Load"; Pmean; "N"
210   PRINT "Creep Load"; Pc; "N"
220   PRINT "Creep Weight"; Wc; "Kg"
230   PRINT "Frequency"; f; "Hz"
240   PRINT " "
250   GOTO 30
260   END
```

APPENDIX 4: TABULATED VALUES

Appendices 4A-F respectively show the parameters and results for all the sets of: chipboard samples tested at R=0.1 at low, medium and high frequencies, chipboard tested at R=0.25 at high frequency, OSB tested at medium frequency and MDF tested at R=0.1 at medium frequency. Each appendix contains three pages of tables where page 1 includes all the data from static testing the outside two samples of each matched set of four. The test number is arbitrary and serves purely to match the data on the three pages of the table. For example, in Appendix 5 test 6 incorporates the outside static samples O-96C (LHS) and O-98 (RHS) on page 1, then inside fatigue/dynamic sample O-97 (LHS) on page 2, and then inside creep sample O-97C on page 3.

Page 2 of each appendix displays all the data from the respective dynamic tests performed. Again the initial columns identify the test and the individual samples tested, followed by the sample dimensions. The maximum, mean and minimum stress values were calculated as percentages of the 100% stress value. The maximum, mean and minimum loads were applied to the samples to obtain the required stress values. The percentage stress level is shown in the final column. Also shown is the R ratio, which was R=0.1 for all but one set of testing, the frequency of loading, which is a function of the stress amplitude, the number of cycles to failure and the $\log_{10}$ cycles to failure.

Page 3 of each appendix shows the data for all the side-matched samples loaded in creep. The first four columns are the same as previously except for the creep samples. Next is the creep load required to equal the peak fatigue stress and the weight applied to produce it.

The formulae used for calculating all values are included as Appendix 1.

Appendix 4A: Page 1 - Static test values. Low frequency testing of chipboard at R=0.1.

Test N^{o}.	Static Sample (left)	Width mm	Thickness mm	Failure Load kN	Failure Stress MPa	Static Sample (right)	Width mm	Thickness mm	Failure Load kN	Failure Stress MPa	Mean Stress MPa
1	C-211	50.0	17.9	1.263	17.75	C-212C	50.1	17.9	1.244	17.48	17.62
2	C-221	50.0	18.0	1.423	19.73	C-222C	50.0	18.0	1.424	19.84	19.79
3	C-237C	49.9	17.9	1.205	16.93	C-239	49.6	17.9	1.315	18.60	17.77
4	C-246	50.2	18.0	1.315	18.27	C-247C	50.0	17.9	1.275	17.85	18.06
5	C-254	49.9	17.9	1.473	20.62	C-255C	50.0	17.9	1.533	21.44	21.03
6	C-256	50.2	18.1	1.440	19.71	C-257C	50.0	18.0	1.412	19.55	19.63
7	C-214	50.1	17.9	1.247	17.48	C-215C	49.6	17.9	1.349	19.09	18.29
8	C-227C	49.9	18.0	1.375	19.15	C-229	49.8	18.0	1.247	18.79	18.97
9	C-244	49.8	17.9	1.246	17.55	C-245C	50.1	17.9	1.193	16.65	17.10
10	C-247C	50.0	17.9	1.275	17.85	C-249	50.0	17.9	1.314	18.46	18.16
11	C-251	50.2	18.0	1.394	19.27	C-252C	50.1	18.0	1.413	19.70	19.49
12	C-269	49.8	18.0	1.497	20.83	C-270C	50.1	18.1	1.452	20.01	20.42
13	C-217C	50.0	17.9	1.428	20.05	C-219	50.0	17.9	1.358	19.07	19.56
14	C-229	49.8	18.0	1.347	18.79	C-230C	50.1	18.0	1.477	20.41	19.60
15	C-239	49.6	17.9	1.315	18.6	C-240C	50.0	17.9	1.286	18.02	18.31
16	C-242C	50.2	17.9	1.177	16.44	C-244	49.8	17.9	1.246	17.55	17.00
17	C-257C	49.9	18.0	1.412	19.55	C-259	49.8	18.0	1.520	21.18	20.37
18	C-262C	49.9	18.0	1.529	21.20	C-264	49.9	18.0	1.466	20.35	20.78
19	C-212C	50.1	17.9	1.244	17.48	C-214	50.1	17.9	1.247	17.48	17.48
20	C-219	50.0	17.9	1.358	19.07	C-220C	49.9	17.9	1.281	17.96	18.52
21	C-226	50.0	18.0	1.271	17.59	C-227C	49.9	18.0	1.375	19.15	18.37
22	C-241	50.2	17.9	1.233	17.23	C-242C	50.2	17.9	1.177	16.44	16.48
23	C-252C	50.1	18.0	1.413	19.70	C-254	49.9	17.9	1.473	20.62	20.16
24	C-267C	49.9	18.0	1.464	20.34	C-269	49.8	18.0	1.497	20.83	20.59
25	C-236	50.2	17.9	1.220	16.99	C-237C	49.9	17.9	1.205	16.93	16.96
26	C-249	50.0	17.9	1.314	18.46	C-250C	49.6	17.9	1.330	18.80	18.63
27	C-264	49.9	18.0	1.466	20.35	C-265C	50.0	18.1	1.506	20.78	20.57

Appendix 4A: Page 2 - dynamic test values. Low frequency testing of chipboard at R=0.1. **(+ = Runout Sample)**

Test N^{O}.	Dynamic Sample	Width mm	Thickness mm	Max Stress MPa	Mean Stress MPa	Min Stress MPa	Max Load kN	Mean Load kN	Min Load kN	R ratio	Freq Hz	Cycles To Failure	$\log_{10}$ Cycles	Stress Level %
1	C-211C	49.8	17.9	14.10	7.75	1.14	1.016	0.559	0.102	0.1	0.047	21	1.32	80
2	C-221C	50.1	18.0	15.83	8.71	1.58	1.145	0.630	0.115	0.1	0.042	78	1.89	80
3	C-238	49.6	17.9	14.22	7.82	1.42	1.005	0.533	0.101	0.1	0.047	60	1.78	80
4	C-246C	49.7	17.9	14.45	7.946	1.45	1.027	0.565	0.103	0.1	0.046	100	2.00	80
5	C-254C	50.1	17.9	16.82	9.25	1.68	1.202	0.660	0.120	0.1	0.040	108	2.03	80
6	C-256C	49.9	18.1	15.70	8.64	1.57	1.135	0.624	0.113	0.1	0.042	147	2.16	80
7	C-214C	50.1	17.9	12.20	7.04	1.28	0.912	0.502	0.091	0.1	0.052	1024	3.01	70
8	C-228	49.8	18.0	13.28	7.30	1.33	0.953	0.524	0.095	0.1	0.050	806	2.91	70
9	C-244C	50.2	17.9	11.97	6.58	1.20	0.789	0.434	0.079	0.1	0.056	3632	3.56	70
10	C-248	50.1	17.9	12.71	6.99	1.27	0.906	0.498	0.091	0.1	0.052	638	2.80	70
11	C-251C	49.8	18.0	13.64	7.50	1.36	0.972	0.535	0.097	0.1	0.049	614	2.79	70
12	C-269C	50.0	18.0	14.29	7.86	1.43	1.032	0.567	0.103	0.1	0.047	164	2.21	70
13	C-218	50.0	17.9	11.74	6.45	1.17	0.835	0.460	0.084	0.1	0.057	8963	3.95	60
14	C-229C	49.9	18.0	11.76	6.47	1.18	0.846	0.465	0.085	0.1	0.057	9260	4.00	60
15	C-239C	49.9	17.9	10.99	6.04	1.10	0.781	0.430	0.078	0.1	0.061	15580	4.19	60
16	C-243	49.8	17.9	10.20	5.61	1.02	0.725	0.399	0.072	0.1	0.065	1852	3.27	60
17	C-258	49.9	18.0	12.22	6.72	1.22	0.881	0.484	0.088	0.1	0.055	4079	3.61	60
18	C-263	49.6	18.0	12.47	6.86	1.24	0.893	0.491	0.089	0.1	0.053	6871	3.94	60
19	C-213	50.08	17.9	8.74	4.81	0.87	0.622	0.342	0.062	0.1	0.076	183598+	5.26+	50
20	C-219C	50.06	17.9	9.26	5.09	0.93	0.660	0.363	0.066	0.1	0.072	103121+	5.01+	50
21	C-226C	50.1	18.0	9.19	5.05	0.92	0.663	0.365	0.066	0.1	0.073	105911+	5.02+	50
22	C-241C	50.1	17.9	8.42	4.63	0.84	0.602	0.331	0.060	0.1	0.079	88285	4.94	50
23	C-253	50.0	17.9	10.08	5.55	1.01	0.720	0.396	0.072	0.1	0.066	101075	5.00+	50
24	C-268	49.4	18.0	10.30	5.66	1.03	0.732	0.403	0.072	0.1	0.065	102336+	5.01+	50
25	C-236C	50.0	17.9	6.78	3.73	0.68	0.485	0.266	0.048	0.1	0.098	109735+	5.04+	40
26	C-249C	50.1	17.9	5.59	3.07	0.56	0.399	0.219	0.040	0.1	0.119	204751+	5.31+	30
27	C-264C	50.0	18.0	4.11	2.26	0.41	0.297	0.164	0.030	0.1	0.162	206573+	5.32+	20

Appendix 4A: Page 3 - creep test values. Low frequency testing of chipbaord at R=0.1.

Test N^{O}.	Creep Sample	Width mm	Thickness mm	Creep Load kN	Creep Weight kg
1	C-212	50.1	17.9	1.001	11.9
2	C-222	50.1	18.0	1.138	13.8
3	C-238C	49.7	17.9	1.008	12.0
4	C-247	49.9	17.9	1.031	12.3
5	C-255	49.9	17.9	1.199	14.7
6	C-257	50.1	18.1	1.140	13.9
7	C-215	50.0	17.9	0.911	10.5
8	C-228C	49.8	18.0	0.952	11.1
9	C-245	50.2	17.9	0.855	9.7
10	C-248C	50.1	17.9	0.908	10.5
11	C-252	50.1	18.0	0.983	11.6
12	C-270	49.6	18.1	1.026	12.2
13	C-218C	50.0	18.0	0.842	9.5
14	C-230	50.1	18.0	0.850	9.7
15	C-240	49.9	17.9	0.783	8.7
16	C-243C	50.0	17.9	0.727	7.9
17	C-258C	49.7	18.0	0.877	10.0
18	C-263C	49.6	18.0	0.892	10.3
19	C-213C	50.1	17.9	0.622	6.3
20	C-220	50.0	17.9	0.662	6.9
21	C-227	49.9	18.0	0.661	6.9
22	C-242	50.2	17.9	0.603	6.1
23	C-253C	50.0	18.0	0.722	7.8
24	C-268C	49.6	18.0	0.737	8.0
25	C-237	49.9	17.9	0.482	4.3
26	C-250	49.8	17.9	0.397	3.1
27	C-265	49.9	18.0	0.297	1.6

Appendix 4B: Page 1 - Static test values. Medium frequency testing of chipboard at R=0.1.

Test N^{o}.	Static Sample (left)	Width mm	Thickness mm	Failure Load kN	Failure Stress MPa	Static Sample (right)	Width mm	Thickness mm	Failure Load kN	Failure Stress MPa	Mean Stress MPa
1	C-141	50.1	17.9	1.463	20.52	C-142C	50.1	17.9	1.371	19.24	19.88
2	C-146	50.1	17.9	1.406	19.72	C-147C	50.1	17.9	1.505	21.16	20.44
3	C-154	50.1	17.9	1.829	25.62	C-155C	50.1	17.9	1.879	26.41	26.02
4	C-159	50.0	17.9	1.543	21.62	C-160C	50.0	17.8	1.547	21.88	21.75
5	C-177C	50.1	17.8	1.259	17.78	C-179	50.1	17.8	1.293	18.25	18.02
6	C-181	50.1	17.9	1.507	21.13	C-182C	50.0	17.9	1.453	20.48	20.81
7	C-142C	50.1	17.9	1.371	19.24	C-144	50.1	17.9	1.397	19.61	19.43
8	C-151	50.1	18.0	1.729	24.05	C-152C	50.0	18.0	1.842	25.20	24.63
9	C-157C	50.0	18.0	1.595	22.27	C-159	50.0	17.9	1.543	21.62	21.95
10	C-162C	49.9	18.0	1.528	21.26	C-164	49.9	18.0	1.670	22.49	21.88
11	C-169	50.0	17.9	1.275	17.97	C-170C	50.0	17.8	1.313	18.60	18.29
12	C-179	50.1	17.8	1.293	18.25	C-180C	49.5	17.9	1.312	18.69	18.47
13	C-144	50.1	17.9	1.397	19.61	C-145C	50.0	17.8	1.454	20.66	20.14
14	C-149	50.1	17.9	1.435	20.16	C-150C	50.0	18.0	1.469	20.40	20.28
15	C-152C	50.0	18.0	1.842	25.20	C-154	50.1	17.9	1.829	25.62	25.41
16	C-171	50.0	17.9	1.356	19.02	C-172C	50.2	17.9	1.396	19.54	19.28
17	C-172C	50.2	17.9	1.396	19.54	C-174	50.0	17.9	1.423	20.06	19.80
18	C-176	50.1	17.9	1.354	19.06	C-177C	50.1	17.8	1.259	17.78	18.42
19	C-147C	50.1	17.9	1.505	21.16	C-149	50.1	17.9	1.435	20.16	20.66
20	C-156	50.1	18.0	1.532	21.27	C-157C	50.0	18.0	1.595	22.27	21.77
21	C-164	49.9	18.0	1.670	22.49	C-165C	50.1	17.9	1.665	23.45	22.97
22	C-167C	49.9	17.9	1.374	19.26	C-169	49.9	17.9	1.247	17.97	18.62
23	C-174	50.0	17.9	1.423	20.06	C-175C	50.2	17.8	1.358	19.19	19.63
24	C-182C	50.0	17.9	1.453	20.48	C-184	50.0	17.9	1.468	20.67	20.58
25	C-161	50.2	18.0	1.572	21.73	C-162C	49.9	18.0	1.528	21.26	21.50
26	C-184	50.0	17.9	1.468	20.67	C-185C	49.9	17.9	1.408	19.83	20.25
27	C-166	50.2	17.9	1.358	18.93	C-167C	49.9	17.9	1.374	19.26	19.10

Appendix 4B: Page 2 - Dynamic test values. Medium frequency testing of chipboard at R=0.1. **(+ = Runout Sample)**

Test N^{o}.	Dynamic Sample	Width mm	Thickness mm	Max Stress MPa	Mean Stress MPa	Min Stress MPa	Max Load kN	Mean Load kN	Min Load kN	R ratio	Freq Hz	Cycles To Failure	$\log_{10}$ Cycles	Stress Level %
1	C-141C	50.0	17.9	15.90	8.75	1.59	1.135	0.642	0.113	0.1	0.417	236	2.37	80
2	C-146C	50.0	17.9	16.35	8.99	1.64	1.163	0.640	0.116	0.1	0.408	228	2.36	80
3	C-154C	50.0	17.9	20.82	11.45	2.08	1.479	0.813	0.148	0.1	0.320	334	2.52	80
4	C-159C	50.0	17.9	17.40	9.57	1.74	1.240	0.682	0.124	0.1	0.383	130	2.11	80
5	C-178	50.1	17.8	14.42	7.93	1.44	1.021	0.562	0.102	0.1	0.462	202	2.31	80
6	C-181C	49.9	17.9	16.65	9.16	1.67	1.187	0.653	0.119	0.1	0.400	139	2.14	80
7	C-143	50.1	17.9	13.60	7.48	1.36	0.968	0.533	0.097	0.1	0.490	3359	3.53	70
8	C-151C	50.1	18.0	17.24	9.48	1.72	1.242	0.683	0.124	0.1	0.387	15336	4.19	70
9	C-158	49.9	18.0	15.37	8.45	1.54	1.100	0.605	0.110	0.1	0.434	2183	3.34	70
10	C-163	49.9	18.0	15.32	8.42	1.53	1.105	0.608	0.111	0.1	0.435	4616	3.66	70
11	C-169C	49.9	17.9	12.80	7.04	1.28	0.907	0.499	0.091	0.1	0.521	2457	3.39	70
12	C-179C	50.0	17.8	12.93	7.11	1.29	0.912	0.502	0.091	0.1	0.516	436	2.64	70
13	C-144C	50.0	17.9	12.08	6.65	1.21	0.858	0.472	0.086	0.1	0.552	44558	4.65	60
14	C-149C	50.0	17.8	12.17	6.69	1.22	0.861	0.474	0.086	0.1	0.548	41938	4.62	60
15	C-153	50.0	18.0	15.25	8.39	1.53	1.092	0.600	0.109	0.1	0.437	26352	4.42	60
16	C-171C	50.3	17.9	11.57	6.36	1.16	0.827	0.455	0.083	0.1	0.576	35629	4.55	60
17	C-173	50.2	17.9	11.88	6.53	1.19	0.847	0.466	0.085	0.1	0.561	50554	4.70	60
18	C-176C	49.7	17.9	11.05	6.08	1.11	0.778	0.428	0.078	0.1	0.603	69393	4.84	60
19	C-148	50.1	17.9	10.33	5.68	1.03	0.736	0.405	0.074	0.1	0.645	895045	5.95	50
20	C-156C	50.2	18.0	10.89	5.99	1.09	0.785	0.432	0.078	0.1	0.612	431184	5.63	50
21	C-164C	50.0	17.9	11.49	6.32	1.15	0.820	0.451	0.082	0.1	0.580	974452	5.99	50
22	C-168	50.0	17.9	9.31	5.12	0.93	0.664	0.365	0.066	0.1	0.716	837667	5.92	50
23	C-174C	50.1	17.9	9.82	5.40	0.98	0.696	0.383	0.070	0.1	0.679	1088931+	6.04+	50
24	C-183	50.0	17.9	10.29	5.66	1.03	0.729	0.401	0.073	0.1	0.648	1123401+	6.05+	50
25	C-161C	50.2	18.0	8.60	4.73	0.86	0.622	0.342	0.062	0.1	0.775	1075351+	6.03+	40
26	C-184C	50.1	17.9	6.08	3.34	0.61	0.431	0.237	0.043	0.1	1.097	1019403+	6.01+	30
27	C-166C	50.2	17.9	3.82	2.10	0.04	0.274	0.151	0.027	0.1	1.745	1.43001+	6.02+	20

Appendix 4B: Page 3 - Creep Test Values. Medium Frequency Testing of Chipboard at R=0.1

Test N^{O}.	Creep Sample	Width mm	Thickness mm	Creep Load kN	Creep Weight kg
1	CM-142	50.0	17.9	1.133	13.8
2	CM-147	50.0	17.9	1.161	14.2
3	CM-155	50.0	17.8	1.470	18.7
4	CM-160	50.1	17.9	1.235	15.3
5	CM-178C	50.1	17.8	1.021	12.1
6	CM-182	50.1	17.9	1.183	14.5
7	CM-143C	50.2	17.9	0.986	11.4
8	CM-152	50.1	18.0	1.239	15.3
9	CM-158C	50.0	17.9	1.098	13.3
10	CM-163C	49.9	18.0	1.221	15.1
11	CM-170	49.8	17.8	0.900	10.4
12	CM-180	49.0	17.9	0.899	10.4
13	CM-145	50.1	17.8	0.855	9.7
14	CM-150	50.0	17.8	0.858	9.8
15	CM153C	50.0	17.9	1.091	13.2
16	CM-172	50.2	17.9	0.827	9.3
17	CM-173C	50.2	17.9	0.846	9.6
18	CM-177	50.1	17.9	0.783	8.7
19	CM-148C	50.1	17.9	0.736	8.0
20	CM-157	50.1	18.0	0.783	8.7
21	CM-165	50.0	17.9	0.815	9.2
22	CM-168C	50.0	17.9	0.670	6.9
23	CM-175	50.1	17.8	0.694	7.4
24	CM-183C	50.0	17.9	0.792	7.9
25	CM-162	50.0	18.0	0.622	6.3
26	CM-185	50.0	17.9	0.432	3.6
27	CM-167	50.0	17.9	0.272	1.2

Appendix 4C: Page 1 - Static Test Values. High Frequency Testing of Chipboard at R=0.1.

Test N^{o}.	Static Sample (left)	Width mm	Thickness mm	Failure Load kN	Failure Stress MPa	Static Sample (right)	Width mm	Thickness mm	Failure Load kN	Failure Stress MPa	Mean Stress MPa
1	C-74	50.2	17.9	1.3582	19.01	C-75C	50.0	17.9	1.2802	17.96	18.49
2	C-92C	49.9	18.0	1.5450	21.57	C-94	50.1	18.0	1.4317	19.86	20.72
3	C-112C	50.2	18.0	1.5696	21.27	C-114	50.1	18.0	1.5398	21.40	21.56
4	C-126	50.2	18.1	1.5631	21.30	C-127C	49.8	18.1	1.5127	20.95	21.13
5	C-132C	49.8	18.0	1.4218	19.89	C-134	50.0	18.0	1.4414	20.08	19.99
6	C-139	50.2	18.0	1.1480	15.94	C-140C	50.2	18.0	1.2060	16.70	16.32
7	C-91	50.2	18.0	1.4717	20.37	C-92C	49.9	18.0	1.5450	21.57	20.97
8	C-114	50.1	18.0	1.5398	21.40	C-115C	50.0	18.0	1.6642	23.08	22.24
9	C-119	50.1	18.1	1.5742	21.70	C-120C	50.2	18.1	1.5158	20.82	21.26
10	C-129	50.0	18.1	1.4830	20.48	C-130C	50.2	18.1	1.5358	21.08	20.78
11	C-131	50.3	18.1	1.4458	19.80	C-132C	49.8	18.0	1.4218	19.89	19.85
12	C-137C	49.9	18.0	1.2350	17.16	C-139	50.2	18.0	1.1480	15.94	16.55
13	C-94	50.1	18.0	1.4317	19.86	C-95C	50.2	18.0	1.4822	20.49	20.18
14	C-97C	49.8	17.9	1.3245	18.64	C-99	50.0	17.9	1.4708	20.64	19.64
15	C-102C	50.1	17.9	1.3128	18.37	C-104	50.3	18.0	1.2976	18.0	18.19
16	C-117C	50.2	18.1	1.5208	20.84	C-119	50.1	18.1	1.5742	21.70	21.27
17	C-127C	49.8	18.1	1.5127	20.95	C-129	50.0	18.1	1.4830	20.48	20.72
18	C-136	50.2	18.0	1.2751	17.63	C-137C	49.9	18.0	1.2350	17.16	17.40
19	C-86	50.0	18.0	1.3512	18.77	C-87C	50.1	18.1	1.3588	18.72	18.75
20	C-87C	50.1	18.1	1.3588	18.72	C-89	50.1	18.0	1.4141	19.54	19.13
21	C-99	50.0	17.9	1.4708	20.64	C-100C	50.0	17.9	1.4338	20.03	20.34
22	C-101	50.3	18.0	1.3441	18.63	C-102C	50.1	17.9	1.3128	18.37	18.50
23	C-107C	50.2	18.0	1.3912	19.36	C-109	50.2	17.9	1.4410	20.09	19.73
24	C-116	50.2	18.1	1.5244	20.89	C-117C	50.2	18.1	1.5208	20.84	20.87
25	C-77C	50.1	17.9	1.5682	22.09	C-79	50.1	17.9	1.6550	23.32	22.71
26	C-111	50.2	18.0	1.5040	20.92	C-112C	50.2	18.0	1.5696	21.72	21.32
27	C-89	50.1	18.0	1.4141	19.54	C-90C	50.2	18.0	1.3994	19.33	19.44
28	C-134	50.0	18.0	1.4414	20.08	C-135C	50.1	18.0	1.4414	19.90	19.99

Appendix 4C: Page 2 - dynamic test values. High frequency testing of chipboard at R=0.1. **(+ = Runout sample)**

Test N°.	Dynamic Sample	Width mm	Thickness mm	Max Stress MPa	Mean Stress MPa	Min Stress MPa	Max Load kN	Mean Load kN	Min Load kN	R ratio	Freq Hz	Cycles To Failure	$\log_{10}$ Cycles	Stress Level %
1	C-74C	50.2	17.9	14.79	8.14	1.48	1.058	0.582	0.106	0.1	4.507	349	2.54	80
2	C-93	49.6	18.0	16.58	9.12	1.66	1.183	0.650	0.118	0.1	4.022	1564	3.19	80
3	C-113	50.2	18.0	17.25	9.49	1.73	1.242	0.683	0.124	0.1	3.865	24	1.38	80
4	C-126C	50.2	18.1	16.90	9.30	1.69	1.233	0.678	0.123	0.1	3.944	583	2.77	80
5	C-133	49.3	18.0	15.99	8.80	1.59	1.131	0.622	0.113	0.1	4.169	200	2.30	80
6	C-139C	49.8	18.0	13.06	7.18	1.31	0.934	0.514	0.093	0.1	5.106	2519	3.40	80
7	C-91C	50.2	18.0	14.68	8.07	1.47	1.058	0.582	0.106	0.1	4.542	22964	4.36	70
8	C-114C	50.2	18.0	15.57	8.56	1.56	1.119	0.615	0.112	0.1	4.282	15459	4.19	70
9	C-119C	50.2	18.1	14.88	8.19	1.49	1.085	0.597	0.108	0.1	4.480	11468	4.06	70
10	C-129C	49.8	18.1	14.55	8.00	1.46	1.050	0.577	0.105	0.1	4.583	15335	4.19	70
11	C-131C	50.2	17.8	13.90	7.642	1.39	1.095	0.602	0.109	0.1	4.798	1146	3.06	70
12	C-138	49.2	18.0	11.59	6.37	1.16	0.819	0.451	0.082	0.1	5.754	36434	4.56	70
13	C-94C	50.0	18.0	12.11	6.66	1.21	0.874	0.480	0.087	0.1	5.506	385810	5.59	60
14	C-98	49.5	17.9	11.78	6.48	1.18	0.831	0.457	0.084	0.1	5.657	461955	5.66	60
15	C-103	49.6	17.9	11.35	6.24	1.14	0.804	0.442	0.084	0.1	5.876	139037	5.14	60
16	C-118	50.1	18.1	12.76	7.02	1.28	0.925	0.509	0.093	0.1	5.224	346277	5.54	60
17	C-128	49.6	18.0	12.43	6.84	1.24	0.981	0.490	0.089	0.1	5.363	49477	4.69	60
18	C-136C	50.2	18.0	10.44	5.74	1.04	0.757	0.416	0.076	0.1	6.386	337511	5.53	60
19	C-86C	50.2	18.0	9.38	5.16	0.94	0.680	0.374	0.068	0.1	7.111	3698783	6.57	50
20	C-88	49.9	18.0	9.57	5.26	0.96	0.688	0.378	0.069	0.1	6.970	3823711	6.58	50
21	C-99C	50.0	17.9	10.17	5.59	1.02	0.727	0.400	0.073	0.1	6.555	1534263	6.14	50
22	C-101C	50.2	18.0	9.25	5.09	0.93	0.665	0.366	0.067	0.1	7.207	1862866	6.27	50
23	C-108	50.2	18.0	9.87	5.43	0.99	0.710	0.391	0.071	0.1	6.758	2086482	6.32	50
24	C-116C	50.2	18.1	10.44	5.74	1.04	0.759	0.417	0.076	0.1	6.389	7269408	6.86	50
25	C-78	50.1	17.9	9.08	5.00	0.91	0.646	0.356	0.064	0.1	7.339	18240189+	7.26+	40
26	C-111C	50.2	18.0	8.53	4.69	0.85	0.617	0.339	0.062	0.1	7.817	11380003+	7.06+	40
27	C-89C	50.1	18.0	5.83	3.21	0.58	0.421	0.231	0.042	0.1	11.431	16567032+	7.22+	30
28	C-134C	49.7	18.0	6.00	3.30	0.60	0.429	0.235	0.043	0.1	11.117	15299002+	7.18+	30

Appendix 4C: Page 3 - creep test values. High frequency testing of chipboard at R=0.1.

Test N°.	Creep Sample	Width mm	Thickness mm	Creep Load kN	Creep Weight kg
1	C-75	50.2	17.9	1.057	12.7
2	C-93C	49.9	18.0	1.193	14.7
3	C-113C	50.1	18.0	1.237	15.3
4	C-127	50.2	18.1	1.231	15.2
5	C-133C	50.0	18.0	1.148	14.0
6	C-140	50.3	18.0	0.945	11.0
7	C-92	50.1	18.0	1.057	12.7
8	C-115	50.2	18.0	1.123	13.6
9	C-120	50.2	18.1	1.084	13.1
10	C-130	50.2	18.1	1.062	12.7
11	C-132	50.1	18.0	1.002	11.9
12	C-138C	50.3	18.0	0.840	9.5
13	C-95	50.1	18.0	0.873	10.0
14	C-98C	50.0	18.0	0.845	9.6
15	C-103C	50.3	17.9	0.814	9.1
16	C-118C	50.0	18.1	0.923	10.7
17	C-128C	50.0	18.0	0.989	10.4
18	C-137	50.3	18.0	0.758	8.3
19	C-87	50.3	18.0	0.682	7.2
20	C-88C	50.0	18.0	0.960	7.3
21	C-100	50.0	17.9	0.727	7.9
22	C-102	50.2	18.0	0.665	7.0
23	C-108C	50.2	17.9	0.707	7.6
24	C-117	50.2	18.0	0.760	8.3
25	C-78C	50.0	17.9	0.644	6.7
26	C-112	50.2	18.0	0.615	6.2
27	C-90	50.2	18.0	0.422	3.4
28	C-135	50.2	18.0	0.434	3.6

Appendix 4D: Page 1 - static test values. High frequency testing of chipboard at R=0.25.

Test N^{O}.	Static Sample (left)	Width mm	Thickness mm	Failure Load kN	Failure Stress MPa	Static Sample (right)	Width mm	Thickness mm	Failure Load kN	Failure Stress MPa	Mean Stress MPa
1	C-31	50.2	18.0	1.438	19.89	C-32C	50.1	17.9	1.379	19.29	19.59
2	C-56	50.1	18.0	1.472	20.49	C-57	49.8	18.0	1.360	18.97	19.73
3	C-59	49.9	18.0	1.399	19.49	C-60C	50.1	18.0	1.471	20.46	19.98
4	C-61	50.2	17.9	1.289	18.00	C-62C	49.9	18.0	1.353	18.96	18.48
5	C-62C	49.9	17.9	1.353	18.96	C-64	49.9	17.9	1.318	18.53	18.75
6	C-69	50.2	17.9	1.453	20.34	C-70C	50.0	17.9	1.287	18.03	19.19
7	C-17C	50.9	18.0	1.720	23.56	C-19	49.8	18.0	1.947	27.23	25.40
8	C-19	49.8	18.0	1.947	27.23	C-20C	50.2	17.9	1.679	23.49	25.36
9	C-27C	49.7	18.0	1.552	21.73	C-29	49.7	17.9	1.434	20.18	20.96
10	C-32C	50.1	17.9	1.379	19.29	C-34	49.8	17.90	1.509	21.26	20.28
11	C-34	49.8	17.9	1.509	21.26	C-35C	49.95	17.9	1.560	21.95	21.61
12	C-49	50.1	18.0	1.624	22.56	C-50C	50.1	18.0	1.589	22.16	22.36
13	C-26	50.2	18.0	1.659	22.98	C-27C	49.70	18.0	1.552	21.73	22.36
14	C-29	49.7	17.9	1.433	20.18	C-30	50.0	17.9	1.450	20.29	20.24
15	C-39	50.1	17.9	1.418	19.90	C-40C	49.5	17.9	1.580	22.54	21.22
16	C-42C	50.1	17.9	1.721	24.10	C-44	50.1	17.9	1.808	25.33	24.72
17	C-46	50.1	18.0	1.418	19.75	C-47C	50.1	18.0	1.449	20.07	19.91
18	C-51	49.9	18.0	1.723	23.98	C-52C	50.0	18.0	1.518	21.19	22.59
19	C-52C	50.0	18.0	1.518	21.19	C-54	50.02	17.9	1.477	20.55	20.87
20	C-54	50.0	17.9	1.477	20.55	C-55C	50.0	17.9	1.700	23.92	22.24
21	C-57	49.8	18.0	1.360	18.97	C-59	49.9	18.0	1.399	19.49	19.23
22	C-67C	50.1	17.9	1.210	16.93	C-69	50.2	17.9	1.453	20.34	18.64
23	C-76	50.1	17.9	1.690	23.72	C-77C	50.1	17.9	1.568	22.09	22.91

Appendix 4D: Page 2 - dynamic test values. High frequency testing of chipboard at R=0.25.

Test N°.	Dynamic Sample	Width mm	Thickness mm	Max Stress MPa	Mean Stress MPa	Min Stress MPa	Max Load KN	Mean Load KN	Min Load KN	R ratio	Freq Hz	Cycles To Failure	$\log_{10}$ Cycles	Stress Level %
1	C-31C	50.2	18.0	15.67	9.80	3.92	1.129	0.705	0.282	0.25	5.105	280	2.45	80
2	C-56C	50.1	18.0	15.78	9.87	3.95	1.138	0.712	0.285	0.25	5.068	824	2.92	80
3	C-59C	50.0	18.0	15.98	9.99	3.99	1.146	0.716	0.286	0.25	5.005	589	2.77	80
4	C-61C	50.1	17.9	14.78	9.24	3.70	1.058	0.661	0.264	0.25	5.411	1133	3.05	80
5	C-63	49.9	18.0	15.00	9.38	3.75	1.072	0.670	0.268	0.25	5.333	4029	3.61	80
6	C-69C	50.2	17.9	15.35	9.60	3.84	1.096	0.685	0.274	0.25	5.211	1404	3.15	80
7	C-18	50.0	18.0	17.78	11.11	4.45	1.274	0.796	0.318	0.25	4.500	2855	3.46	70
8	C-19C	50.1	18.0	17.75	11.10	4.44	1.274	0.796	0.318	0.25	4.507	11063	4.04	70
9	C-28	49.9	18.0	14.67	9.17	3.67	1.056	0.660	0.264	0.25	5.453	2967	3.47	70
10	C-33	50.2	17.9	14.20	8.87	3.55	1.017	0.635	0.254	0.25	5.635	23222	4.37	70
11	C-34C	50.2	17.9	15.13	9.45	3.78	1.085	0.678	0.271	0.25	5.289	1697	3.23	70
12	C-49C	50.1	17.9	15.65	9.78	3.91	1.220	0.701	0.281	0.25	5.111	6074	3.78	70
13	C-26C	50.1	18.0	13.42	8.39	3.354	0.97	0.606	0.242	0.25	5.963	345619	5.54	60
14	C-29C	50.1	17.9	12.14	7.59	3.04	0.870	0.544	0.217	0.25	6.588	817593	5.91	60
15	C-39C	50.1	17.9	12.73	7.96	3.18	0.903	0.564	0.226	0.25	6.283	810485	5.91	60
16	C-43	50.1	17.9	14.83	9.27	3.71	1.062	0.664	0.265	0.25	5.392	236749	5.37	60
17	C-46C	50.1	18.0	11.95	7.47	2.99	0.860	0.537	0.215	0.25	6.697	489365	5.69	60
18	C-51C	50.1	17.9	13.55	8.47	3.39	0.971	0.607	0.243	0.25	5.902	311549	5.49	60
19	C-53	50.0	17.9	10.44	6.52	2.61	0.744	0.465	0.186	0.25	7.666	10010004	7.00	50
20	C-54C	50.0	17.9	11.12	6.95	2.78	0.791	0.495	0.198	0.25	7.192	6996271	6.84	50
21	C-58	49.9	18.0	9.62	6.01	2.40	0.691	0.432	0.173	0.25	8.320	9691000	6.99	50
22	C-68	50.2	17.9	9.32	5.83	2.33	0.666	0.416	0.166	0.25	8.584	8558612	6.93	50
23	C-76C	50.1	17.9	11.45	7.16	2.86	0.813	0.508	0.203	0.25	6.983	3411128	6.53	50

Appendix 4D: Page 3 - creep test values. High frequency testing of chipboard at R=0.25.

Test N^{O}.	Creep Sample	Width mm	Thickness mm	Creep Load kN	Creep Weight kg
1	C-32	50.1	18.0	1.124	13.7
2	C-57	50.0	18.0	1.140	13.9
3	C-60	50.1	18.0	1.146	14.0
4	C-62	49.9	17.9	1.052	12.6
5	C-63C	49.9	18.0	1.075	12.9
6	C-70	50.0	17.9	1.093	13..2
7	C-18C	50.0	18.0	1.271	15.8
8	C-20	50.1	18.0	1.280	15.9
9	C-28C	49.8	18.0	1.050	12.6
10	C-33C	50.2	17.9	1.016	12.1
11	C-35	50.1	18.0	1.090	13.2
12	C-50	50.1	18.0	1.124	13.6
13	C-27	50.1	18.0	0.963	11.3
14	C-30	50.0	18.0	0.870	10.0
15	C-40	50.1	17.9	0.905	10.5
16	C-43C	50.1	17.9	1.057	12.7
17	C-47	50.2	18.0	0.826	9.8
18	C-52	50.0	17.9	0.968	11.4
19	C-53C	49.9	17.9	0.744	8.1
20	C-55	50.1	17.9	0.791	8.8
21	C-58C	50.0	18.0	0.770	8.5
22	C-68C	50.1	17.9	0.665	7.0
23	C-77	50.1	17.8	0.812	9.1

Appendix 4E: Page 1 - static test values. Medium frequency testing of OSB at R=0.1.

Test N^{O}.	Static Sample (left)	Width mm	Thickness mm	Failure Load kN	Failure Stress MPa	Static Sample (right)	Width mm	Thickness mm	Failure Load kN	Failure Stress MPa	Mean Stress MPa
1	O-8C	50.1	19.4	2.298	27.50	O-10	50.06	19.5	2.141	25.31	26.41
2	O-12	50.1	19.2	N/A	32.77	O-13C	50.34	19.3	2.662	32.07	32.42
3	O-43	50.3	19.1	2.236	27.42	O-44C	50.20	19.2	2.080	25.42	26.42
4	O-51	50.3	18.9	2.082	26.15	O-52C	50.22	19.0	2.248	28.01	27.08
5	O-74C	50.3	18.7	1.989	25.39	O-76	50.42	18.6	1.862	23.99	24.69
6	O-96C	50.4	18.7	2.040	26.13	O-98	50.36	18.6	2.101	27.04	26.59
7	O-5C	50.2	19.3	2.510	30.20	O-7	50.15	19.4	2.757	32.93	31.57
8	O-21	50.2	19.4	2.238	26.74	O-22C	50.04	19.2	2.323	28.22	27.48
9	O-37	50.3	18.9	2.636	32.95	O-38C	50.30	19.0	N/A	30.92	31.94
10	O59	50.3	18.8	2.710	34.37	O-60C	50.20	18.9	2.598	32.50	33.44
11	O-76	50.4	18.6	1.862	23.99	O-77C	50.22	18.8	1.721	21.91	22.95
12	O-79C	50.3	18.8	2.065	33.13	O-81	50.31	18.7	2.382	30.50	31.82
13	O-4	50.1	19.1	2.596	31.73	O-5C	50.20	19.3	2.510	30.20	30.97
14	O-41C	50.3	19.0	2.368	29.21	O-43	50.30	19.1	2.236	27.42	28.32
15	O-48	50.3	18.8	2.782	35.39	O-49C	50.26	19.0	2.944	36.59	35.99
16	O-63C	50.1	18.6	2.322	30.03	O-65	50.19	18.7	2.542	32.52	31.28
17	O-73	50.4	18.8	2.093	26.60	O-74C	50.30	18.7	1.989	25.39	26.00
18	O-87	50.3	18.7	2.070	26.62	O-88C	50.11	18.6	2.061	26.78	26.70
19	O-2C	50.1	19.3	2.708	32.62	O-4	50.14	19.2	2.596	31.73	32.18
20	O-18	50.3	19.0	1.996	24.68	O-19C	50.27	19.3	2.160	26.04	25.36
21	O-19C	50.3	19.3	2.160	26.04	O-21	50.24	19.4	2.238	26.74	26.39
22	O-38C	50.3	19.0	N/A	30.92	O-40	50.28	19.0	2.655	33.02	31.97
23	O-67	50.2	18.8	2.340	29.75	O-68C	50.29	18.8	2.474	31.18	30.47
24	O-82C	50.3	18.7	2.371	30.28	O-84	50.36	18.7	2.302	29.57	29.93
25	O-60	50.2	18.9	2.598	32.50	O-62	50.16	18.7	2.592	33.43	32.97

Appendix 4E: Page 2 - dynamic test values. Medium frequency testing of OSB at R=0.1. **(+ = Runout Sample)**

Test N°.	Dynamic Sample	Width mm	Thickness mm	Max Stress MPa	Mean Stress MPa	Min Stress MPa	Max Load kN	Mean Load kN	Min Load kN	R ratio	Freq Hz	Cycles To Failure	$\log_{10}$ Cycles	Stress Level %
1	O-9	50.2	19.5	21.13	11.62	2.11	1.787	0.983	0.178	0.1	0.316	213	2.33	80
2	O-12C	49.8	19.3	25.94	14.67	2.59	2.130	1.171	0.213	0.1	0.257	3	0.48	80
3	O-43C	50.2	19.0	21.14	11.62	2.11	1.694	0.932	0.169	0.1	0.315	73	1.86	80
4	O-51C	50.3	19.0	21.66	11.92	2.17	1.727	0.950	0.173	0.1	0.308	30	1.47	80
5	O-75	50.3	18.7	19.75	10.86	1.98	1.547	0.851	0.155	0.1	0.338	771	2.89	80
6	O-97	50.3	18.7	21.27	11.70	2.13	1.656	0.911	0.166	0.1	0.313	36	1.56	80
7	O-6	50.2	19.4	22.10	12.15	2.21	1.848	1.017	0.185	0.1	0.302	1520	3.18	70
8	O-21C	50.3	19.4	19.24	10.58	1.92	1.625	0.984	0.162	0.1	0.347	1509	3.18	70
9	O-37C	50.3	19.0	22.36	12.30	2.24	1.802	0.992	0.180	0.1	0.298	1422	3.15	70
10	O-59C	50.2	19.0	23.41	12.87	2.34	1.865	1.026	0.187	0.1	0.285	8	0.90	70
11	O-76C	50.4	18.5	16.07	8.84	1.61	1.233	0.678	0.123	0.1	0.415	10364	4.02	70
12	O-80	50.3	18.8	22.27	12.25	2.23	1.759	0.968	0.176	0.1	0.299	89	1.93	70
13	O-4C	50.2	19.3	18.58	10.22	1.86	1.546	0.850	0.155	0.1	0.359	11070	4.04	60
14	O-42	50.3	19.0	16.99	9.35	1.70	1.365	0.751	0.137	0.1	0.392	9604	3.98	60
15	O-48C	50.2	19.0	21.59	11.88	2.16	2.159	1.733	0.953	0.1	0.309	4515	3.65	60
16	O-64	50.1	18.7	18.77	10.32	1.88	1.456	0.801	0.146	0.1	0.355	17	1.23	60
17	O-73C	50.4	18.8	15.60	8.58	1.56	1.230	0.677	0.123	0.1	0.427	146533	5.17	60
18	O-87C	50.3	18.4	16.02	8.81	1.60	1.214	0.668	0.121	0.1	0.416	348217	5.54	60
19	O-3	50.2	19.2	16.09	8.85	1.61	1.323	0.728	0.132	0.1	0.414	563222	5.75	50
20	O-18C	50.3	19.1	12.68	6.97	1.27	1.029	0.566	0.103	0.1	0.526	1129700+	6.05+	50
21	O-20	50.3	19.3	13.20	7.26	1.32	1.094	0.602	0.109	0.1	0.505	0.25	-0.6	50
22	O-39	50.3	19.1	15.99	8.79	1.60	1.299	0.714	0.130	0.1	0.417	640466	5.81	50
23	O-67C	50.3	18.9	15.24	8.38	1.52	1.222	0.672	0.122	0.1	0.438	350572	5.54	50
24	O-83	50.3	18.7	14.97	8.23	1.50	1.175	0.646	0.188	0.1	0.445	1076016+	6.03+	50
25	O-61C	50.2	18.8	6.59	3.63	0.66	0.522	0.287	0.052	0.1	1.011	1916050+	6.28+	20

Appendix 4E: Page 3 - creep test values. Medium frequency testing of OSB at R=0.1.

Test N^{O}.	Creep Sample	Width mm	Thickness mm	Creep Load kN	Creep Weight kg
1	O-9C	50.2	19.6	1.082	23.5
2	O-13	50.3	19.3	2.164	28.8
3	O-44	50.3	19.0	1.704	22.1
4	O-50	50.3	19.	1.739	22.6
5	O-75C	50.4	18.8	1.560	20.0
6	O-97C	50.3	18.8	1.677	21.7
7	O-6C	50.2	19.3	1.843	24.1
8	O-22	50.3	19.4	1.612	20.8
9	O-37C	50.3	19.0	1.811	23.7
10	O-59C	50.2	19.0	1.863	24.4
11	O-77	50.4	18.8	1.268	15.7
12	O-80C	50.3	18.8	1.766	23.0
13	O-5	50.2	19.3	1.536	19.6
14	O-43	50.3	19.1	1.391	17.5
15	O-49	50.2	19.0	1.740	22.6
16	O-64C	50.0	18.6	1.440	18.3
17	O-74	50.4	18.8	1.224	15.1
18	O-88	50.3	18.6	1.235	15.3
19	O-3C	50.1	19.2	1.319	16.5
20	O-19	50.3	19.2	1.044	12.5
21	O-20C	50.3	19.4	1.104	13.4
22	O-39C	50.3	19.0	1.283	16.0
23	O-67C	50.4	19.0	1.225	15.1
24	O-83C	50.3	18.7	1.170	14.3
25	O-62	50.1	18.7	0.513	4.8

Appendix 4F: Page 1 - static test values. Medium frequency testing of MDF at R=0.1.

Test N^{O}.	Static Sample (left)	Width mm	Thickness mm	Failure Load kN	Failure Stress MPa	Static Sample (right)	Width mm	Thickness mm	Failure Load kN	Failure Stress MPa	Mean Stress MPa
1	M-1	50.5	18.0	3.080	42.55	MM-2C	50.9	17.9	3.201	44.01	43.28
2	M-15	50.3	17.8	3.349	47.05	MM-16C	50.5	17.8	3.350	47.03	47.04
3	M-43	50.3	17.8	2.952	41.53	MM-44C	50.3	17.8	2.773	38.96	40.25
4	M-46C	50.9	17.9	3.099	42.81	MM-48	50.9	17.9	3.198	44.37	43.59
5	M-65	50.3	17.8	3.103	43.75	MM-66C	50.4	17.8	2.939	41.27	42.51
6	M-70	50.6	17.9	3.081	42.77	MM-71C	50.3	17.9	3.154	44.12	43.45
7	M-5C	50.3	17.9	3.285	46.04	MM-7	50.7	17.9	3.419	47.53	46.79
8	M-19C	50.6	17.8	3.210	45.07	MM-21	50.9	17.8	3.320	46.31	45.69
9	M-37	50.2	17.8	3.036	42.76	MM-38C	50.6	17.8	3.150	44.07	43.42
10	M-51	50.5	17.8	3.062	42.95	MM-52C	50.2	17.8	3.019	42.59	42.77
11	M-59	50.8	17.8	3.208	44.64	MM-60C	50.5	17.8	3.068	43.06	43.85
12	M-67	50.4	18.0	2.924	40.40	MM-68C	50.9	17.9	3.062	42.21	41.31
13	M-4	50.5	17.9	3.469	48.19	MM-5C	50.3	17.9	3.285	46.04	47.12
14	M-21	50.9	17.8	3.320	46.31	MM-22C	50.4	17.8	3.285	46.20	46.26
15	M-40	51.1	17.8	3.215	44.59	MM-41C	50.4	17.8	3.074	43.27	43.93
16	M-49C	51.1	17.8	3.020	41.79	MM-51	50.5	17.8	3.062	42.95	42.37
17	M-57C	50.6	17.9	3.184	44.37	MM-57C	50.6	17.9	3.184	44.37	41.26
18	M-74C	50.3	17.9	3.215	45.13	MM-76	50.6	17.9	3.148	43.85	44.49
19	M-7	50.7	17.9	3.419	47.53	MM-8C	50.4	17.9	3.375	47.33	47.43
20	M-12	50.5	17.9	3.187	44.19	MM-13C	50.5	17.9	3.364	47.02	45.61
21	M-35C	50.6	17.9	3.137	43.66	MM-37	50.2	17.8	3.036	42.76	43.21
22	M-54	50.4	17.8	3.028	42.56	MM-55C	50.3	17.9	2.977	41.72	42.14
23	M-60C	50.5	17.8	3.068	43.06	MM-62	50.6	17.8	3.192	44.77	43.92
24	M-73	50.3	17.9	3.090	43.42	MM-74C	50.3	17.9	3.215	45.13	44.28
25	M-41C	50.4	17.8	3.074	43.27	MM-43	50.25	17.8	2.952	41.53	42.40
26	M-10	50.7	17.9	3.189	44.34	MM-11C	50.4	17.9	3.078	43.06	43.7

Appendix 4F: Page 2- Dynamic test values. Medium frequency testing of MDF at R=0.1 **(+ = Runout Samples)**

Test N^{0}.	Dynamic Sample	Width mm	Thickness mm	Max Stress MPa	Mean Stress MPa	Min Stress MPa	Max Load kN	Mean Load kN	Min Load kN	R ratio	Freq Hz	Cycles To Failure	$\log_{10}$ Cycles	Stress Level %
1	M-1C	50.3	18.0	34.62	19.04	3.46	2.494	1.372	0.249	0.1	0.193	55	1.74	80
2	M-15C	50.4	17.8	37.63	20.70	3.76	2.678	1.473	0.268	0.1	0.177	120	2.08	80
3	M-43C	50.2	17.8	32.20	17.71	3.22	2.287	1.258	0.229	0.1	0.207	415	2.62	80
4	M-47	50.6	17.9	34.87	19.18	3.49	2.509	1.380	0.251	0.1	0.191	54	1.73	80
5	M-65C	50.1	17.8	34.01	18.70	3.40	2.406	1.323	0.241	0.1	0.196	322	2.51	80
6	M-70C	50.4	17.9	34.76	19.12	3.48	2.493	1.371	0.249	0.1	0.192	403	2.61	80
7	M-6	50.9	17.9	32.75	18.01	3.28	2.365	1.301	0.237	0.1	0.204	1499	3.18	70
8	M-20	50.8	17.8	31.98	17.59	3.20	2.287	1.258	0.229	0.1	0.208	1146	3.06	70
9	M-37C	50.3	17.8	30.39	16.72	3.04	2.161	1.189	0.216	0.1	0.219	660	2.82	70
10	M-51C	50.4	17.8	29.94	16.47	3.99	2.133	1.173	0.213	0.1	0.223	925	2.97	70
11	M-59C	50.9	17.8	30.70	16.88	3.07	2.205	1.213	0.221	0.1	0.217	763	2.88	70
12	M-67C	50.8	17.9	28.92	15.90	2.89	2.101	1.156	0.210	0.1	0.231	330	2.52	70
13	M-4C	50.3	17.9	28.27	15.55	2.83	2.023	1.113	0.202	0.1	0.236	4687	3.67	60
14	M-21C	50.9	17.8	27.76	15.27	2.78	1.993	1.096	0.199	0.1	0.240	2771	3.44	60
15	M-40C	51.1	17.8	26.36	14.50	2.64	1.905	1.047	0.191	0.1	0.253	9054	3.96	60
16	M-50	50.4	17.8	25.42	13.98	2.54	1.807	0.994	0.180	0.1	0.262	5711	3.76	60
17	M-58	50.8	17.9	26.71	14.69	2.67	1.925	1.059	0.193	0.1	0.250	2834	3.45	60
18	M-75	50.4	17.8	26.69	14.68	2.67	1.904	1.047	0.190	0.1	0.250	6278	3.80	60
19	M-7C	50.4	17.9	23.72	13.04	2.37	1.696	0.933	0.170	0.1	0.281	70484	4.85	50
20	M-12C	51.0	17.9	22.09	12.54	2.28	1.656	0.911	0.166	0.1	0.292	20920	4.32	50
21	M-36	50.9	17.9	21.61	11.88	2.16	1.560	0.858	0.156	0.1	0.309	37059	4.57	50
22	M-54C	50.2	17.8	21.07	11.59	2.11	1.496	0.823	0.150	0.1	0.316	68143	4.83	50
23	M-61	51.0	17.8	21.96	12.08	2.20	1.580	0.869	0.158	0.1	0.304	57049	4.76	50
24	M-73C	50.8	17.9	20.66	11.36	2.07	1.501	0.825	0.150	0.1	0.323	111191	5.05	50
25	M-42	51.1	17.8	17.57	9.67	1.76	1.270	0.698	0.127	0.1	0.379	1079538+	6.03+	40
26	M-10C	50.5	17.9	8.74	4.81	0.87	0.627	0.345	0.063	0.1	0.762	1029800+	6.02+	20

Appendix 4F: Page 3 - creep test values. Medium frequency testing of MDF at R=0.1.

Test N^{o}.	Creep Sample	Width mm	Thickness mm	Creep Load kN	Creep Weight kg
1	M-2	50.5	18.0	2.518	33.9
2	M-15	50.3	17.8	2.675	36.2
3	M-44	50.4	17.8	2.294	30.7
4	M-47C	51.0	17.9	2.523	34.0
5	M-66	50.5	17.8	2.426	32.6
6	M-71	50.3	17.9	2.482	33.4
7	M-6C	50.8	17.9	2.361	31.7
8	M-20C	50.9	17.8	2.290	30.6
9	M-38	50.5	17.8	2.167	28.8
10	M-52	50.4	17.8	2.129	28.3
11	M-60	50.5	17.8	2.186	29.1
12	M-68	50.4	18.0	2.102	27.9
13	M-5	50.2	17.9	2.018	26.7
14	M-22	50.5	17.8	1.974	26.0
15	M-41	50.5	17.8	1.878	24.6
16	M-50C	50.9	17.8	1.827	23.9
17	M-58C	51.0	17.9	1.927	25.4
18	M-75C	50.4	17.9	1.907	25.1
19	M-8	50.6	17.9	1.702	22.1
20	M-13	50.3	17.9	1.633	21.1
21	M-36C	50.4	17.9	1.540	19.7
22	M-55	50.4	17.8	1.503	19.2
23	M-61C	50.7	17.8	1.568	20.1
24	M-74	50.5	17.9	1.501	19.1
25	M-42C	50.5	17.9	1.241	15.3
26	M-11	50.6	17.9	0.626	6.4

APPENDIX 5: Statistical Terms

APPENDIX 5A: Skewness

Skewness provides a non-dimensional quantity to measure the "shape" of a distribution rather than its moment, which is measured in the same units as the distribution. The skewness is determined by:

$$\frac{n}{(n-1)(n-2)}\sum\left(\frac{x_1-\bar{x}}{s}\right)^3$$

A positive result means that the distribution is skewed to the right (the median is less than the mean). A negative result means that the distribution is skewed to the left (the median is greater than the mean). If a zero result is returned then the distribution is symmetrical about its mean.

APPENDIX 5B: Cumulative Distribution Function

If there are many observations in a histogram they can be replaced by a smooth curve drawn through the midpoints of each bar giving a frequency curve. If the height of the curve is then standardised so that the area underneath the curve is equal to unity, then a probability curve is produced. The function describing this curve is called the probability density function and is usually denoted by f(x). It gives the probability of finding a value within a certain range under the curve.

Another way of describing the probability curve is to consider the probability of observing a value less than or equal to a defined value. This function is called the cumulative distribution function, denoted by F(x).

The above density functions are related by:

$$f(x)=\frac{dF(x)}{dx}$$